NONLINEAR BEHAVIOUR OF PRECAST CONCRETE PANEL WALLS UNDER SIMULATED QUASI-STATIC AND DYNAMIC CONDITIONS OF LOCAL PANEL COLLAPSE

Alan W. K. Lee

A Thesis

in

The Department

of

Civil Engineering

Presented in Partial Fulfillment of the Requirements
for the degree of Master of Engineering at
Concordia University
Montreal, Quebec, Canada

December 1982

ABSTRACT

ABSTRACT

NONLINEAR BEHAVIOUR OF PRECAST CONCRETE PANEL WALLS UNDER SIMULATED QUASI-STATIC AND DYNAMIC CONDITIONS OF LOCAL PANEL COLLAPSE

Alan W. K. Lee

Precast concrete panel walls are investigated for simulated quasi-static and dynamic conditions of local panel collapse. A finite element procedure is employed to examine the nonlinear static and dynamic behaviour of a typical precast panel shear wall structure of the cross-wall type. Analyses are also performed for elastic behaviour and the rigid-cantilever approximation for static loading.

Individual precast panels are modelled as multilevel substructures comprising of plane stress rectangular elements with linear elastic behaviour. Horizontal and vertical joints are represented by discrete orthogonal spring elements with nonlinear constitutive material relationships, whereas elastic bar elements are used to model the transverse and vertical ties.

The static conditions of local collapse are simulated by assuming individual exterior panels to fail quasi-statically at various levels within the precast system. To simulate the dynamic force conditions of local failure, an exterior panel is assumed to collapse in a short duration of time in response to a domestic gas explosion. The nonlinear static and dynamic response of the precast system in this damaged state is evaluated in terms of overall structural response, the magnitude and distribution of forces and deformations in the horizontal and vertical joints, as well as forces in the ties. In particular, the results assess the validity of the rigid-cantilever approximation for the design of transverse and vertical ties.

A parameter study is performed to evaluate the influence of joint design parameters, vertical tie reinforcement details, as well as loading conditions on the nonlinear static and dynamic response of the precast system.

ACKNOWLEDGEMENTS

ACKNOWLEDGEMENTS

The author wishes to acknowledge with sincere gratitude his supervisor Dr. O.A. Pekau and his co-supervisor Dr. Z.A. Zielinski for their encouragement in the preparation of this thesis. The author is especially indebted to Dr. O.A. Pekau for his valuable criticism and suggestions during the course of this investigation.

The author also acknowledges Dr. Armin Wulf for his work in the programming of original versions of several of the computer routines while at the University of California at Berkeley. The substantial computer costs involved in this work were financed from NSERC grant A8258.

The investigation was performed with the financial support of La Formation de Chercheurs et d'Action Consertée du Québec and the Natural Sciences and Engineering Research Council of Canada. The author expresses his gratitude for this assistance. Acknowledgement is also extended to the Computer Center of Concordia University for providing the computing facilities.

Finally, the author wishes to thank Hilary and his parents for their understanding and encouragement.

TABLE OF CONTENTS

TABLE OF CONTENTS

PAGE

LIST OF TABLES

LIST OF TABLES

LIST OF FIGURES

LIST OF FIGURES

NOTATIONS

NOTATIONS

A_s = cross-section area of tie reinforcement

C_R = cantilever compression force resultant

d = effective lever arm in number of storeys, representing the distance from tension force resultant to the compression force resultant of the cantilever

F_a, F_s = axial and shear force in orthogonal spring elements, respectively

F_c, F_t = compression and tension force in bar element or orthogonal spring elements, respectively

F_p = postensioning force in vertical ties

F_y = shear strength of welded headed stud mechanical connectors

H = cantilever height in number of storeys

k_1, k_2, k_3 = compression stiffnesses of orthogonal spring elements in horizontal joints

k_a, k_s = axial and shear stiffnesses of orthogonal spring elements, respectively

k_c, k_t = compression and tension stiffnesses of bar elements or orthogonal spring elements, respectively

R = maximum resistance of cantilever

r_1, r_2, r_3, r_4 = displacement degrees of freedom of orthogonal spring elements

t = time

t_c = panel collapse time

t_d = duration of idealized pressure-time curve

t_m = time of maximum pressure

T_{max}, $\bar{T}_{max}$ = maximum force in transverse ties for static and dynamic behaviour, respectively

T_R = force resultant in transverse ties

u_a, u_s = relative axial and shear displacement in orthogonal spring elements, respectively

u_c, u_t = relative compression and tension displacement in bar elements or orthogonal spring elements, respectively

u_e, u_y = elastic and yield displacement limits in horizontal joints

W = design load consisting of wall and floor loads, per unit width of wall

W_d, W_ℓ = dead and live load per unit width of wall, respectively

$\delta_g, \bar{\delta}_g$ = gap opening in horizontal joints for dynamic and static behaviour, respectively

$\delta_s, \bar{\delta}_s$ = shear slip in horizontal joints for dynamic and static behaviour, respectively

$\delta_v, \bar{\delta}_v$ = cantilever tip deflection for dynamic and static behaviour, respectively

$\mu, \bar{\mu}$ = ductility factor in welded headed stud mechanical connectors for dynamic and static behaviour, respectively

μ_f = coefficient of friction between precast concrete panels and in-situ joint grout

CHAPTER I

INTRODUCTION

CHAPTER I

INTRODUCTION

1.1 GENERAL

In large precast panel buildings, the basic structural system resisting the lateral load is usually constructed of storey-height wall panels, connected along vertical and horizontal joints and functioning as precast panel shear walls. Due to the nature of large panel building construction, the strength and stiffness characteristics of the joints are different from those of the panels. This lack of continuity through the joints provides a fundamental mechanism for altering the structural behaviour of precast shear wall systems, compared to monolithically cast shear walls.

The stability of a large panel system is further questioned when a structural component fails due to an abnormal load, such as a gas explosion, vehicle or aircraft collision, impact or shock loading, etc. In the event that the structure is unable to redistribute the stresses away from the damaged area, failure may propagate, resulting in the collapse of the whole structure, or a large part of it. This phenomenon, in which the structural damage is dis-

proportionate to the significance of the initiating cause, is known as "progressive collapse."

Following the Ronan Point accident in London [1], in which the partial collapse of a large panel building was initiated by an internal gas explosion, several studies have been carried out in recent years to assess the liability of large panel structures to progressive collapse.

1.2 PREVIOUS INVESTIGATIONS

Alexander and Hambly [2] developed a method for the design of wall panels and slabs to withstand the dynamic loading from gaseous explosions. The major assumptions made in the dynamic analysis of individual walls or slab elements are that reinforced concrete behaves as a rigid-plastic material, and that plastic hinges form at points of maximum moment. Equations of motion were derived based on the formation of hinge mechanisms. It was shown that a relatively small amount of reinforcement provides substantial resistance to explosions.

Stafford-Smith and Rahman [3] have used the finite element method to study the sequence of failure in precast panel shear walls. Storey-height panels were modelled as single elements, and various joint strengths were assumed. The results suggest that a substantial reserve of strength

exists beyond the initial tension failure of the precast walls.

The Portland Cement Association (PCA) [4],[5] has conducted analytical and experimental studies on the behaviour of large panel structures under abnormal loads. By considering various panels ineffective within a precast wall, structures were tested statically under the simulated progressive collapse conditions. Analyses were made based on a rigid-cantilever assumption for various damaged configurations. Design charts are available for determining the forces required in the proposed tie system to maintain structural integrity.

Muskitvitch and Harris [6],[7] investigated the behaviour of large panel structures by means of small scale models. A 3/32 scale 3-dimensional large panel building was tested under simulated progressive collapse conditions, consisting of the removal of individual panels at different locations within the building. The effects of joint details on the behaviour of the damaged structure were studied using the finite element method [8]. The analytical results indicate that the nonlinear behaviour and proper functioning of cantilever walls are mainly governed by three factors: the bond slip characteristics of the transverse ties, the shear slip behaviour of the horizontal

joints, and the degree of vertical support provided for the cantilever walls.

Llorente [9] investigated the effect of opening of horizontal joints on the seismic response of precast panel walls using a finite element procedure. Elastic wall panels were modelled as substructures, whereas horizontal joints were modelled by plane stress rectangular elements with nonlinear material behaviour. It was concluded that under seismic loadings the rocking motion may contribute to a lessening of force levels.

Becker et al [10],[11],[12] presented a series of investigations examining the seismic resistance of simple and composite precast walls. A finite element idealization was used for the simple precast walls with coupling of shear and normal behaviour in the horizontal joints. The seismic response of simple precast walls was found to be governed mainly by a rocking phenomenon, and shear slippage between panels cannot be counted upon for seismic force isolation. Moreover, the seismic behaviour of composite precast walls were studied using the shear medium theory. The results indicate that if vertical connections can be designed to exhibit a stable elasto-plastic hysteretic behaviour, the walls and horizontal joints can be protected against seismic forces by deliberately installing weak vertical joints.

Schricker and Powell [13] reported a detailed study on the effect of nonlinear connection behaviour on the seismic response of simple precast walls. Wall panels were idealized by elastic beam elements and also by 2-dimensional finite elements. Horizontal joints were modelled by nonlinear spring elements with various material behaviour. It was concluded that the response can be very sensitive to the assumed strain hardening behaviour and joints should be designed to gain strength after yielding begins.

The recent work by Pekau [14] examined the structural integrity of precast panel walls for conditions simulating progressive collapse. The analyses were performed by a finite element substructuring procedure for static and seismic loadings assuming elastic material behaviour. The results indicate that the distributions of shear and axial force in the vertical and horizontal joints are different from those of the rigid-cantilever mechanism of Reference [5].

1.3 SCOPE OF PRESENT STUDY

The PCA [5] recommends a tie reinforcement system for structural integrity of precast panel walls. The analyses were made based on a rigid-cantilever model for the critical condition where an exterior panel in a precast wall becomes ineffective, which requires that the nonlinear

behaviour such as shear slip and opening in the joints are insignificant. Hence this analytical model may not be adequate to predict the behaviour of the damaged structure.

In related studies, the more refined finite element procedure used by Pekau [14] has shown that the flexibility introduced by the joints can lead to critical force requirements in the structure which are not predicted by the rigid-cantilever approach.

The foregoing studies related to progressive collapse have been confined to evaluations of the behaviour of the damaged structure with elastic joint characteristics, therefore limiting the practical applicability of the results. Furthermore, the investigations were carried out under static conditions, i.e., the local panel failure was assumed to take place in a quasi-static manner. The only study on the dynamic behaviour of precast systems under local failure conditions appears to be that of Reference [2], which is restricted to the response of individual panels or slabs. Corresponding studies on the overall dynamic behaviour of precast systems have not been reported to-date. The question arises as to whether the resistance of a precast structure is the same if the abnormal loading is a dynamic one, such as a gas explosion.

It is the purpose of the present study to examine the static and dynamic behaviour of precast panel walls under simulated progressive collapse conditions. A finite element procedure is employed to examine the nonlinear behaviour of a large precast panel building of the cross wall type. Individual wall panels are represented by multi-level substructures consisting of plane stress finite elements with linear elastic behaviour, whereas horizontal and vertical joints are modelled by orthogonal spring elements with nonlinear constitutive relationships. Transverse and vertical ties required for structural integrity are modelled as linear elastic uniaxial spring elements.

The investigation reported herein is organized in the following manner:

The modelling concept used for large panel structures is discussed in Chapter II. Here, the finite element substructuring procedure used for the elastic wall panels is presented. The constitutive models used for the horizontal and vertical joints, as well as the transverse and vertical ties are described in detail. Furthermore, the dimensions and properties of the prototype structure are presented in this Chapter.

The nonlinear static behaviour of a 12-storey prototype structure is presented in Chapter III. Also, the elastic

behaviour as well as the rigid-cantilever approach of Reference [5] are examined. The influence of various tie reinforcement details and joint parameters on expected performance of a 6-storey precast panel wall is presented in detail.

In Chapter IV, the nonlinear dynamic behaviour of a 6-storey prototype structure is examined. The modelling procedure and dynamic force conditions of local panel failure associated with a typical domestic gas explosion is described. Also, the effects of various joint properties and dynamic response parameters on a precast wall are discussed in detail.

Finally, general conclusions and proposed design recommendations are listed in Chapter V.

CHAPTER II

IDEALIZATION OF LARGE PRECAST PANEL WALLS

CHAPTER II

IDEALIZATION OF LARGE PRECAST PANEL WALLS

2.1 INTRODUCTION

Joints in large panel buildings are recognized as the weak elements; hence, it is reasonable to assume that nonlinear behaviour occurs only in the joints. Precast panel walls have been modelled as linear elastic 2-dimensional finite elements by many authors for static and seismic analysis [9],[10],[13],[14]. Two common approaches have been used for modelling the nonlinear behaviour of the joints, either by orthogonal spring elements [13], or by contact (or interface) elements [8],[9],[10].

Becker et al [10] modelled the horizontal joints as rectangular finite elements using elasto-plastic shear behaviour with strength dependent upon the normal compressive stress. The joint opening was modelled by assigning zero strength and stiffness in tension.

Mueller and Becker [12] have used an elasto-plastic model with stiffness degradation for vertical mechanical joints. Schricker and Powell [13] have developed several joint elements to model interface shear transfer, joint opening and crushing behaviour of the joints for seismic analysis.

For the present investigation, a precast panel wall is modelled as an assembly of linear elastic panel elements connected by discrete inelastic joint elements. Each precast panel is modelled as a substructure comprising of four-node plane stress rectangular finite elements with linear elastic behaviour. A horizontal or vertical joint is modelled by one or more orthogonal spring elements with nonlinear constitutive relations chosen to model the actual material behaviour. The analysis was performed using the general purpose program ANSR-I [27], with panel and joint elements attached as subroutines in earlier investigations [20],[21],[22]. Furthermore, the transverse and vertical ties required for structural integrity are modelled as uniaxial spring elements with elastic behaviour.

2.2 SUBSTRUCTURING OF LARGE PRECAST PANELS

For more refined modelling of precast panel shear walls connected by discrete joint elements, it is efficient to represent each linear elastic panel element as a substructure. The basis for panel substructuring described in detail in References [20],[21], consists of the systematic condensation of internal nodes as well as nodes not incident to the joints, in each individual panel. The overall system is then composed of an assembly of panel substructures which are represented in the subsequent

analysis by only the joint nodes.

The present investigation, employed the versatile panel element substructure described by Pekau and Huttelmaier [20]. The growth scheme applied in the development of a panel substructure follows the multilevel substructuring technique developed by Huttelmaier [21] based on a series of static condensation (see Figure 2.1). The stepwise formation of panel substructures is based on a single progression scheme composed of three stages: Stage 1 - end elements, as well as first and second level elements, are created with optional boundary node elimination in both end elements, as well as the level 2 elements; Stage 2 - elements created in Stage 1, are assembled into level 3, with optional node elimination; Stage 3 - by symmetry, level 4 elements are created, again with optional boundary elimination.

Plane stress four-node rectangular elements are employed to model the precast panel walls. There are two degrees of freedom at each retained boundary node incident to the joints. A lumped mass representation [21], derived by the use of a consistent lumping procedure and expressed by the retained degrees of freedom, is used to represent panel masses. The additional floor masses are inserted separately at each floor level.

2.3 MODELLING OF JOINTS IN LARGE PRECAST PANEL BUILDINGS

Finite element models of horizontal and vertical joints were developed and attached to ANSR-I [27] by Pekau and Wulf [22]. These were employed in this study after minor modification. A summary of the constitutive material relationships is provided below.

The joints are modelled by nonlinear orthogonal spring elements placed parallel and normal to the joint surfaces. A series of such spring elements is used to model a continuous joint of the "wet" type. In the case of a mechanical connector, a single element is employed to model the joint behaviour. Each spring element consists of a shear and axial spring, representing the shear and axial behaviour of the joint, respectively. The incremental behaviour of the element is governed by the tangent stiffnesses in the directions tangent and normal to the joint surfaces.

A 2-node spring element has four degrees of freedom and zero dimensions in space, as shown in Figure 2.2. If u_s and u_a are the shear and axial deformation of the element, hence, the relationship between the element deformations, $\underline{u}$, and nodal displacements, $\underline{r}$, is then given by

$$\begin{bmatrix} u_s \\ u_a \end{bmatrix} = \begin{bmatrix} -1 & 0 & 1 & 0 \\ 0 & -1 & 0 & 1 \end{bmatrix} \begin{bmatrix} r_1 \\ r_2 \\ r_3 \\ r_4 \end{bmatrix}$$

or in matrix form,

$$\underline{u} = \underline{A}\ \underline{r}$$

where

$\underline{A}$ is the element deformation-nodal displacement transformation matrix.

The force-deformation relationship for the element is

$$\begin{bmatrix} F_s \\ F_a \end{bmatrix} = \begin{bmatrix} k_s & 0 \\ 0 & k_a \end{bmatrix} \begin{bmatrix} u_s \\ u_a \end{bmatrix}$$

or in matrix form,

$$\underline{F} = \underline{k}\ \underline{u}$$

where

$\underline{F}$ is the element force vector, and

$\underline{k}$ is the element force-deformation matrix.

Hence, the element stiffness matrix $\underline{K}$ related to the nodal displacements, $\underline{r}$, may be expressed as

$$\underline{K} = \underline{A}^T \underline{k} \underline{A}$$

or,

$$\underline{K} = \begin{bmatrix} k_s & 0 & -k_s & 0 \\ 0 & k_a & 0 & -k_a \\ -k_s & 0 & k_s & 0 \\ 0 & -k_a & 0 & k_a \end{bmatrix}$$

In the remainder of this Chapter, the constitutive material relationships used for the vertical and horizontal joints, as well as the transverse and vertical ties are described.

2.3.1 Constitutive Model for Horizontal Joint

Karsan and Jirsa [23] conducted tests on the cyclic behaviour of concrete under uniaxial compressive load. The results indicate that concrete deteriorates under load level beyond the maximum stress with further degradation of stresses under cyclic load.

Test results by Mattock [17],[18] and others [16] on interface shear transfer of concrete with little or no reinforcement suggested that behaviour in shear is predominantly governed by friction. The hysteretic shear-slip behaviour of such joints under cyclic load tests with constant bearing force is essentially elasto-plastic.

To model the widely used "platform" type horizontal joints, a trilinear constitutive model is adopted for the compressive behaviour of the axial spring, with tensile stiffness reduced to zero during joint opening, as shown in Figure 2.3.

The compressive unloading or reloading is assumed to follow the initial stiffness, k_1. It should be noted that the compressive stiffness after crushing, k_3, is negative, which may cause computational problems. Therefore, to facilitate the numerical solution of the present analysis, a zero stiffness is used instead of a negative one.

When a series of spring elements is used to model a continuous horizontal joint, opening and closing along the joint will take place progressively. However, when only a few spring elements are used, opening and closing of the joint can cause drastic changes in stiffness behaviour, resulting in large unbalanced forces during the analysis. These large unbalanced forces may again lead to certain numerical instabilities. It is therefore essential to employ a sufficient number of spring elements when modelling a "wet" type horizontal joint.

An elasto-plastic constitutive model is used for the shear friction behaviour of the shear spring in the horizontal joint shown in Figure 2.4. Shear strength at any

instant is equal to the normal compressive force, F_c, multiplied by the coefficient of friction, μ_f, i.e., $\mu_f F_c$. Shear slip occurs when the shear force, F_s, is greater than or equal to the shear strength, $\mu_f F_c$. Inelastic unloading is assumed to follow the initial stiffness, k_s.

The coupling of axial-shear behaviour in the horizontal joint model allows the shear strength to vary with the bearing force; this produces a relatively complex shear-slip behaviour as shown in Figure 2.5. The plastic slip, as indicated in Figure 2.5, represents a measure of the energy dissipated by the inelastic shear-slip mechanism.

2.3.2 Constitutive Model for Vertical Joint

The vertical joint element allows modelling of mechanical connectors commonly used in North America. This joint model can also be used to approximate the behaviour of "wet" vertical joints.

Experimental tests [19],[28],[33] on welded headed stud mechanical connectors subjected to monotonic loadings indicate that the shear slip behaviour is essentially elasto-plastic exhibiting excellent ductility prior to failure, as shown in Fig. 2.6. It was shown that the shear strength is approximately proportional to the cross-sectional area of the studs [28],[33], with values ranging from 24 kN to 289 kN per connector (for two headed stud anchors of

sizes ranging from 6.4 × 68.3 mm to 22.2 × 207.9 mm embedded in normal weight concrete).

An empirical formula for the shear-slip relationship of monotonically loaded connectors was suggested as [33]:

$$F_s = F_{su}(1-e^{-18\,u_s})^{2/5}$$

where

F_s is the shear force,

F_{su} is the ultimate shear strength of the connector, and

u_s is the slip in inches.

For a slip equal to 0.5 in. (12.7 mm), the equation yields approximately 100% of the ultimate strength.

The constitutive model used for the shear behaviour of the mechanical connector is shown in Figure 2.7. Inelastic unloading or reloading of the elasto-plastic model is assumed to follow the initial elastic stiffness k_s. The parameter F_y indicated in Figure 2.7, denotes the shear strength of the connector.

An earlier study by Pekau [24] showed that the across-the-joint axial stiffness is of much less importance to the integrity of the panel system. It was suggested that the provision of a minimum axial stiffness ($k_a \simeq 14.6 \times 10^2$ kN/m) will guarantee integrity of the precast system in

the direction across the vertical joint.

The linear elastic constitutive model assumed for the axial behaviour of the axial spring is shown in Figure 2.8. For modelling of the welded headed stud connectors, the stiffness in tension and compression, k_t and k_c, respectively, are expected to be of the same order. However, when the joint model is used to represent a "wet" vertical joint, reduction in stiffness due to shrinkage and creep of the joint mortar can result in k_t being substantially less than k_c.

2.4 MODELLING OF TIES IN LARGE PRECAST PANEL WALLS

When an exterior wall panel of a particular storey fails in a multipanel wall assembly, the PCA [5] recommends the provision of transverse and vertical ties to ensure the monolithic behaviour of the cantilever mechanism. Transverse ties lie horizontally in the plane of the wall panels and pass through the horizontal joints, whereas vertical ties are placed within the wall panels vertically through tubular voids.

2.4.1 Constitutive Model for Transverse Tie

An effective cantilever mechanism requires high tensile forces to be developed in the transverse ties. These high

tensile forces induced in the ties in turn must be transferred to the surrounding joint concrete through bond stresses, such that the capacity of the ties can be fully utilized. Experimental tests [5] indicate maximum debonding of the transverse ties is in the range of 60 to 120 times that of the tie diameter.

The transverse ties are modelled by uniaxial spring elements. The linear elastic constitutive model for the spring element, shown in Figure 2.9, is selected to describe the behaviour of high strength unstressed prestressing strands. The equivalent tensile stiffness of the spring element, k_t, is dictated by the maximum debonding length of the strand. It is clear that the choice of a smaller debonding length will result in a higher tensile stiffness.

2.4.2 Constitutive Model for Vertical Tie

In the development of the cantilever mechanism [5], vertical ties are provided between consecutive lifts of wall panels to assure clamping and dowel action within the horizontal joints. In addition, these ties also provide a suspension mechanism to resist tensile forces incurred in the horizontal joints. High strength steel bars are suggested [5] for use as vertical ties. To provide additional vertical continuity in the wall assembly, postensioning can be introduced in the high strength steel bars.

The constitutive model employed for the transverse ties is also used to represent vertical ties. When post-tensioned vertical ties are used in design, the post-tensioning force, F_p, can be easily introduced as an initial force in the spring element, as shown in Figure 2.10. The equivalent tensile stiffness, k_t, of the element is now based on the actual development length rather than the debonding length.

2.5 PROTOTYPE STRUCTURE

The structure selected for study consists of the 12-storey cross wall system shown in Figure 2.11. Each solid precast wall panel is 2.97 × 3.67 m and 200 mm thick. The wall panels are constructed from normal weight concrete (23.6 kN/m^3), Young's modulus, Poisson's ratio and mass density are, respectively: $E = 2.76 \times 10^4$ MPa; $\nu = 0.17$; and $\rho = 2.40 \times 10^3$ kg/m^3. 200 mm precast hollow core slabs are used for the floor and roof slabs with a dead weight of 2.63×10^3 MPa.

Allowance for loads due to precast wall panels, partitions, mechanical equipment and hollow core slabs leads to an equivalent distributed dead load of 43 kN/m at floor levels. Live load is specified as 1.92 kN/m^2, corresponding to an equivalent distributed live load of 16 kN/m. The equivalent lumped masses assigned to the individual walls at

each floor level is 57.24×10^3 kg at each floor level.

The effect of wind load is not considered in the present investigation; therefore, according to the design recommendations of the PCA [5], the strength, U, required to resist dead load, D, and live load, L, should be at least equal to the following:

$$U = D + 0.5L$$

Accordingly, the resulting wall and floor loading to be used in the analysis is determined as 51 kN/m at each level per unit width of the wall. Details of the loading and lumped mass calculations are given in Appendices A.1 - A.3.

Since a precast hollow core slab system provides questionable coupling action, each of the cross wall is assumed to perform as a multipanel precast wall, as shown in Figure 2.11(b). The dimensions and properties of the prototype wall are summarized in Table 2.1. The "Platform" type continuous joints are used for the horizontal joints. (See Figure 2.11(c)). The vertical joint between wall panels employs welded headed stud connectors with two connectors per panel. (See Figure 2.11(d)). Transverse ties are provided at the floor levels and passing through the horizontal joints.

The analytical model adopted in the present study is shown in Figure 2.12. Each wall is modelled as a finite element substructure comprising of 4-node plane stress rectangular elements. The "platform" type horizontal joint is modelled by three orthogonal spring elements, whereas a single orthogonal spring element is used to represent a welded headed stud vertical connector. At floor levels, the equivalent stiffnesses of the uniaxial spring elements which represent the transverse ties are lumped at the panel corners. This arrangement allows the transverse tie stiffness properties to be represented by the axial spring of the vertical joint elements at floor levels.

2.5.1 Material Properties of Horizontal and Vertical Joints

Each horizontal joint is modelled by three joint elements presented in Section 2.4.1. The total stiffness of the entire joint is divided among the three joint elements in proportion to their tributary areas. Five parameters are needed to describe the compressive behaviour of the model: the initial elastic stiffness, k_1; the corresponding elastic deformation limit, u_e; the yielding stiffness, k_2; the corresponding yield limit, u_y; and the crushing stiffness, k_3. Tensile stiffness is specified as zero to represent the joint opening.

Based on a joint grout strength of 29×10^3 MPa, the above parameters are determined by an empirical equation suggested by Desayi and Krishnan [26] which describes the stress-strain behaviour of concrete in compression. Shear stiffness of the horizontal joint, k_s, is selected based on experimental results by Verbic and Terzic [16], assuming a constant coefficient of friction, $\mu_f = 0.4$.

Each headed stud mechanical connector is modelled by the vertical joint element described in Section 2.4.2. The value of the tensile stiffness parameter k_t of the element, representing the transverse ties, will be discussed in the following section. The value of the compressive stiffness parameter k_c is calculated based on the axial stiffnesses of the head studs (2-12.7 mm diameter studs per connector) used in the mechanical connectors. The shear strength F_y and shear stiffness k_s of the headed stud connectors are adopted from design data and experimental results of References [19],[28],[33]. Table 2.2 summarizes the values of various joint parameters for both the horizontal and vertical joints.

2.5.2 Material Properties of Transverse and Vertical Ties

The design of transverse and vertical ties is based on the design charts provided by the Portland Cement Association [5]. Details of the design procedure are presented in

Appendices A.4 and A.5. 12.7 mm unstressed prestressing strands are used as transverse ties at floor levels with a design strength of 142.0 kN per tie. The equivalent tensile stiffness, k_t, is calculated based on a debonding length of 60 times that of the strand diameter.

High strength steel bars of 17.5 mm diameter with a design strength of 179.2 kN are used as vertical ties with two bars per panel. The bars are placed within consecutive lifts of panels vertically through tubular voids, located near the ends of panels, as shown in Figure 2.11(b). To facilitate the construction, the bars are anchored at floor levels by means of threaded couplers, as shown in Figure 2.11(c), Detail A. In the event of a local panel failure, this design detail allows the ties to remain effective above and below the damaged panel.

Each vertical tie is modelled by the uniaxial spring element described in Section 2.4.2, connecting the uppermost panel to the foundation, or to the anchorage above the ineffective panel in the case of a local failure. It should be noted that the dowel effect of the bars is not considered in the present analysis. The value of the tensile stiffness of ungrouted ties is calculated based on the length of the bars. Details of the calculation of stiffnesses for transverse and vertical ties are presented in Appendices A.4 and A.5, whereas the values of the tie stiffnesses are summarized in Table 2.2.

TABLE 2.1 DIMENSIONS AND PROPERTIES FOR PROTOTYPE WALL

DIMENSION/PROPERTIES	VALUE
Overall height, in m - 12 storeys	35.64
- 6 storeys	17.82
Overall width, in m	11.0
Thickness of panels, t, in m	0.20
Height of panels, h, in m	2.97
Width of panels, b, in m	3.67
Properties of panels,	
- Young's Modulus, E, in MPa	2.76×10^4
- Poisson's ratio, ν	0.17
- Concrete compressive strength, f_c', in MPa	34.0
- Unit weight of concrete, in kN/m^3	23.60
- Mass density, ρ, in kg/m^3	2.4×10^3
Equivalent uniform dead load per unit width of wall, W_d, in kN/m	43.0
Equivalent uniform live load per unit width of wall, W_ℓ, in kN/m	16.0
Design load level, $W = W_d + 0.5W_\ell$, in kN/m	51.0
Equivalent lumped mass at each floor level, m, in kg	57.24×10^3

TABLE 2.2 VALUES OF JOINTS AND TIES STIFFNESS PARAMETERS FOR PROTOTYPE WALL

JOINT/TIE		VALUE OF PARAMETER
Horizontal joint,*		
- Axial	k_1	60.66×10^6 kN/m
	k_2	14.52×10^6 kN/m
	k_3	1.00×10^{-5} kN/m
	k_t	1.00×10^{-5} kN/m
	u_e	2.94×10^{-4} m
	u_y	5.38×10^{-4} m
- Shear	k_s	21.68×10^{-6} kN/m
	μ_f	0.4
Vertical joint,**		
- Axial	k_c	22.4×10^4 kN/m
	k_t	12.0×10^3 kN/m
- Shear	k_s	29.4×10^4 kN/m
	F_y	104.0 kN
Transverse tie,†		
	k_t	24.0×10^3 kN/m
	F_y †††	142.0 kN
Vertical tie,††		
	k_t - 12 storeys	13.47×10^2 kN/m
	- 6 storeys	26.94×10^2 kN/m
	F_y ††† -	224.0 kN

* Total stiffness for 3 spring elements per panel.
** Stiffness per mechanical connector.
† Stiffness per tie, lumped at the axial spring of vertical joint element.
†† Stiffness per tie.
††† Design strength per tie.

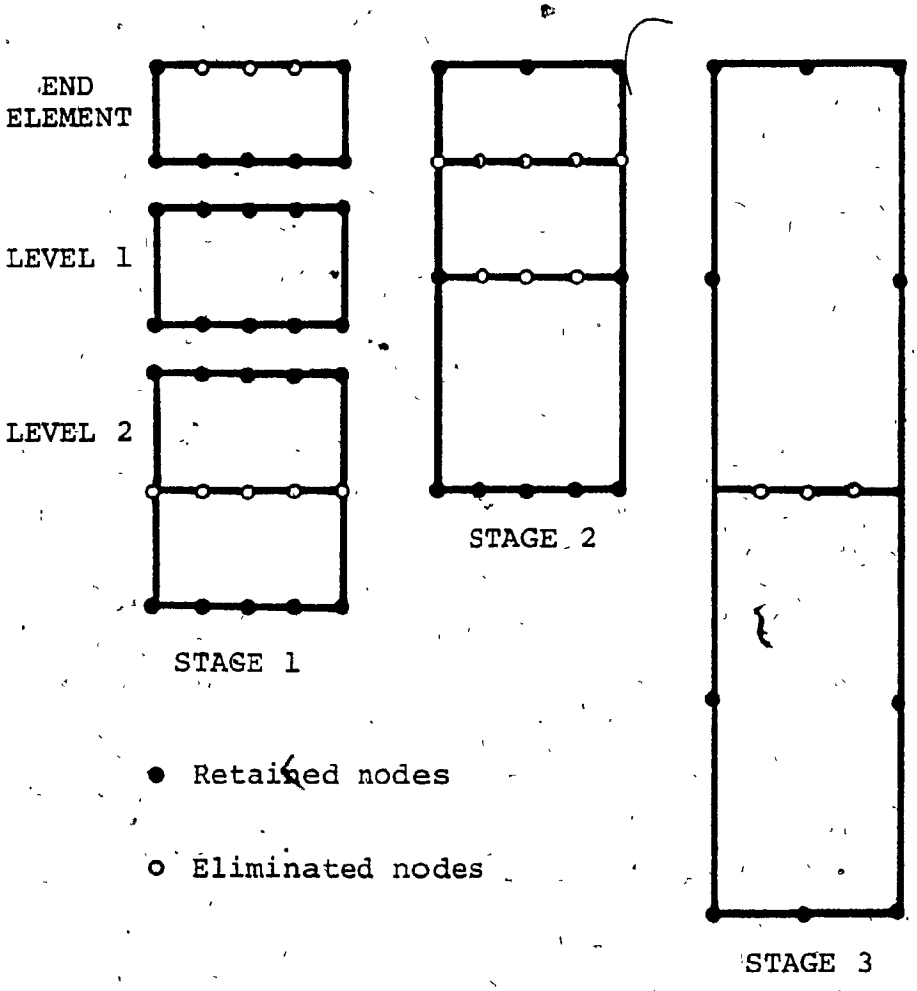

FIG. 2.1 SCHEME FOR MULTILEVEL PANEL SUBSTRUCTURING [21]

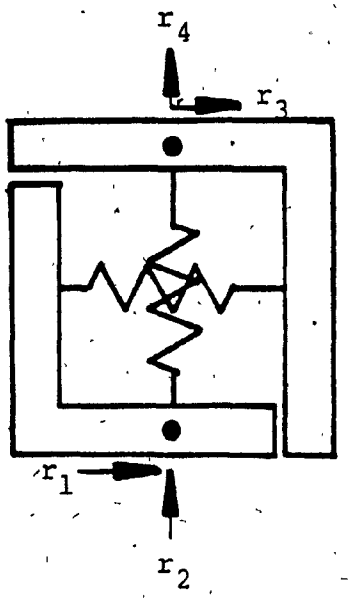

FIG. 2.2 2-NODE ORTHOGONAL SPRING ELEMENT

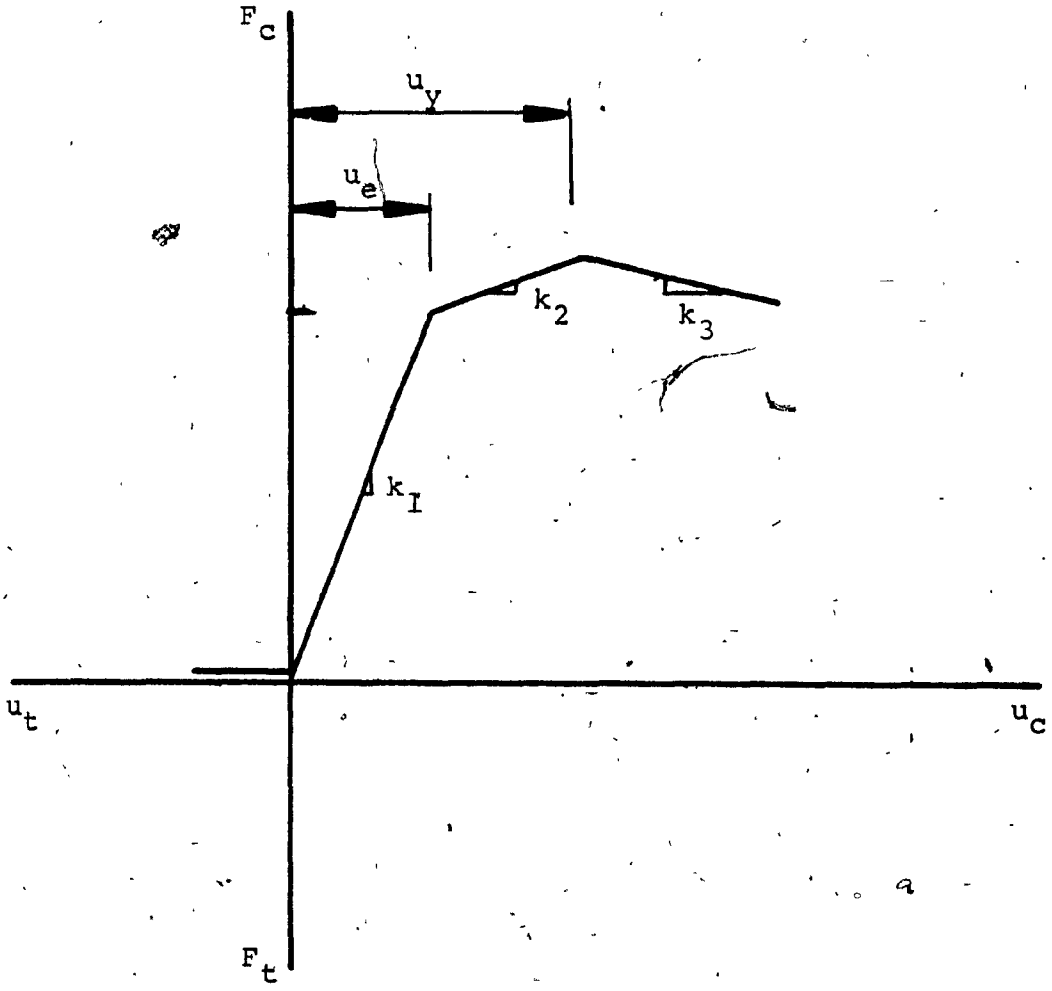

FIG. 2.3 CONSTITUTIVE MODEL FOR AXIAL BEHAVIOUR - HORIZONTAL JOINT

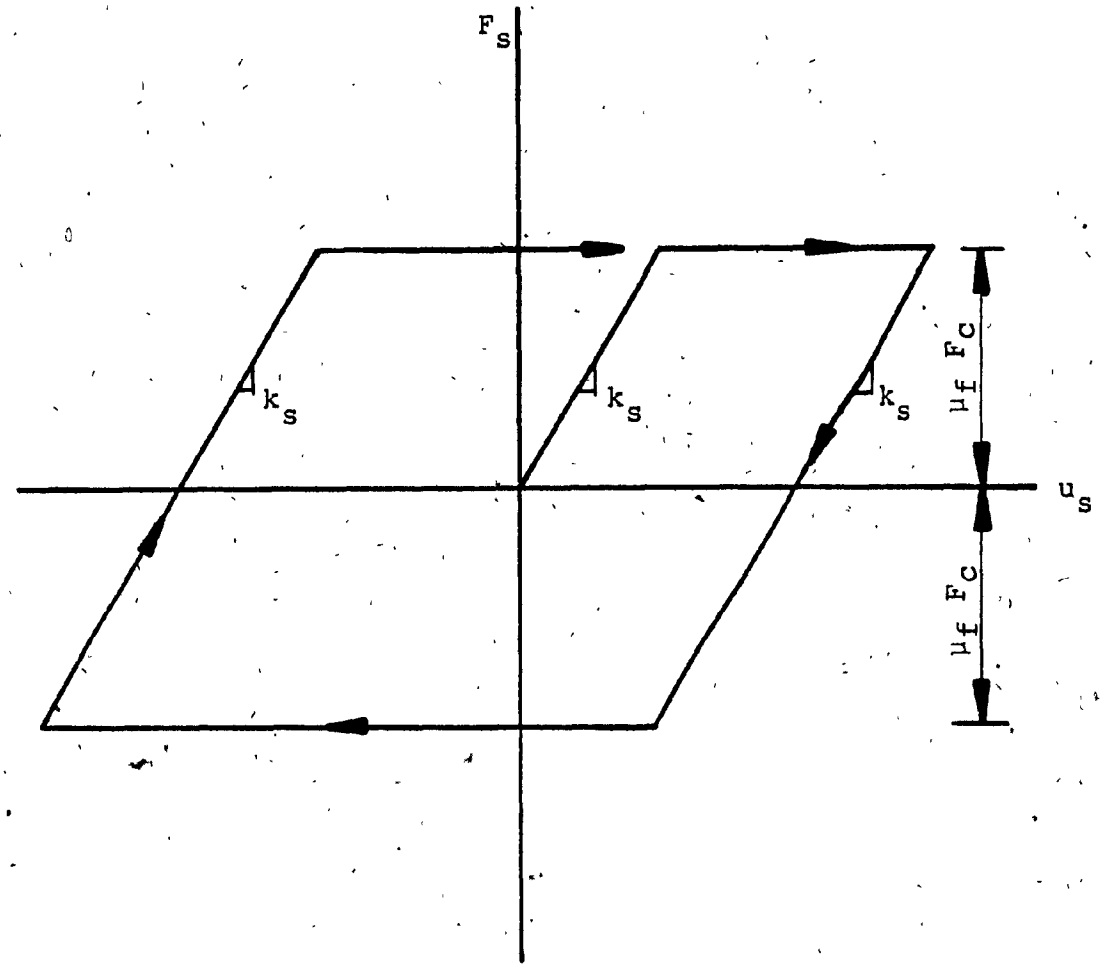

FIG. 2.4 CONSTITUTIVE MODEL FOR SHEAR BEHAVIOUR - HORIZONTAL JOINT

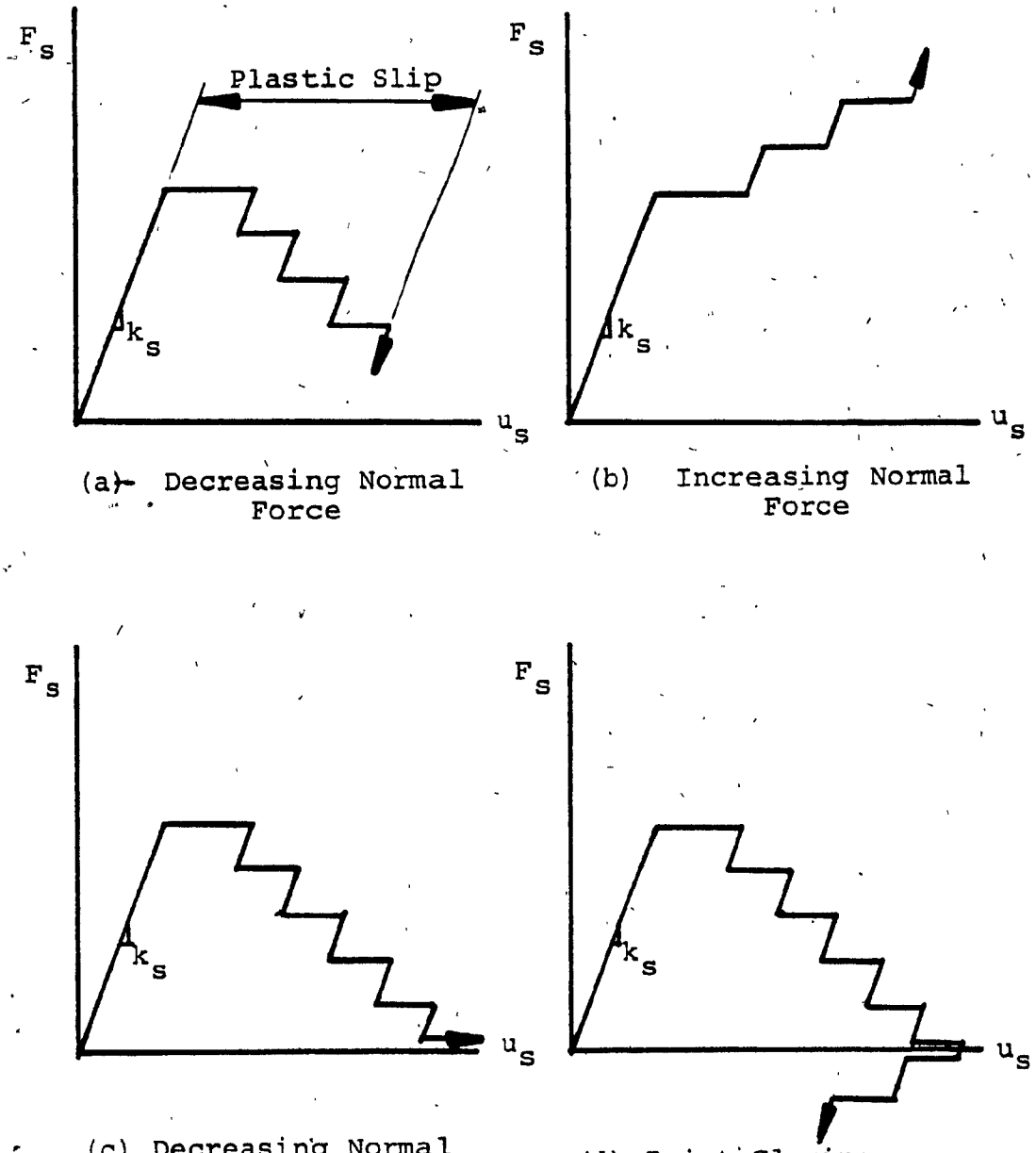

(a) Decreasing Normal Force

(b) Increasing Normal Force

(c) Decreasing Normal Force Followed by Joint Opening

(d) Joint Closing Followed by Shear Slip

FIG. 2.5 SHEAR SLIP BEHAVIOUR OF SHEAR SPRING ELEMENT - HORIZONTAL JOINT [22]

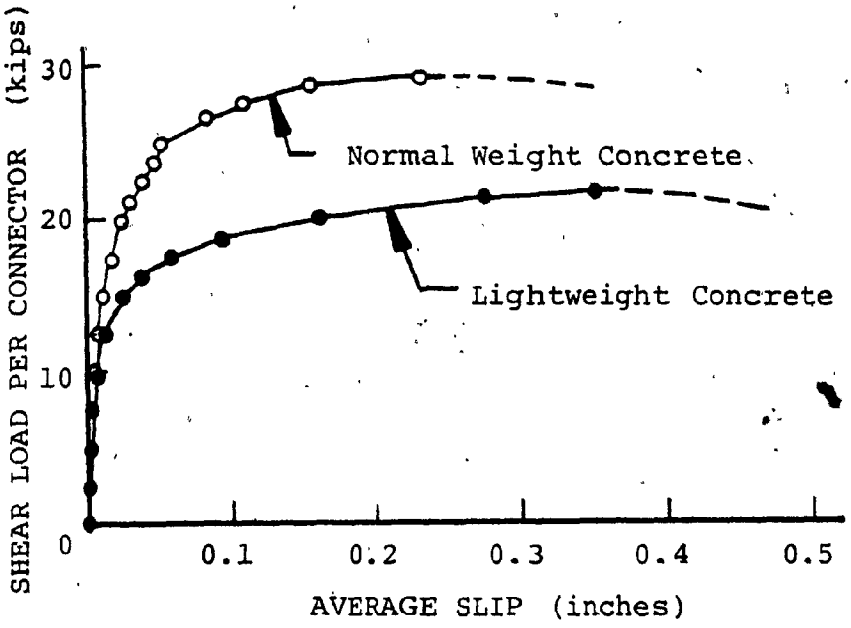

FIG. 2.6 TYPICAL SHEAR-SLIP BEHAVIOUR OF HEADED STUD CONNECTORS [33]

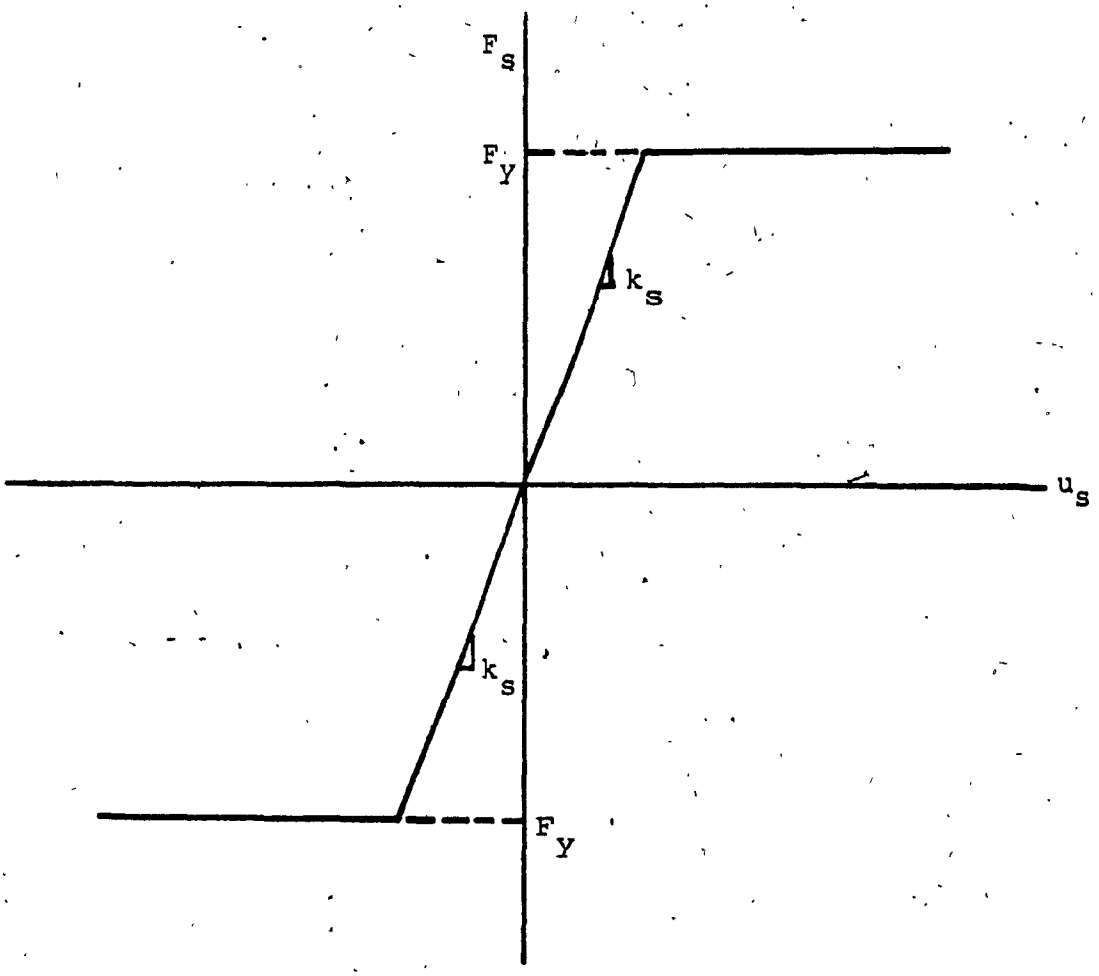

FIG. 2.7 CONSTITUTIVE MODEL FOR SHEAR BEHAVIOUR - VERTICAL JOINT

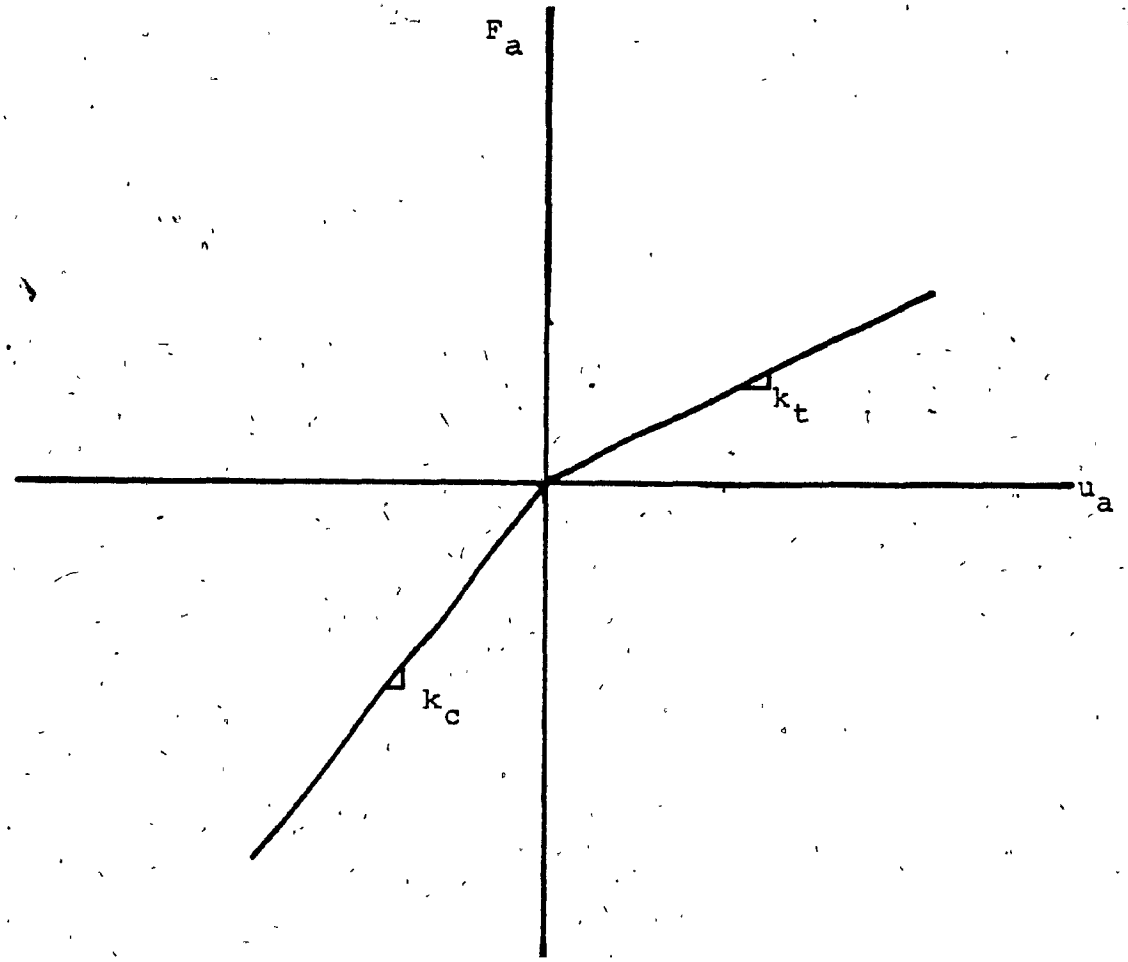

FIG. 2.8 CONSTITUTIVE MODEL FOR AXIAL BEHAVIOUR - VERTICAL JOINT

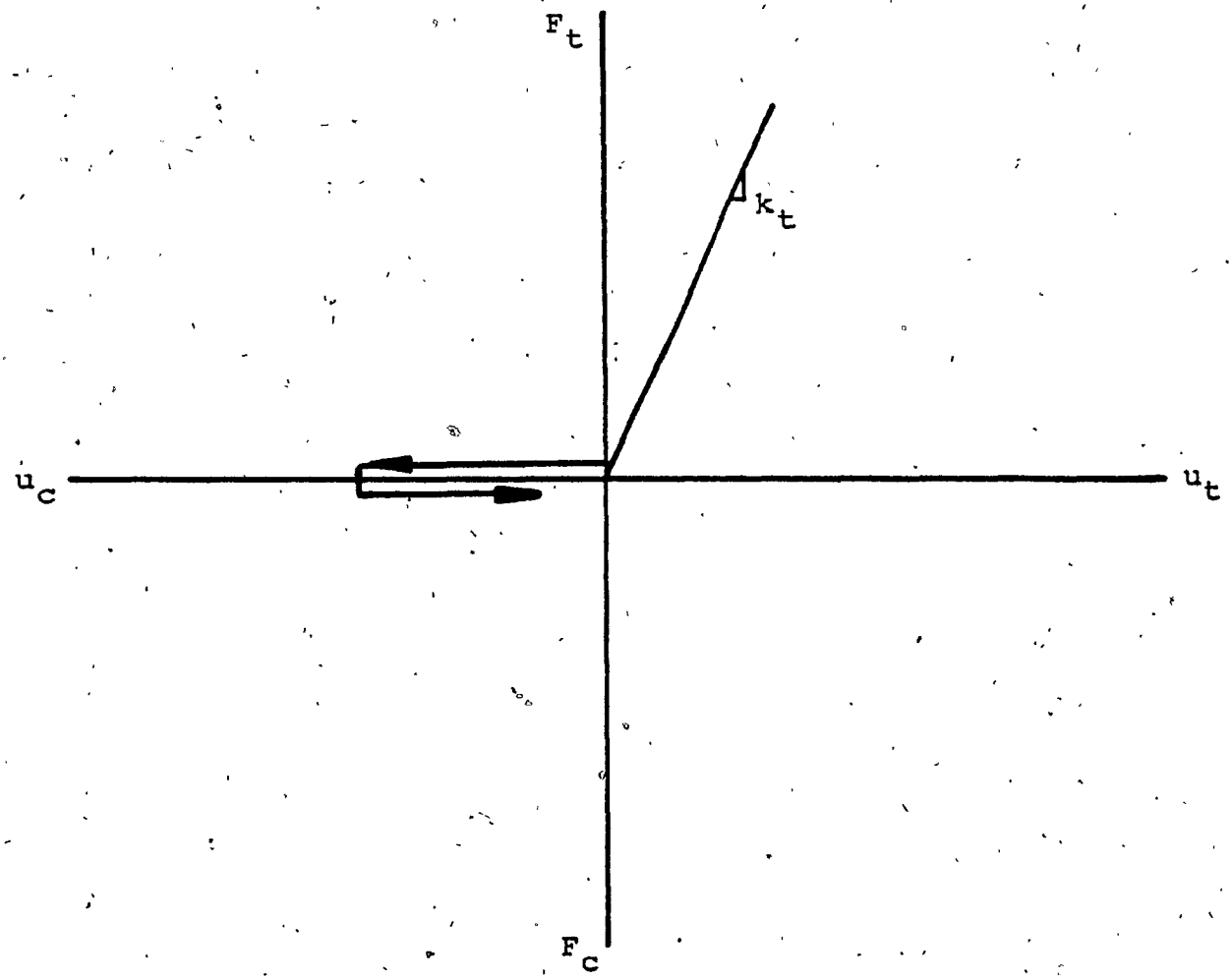

FIG. 2.9 CONSTITUTIVE MODEL FOR TRANSVERSE TIE

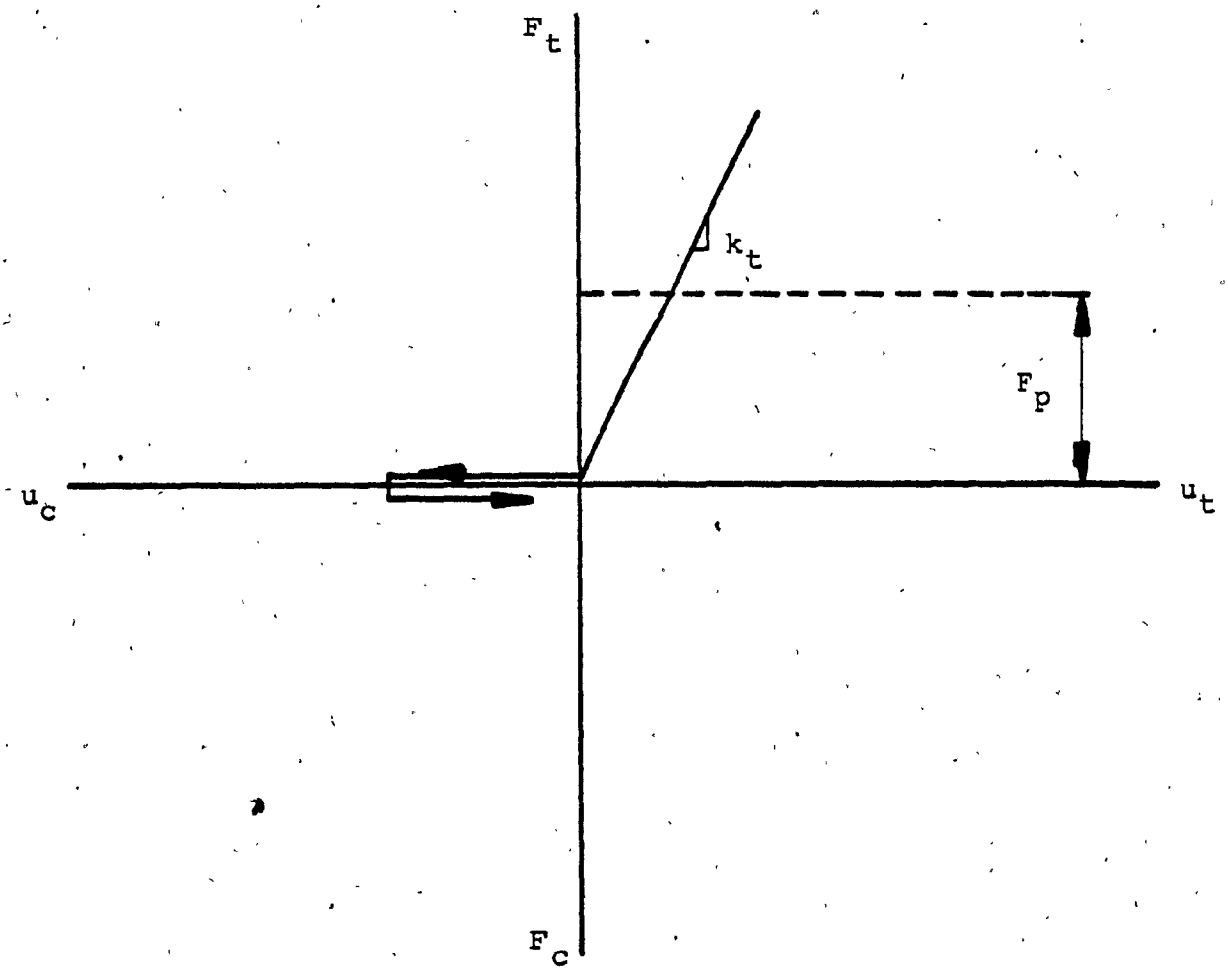

FIG. 2.10 CONSTITUTIVE MODEL FOR VERTICAL TIE

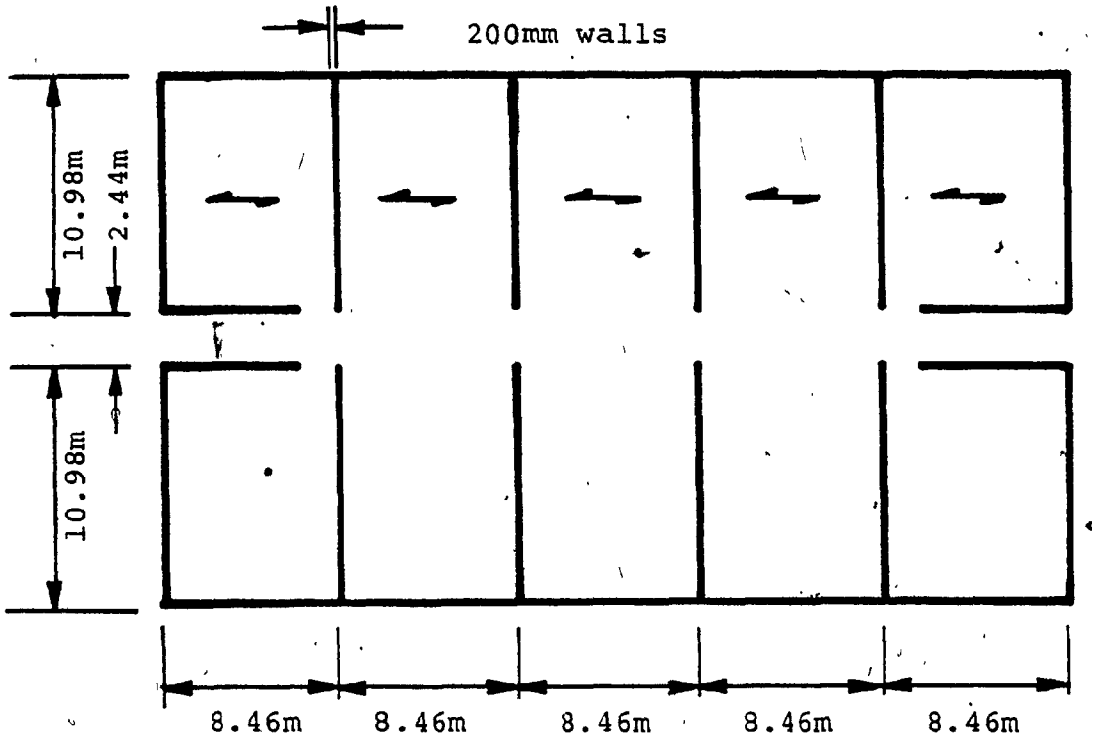

(a)

FIG. 2.11 PROTOTYPE BUILDING

(a) FLOOR PLAN ;
(b) TYPICAL PRECAST PANEL WALL ;
(c) PLATFORM CONNECTION DETAILS ;
(d) WELDED HEADED STUD CONNECTOR DETAILS

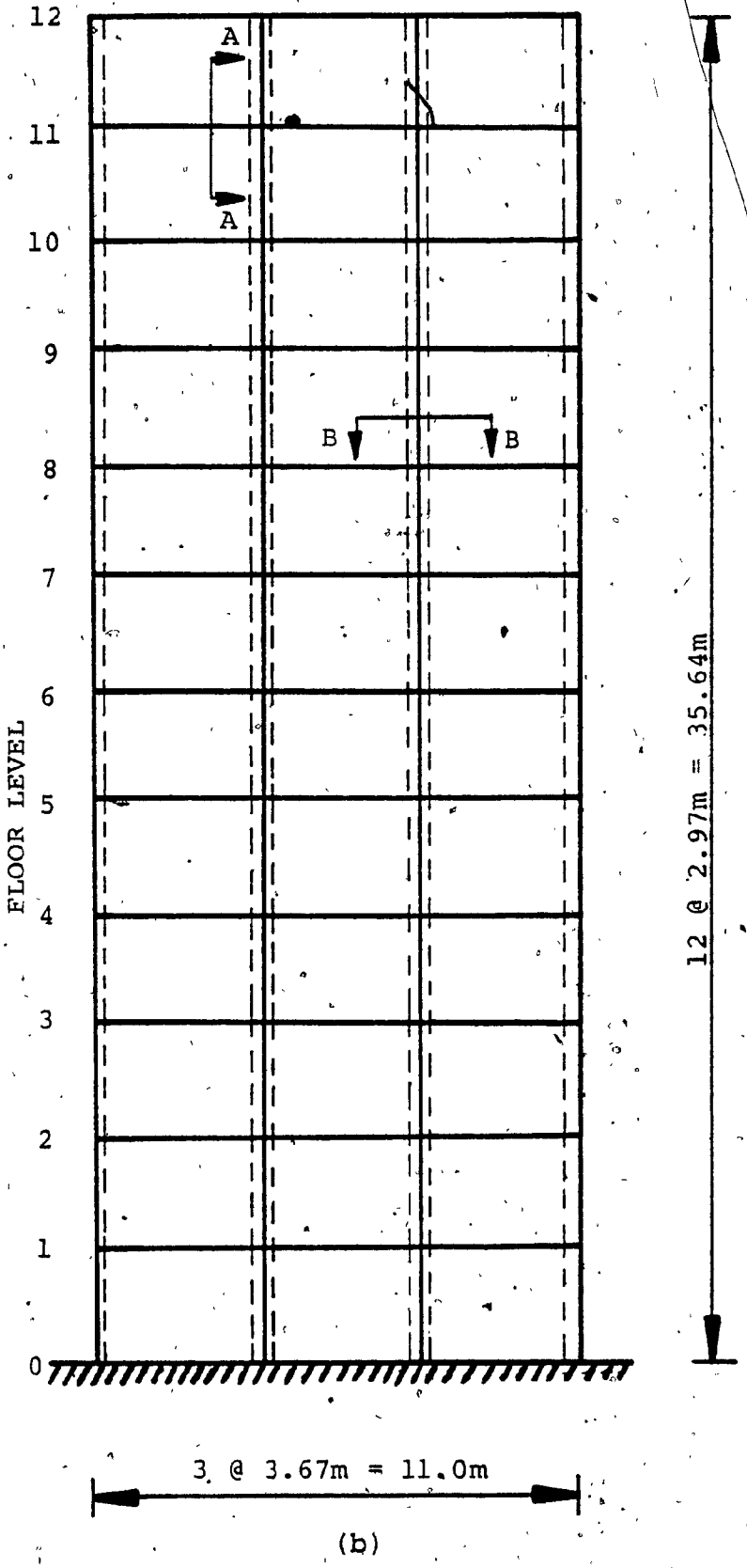
12
11
10
9
8
7
6
5
4
3
2
1
0
FLOOR LEVEL
A
A
B
B
12 @ 2.97m = 35.64m
3 @ 3.67m = 11.0m

(b)

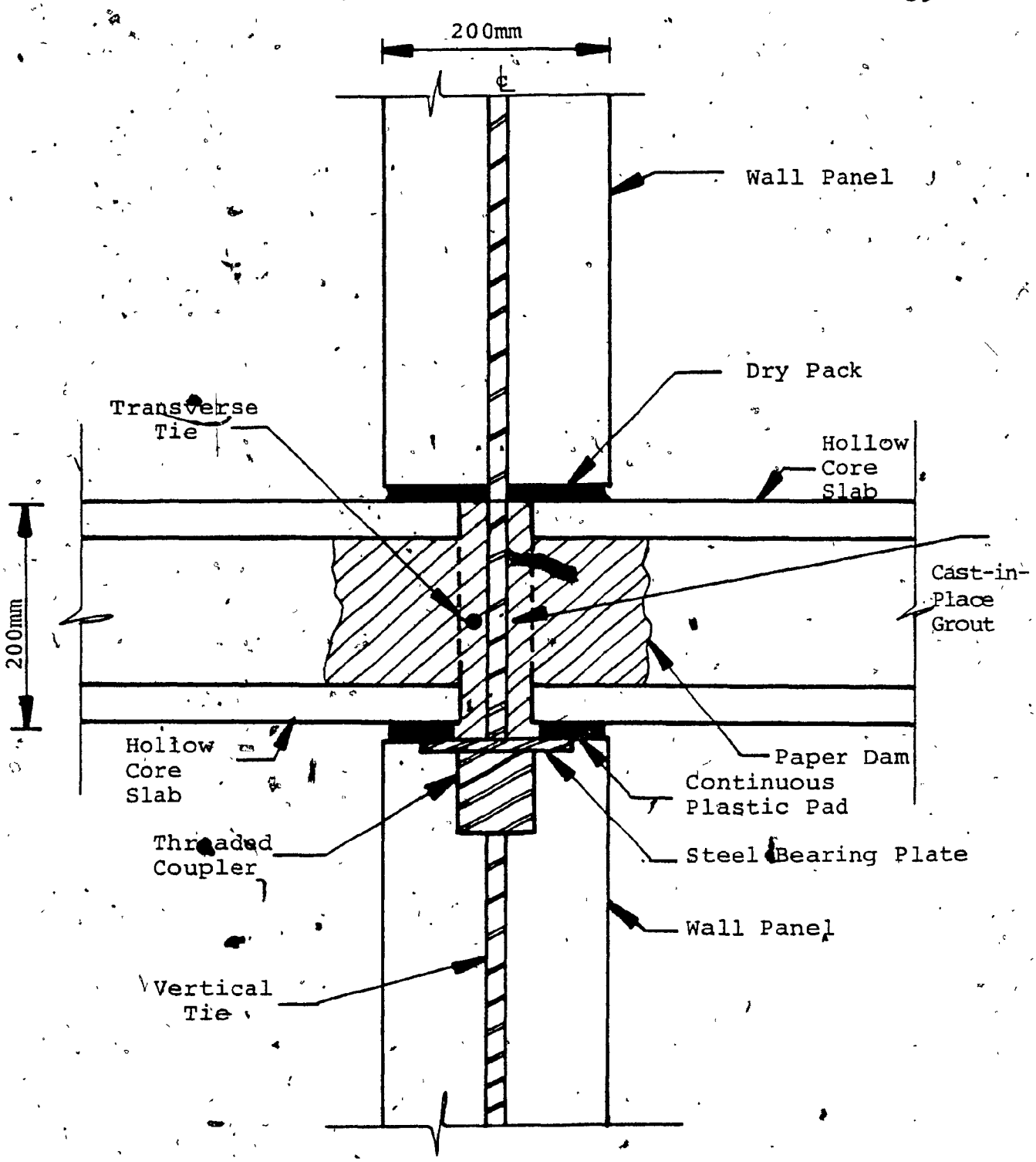

SECTION A-A TYPICAL PLATFORM CONNECTION

(c)

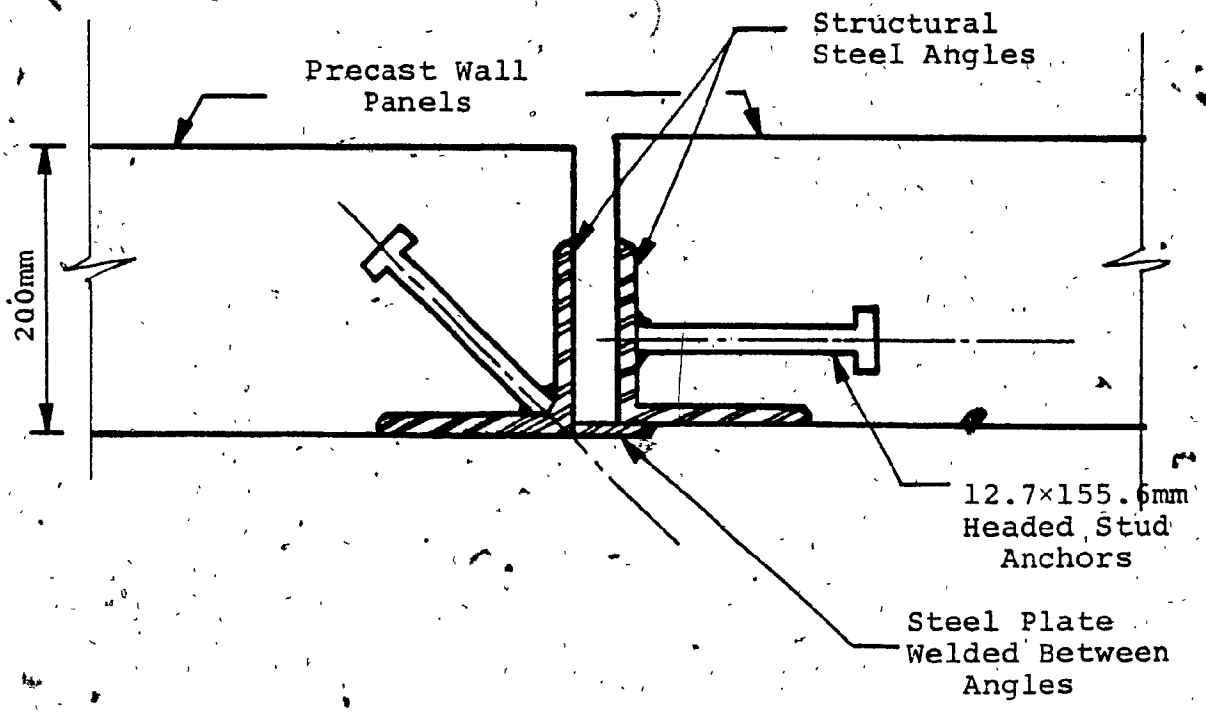

SECTION B-B TYPICAL WELDED HEADED STUD CONNECTOR

(d)

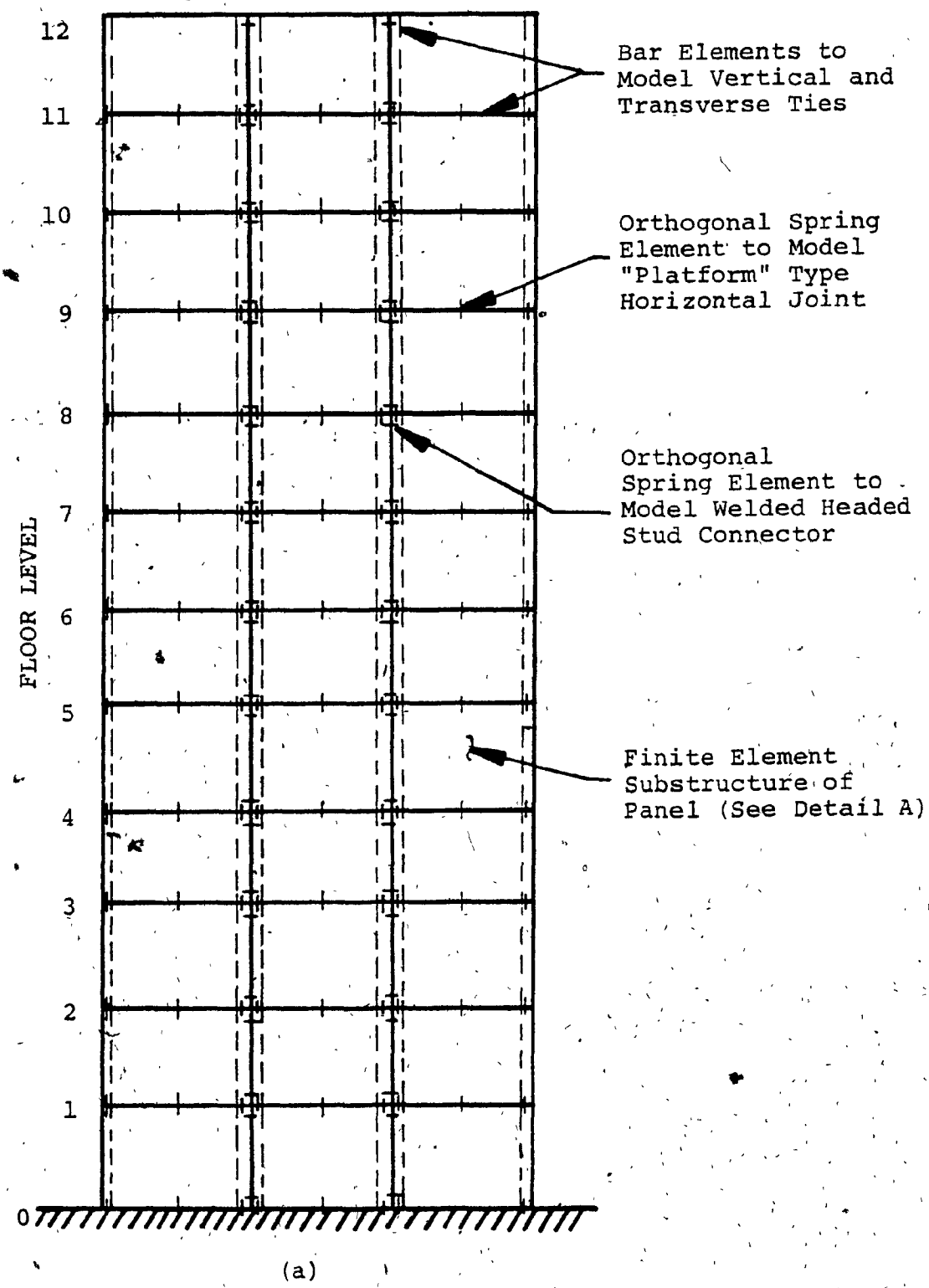

FIG. 2.12 FINITE ELEMENT IDEALIZATION:
(a) PRECAST PANEL WALL ;
(b) SUBSTRUCTURE OF TYPICAL PANEL

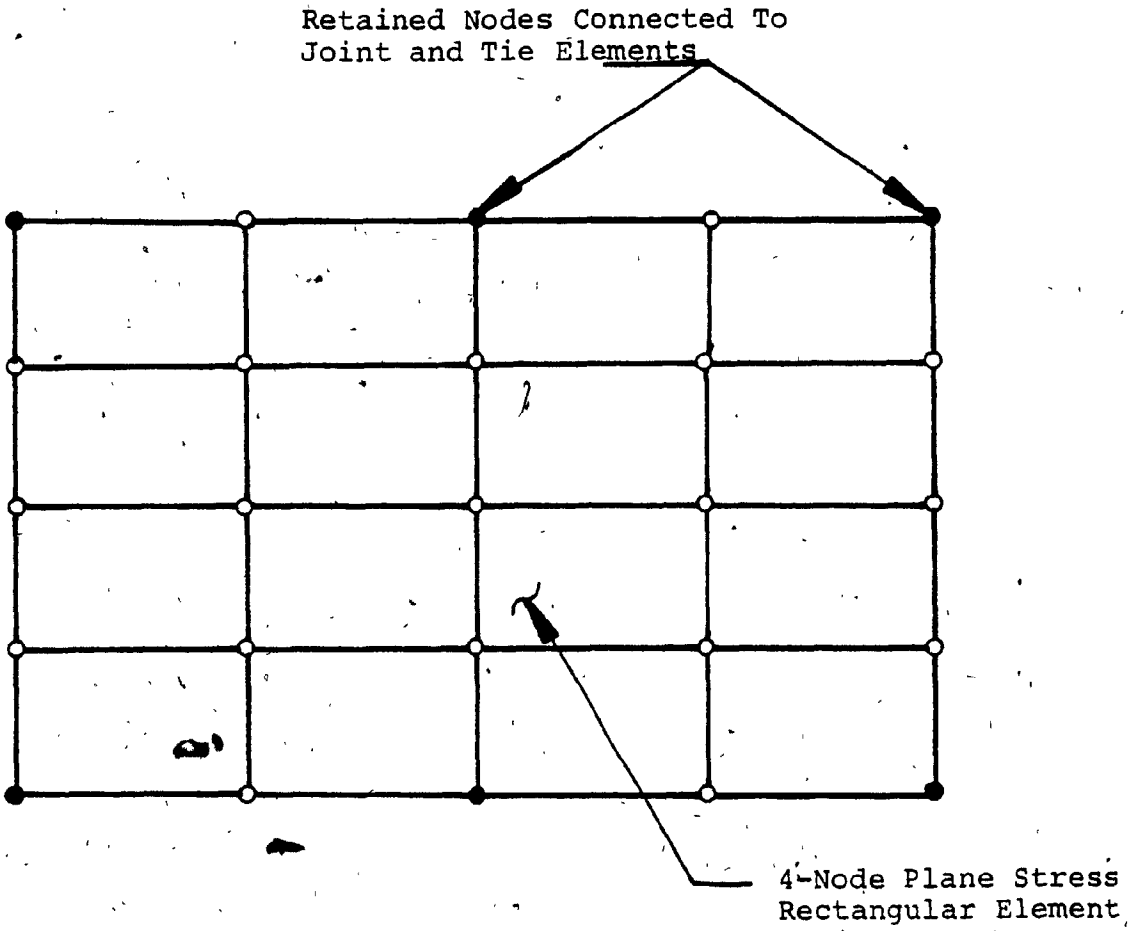

DETAIL A FINITE ELEMENT SUBSTRUCTURE OF TYPICAL PANEL

(b)

CHAPTER III

STATIC BEHAVIOUR

CHAPTER III

STATIC BEHAVIOUR

3.1 INTRODUCTION

Large precast panel buildings are more susceptible to progressive collapse than traditional monolithic concrete structures. This is due primarily to the lack of continuity and ductility through the joint regions. The need for continuity in a precast panel building system is demonstrated by the case history of the partial collapse at Ronan Point [1]. Progressive collapse is a complex phenomenon, and preventive mechanisms are not explicitly included in current codes of practice.

The general structural integrity approach presented by the Portland Cement Association (PCA) [4] recommends a structural tie system to resist abnormal loads. Design charts are provided to evaluate the required capacity of the ties in a precast wall based on a cantilever mechanism. However, in order to effectively develop the cantilever mechanism, the nonlinear behaviour such as shear slip and opening in the joints are assumed insignificant, so that the cantilever portion of the panel wall behaves in a rigid manner. Hence, this analytical model may not be adequate to predict the behaviour of the damaged structure.

The more refined finite element study of the same problem by Pekau [14] indicates that excessive shear force concentration occurs in the lower vertical connectors, which is not predicted by the rigid-cantilever mechanism. Also, the distributions of shear and axial force along the vertical joint were found to be different from those of the rigid-cantilever analysis. The high shear force concentration in the vertical connection shows that joints must be designed with adequate strength and ductility. In the case that connections cannot develop sufficient strength to sustain the excessive shear force, the post-yielded joints require a re-distribution of the internal forces in the structure. Furthermore, since joint openings were not allowed in the analytical model, the results may not be applicable in some cases.

The recent work by Muskitvitch and Harris [7],[8] examined the behaviour of large panel structures under simulated progressive collapse conditions. A 3/32 scale 6-storey building was tested with panels missing at different locations to model conditions of local failure. Analytical studies were also carried out on isolated cantilever walls to parallel the tests. Precast panels and horizontal joints were represented by plane stress finite elements with non-linear behaviour, whereas elasto-plastic bar and slip elements were used to model ties and the shear behaviour of

joint regions, respectively. It was concluded that the nonlinear behaviour and proper functioning of cantilever walls are mainly governed by three factors: the bond slip characteristic of the transverse ties, the shear slip behaviour of the horizontal joints, and the degree of vertical support provided for the cantilever walls.

The purpose of this Chapter is to investigate the static behaviour of precast panel walls (see Figure 2.11) under simulated progressive collapse conditions. A finite element procedure is used to model the linear elastic panels as substructures comprising plane stress rectangular elements, connected by nonlinear orthogonal spring elements to model the joint behaviour, and elastic spring elements to model the ties. Material properties of the joints and ties are chosen to approximate their behaviour in practice. Progressive collapse conditions are simulated by assuming that an exterior panel fails quasi-statically at various levels within the precast wall. Thus, the damaged structure is subjected to the imposed loading only in a static manner.

Consider the 12-storey prototype wall described earlier (Figure 2.12). The multipanel wall must be designed to resist the stresses induced by all predominant modes of panel failures. Results from other studies [5],[14] indicate that the most critical damaged configuration for a multipanel wall occurs when an exterior panel fails; this requires

the system above to behave as a cantilever. The potential cantilever height in a damaged 12-storey wall may vary from one to eleven panels in depth. Figure 3.1 shows a typical damaged configuration of the prototype wall. The dimensions and properties of the prototype structure, as well as the loading condition are summarized in Tables 2.1 and 2.2.

The present investigation was performed using the general purpose finite element program ANSR-I [27] for the analysis of nonlinear structures. Auxiliary subroutines for panel and joint element were added to the program [22] for the analysis of large panel structures. The solution scheme for the nonlinear static analysis of structures uses a Newton-Raphson iteration procedure. In the iterative solution procedure the load is applied in small steps and the structure is assumed to respond linearly within each step with Newton-Raphson iteration. The structure tangent stiffness matrix is reformed and stresses are updated at the end of each iteration, based on the strain increment computed for that iteration.

3.2 STATIC BEHAVIOUR OF A 12-STOREY PROTOTYPE WALL

To investigate the behaviour of precast panel walls under progressive collapse conditions, analyses were conducted on the 12-storey prototype wall for cantilever heights of one to eleven panels in depth, assuming nonlinear behaviour

in their connections. For comparison, analyses were also performed assuming the material properties of the joints to behave linearly elastic. However, to provide a meaningful comparison, joint opening and shear slip are allowed in the horizontal joints of the elastic analysis. The results are then compared to the rigid-cantilever approach to assess the validity of the design model proposed by the PCA [5].

The design features which have been studied for the prototype structure under damaged configurations are as follows:

1) Axial force distribution in vertical joints;
2) Compressive stress block;
3) Shear force distribution in vertical joints;
4) Ductility demand in vertical mechanical connectors; and
5) Coupled axial - shear behaviour in horizontal joints.

3.2.1 Axial Force Distribution in Vertical Joints

The distribution of axial force at floor levels along the vertical joints for cantilever height, H, of 1,3,5,7,9 and 11 storeys are shown in Figure 3.2. For cantilevers deeper than one storey, the force distribution pattern is character-

ized by a relatively high tensile force at the uppermost level, then followed by an increase of tensile force to a maximum at the eleventh level. The tensile force then starts to decrease progressively at successively lower levels to zero, after which the force changes to compression and increases rapidly to a maximum value at the base of the lowest panel.

In response to the failure of an exterior panel and subsequent loss of support for the wall panels above that level, the damaged structure is required to redistribute the loading from the cantilever to the remaining portions of the structure. Two predominant modes of behaviour are therefore anticipated by the cantilever assembly:

1) Bending action accompanied by an in-plane outward rotation of the panels; and

2) Shear action combined with a downward displacement along the vertical joint providing support.

The force distributions shown in Figure 3.2 are mainly influenced by the first mode. The overturning moment induced by the loading on the cantilever, is resisted by the tensile forces developed in the transverse ties acting in combination with the compressive forces distributed over the lower quarter of the cantilever assembly (see Figure 3.2) forming an internal resisting couple. For overall equilibrium of the

cantilever assembly the resultant of the transverse tie forces, T_R, must be equal to that of the resultant compressive force, C_R.

Table 3.1 presents the resultant forces for cantilevers of various depths. The effective lever arm, d, represents the distance between the resultant force couple expressed in terms of the number of storeys. With the exception of one storey cantilever, the data show that as the depth of the cantilever increases the resultant force is approximately constant for all cantilever heights (within 5%). This suggests that as the overturning moment increases in direct proportion to the cantilever depth, the internal resisting moment also increases, but only by extending the effective lever arm. This provides a larger resisting couple with the resultant force essentially constant (see Table 3.1). In practice, this behaviour is desirable since the force requirement is not influenced by the cantilever depth. Furthermore, the ratio between the effective lever arm, d, and the cantilever height, H, is approximately the same at $d/H = 0.80$ for all cantilever heights shown in Table 3.1. It can also be observed from Figure 3.2 that the tensile force region is limited within the upper portions of the cantilevers (approximately 6 storeys), with relatively small corresponding compressive force regions. For design purposes, the results suggest that the principal transverse tie reinforcement should be placed

within the top six floor levels, regardless of the cantilever height.

In the development of the rigid-cantilever action, Burnett and Howson [15] also observed that the transverse tie force decreases rapidly from the top of the building. As a result, an alternate tie design method was suggested which involves only the placement of transverse floor ties at the upper four levels of interior walls.

For comparison, further investigations were performed for (1) elastic behaviour based on the assumption that all joints and ties behave elastically but allowing slip and opening to occur in the horizontal joints, and (2) the rigid-cantilever analysis of Reference [5]. Figures 3.3 and 3.4 present the axial force distributions in the vertical joint for cantilever assemblies of 5 and 11 storeys, respectively.

For a cantilever of one storey, the force distribution is identical to that of the corresponding inelastic analysis. However, for cantilevers deeper than one panel, the force distribution follows the stress pattern typically found in isotropic homogeneous deep beams before cracking. For cantilever depth of 5 storeys, the maximum tensile force occurs at the eleventh level, as was the case for inelastic analysis; the force then decreases gradually to zero followed by a large

compressive force at the base of the cantilever (see Figure 3.3). However, as the cantilever depth increases to 11 storeys, there is a more pronounced deviation of the force pattern from that of the inelastic analysis (see Figure 3.4). The maximum tensile force in this case is seen to occur at a lower floor level. The rigid-cantilever mechanism assumes that the opening of the vertical joint is linearly related to the distance from the base of the cantilever; therefore, the force distribution follows a linear pattern with the maximum tensile force at the uppermost level (see Figures 3.3 and 3.4). The resultant compressive force, C_R, is assumed to act at the base of the cantilever through a single point.

Figures 3.5 and 3.6 show the resultant transverse tie force and the effective lever arm for varying cantilever depths. For a cantilever of one storey, all analyses indicate identical resultant force. However, as the cantilever depth increases, the elastic analysis indicates considerable increase in resultant force, whereas the force is approximately constant for the inelastic case (Figure 3.5). The results from the rigid-cantilever analysis also show constant force and a gradual increase in lever arm (Figure 3.6) for deeper cantilevers. The effective lever arm obtained is comparable for all analyses for cantilevers up to 3 storeys in height, after which the inelastic analysis shows an approximately

linear increase for deeper cantilevers (Figure 3.6). The elastic analysis, however, indicates steadily increasing force clearly due to the fact that the bending capacity of the cantilever is increased by developing higher transverse tie forces rather than increasing the effective lever arm. In the case of the rigid-cantilever analysis, the lever arm also shows an approximately linear increasing pattern for effective lever arm. This is mainly due to the fact that a constant triangular force pattern is assumed for the analysis with the resultant compressive force acting at a single point, instead of over a finite region.

As was noted earlier, a precast panel wall must be designed to resist the stresses induced by all potential cantilever heights, i.e., the cantilever height may vary from one to eleven storeys in depth. Hence, the maximum transverse tie force for any level must be determined by examining all cases for optimum design. Throughout the text, the term "envelope" will refer to the distribution of maximum force or deformation over the height of the structure, induced by all possible cantilever heights. Figure 3.7 shows the envelopes of the maximum transverse tie force for the 12-storey prototype wall. The more refined inelastic analysis produces a force envelope which decreases rapidly from the top level. The force envelope generated by the elastic analysis shows a similar pattern for the top three levels

and then increases considerably to a maximum (but smaller than the force at top level) at the fourth floor level, followed by a substantial reduction toward the base. On the other hand, the rigid-cantilever analysis indicates that the tie force requirement reduces progressively with distance from the top of the structure. Based on the capacity of a 9.5 mm diameter prestressing strand, the PCA [5] recommends that the design force for transverse ties should not be taken less than 80 kN, as indicated by the dashed line in Figure 3.7.

Figure 3.7 also shows that the maximum force occurs in the uppermost transverse tie for all three analyses, which corresponds to a cantilever of one storey. The value of the maximum tie force obtained in this case, is equal to 115.6 kN, still below the provided design strength of 142 kN. It can therefore be concluded that the transverse ties designed according to the PCA recommendations will behave in an elastic manner throughout all storeys at design load level.† Furthermore, by comparing the force envelopes presented in Figure 3.7, it can be observed that the rigid-cantilever approach provides conservative design forces for transverse ties below

---

†Design load, $W = W_d + 0.5\ W_\ell$, where W_d and W_ℓ are the dead load and live load, respectively.

the top four levels, compared to those of the inelastic analysis. However, for optimum design the recommended minimum tie force of 80 kN appears to be relatively inefficient, as indicated by the force envelopes associated with both elastic and inelastic analyses.

3.2.2 Compressive Stress Block

It was noted that compressive force develops near the base of the lowest panel in a cantilever assembly due to the bending mode. Assuming this compressive force is concentrated at the floor level in direct bearing and distributed over a finite area of the precast floor slab, it is essential to protect this compression zone where critical stresses may develop. Experimental study by Muskivitch and Harris [8] showed that local failure occurred in the floor slab due to this compressive stress, even at a stress level much less than the anticipated allowable bearing stress.

Since a panel may become ineffective at any storey, the compressive force can occur near the base of every panel as noted previously. The value of this resultant compressive force for varying cantilever height was presented in Figure 3.5. For inelastic analysis, this force is seen to be approximately constant (150 kN) for cantilever heights deeper than one storey. Using the ACI 318-77 code provision for bearing, the capacity can be calculated as follows in terms

of stress

$$f_{brg} = 0.85\phi\, f_c' \sqrt{A_2/A_1}$$

$$= 0.85\ (0.70)\,(34.0 \times 10^3)\,(\sqrt{2})$$

$$= 28.6 \text{ MPa}$$

where

ϕ is the capacity reduction factor,

f_c' is the concrete compressive strength,

A_1 is the loaded area, and

A_2 is the maximum area of the portion of the supporting surface that is geometrically similar to and concentric with the loaded area.

Consequently, the bearing capacity becomes

$$F_{brg} = f_{brg} \times \text{area}$$

$$= (28.6 \times 10^3)\,(0.20)\,(0.20)$$

$$= 1{,}144 \text{ kN}$$

It is obvious that this value is much greater than the maximum compressive force (150 kN). However, it was suggested that the bearing capacity of the compression zone can be significantly reduced by two factors [8]:

(1) by in-plane rotation of the panel assembly under bending action which considerably reduces the effective bearing area, and (2) the presence of vertical shear in this region. Since mechanical connectors are widely used in vertical joints, to transfer the compressive force effectively from the cantilever to adjacent wall stacks larger bearing areas should be provided by dry packing the lower quarter of vertical joints at every storey.

3.2.3 Shear Force Distribution in Vertical Joints

As stated earlier, the overturning moment due to the loading on the cantilever is mainly resisted by the bending and shear mechanisms of the panel assembly. The latter induces in-plane shear forces in the vertical joints between wall stacks, which are transferred by mechanical connections with two connectors per storey (see Figure 2.11 (d), detail B). It is evident that the primary function of these connectors is analogous to that of the coupling beams in coupled shear walls. Figures 3.8 and 3.9 show shear force distributions in vertical joints 1 and 2 (Figure 3.1) for cantilevers of 5 and 11 storeys, respectively. The force distribution in joint 1 produces a pattern typical of the elastic shear distribution for coupled shear walls under lateral loads. However, the distribution in joint 2 adjacent to the cantilever follows a pattern similar to the elasto-

plastic shear distribution in coupled shear walls.

Initially, when the loading on the cantilever is at a low level, the mechanical connectors behave elastically expressing the elastic shear distributions in joint 1 shown in Figures 3.8 and 3.9. The next increment of loading brings the connectors of the lowest panel to the elastic limit (F_y = 104 kN for 2 - 12.7 × 155.6 mm headed anchors). Further load increment causes redistribution of forces to successive higher levels, until the distribution becomes uniform along the height of the structure, with the upper connectors remaining elastic (see Figures 3.8 and 3.9, joint 2).

If the mechanical connectors were allowed to remain elastic throughout the loading, the shear force would follow the distribution shown in Figures 3.10 and 3.11. However, experimental tests [33] and practical design data [28] suggest the behaviour of such connectors is essentially elasto-plastic with ultimate shear strength ranging from 24 kN to 289 kN per connector (headed anchors embedded in normal weight concrete). Thus, the excessive shear force concentrations in the lower connectors of the cantilevers presented in Figures 3.10(b) and 3.11(b) do not actually occur in practical consideration. The rigid cantilever analysis assumes the total applied load from a particular level in the cantilever is to be carried by the adjacent vertical

shear connectors at that storey, which results in constant shear distributions in joint 2 as shown in Figures 3.10(b) and 3.11(b).

Figure 3.12 shows envelopes of maximum shear force in vertical joint of the 12-storey prototype wall for elastic, inelastic and rigid cantilever behaviour.

3.2.4 Ductility Demand in Vertical Mechanical Connectors

The nonlinear behaviour of the mechanical connectors discussed earlier allows redistribution of forces to occur in the vertical joints, leading to full utilization of the capacity. Once the connectors have reached ultimate strength, inelastic shear deformations will take place which require that the connectors be able to sustain large deformations without premature failure.

Experimental tests [33] of headed stud mechanical connectors indicate two modes of failure, namely ductile failure of the stud anchor and brittle failure in the concrete. The brittle failure mode is characterized by little or no shear deformation prior to catastrophic failure and is therefore to be avoided in design. Test results [19],[28], [33] also indicate that properly design headed stud connectors exhibited excellent ductility prior to failure.

Figures 3.13 and 3.14 show shear deformations of the connectors in vertical joint 1 for cantilevers of 5 and 11 storeys. Experimental tests [19] indicate the elastic shear deformation limit of such connectors is in the order of 0.35 mm shown in Figures 3.13 and 3.14. These diagrams clearly show that considerable deformation beyond the elastic limit occurs in all connectors except for those at the upper two levels. Deformations of the elastic connectors (Figures 3.13 and 3.14) are shown to be substantially lower at all levels than the corresponding inelastic connectors. However, elastic behaviour is only valid if the connectors can provide unusually high shear capacity which has already shown to be unacceptable in design practice (Section 3.2.3).

Nonlinear behaviour requires connectors be able to deform and sustain large yielding without failure, i.e., high ductility. The maximum shear deformation in each connector, u_{max}, and the elastic limit, u_y, can be related through

$$\mu = \frac{u_{max}}{u_y}$$

where

μ will be referred to as the ductility factor for the connector.

Based on an empirical formula suggested in Reference [33]

describing the shear-slip behaviour of headed stud connectors for monotonic loading (see Section 2.3.2), which gives a maximum shear deformation of 12.8 mm at approximately 100% of the connector's ultimate strength. This shear deformation corresponds to a practical ductility limit of $\mu = 36$, considering the elastic limit of $u_y = 0.355$ mm from Reference [19].

The envelope of maximum ductility factors in vertical mechanical connectors of the 12-storey prototype wall is shown in Figure 3.15. The practical ductility limit is also indicated in the diagram. It can be seen that the ductility demand is met for all connectors except at the lowest floor levels. This suggests that for higher structures it is important that mechanical connectors are properly designed and detailed to ensure that sufficient ductility is provided, thereby preventing catastrophic failure.

3.2.5 Coupled Axial - Shear Behaviour in Horizontal Joints

The coupling of axial and shear behaviour in the horizontal joint model (see Section 2.3.1) allows the shear strength to vary with normal force across the joint. Thus, shear strength at any instant is equal to the normal compressive force multiplied by the coefficient of friction, μ_f. and reduces to zero during joint openings. Experimental observations by the PCA [5] and others [7] show shear slip and

joint opening to occur in the horizontal joints in response to cantilever behaviour.

In Figure 3.16, the distributions of axial and shear stresses across the horizontal joints are examined at floor levels 11, 8, 5 and 2 for a cantilever of 11 storeys. At the upper horizontal joints axial and shear stresses are approximately uniform with relatively low magnitude for both inelastic and elastic analyses. However, in the inelastic case stress distribution varies from compression at the unsupported edge of the cantilever to joint opening near the face of support for intermediate floor levels. Therefore, the corresponding shear stress distribution is reduced to zero near the face of the support. Similar distributions occur in the lowest joint in the cantilever. In contrast, the elastic case shows substantially higher compressive stress distribution across the entire joint at intermediate levels, which varies from compression at the supported edge to joint opening at the free edge for the lowest level.

The distributions of maximum joint openings in horizontal joints for cantilevers of 5 and 11 storeys are shown in Figures 3.17 and 3.18. The distribution for the inelastic case is significantly higher than the elastic case. Figure 3.19 shows envelopes of maximum gap in horizontal joints for the 12 storey prototype wall.

Due to the participation of the overall structure in resisting the unbalanced cantilever moment, vertical tensile stresses may develop in the horizontal joints of Wall 1 (see Figure 3.1). The results show joint openings to occur in lower horizontal joints near the exterior face of Wall 1. Envelopes of maximum joint openings in horizontal joints of Wall 1 for the 12 storey prototype wall are presented in Figure 3.20. The envelopes are seen to follow the same pattern in both analyses but larger gap openings are predicted for inelastic behaviour.

In the above analyses, no compressive yielding was found in horizontal joints under the cantilever action, which indicates the across-the-joint compressive behaviour is linearly elastic. However, shear slip was observed in the horizontal joints within the cantilever at all levels. The distributions of shear slip for cantilevers of 5 and 11 storeys are shown in Figures 3.21 and 3.22. In the inelastic analysis, shear slip is maximum in the lower horizontal joints with relatively smaller slip for joints in the upper portion of the cantilever, whereas the elastic analysis shows considerably smaller slip only in the lowest joints. Figure 3.23 shows envelopes of maximum slip in horizontal joints for the 12-storey prototype wall.

The envelopes of Figures 3.19, 3.20 and 3.23 demonstrate that vertical reinforcing is necessary across the horizontal

joints of the cantilever and Wall 1 (Figure 3.1) to resist the vertical tensile stresses, and also to provide additional shear resistance for slippage. Ideally, vertical reinforcement may be provided by reinforcing loops projecting from panel edges and interlaced by continuous bars through the horizontal joints. However, such design details are seldom used in North America because of the high construction cost involved. The PCA [5] recommends placing of continuous vertical ties between wall panels (see Figure 2.11). When joint opening occurs, these ties are assumed to act as tension ties, creating a clamping effect on the joint surfaces which consequently provides additional shear resistance in the joint. The effectiveness of these ties will be examined in the following section.

3.3 PARAMETRIC INVESTIGATION OF A 6-STOREY PRECAST PANEL WALL

The investigation follows a parametric scheme which is intended to evaluate the influence of different tie reinforcement details and joint parameters on expected performance of precast panel shear walls for conditions simulating progressive collapse (Section 3.1). Nonlinear static behaviour of the damaged structure for loading until ultimate capacity is also examined. In particular, the effects of the following are studied in detail:

1) Mechanical connector shear strength F_y;

2) Vertical tie reinforcement and postensioning;

3) Coefficient of friction μ_f; and

4) Loading capacity and behaviour of cantilever at failure.

The series of structures analysed was generated by variation of a particular parameter using a 6-storey precast panel wall. The dimensions and properties of panels and joints for the basic wall are the same as those summarized in Tables 2.1 and 2.2. The results are expressed in terms of magnitude and distribution of forces and deformations in the joints, as well as forces in the ties.

3.3.1 Effect of Mechanical Connector Shear Strength F_y

In Section 3.2.3, it was noted that the shear force requirement for headed stud mechanical connectors in vertical joint 2 is uniform throughout the height of the structure at design load level. This is primarily due to the fact that the connector shear strength F_y, specified at 104 kN (2 - 12.7 × 155.6 mm headed anchors), has been reached for all connectors along the joint, with the exception of the uppermost level. Hence, for design purposes the connector shear strength F_y is an important parameter.

The influence of the parameter F_y on the structure for a cantilever of 5 storeys is shown in Figures 3.24 through 3.30, for F_y = 104 kN and F_y = 146 kN (2 - 15.9 × 166.7 mm headed anchors). In Figure 3.24, it is observed that the shear force distribution in vertical joint 1 is not influenced greatly by the higher shear strength F_y, with elastic behaviour throughout the joint. However, in Figure 3.25, the shear strength F_y = 146 kN is attained only at the two lowest floor levels, as compared to F_y = 104 kN, where the strength is reached at the lower four levels. As expected, the corresponding ductility demands in connectors are reduced considerably for all levels as shown in Figure 3.26. The distribution of axial force (Figure 3.27) in the vertical joint for F_y = 146 kN was found to be similar to that of the elastic distribution described in Section 3.2.1. In general, the magnitude of joint opening and shear slip decrease at all levels for the structure with higher shear strength F_y (Figures 3.28 through 3.30).

The comparison of envelopes of forces and deformations in the joints for the 6-storey basic structure for F_y = 104 kN and F_y = 146 kN is presented in Figures 3.31 through 3.35. The following observations are noted:

(i) The force requirement in transverse ties increases with higher values of F_y (Figure 3.31). It is evident that this increase is due to the shift in force distribution in the vertical joint for F_y = 146 kN, which now follows closer to that of the elastic behaviour, as shown in Figure 3.26.

(ii) The maximum ductility demand which occurs in the lowest mechanical connector is decreased by approximately 57% for F_y = 146 kN (Figure 3.32).

(iii) The magnitude of maximum opening in horizontal joints within the cantilever reduces significantly for higher value of F_y, as shown in Figure 3.33. However, in Figure 3.34, the magnitude of opening in horizontal joints of Wall 1 is shown to be unaffected by the variation in F_y.

(iv) The maximum slip in horizontal joints decreases considerably at all levels for F_y = 146 kN, except at the third floor level, where the slip was found to be comparable to that of F_y = 104 kN (Figure 3.35).

It can be concluded that shear strength parameter F_y of mechanical connectors has a significant effect on the magnitude and distribution of joint forces and deformations in the structure under abnormal loads. As expected,

the ductility demand of these connectors is considerably reduced by the use of higher shear strength F_y. Therefore, for structures higher than twelve storeys, where the demand in the lower connectors may be expected to exceed the practical design ductility (Section 3.2.4), mechanical connectors with relatively higher design shear strength should be employed.

3.3.2 Effect of Vertical Tie Reinforcement and Postensioning

The analyses described earlier (Section 3.2.5) indicate that reinforcement is necessary in the horizontal joints to provide additional resistance for shear slippage and joint openings.

In this section, vertical continuity is provided in two ways: (1) by vertical ties; and (2) by postensioned vertical ties. Based on the design recommendation by the PCA [5], high strength steel bars of 17.5 mm diameter (A_s = 240 mm^2, f_{pu} = 1,035 MPa, F_y = 224 kN) are used as vertical ties with two bars per panel (see Appendix A.5). The postensioned ties are stressed to 60% of ultimate stress corresponding to a force of 150 kN per tie. The modelling of vertical ties is described in Section 2.5.2, whereas the stiffness properties are given in Table 2.2.

The effect of vertical ties and postensioning on the structural performance of the 6-storey precast wall for maximum height cantilever are shown in Figures 3.36 - 3.39. The following observations are noted:

(i) The axial force distribution for vertical joints which indicates the transverse tie force requirements is not significantly affected by the introduction of vertical ties and postensioning force (see Figure 3.36).

(ii) Although it was observed that the presence of vertical ties and postensioning force does not greatly affect the shear force distribution in vertical joints, Figure 3.37 shows the ductility demand in vertical mechanical connectors is more sensitive to the effect of vertical ties. A maximum decrease in ductility factor μ at the lowest connector in the cantilever of 7 and 24 percent was found, respectively, for structures with vertical ties and postensioning.

(iii) As expected, the provision of vertical ties reduces the joint opening occurring in the horizontal joints of the cantilever (Figure 3.38). In the case of postensioned ties, horizontal joint openings were completely eliminated throughout the structure.

(iv) Figure 3.39 indicates that the vertical ties reduce the magnitude of shear slip in horizontal joints for lower storeys in the cantilever. This is particularly evident when ties are postensioned.

It can be concluded that joint openings and inelastic shear deformations in horizontal and vertical joints can be reduced by means of vertical ties and postensioning. However, it appears that the provision of untensioned vertical ties does not significantly decrease the magnitude of the joint deformations in the structure in response to the cantilever action. The use of postensioned ties was shown to be more effective within this context. Nevertheless, it can be seen that both untensioned and postensioned ties reduce the ductility demand in the mechanical connectors along the vertical joint, desirable from the design viewpoint. As was shown in an earlier section, structures higher than 12 storeys require ductility factors in mechanical connectors that exceed the practical ductility limit. This suggests that for such structures the ductility demand should be appropriately reduced by providing either untensioned or the more effective postensioned vertical ties.

3.3.3 Effect of Coefficient of Friction μ_f

In the analyses of the previous sections a constant coefficient of friction, $\mu_f = 0.4$, between precast concrete

panels and joint grout was assumed for the horizontal joints. This implies that frictional shear strength at any instant is directly proportional to the compressive force acting across the joints. Fintel et al [4] reported that coefficients of friction specified by design codes vary from 0.2 to 0.8. In order to investigate the sensitivity of the 6-storey precast panel wall to this design parameter in the damaged state, the response of two values of the coefficient of friction is examined.

The influence of the coefficient friction on the structure for the 5-storey cantilever is shown in Figures 3.40 through 3.42. It was observed that the distributions of axial and shear force in the vertical joint are not affected by varying the coefficient of friction, and virtually identical forces were obtained in both cases. However, the following observations are noted:

(i) Figure 3.40 indicates that the ductility requirement in the vertical mechanical connections is slightly reduced as μ_f is increased from 0.4 to 0.7.

(ii) The magnitude of joint opening is decreased substantially at all levels in the cantilever for $\mu_f = 0.7$ (see Figure 3.41). This is particularly evident at the fourth level, where joint opening is maximum.

(iii) It is apparent that the increase of μ_f from 0.4 to 0.7 will provide relatively higher frictional resistance against shear slip. Figure 3.42 shows that the shear slip is reduced at all levels in the cantilever for $\mu_f = 0.7$.

The results of the above comparison indicate that the coefficient of friction, μ_f, if specified within the range 0.2 - 0.8 used in current design codes, has little effect on the performance of the precast system under abnormal loads. This is particularly important for the design of transverse ties where the force requirement was shown to be relatively unaffected by this joint parameter.

3.3.4 Load Capacity and Behaviour of Cantilever at Failure

The analyses described in the preceding sections evaluate the performance under the design loading conditions in the damaged state. The design load level was specified according to the strength requirement recommended by the PCA [5] for resisting abnormal loads (see Section 2.5). In practice, however, it is important to examine the ultimate load capacity and the mechanism of failure of the cantilever, to determine critical design features as well as strength reserve not indicated by the design load conditions.

Figure 3.43 illustrates the load-displacement behaviour of the 5-storey cantilever for structures with and without vertical ties (untensioned or postensioned). The dashed line in Figure 3.43 indicates the specified design load level. In all cases, the mode of failure of the cantilever is due to shear failures of mechanical connectors along the vertical joint 2 (see Figure 2.11 (c)). This behaviour is in contrast with results observed in experimental tests [5],[7], where failure mode was either due to brittle shear failure of the vertical tie, or due to ductile failure of the transverse ties. However, shear resistance due to the dowel effect of vertical ties across the horizontal joints was not considered in the present analysis. Consequently, the brittle shear failure of the vertical tie in the cantilever is not anticipated. Furthermore, continuous vertical "wet" joints were used between the cantilever and support in some of the experimental models [5],[7], thus providing relatively higher strength which precludes the mechanical shear connector failure mode as indicated in the present analyses.

As indicated in Figure 3.43, the provision of vertical ties increases the ultimate capacity of the cantilever by 4 and 14 percent, for structures with untensioned and postensioned ties, respectively. The axial force distributions for the vertical joint at ultimate capacity of the canti-

lever are shown in Figure 3.44. The distribution is not significantly affected by the presence of vertical ties. However, when ties are postensioned the distribution follows a pattern similar to that of the structure without vertical ties at design load level (see Figure 3.36). This indicates the effectiveness of postensioning force in response to cantilever behaviour. The maximum transverse tie force requirement now occurs at the uppermost tie with values of 88 kN and 97 kN, for structures with and without ties, respectively, which are still less than the design strength (F_y = 142 kN) of the ties.

Figure 3.45 shows distributions of shear force in vertical joints at ultimate capacity of the cantilever for the structure without ties. As the load increases from the design load to the ultimate load level, shear forces in the upper connectors of joint 1 increase slightly with essentially elastic behaviour throughout. On the other hand, yielding in the vertical connectors progresses upward along vertical joint 2 until the ultimate capacity of all the connectors is reached.

Ductility demand and joint deformations at this ultimate load stage are presented in Figure 3.46 through 3.48. The following observations are noted:

"(i) Figure 3.46 indicates that vertical ties reduce ductility requirements for mechanical connectors at all levels. The maximum ductility factor is significantly reduced when postensioned ties are provided.

(ii) The computed gap openings and shear slip are considerably lowered with the introduction of vertical ties as shown in Figures 3.47 and 3.48.

The above analysis indicates that the ultimate load capacity of the cantilever is governed by the shear strength of the mechanical connectors in the vertical joint. Furthermore, the results confirm the effectiveness of postensioned vertical ties in improving the structural performance of the precast system under abnormal loads. The postensioned ties are seen to be more effective in limiting joint deformations at ultimate load level, as compared to those at design load level.

3.4 CONCLUSIONS

A 12-storey precast panel shear wall structure has been analyzed for conditions simulating progressive collapse. The influence of various joint parameters and tie reinforcement details, as well as loading conditions of this damaged state, was investigated by means of a parameter study on a

6-storey precast wall. Within the assumptions and the analytical model considered, the following conclusions were noted:

1) Tensile forces developed in transverse ties are confined within the upper six floor levels, regardless of the cantilever height. The resultant force in transverse ties is essentially constant for cantilevers deeper than one storey, whereas the effective lever arm of the internal resisting couple increases with increasing cantilever depth. However, the ratio between the effective lever arm d and the overall cantilever height H is approximately constant (d/H = 0.8). At design load level, results indicate that transverse ties which are designed according to the PCA recommendations [5] will remain elastic. Furthermore, it was observed that the rigid-cantilever analysis produces conservative design forces for transverse ties below the top four levels, as compared to those of the nonlinear analysis. Finally, the recommended minimum tie force (80 kN) by the PCA [5] was shown to be overly conservative for design purposes.

2) The ductility demand in mechanical connectors increases with increasing cantilever depth. For structures higher than 12 storeys, results indicate that the ductility demand will exceed the practical ductility limit.

3) Significant gap openings were observed in the horizontal joints of the cantilever and Wall 1. This demonstrates that vertical reinforcing is necessary across the horizontal joints to resist the vertical tensile stresses developed. In particular, the magnitude of maximum gap openings in the horizontal joints of the cantilever ranges from 0.31 to 0.89 mm for the prototype wall. On the other hand, the magnitude of maximum gap openings of Wall 1 ranges from 0.08 to 0.63 mm in the horizontal joints.

4) In the horizontal joints of the cantilever, the induced shear force exceeds the frictional resistance between the precast concrete panels and the in situ joint grout. As a result, horizontal shear slip occurs at all floor levels of the cantilever joints, with maximum values ranging from 0.07 to 0.86 mm for the prototype wall.

The results of the parameter study allow the following conclusions:

5) The nonlinear behaviour of the precast system is significantly influenced by the design shear strength of mechanical connectors. It was observed that the magnitude of nonlinear joint deformations decreases with increasing shear strength. In particular, the ductility demand of mechanical connectors can be effectively reduced by introducing connectors with higher design shear strength.

6) The coefficient of friction between the precast concrete and the grout in horizontal joints, if specified within the range 0.2 - 0.8 used in current design codes, has insignificant effect on the performance of the precast system.

7) Vertical ties reduce the magnitude of nonlinear joint deformations and ductility demand in the structure. However, postensioned vertical ties were shown to be relatively more effective.

8) The ultimate load capacity of the cantilever is governed by the shear strength of the mechanical connectors. The ultimate capacity of the cantilever can be increased by introducing vertical ties with or without postensioning.

The present study examined the static behaviour of precast panel shear walls for conditions simulating progressive collapse. The latter was simulated by assuming the panel failure to take place quasi-statically within the structure. However, for design purposes it is important to examine the dynamic behaviour of precast systems under the effects of abnormal loads, in order to assess the validity of the preceding conclusions. The influence of the dynamic effects on the performance of precast panel walls are therefore examined in the following Chapter.

TABLE 3.1 SUMMARY OF RESULTANT FORCE AND EFFECTIVE LEVER ARM FOR 12 STOREY PROTOTYPE WALL - NONLINEAR STATIC BEHAVIOUR

CANTILEVER HEIGHT IN NO. OF STOREYS, H	RESULTANT FORCE, T_R OR C_R (kN)	EFFECTIVE LEVER ARM IN NO. OF STORIES, d	d/H
1	115.6	1.00	1.00
3	143.9	2.35	0.78
5	149.5	3.87	0.77
7	147.0	5.58	0.80
9	145.3	7.23	0.80
11	142.4	8.87	0.81

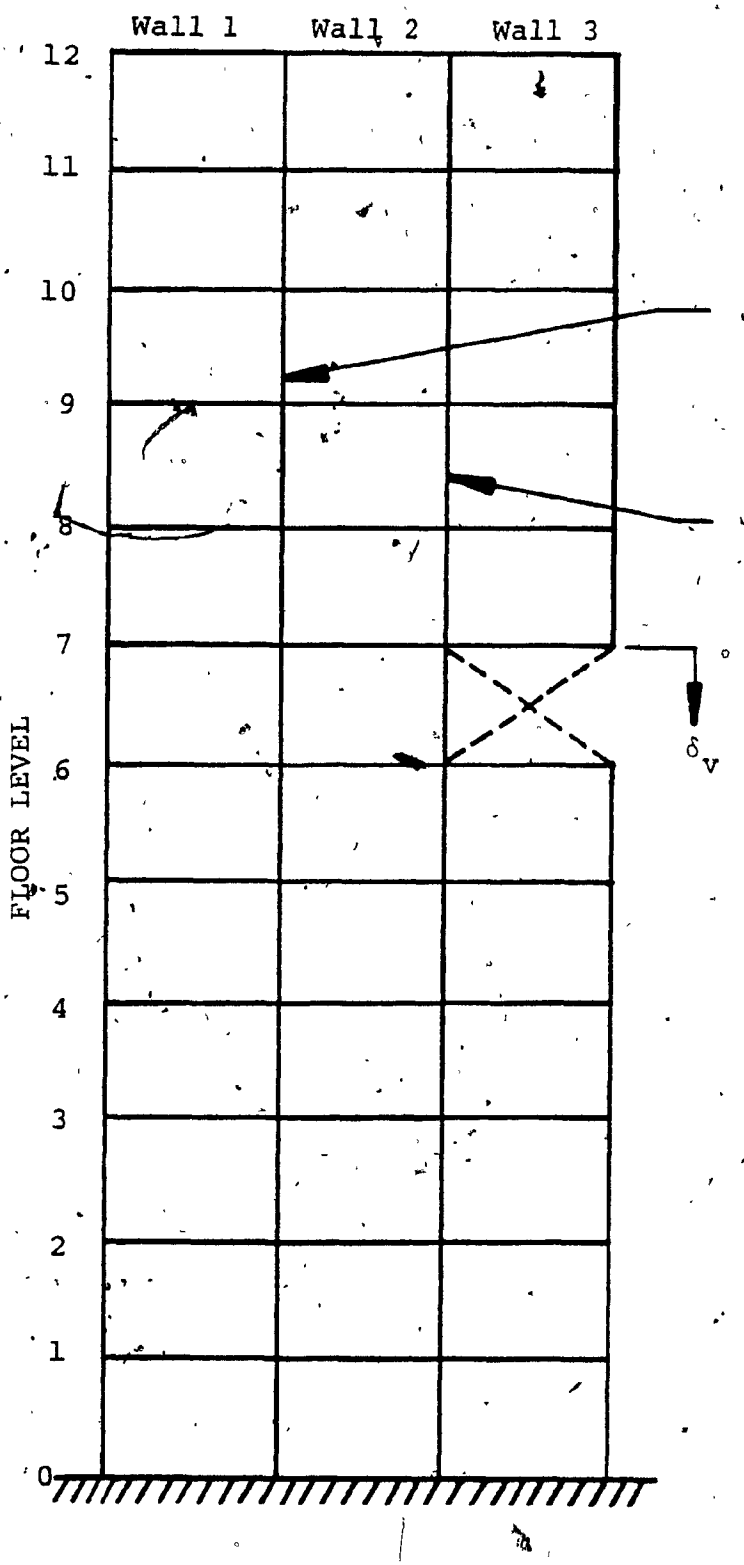

FIG. 3.1 TYPICAL DAMAGED CONFIGURATION OF 12-STOREY PROTOTYPE WALL

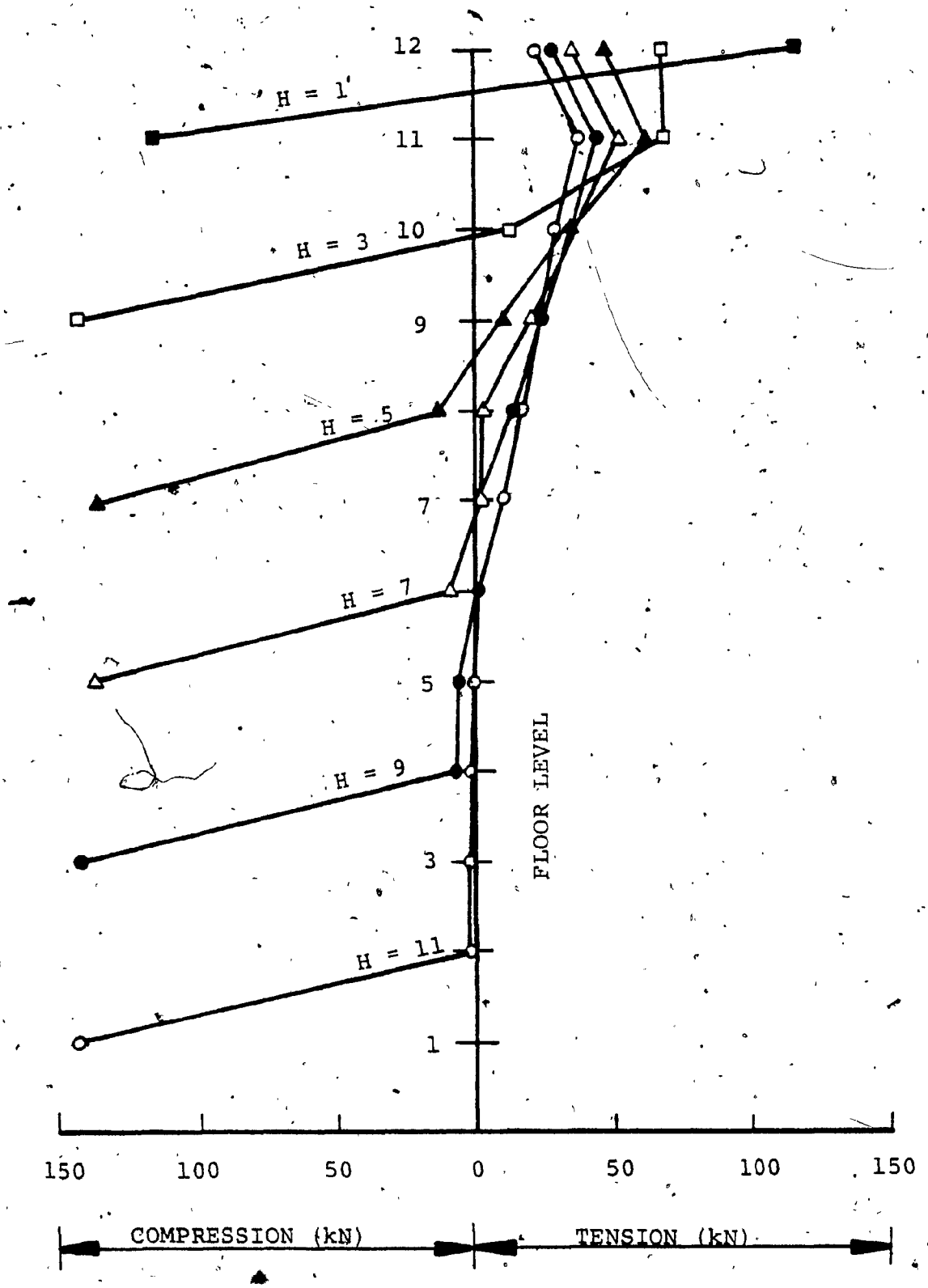

FIG. 3.2 AXIAL FORCE DISTRIBUTION IN VERTICAL JOINT FOR VARIOUS CANTILEVER DEPTHS - INELASTIC BEHAVIOUR
(H = NUMBER OF STOREYS IN CANTILEVER)

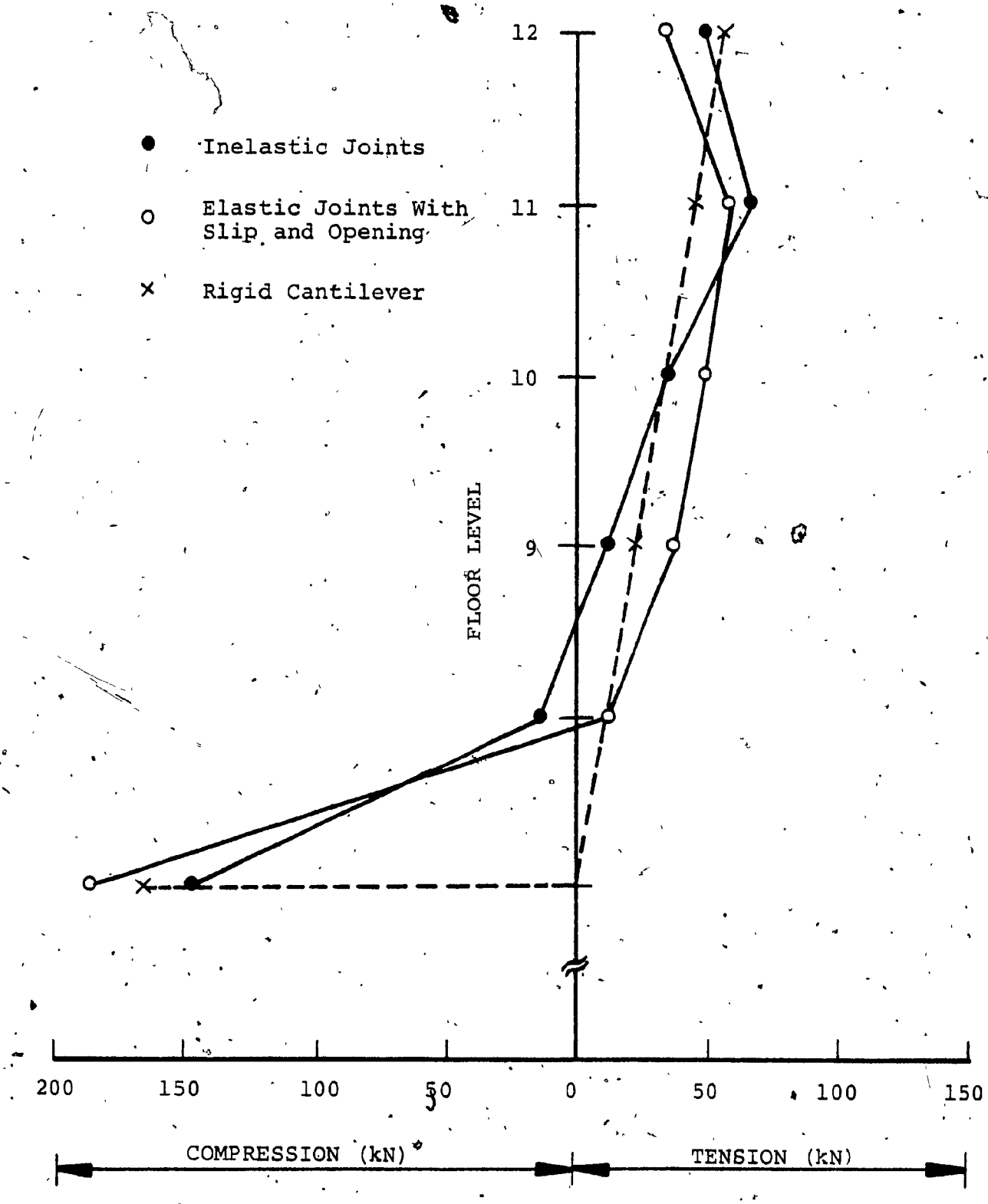

FIG. 3.3 AXIAL FORCE DISTRIBUTION IN VERTICAL JOINT FOR ELASTIC, INELASTIC AND RIGID CANTILEVER BEHAVIOUR - 5 STOREY CANTILEVER

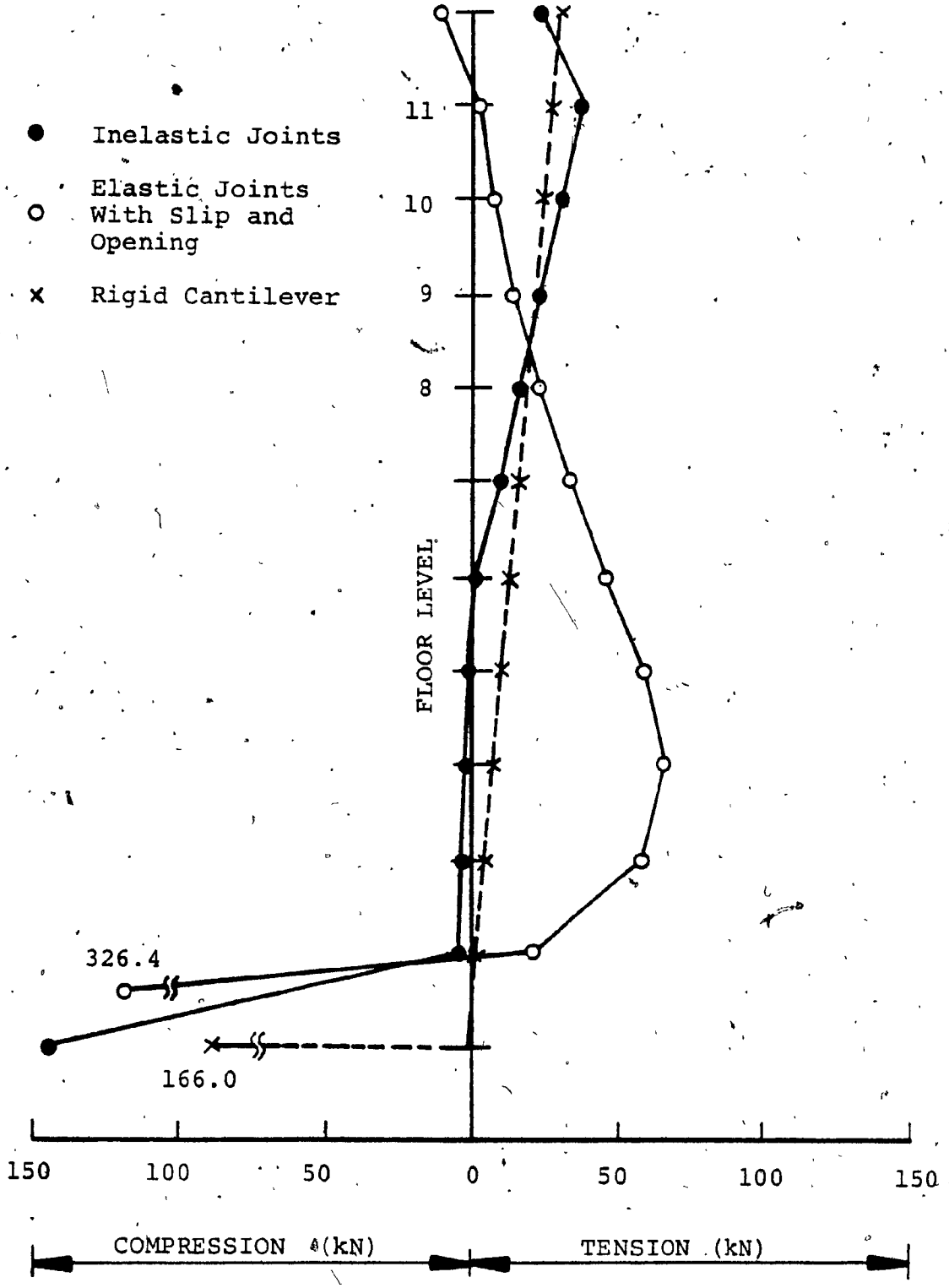

FIG. 3.4 AXIAL FORCE DISTRIBUTION IN VERTICAL JOINT FOR ELASTIC, INELASTIC AND RIGID CANTILEVER BEHAVIOUR - 11 STOREY CANTILEVER

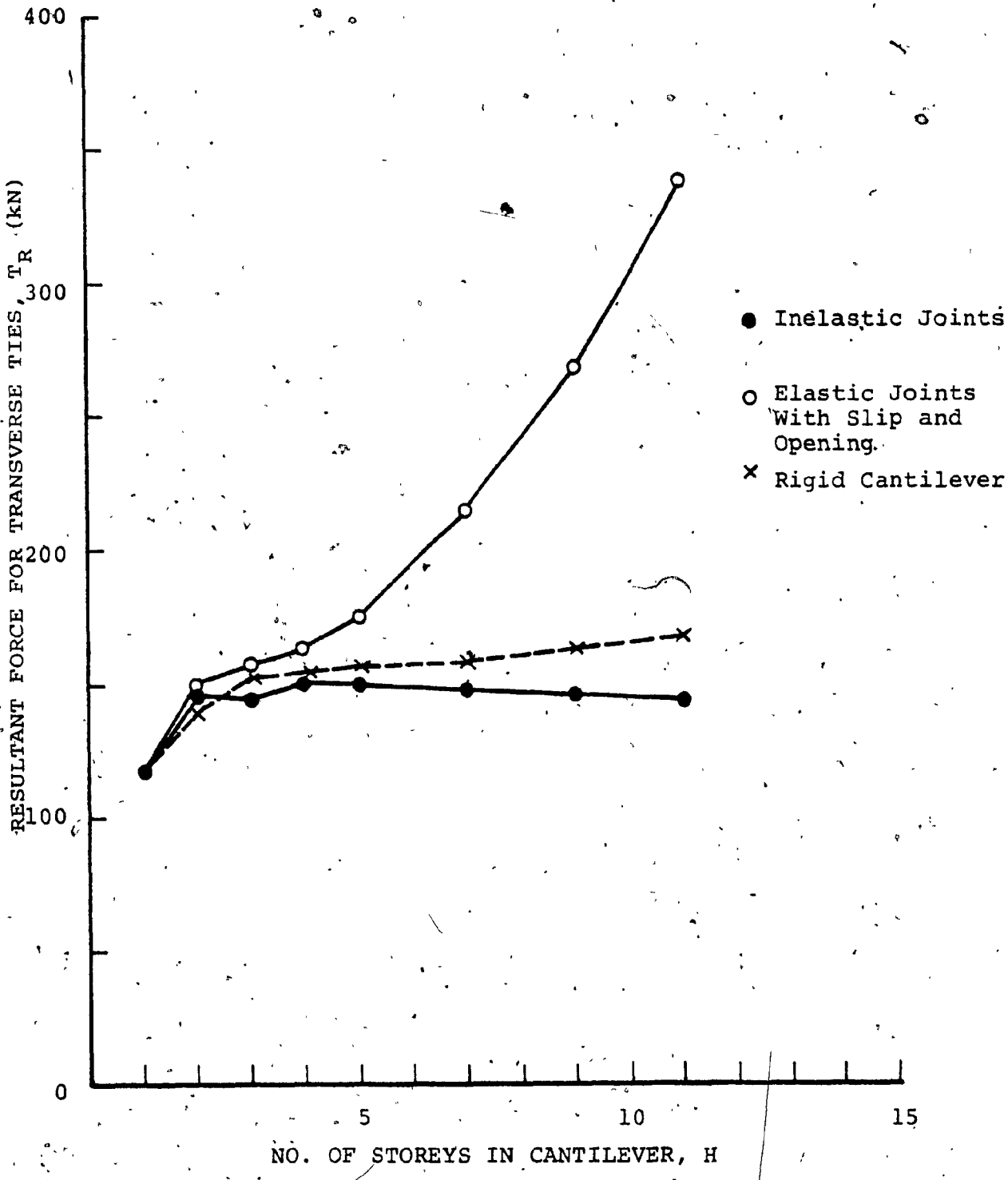

FIG. 3.5 VARIATION IN RESULTANT FORCE OF TRANSVERSE TIES WITH CANTILEVER DEPTH FOR ELASTIC, INELASTIC AND RIGID CANTILEVER BEHAVIOUR

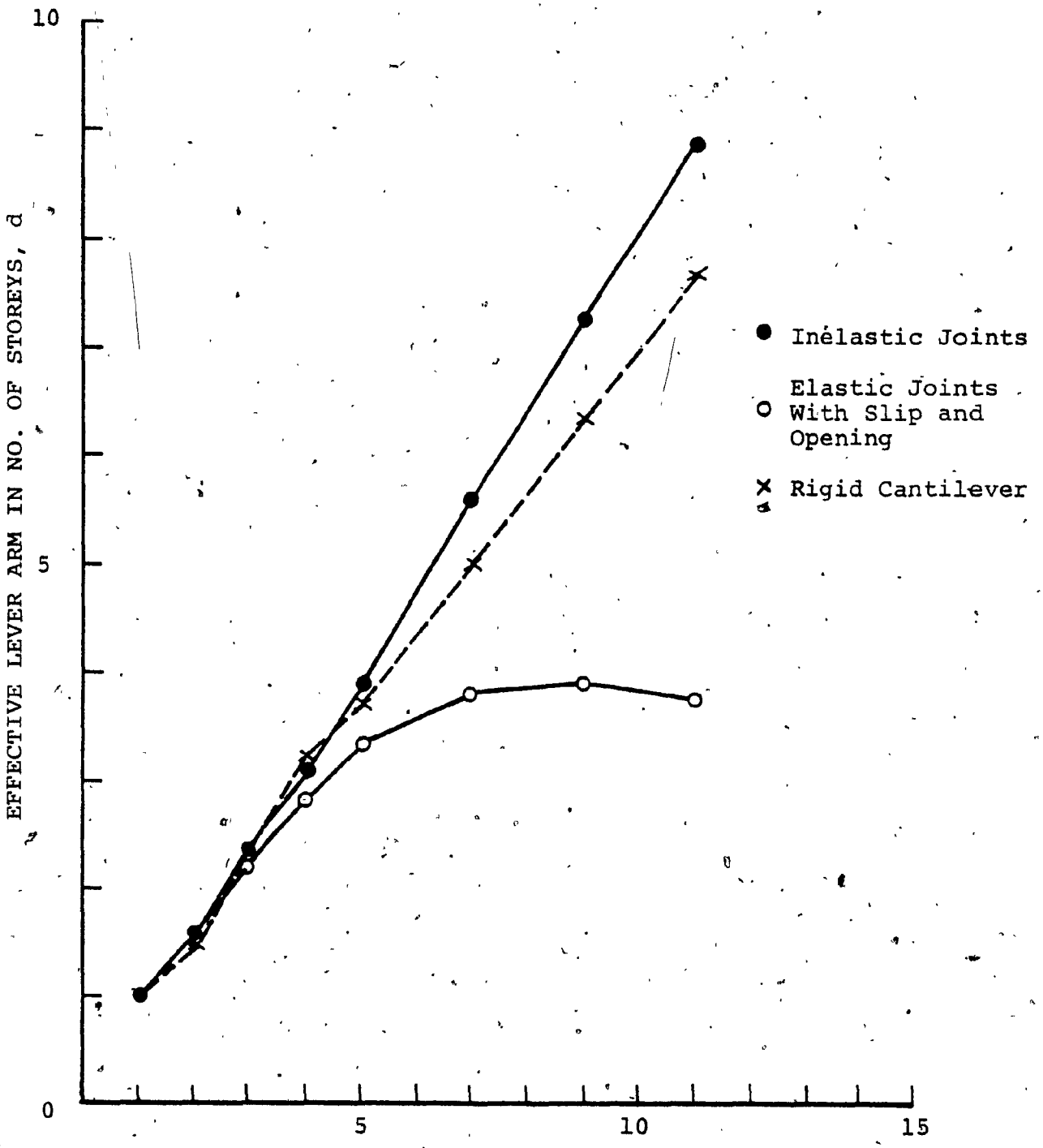

FIG. 3.6 VARIATION IN EFFECTIVE LEVER ARM WITH CANTILEVER DEPTH FOR ELASTIC, INELASTIC AND RIGID CANTILEVER BEHAVIOUR

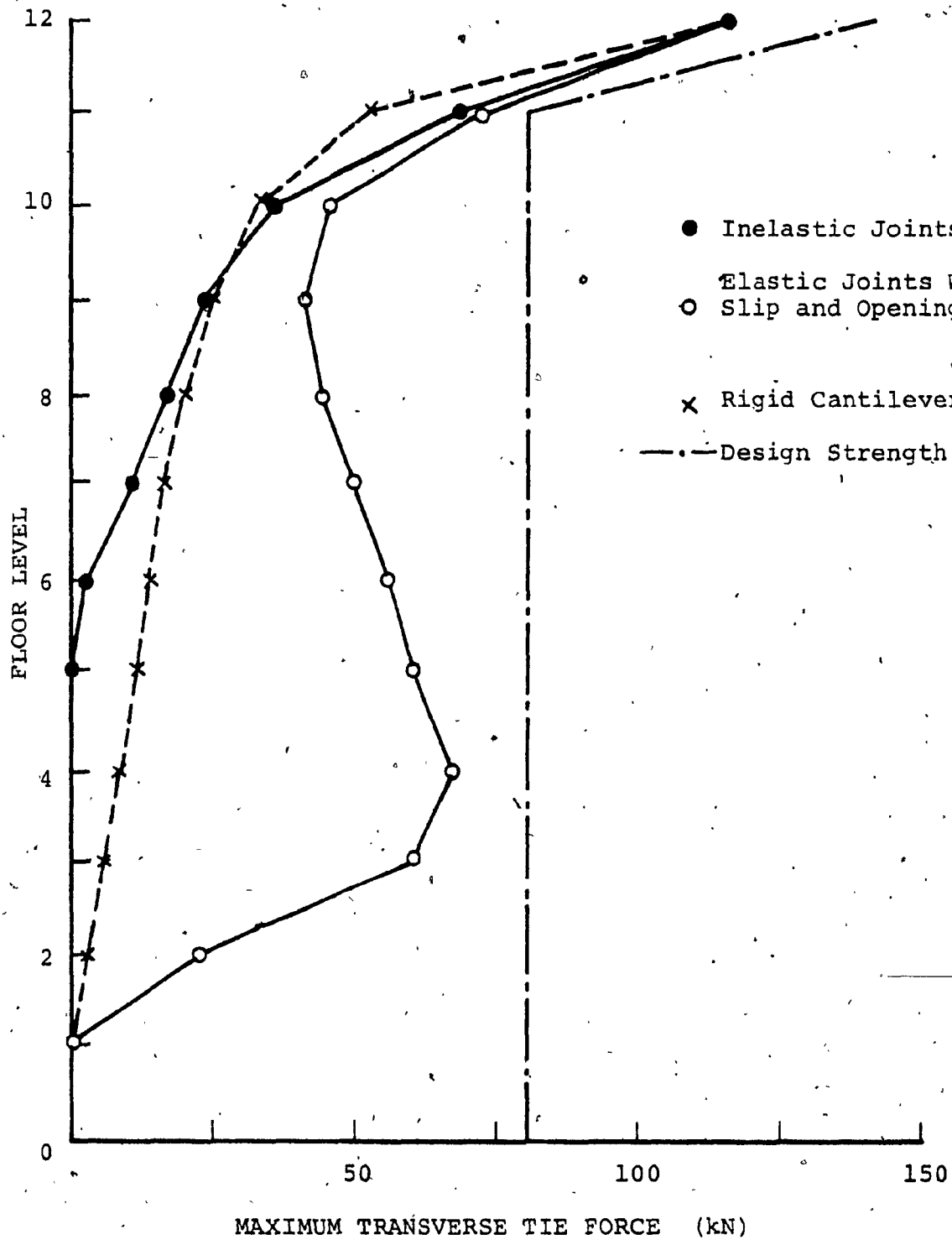

FIG. 3.7 ENVELOPES OF MAXIMUM FORCE IN TRANSVERSE TIES OF 12 STOREY PROTOTYPE WALL FOR ELASTIC, INELASTIC AND RIGID CANTILEVER BEHAVIOUR

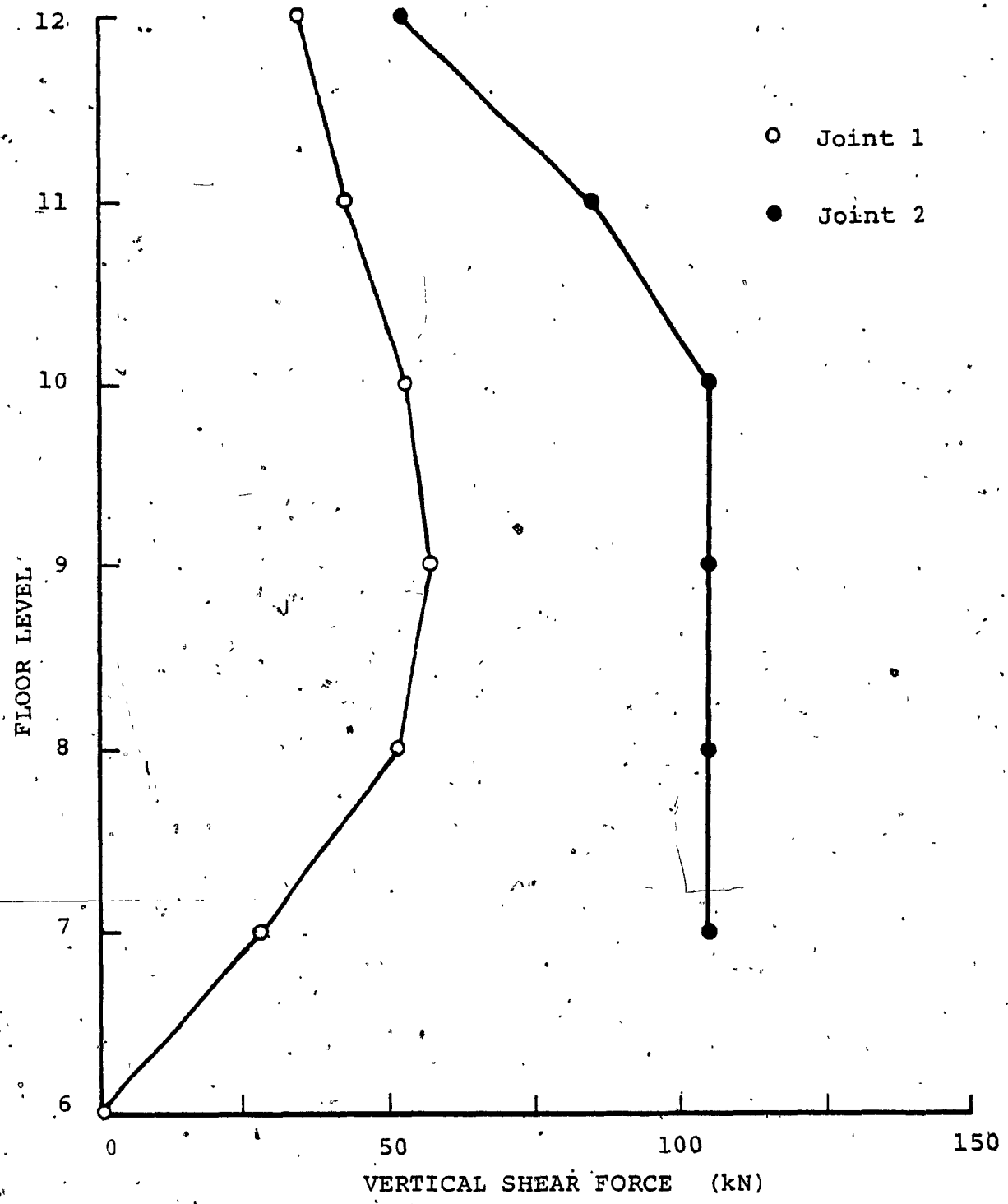

FIG. 3.8 SHEAR FORCE DISTRIBUTION IN VERTICAL JOINTS 1 AND 2 FOR INELASTIC BEHAVIOUR - 5 STOREY CANTILEVER

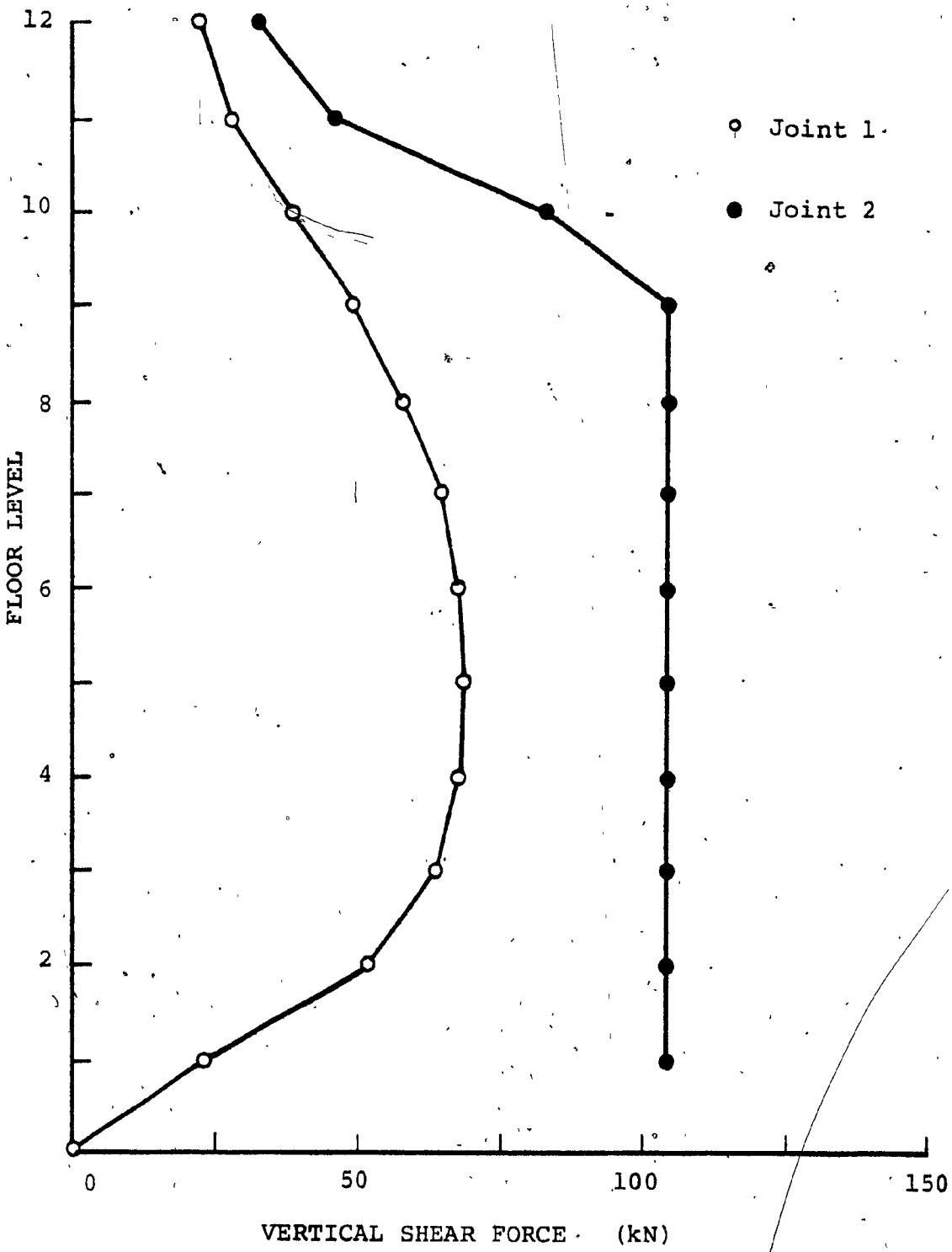

FIG. 3.9 SHEAR FORCE DISTRIBUTION IN VERTICAL JOINTS 1 AND 2 FOR INELASTIC BEHAVIOUR - 11 STOREY CANTILEVER

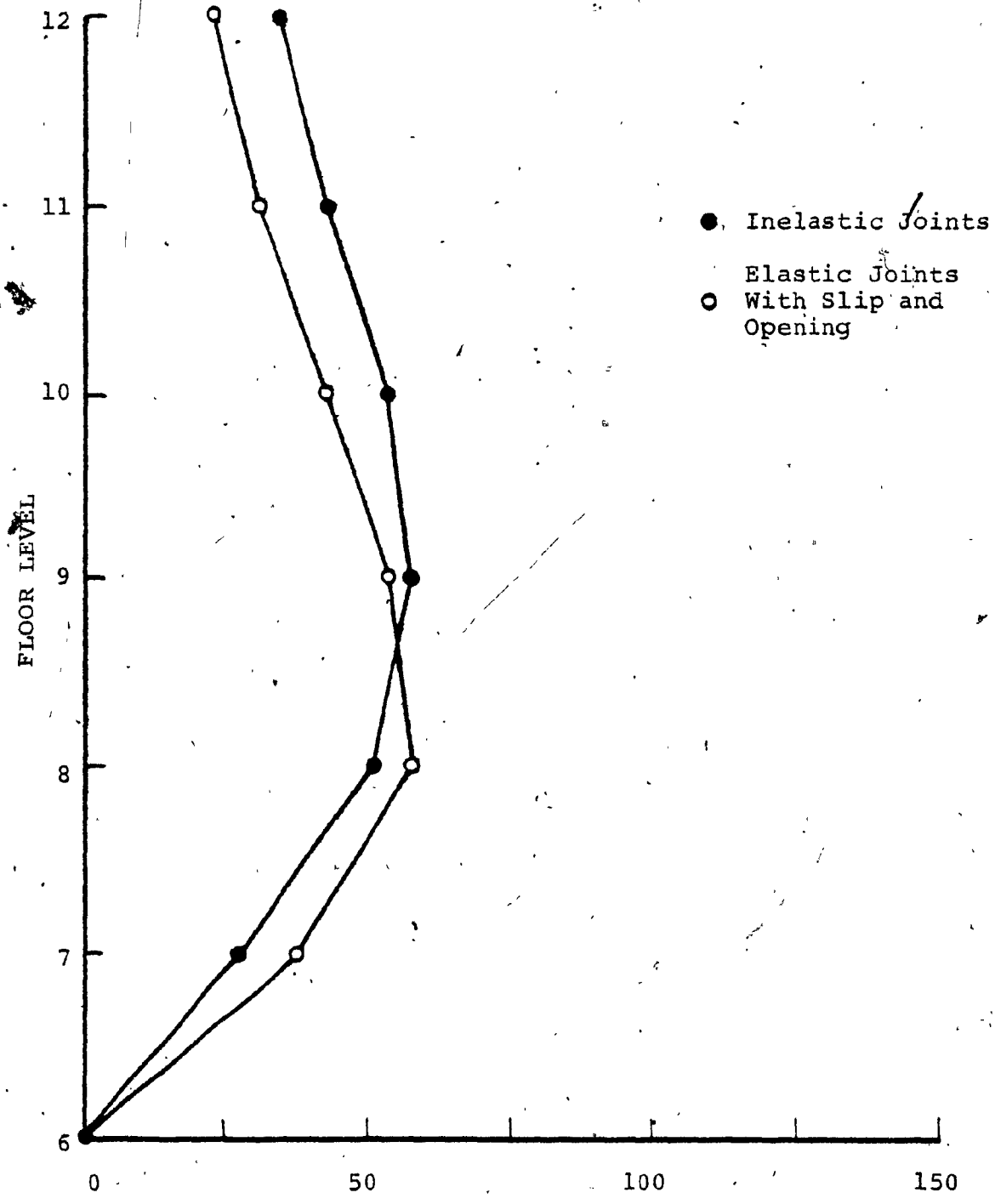

(a)

FIG.3.10 SHEAR FORCE DISTRIBUTION IN VERTICAL JOINTS 1 AND 2 OF 5 STOREY CANTILEVER FOR ELASTIC, INELASTIC AND RIGID CANTILEVER BEHAVIOUR: (a) JOINT 1; (b) JOINT 2

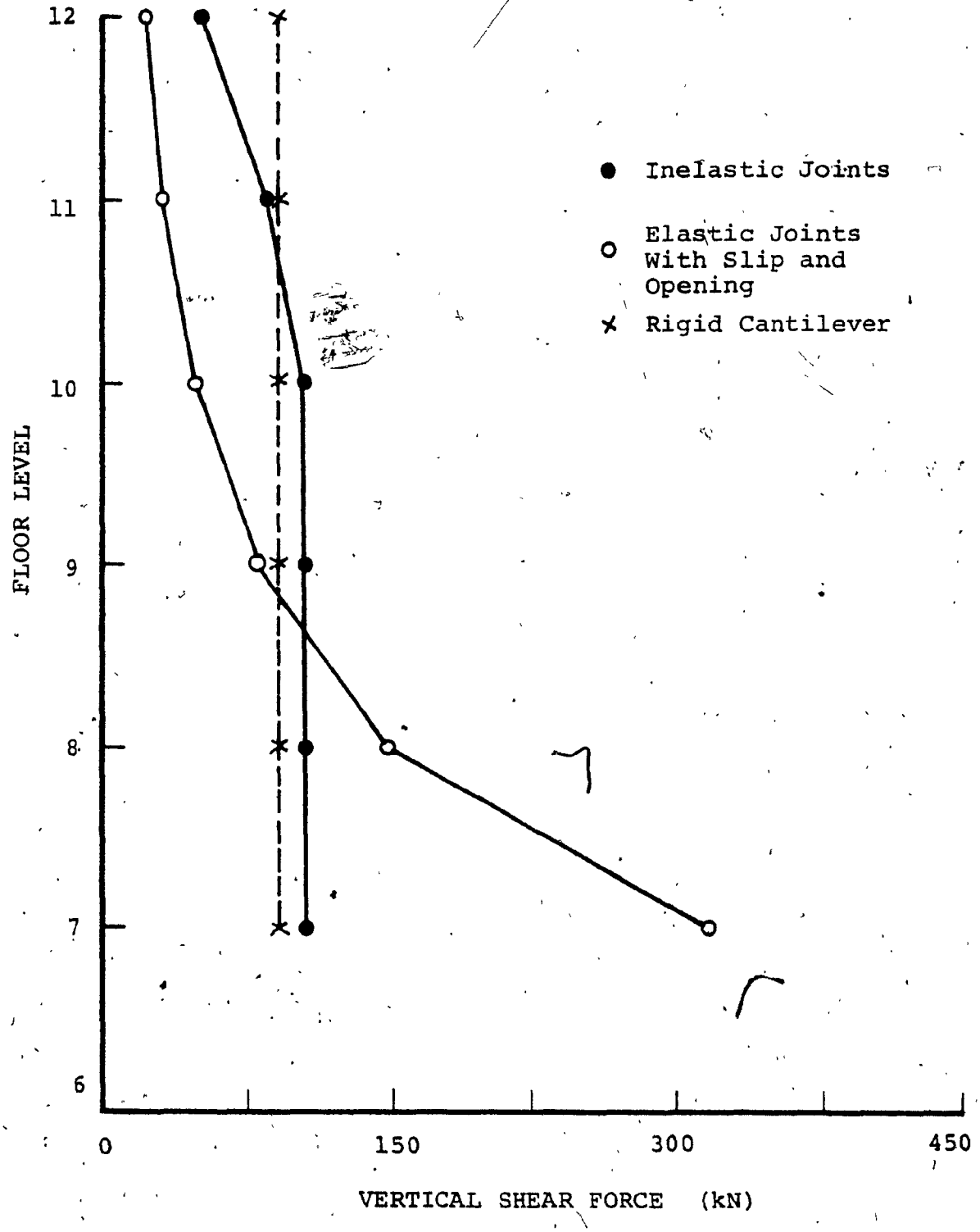
12
11
10
9
8
7
6
FLOOR LEVEL
0
150
300
450
VERTICAL SHEAR FORCE (kN)
Inelastic Joints
Elastic Joints With Slip and Opening
Rigid Cantilever

(b)

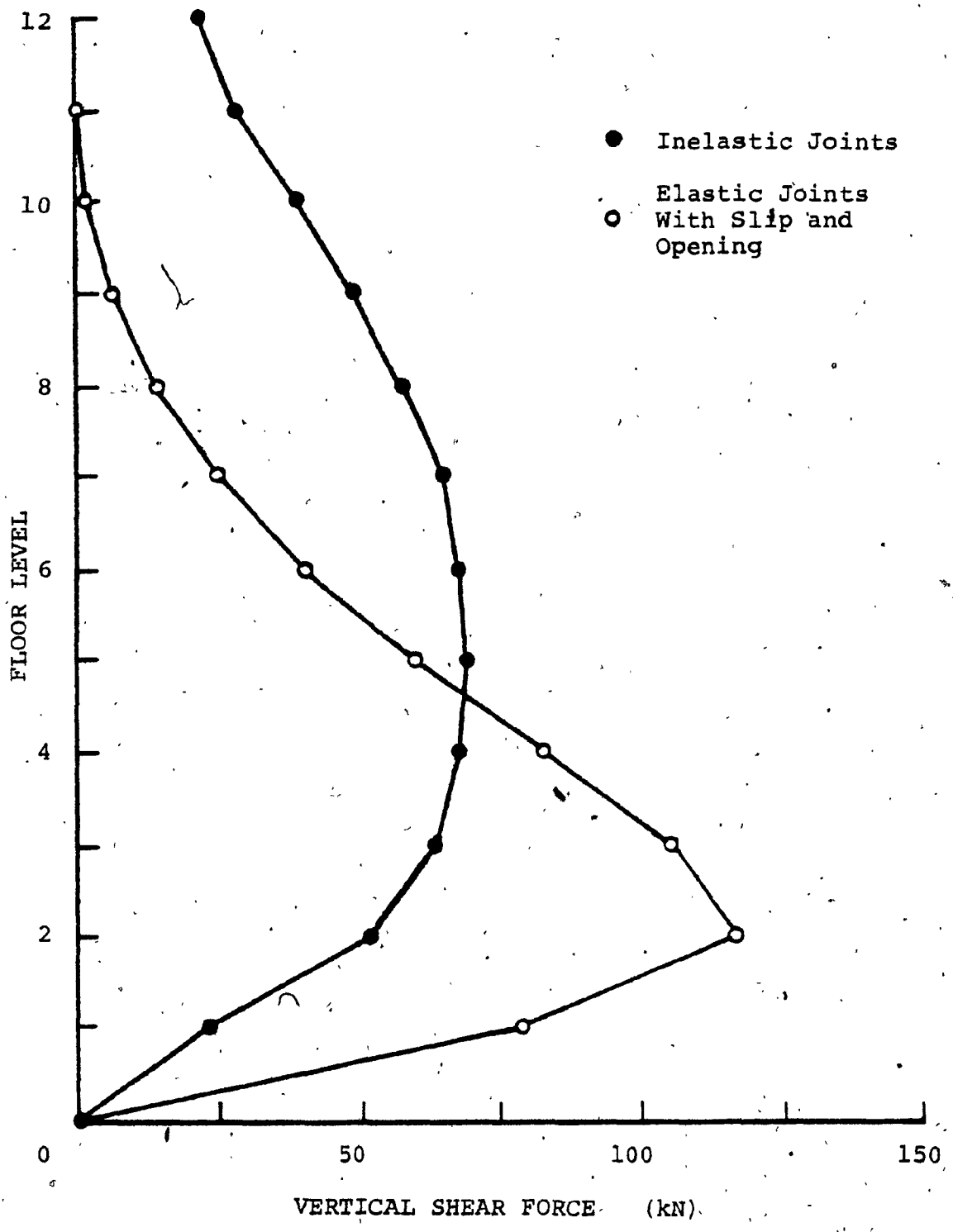

(a)

FIG. 3.11 SHEAR FORCE DISTRIBUTION IN VERTICAL JOINTS 1 AND 2 OF 11 STOREY CANTILEVER FOR ELASTIC, INELASTIC AND RIGID CANTILEVER BEHAVIOUR: (a) JOINT 1; (b) JOINT 2

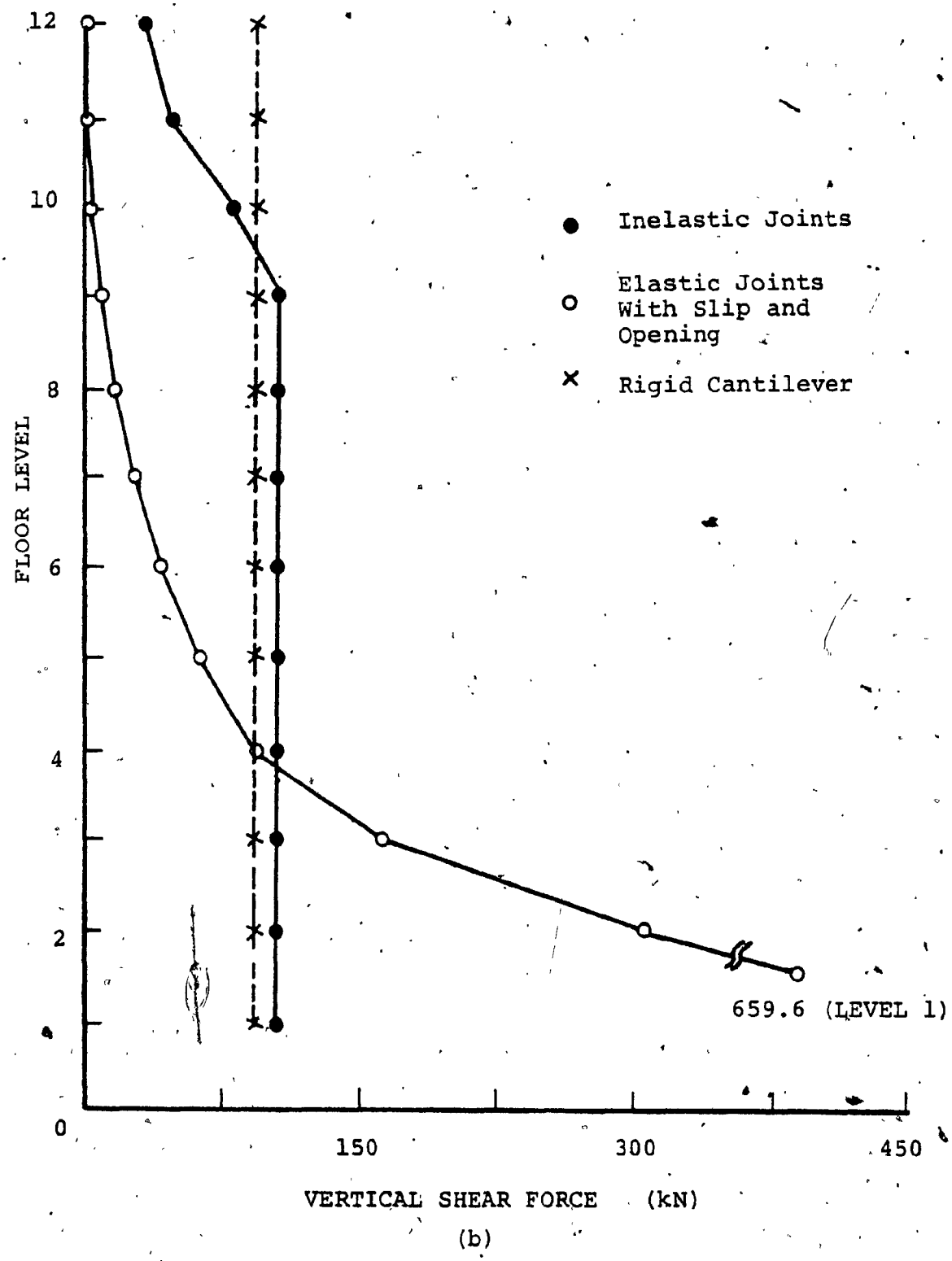
12
10
8
6
4
2
0
FLOOR LEVEL
Inelastic Joints
Elastic Joints With Slip and Opening
Rigid Cantilever
659.6 (LEVEL 1)
150
300
450
VERTICAL SHEAR FORCE (kN)

(b)

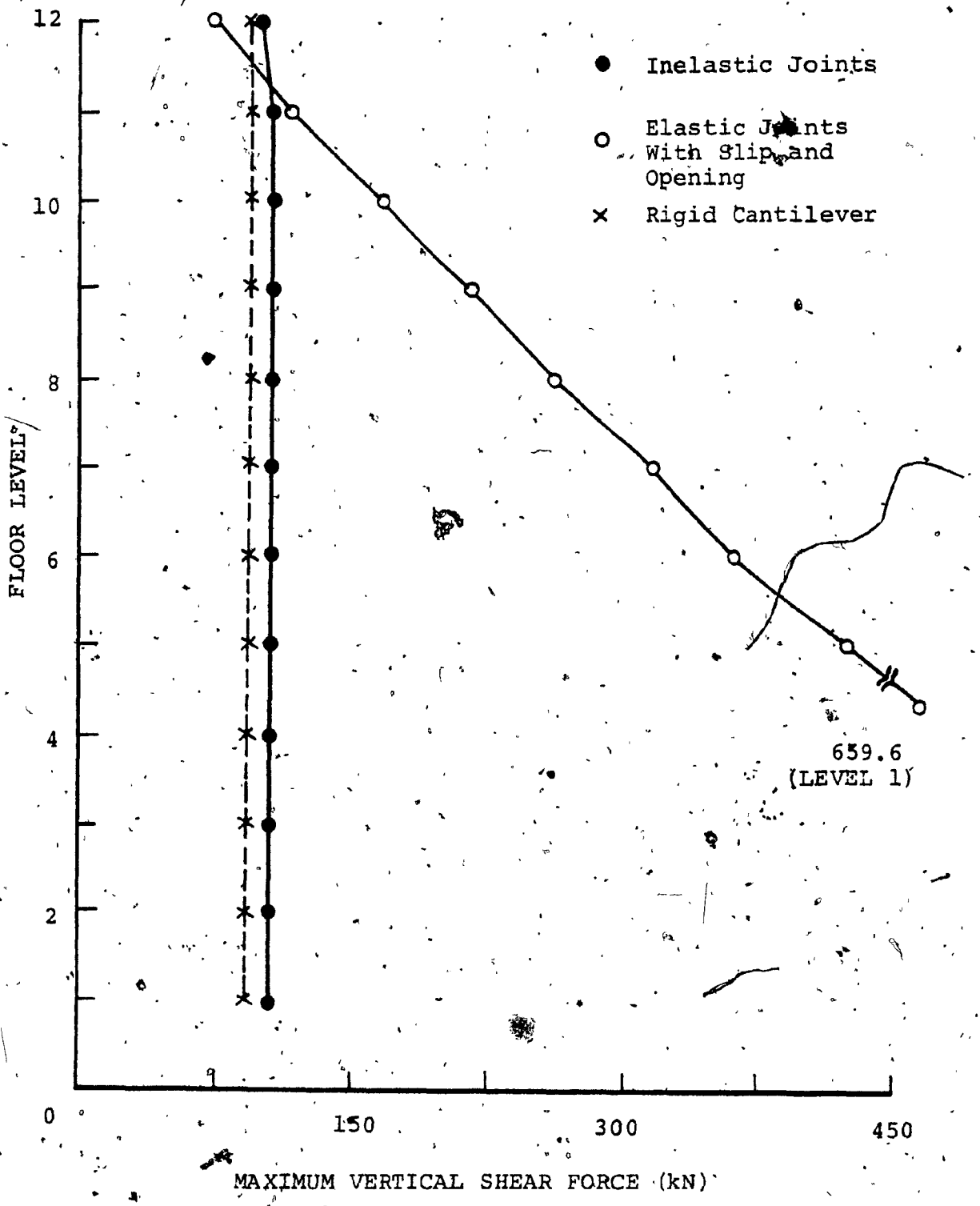

FIG. 3.12 ENVELOPES OF MAXIMUM SHEAR FORCE IN VERTICAL JOINT OF 12 STOREY PROTOTYPE WALL FOR ELASTIC, INELASTIC AND RIGID CANTILEVER BEHAVIOUR

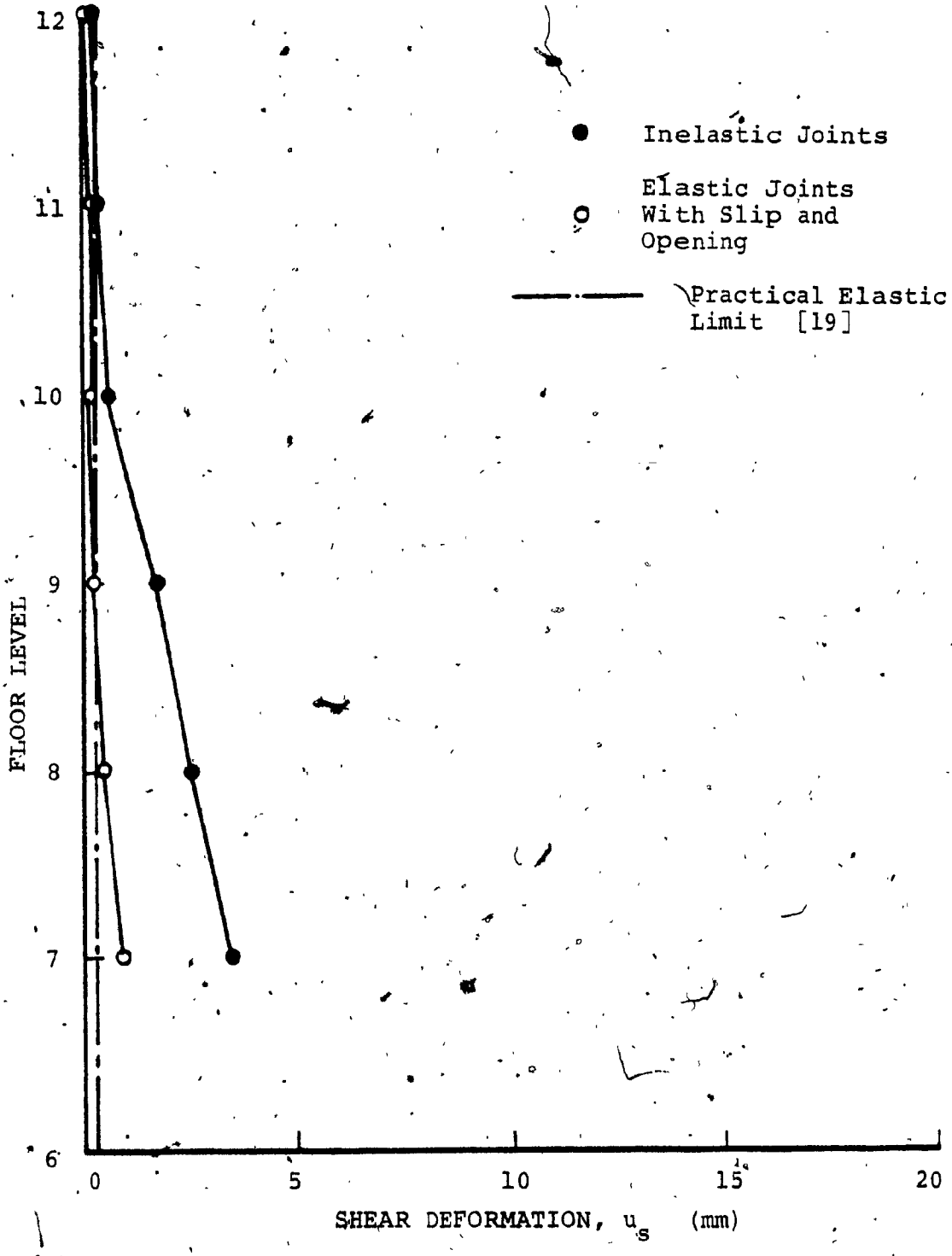

FIG. 3.13 DISTRIBUTION OF SHEAR DEFORMATION IN VERTICAL MECHANICAL CONNECTORS OF JOINT 2 FOR ELASTIC AND INELASTIC BEHAVIOUR - 5 STOREY CANTILEVER

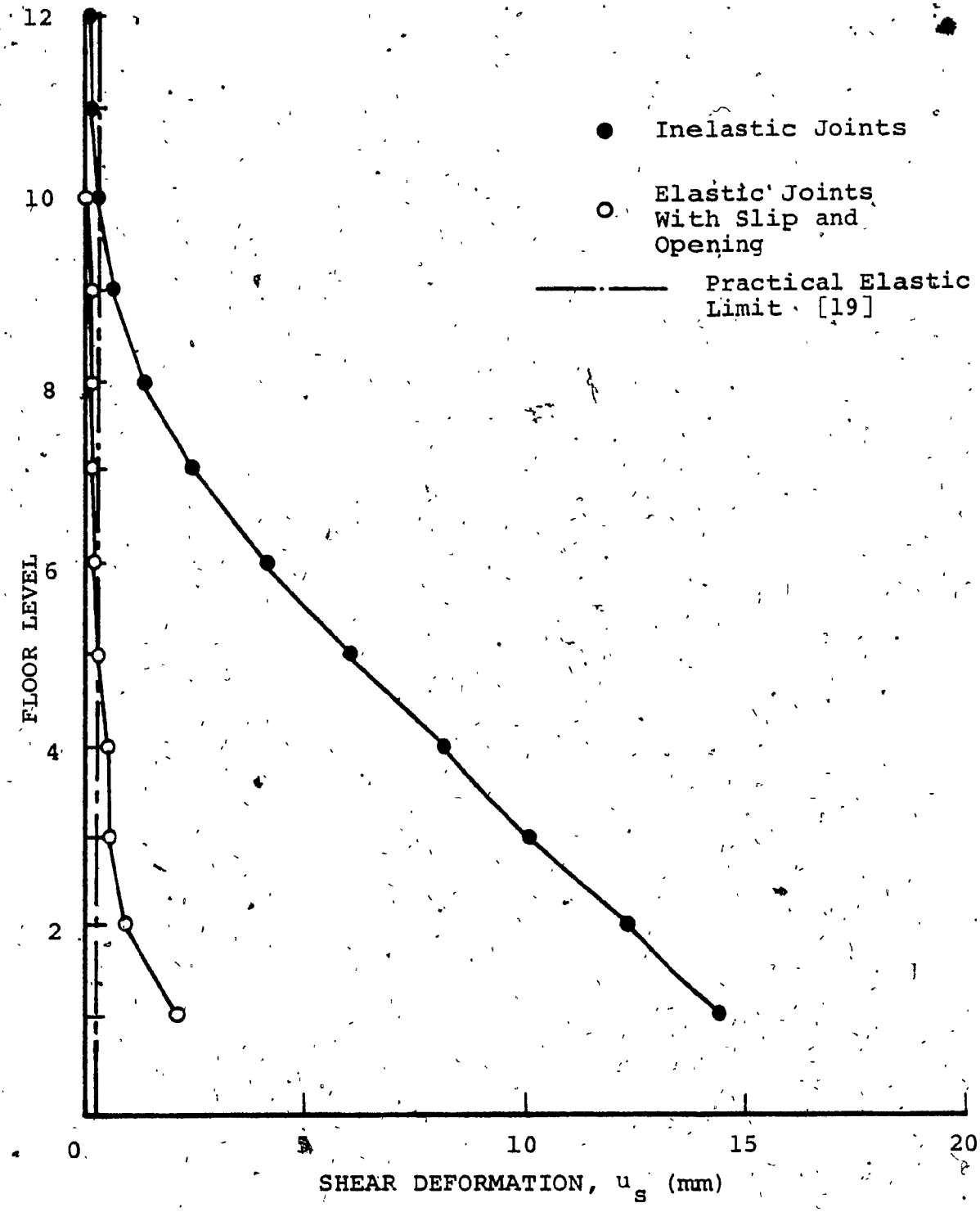

FIG. 3.14 DISTRIBUTION OF SHEAR DEFORMATION IN VERTICAL MECHANICAL CONNECTORS OF JOINT 2 FOR ELASTIC AND INELASTIC BEHAVIOUR - 11 STOREY CANTILEVER

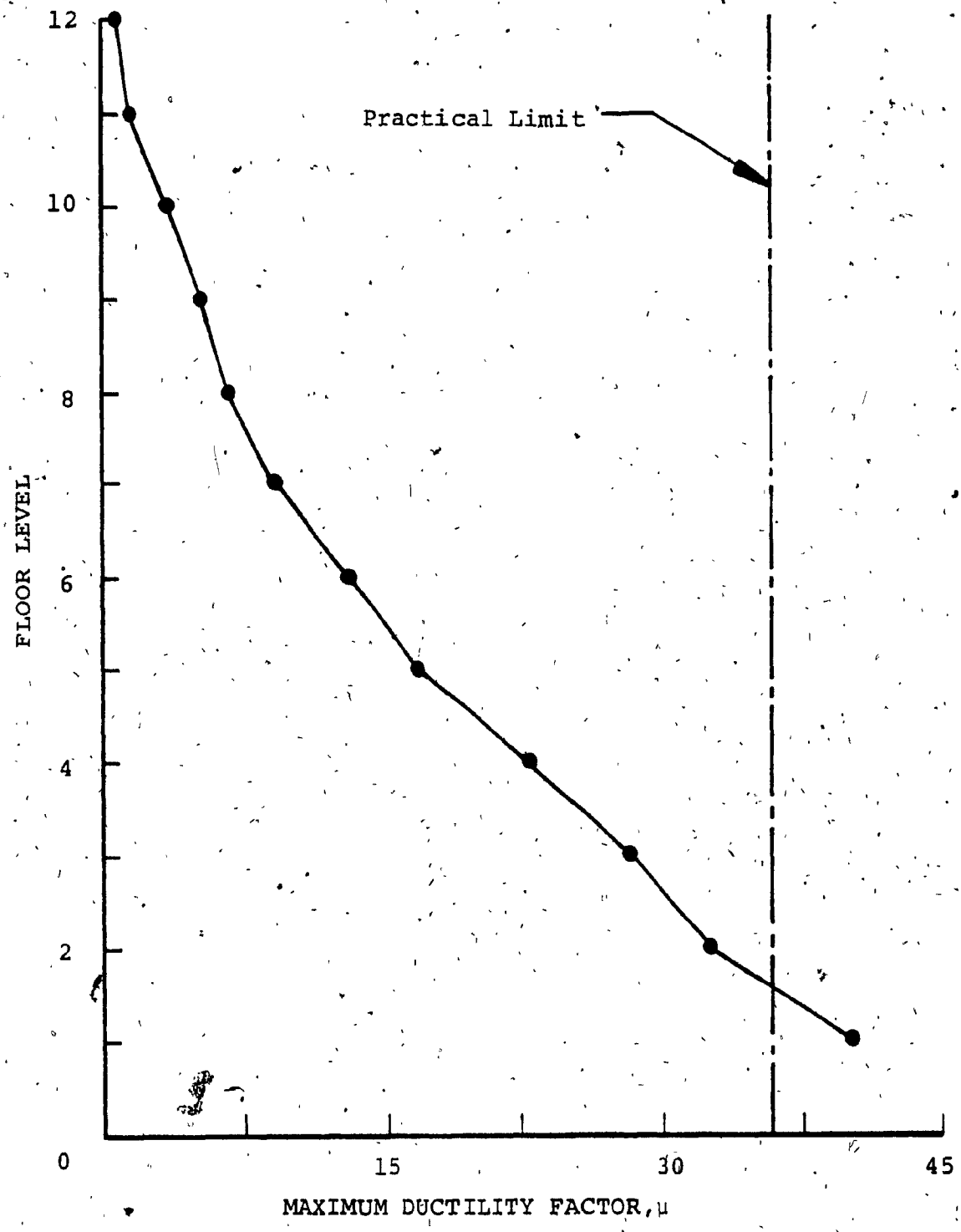

FIG. 3.15 ENVELOPE OF MAXIMUM DUCTILITY DEMAND IN VERTICAL MECHANICAL CONNECTORS OF 12 STOREY PROTOTYPE WALL FOR INELASTIC BEHAVIOUR

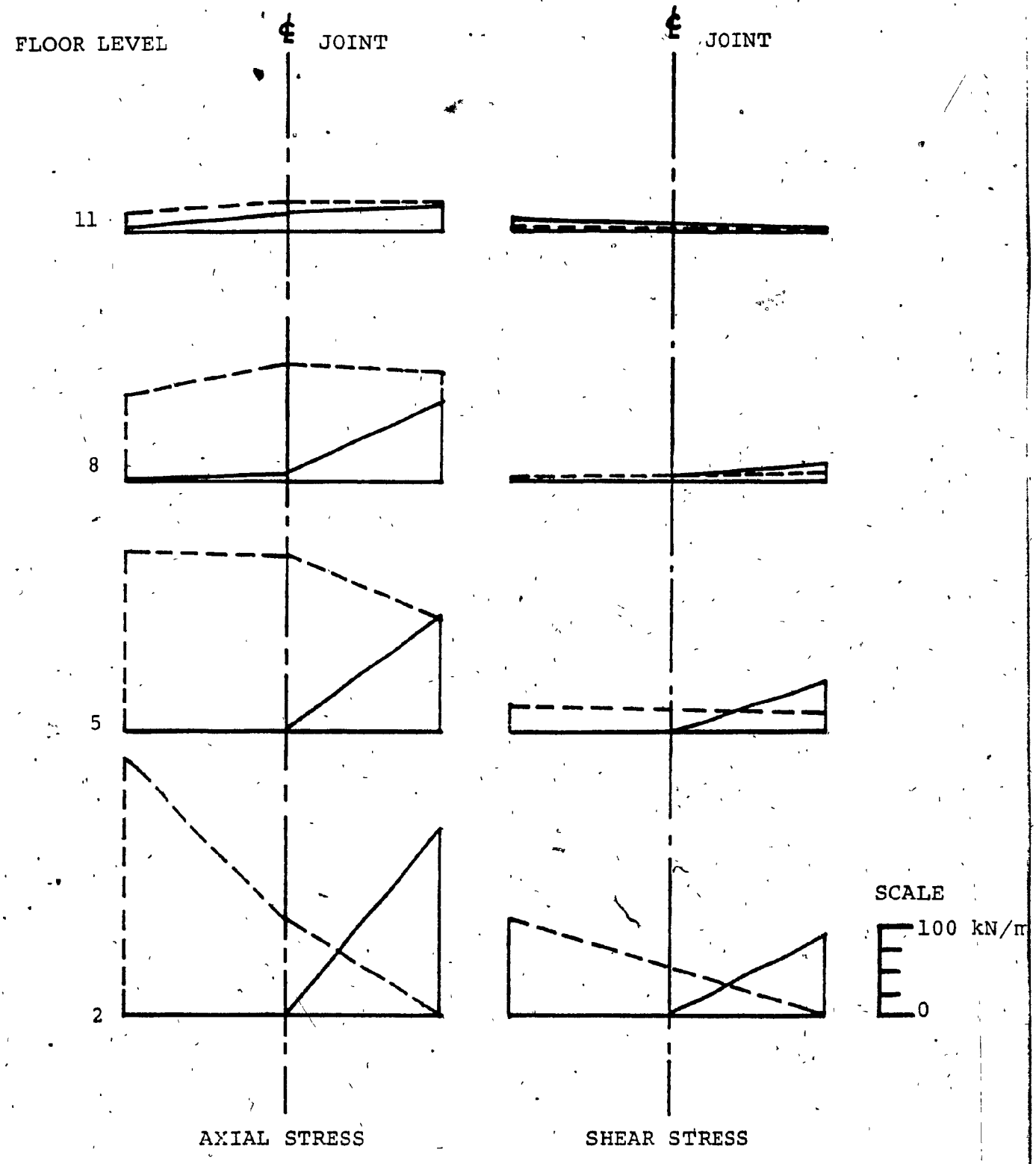

FIG. 3.16 VARIATION OF AXIAL AND SHEAR STRESS ACROSS HORIZONTAL JOINTS AT VARIOUS FLOOR LEVELS OF 11 STOREY CANTILEVER FOR ELASTIC AND INELASTIC BEHAVIOUR
(—INELASTIC JOINTS; ---ELASTIC JOINTS)

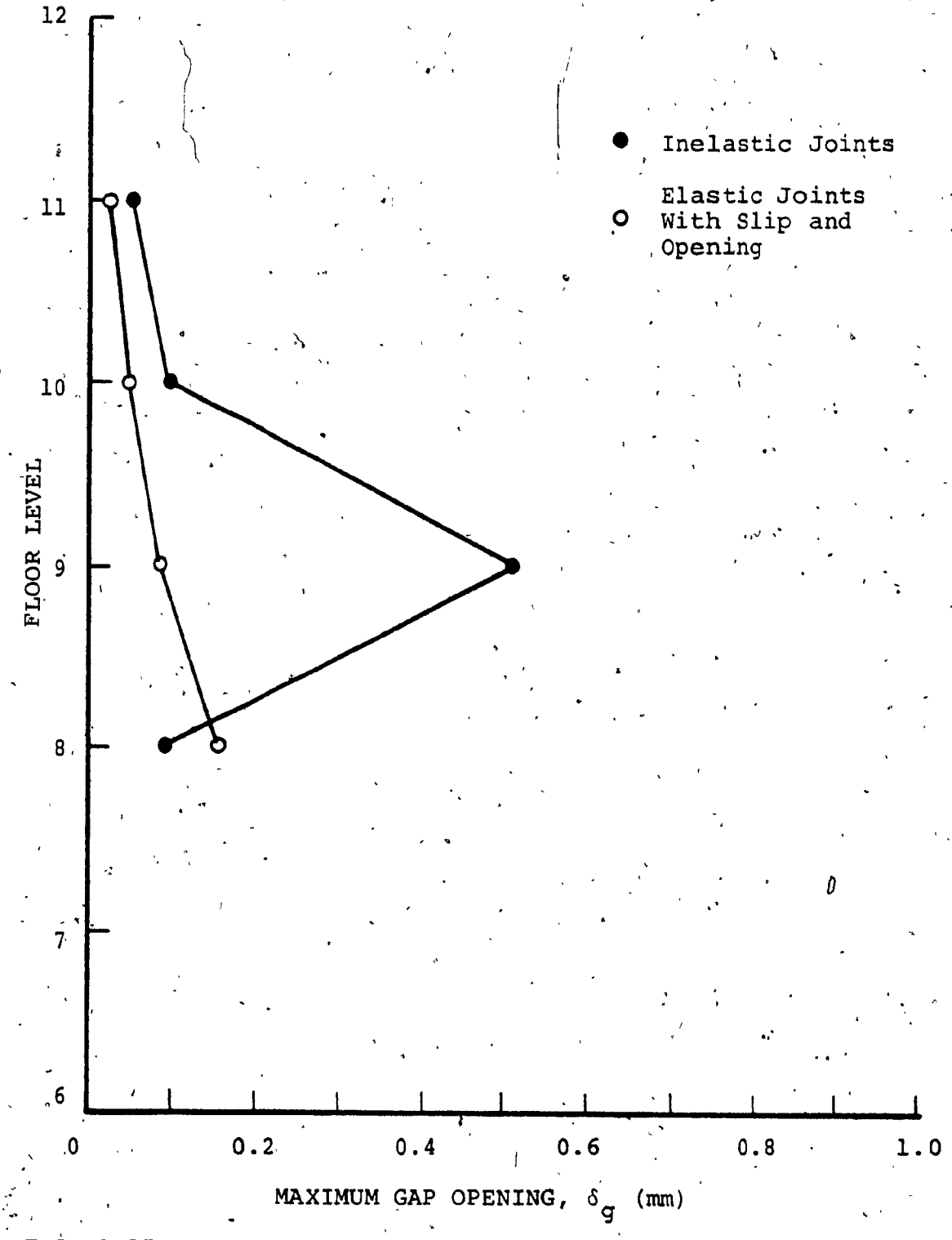

FIG. 3.17 DISTRIBUTION OF MAXIMUM GAP OPENING IN HORIZONTAL JOINTS OF CANTILEVER FOR ELASTIC AND INELASTIC BEHAVIOUR - 5 STOREY CANTILEVER

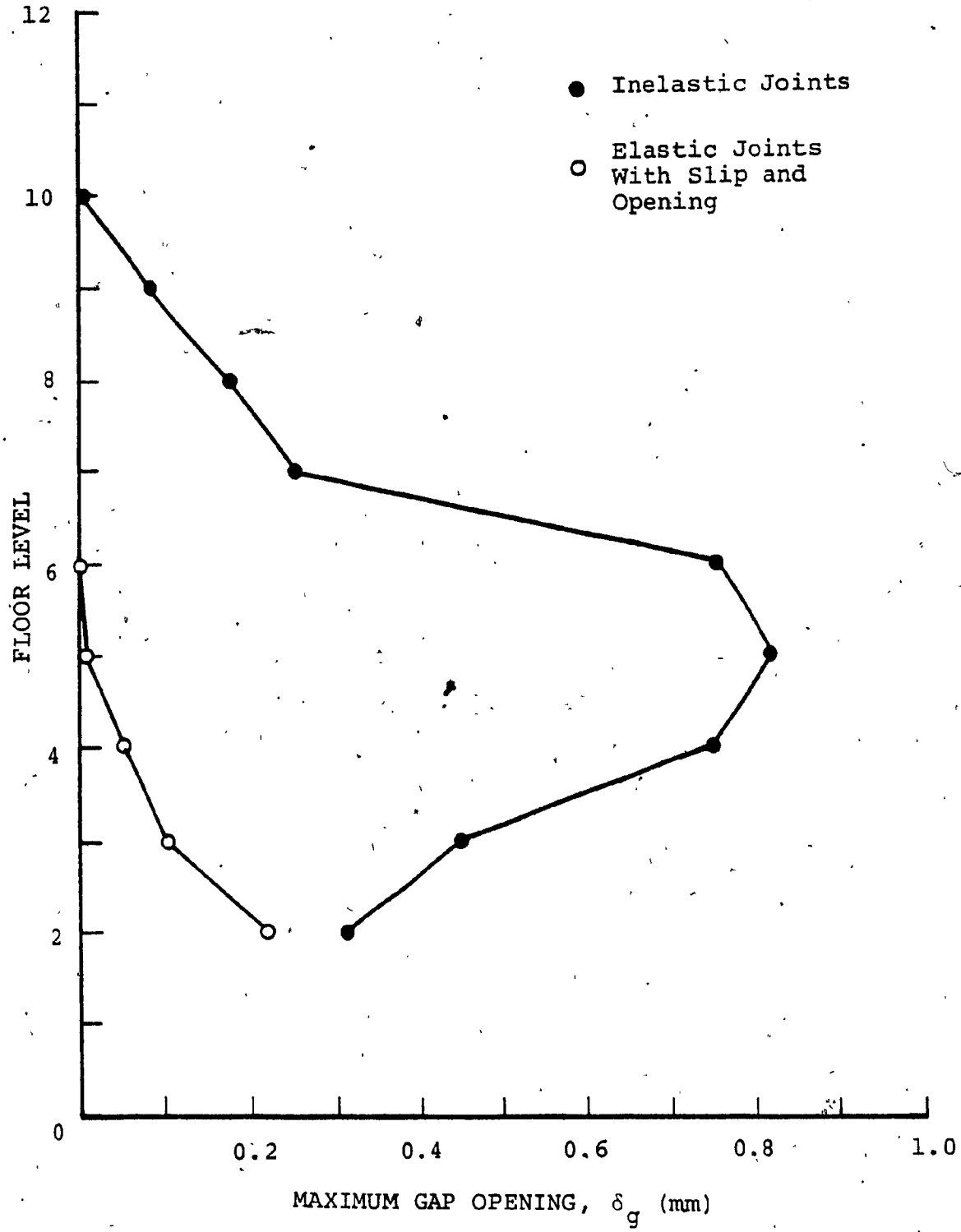

FIG. 3.18 DISTRIBUTION OF MAXIMUM GAP OPENING IN HORIZONTAL JOINTS OF CANTILEVER FOR ELASTIC AND INELASTIC BEHAVIOUR - 11 STOREY CANTILEVER

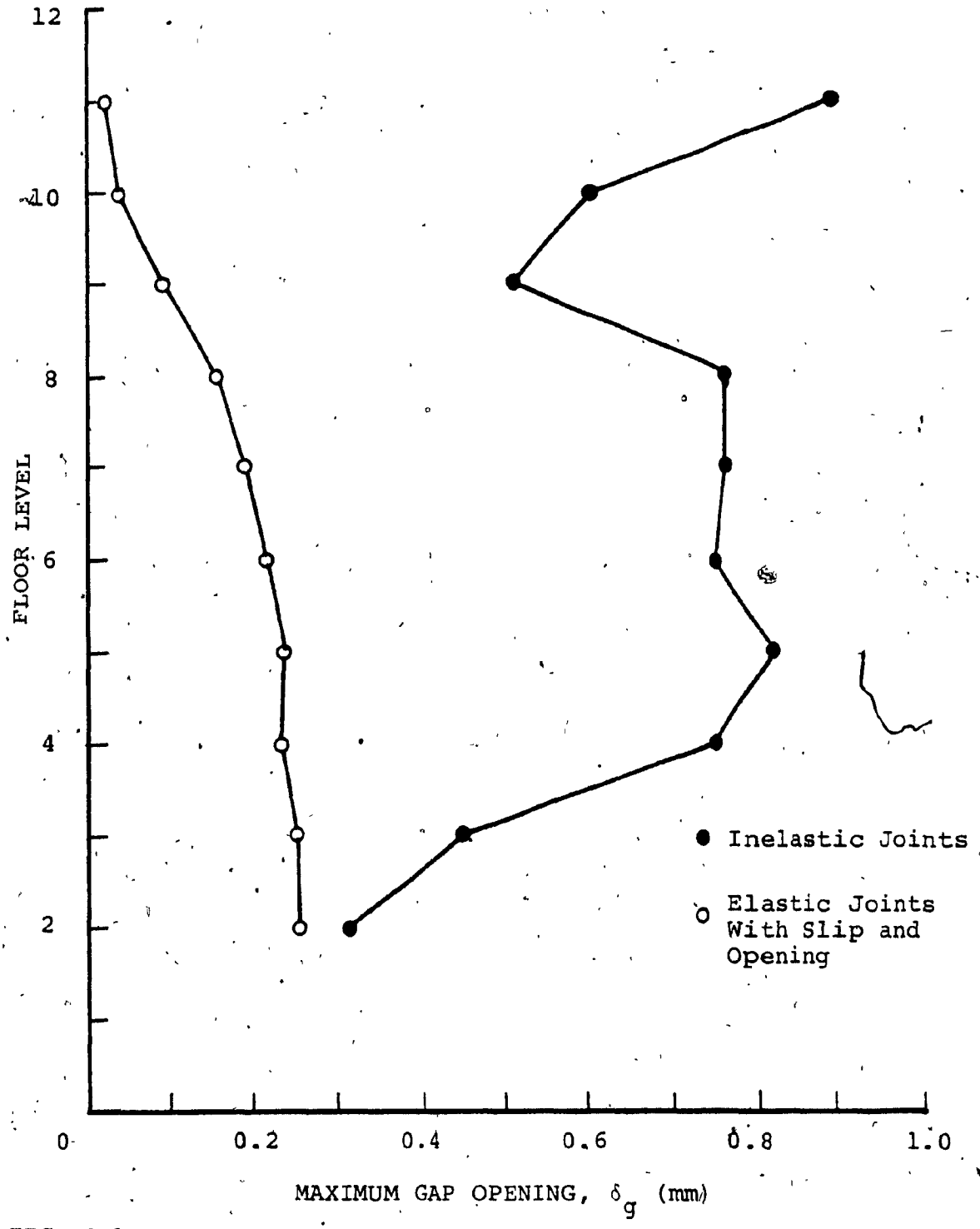

FIG. 3.19 ENVELOPES OF MAXIMUM GAP OPENING IN HORIZONTAL JOINTS OF CANTILEVER FOR ELASTIC AND INELASTIC BEHAVIOUR - 12 STOREY PROTOTYPE WALL

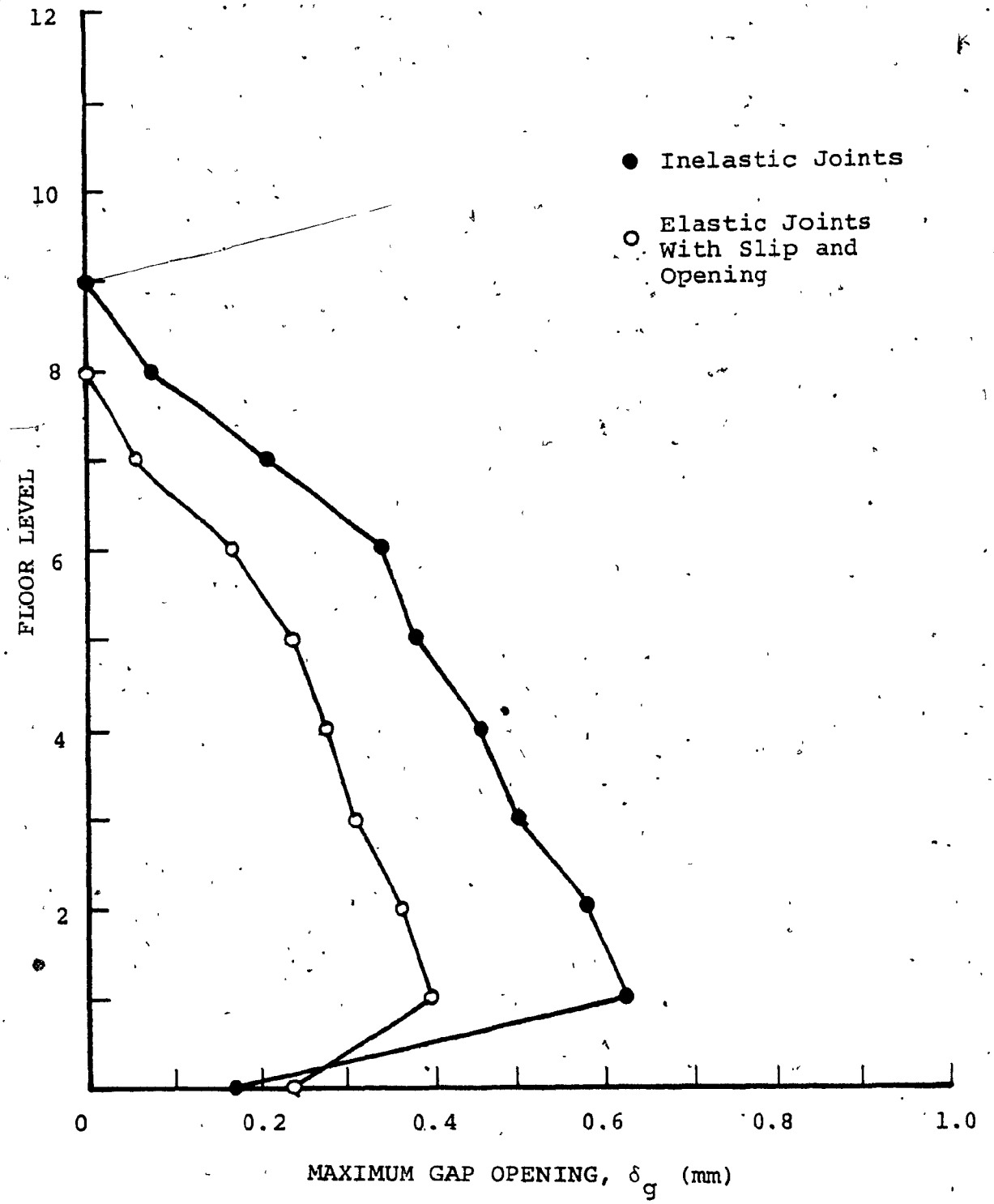

FIG. 3.20 ENVELOPES OF MAXIMUM GAP OPENING IN HORIZONTAL JOINTS OF WALL 1 FOR ELASTIC AND INELASTIC BEHAVIOUR - 12 STOREY PROTOTYPE WALL

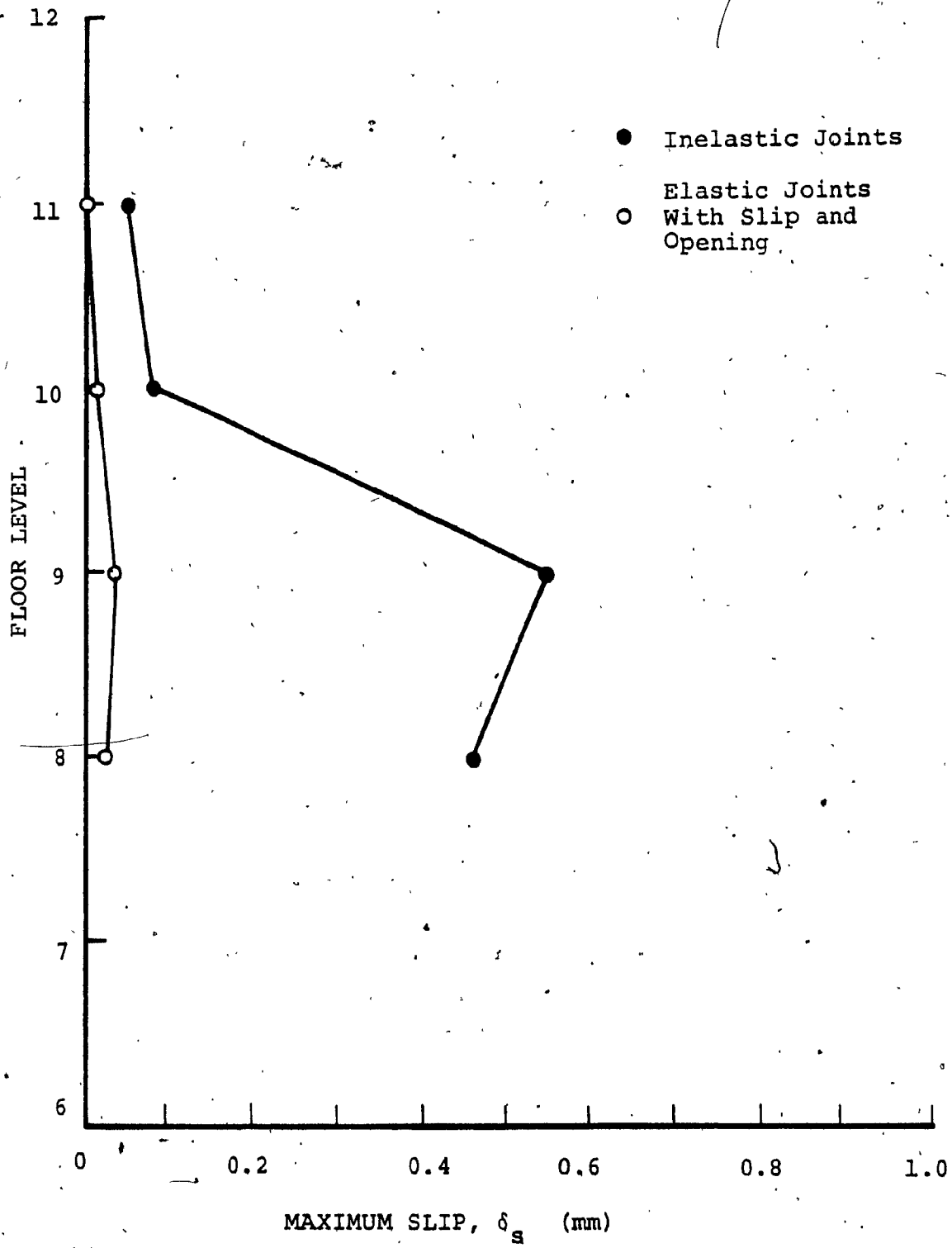

FIG. 3.21 DISTRIBUTION OF MAXIMUM SLIP IN HORIZONTAL JOINTS OF CANTILEVER FOR ELASTIC AND INELASTIC BEHAVIOUR - 5 STOREY CANTILEVER

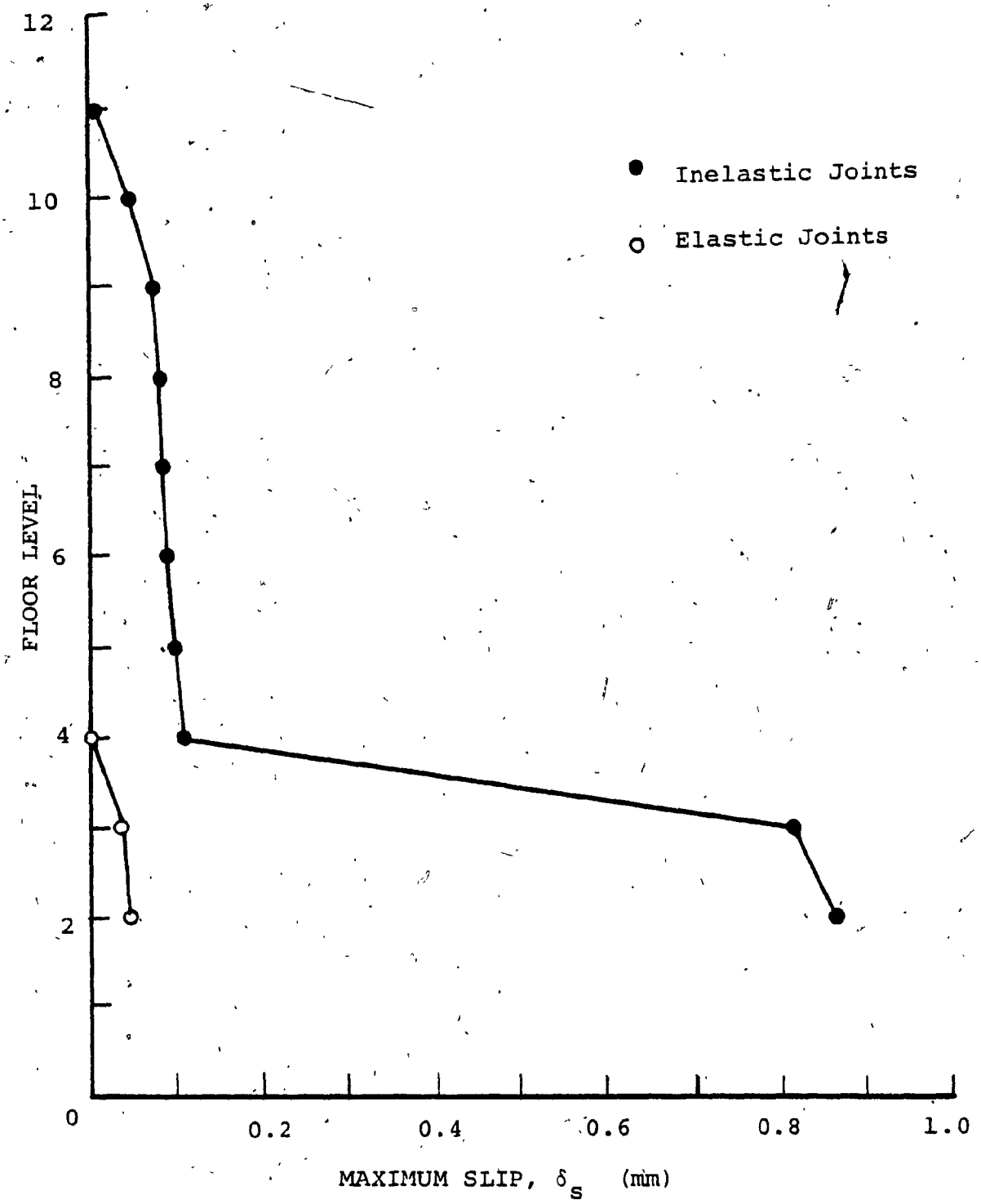

FIG. 3.22 DISTRIBUTION OF MAXIMUM SLIP IN HORIZONTAL JOINTS OF CANTILEVER FOR ELASTIC AND INELASTIC BEHAVIOUR - 11 STOREY CANTILEVER

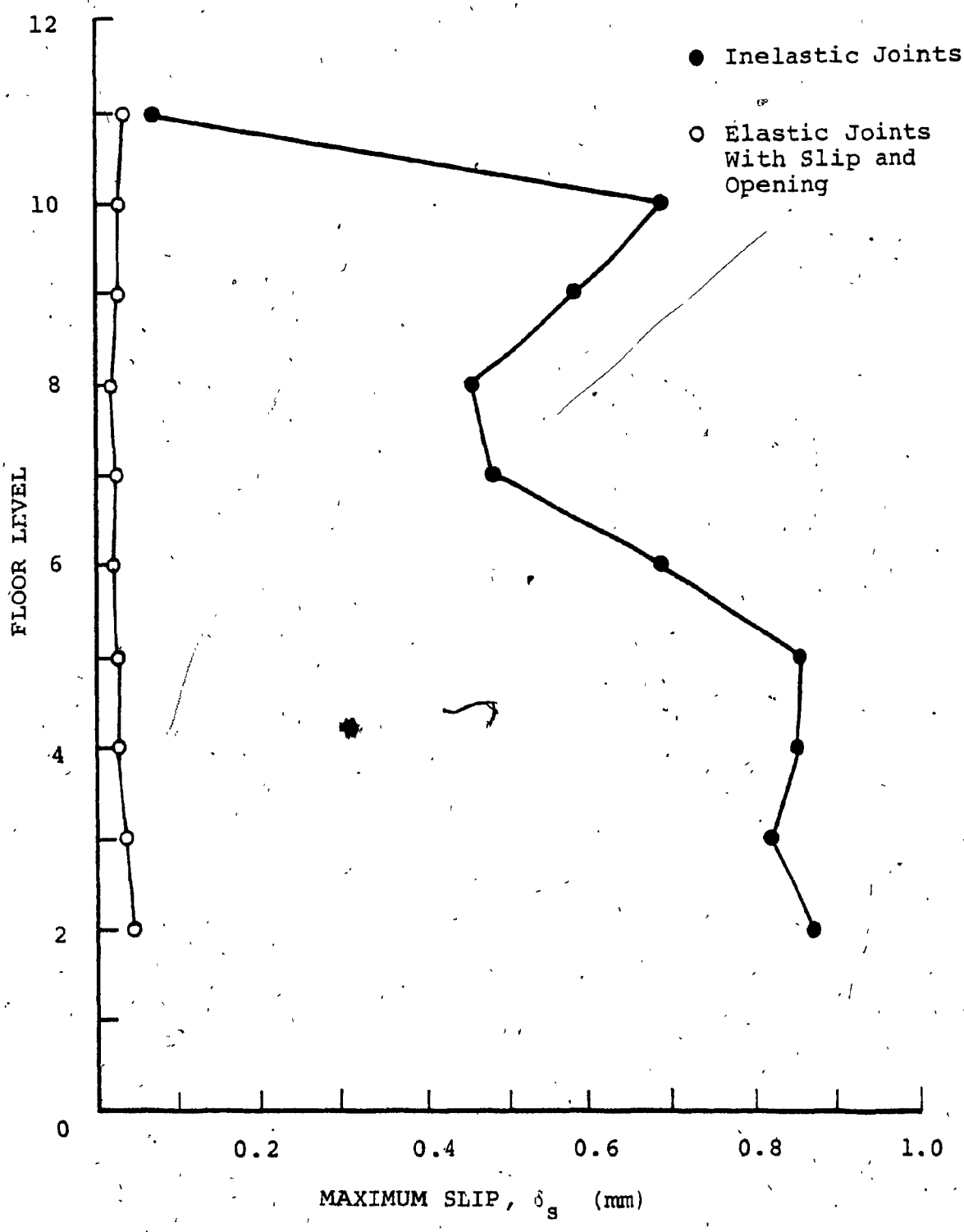

FIG. 3.23 ENVELOPES OF MAXIMUM SLIP IN HORIZONTAL JOINTS OF CANTILEVER FOR ELASTIC AND INELASTIC BEHAVIOUR - 12 STOREY PROTOTYPE WALL

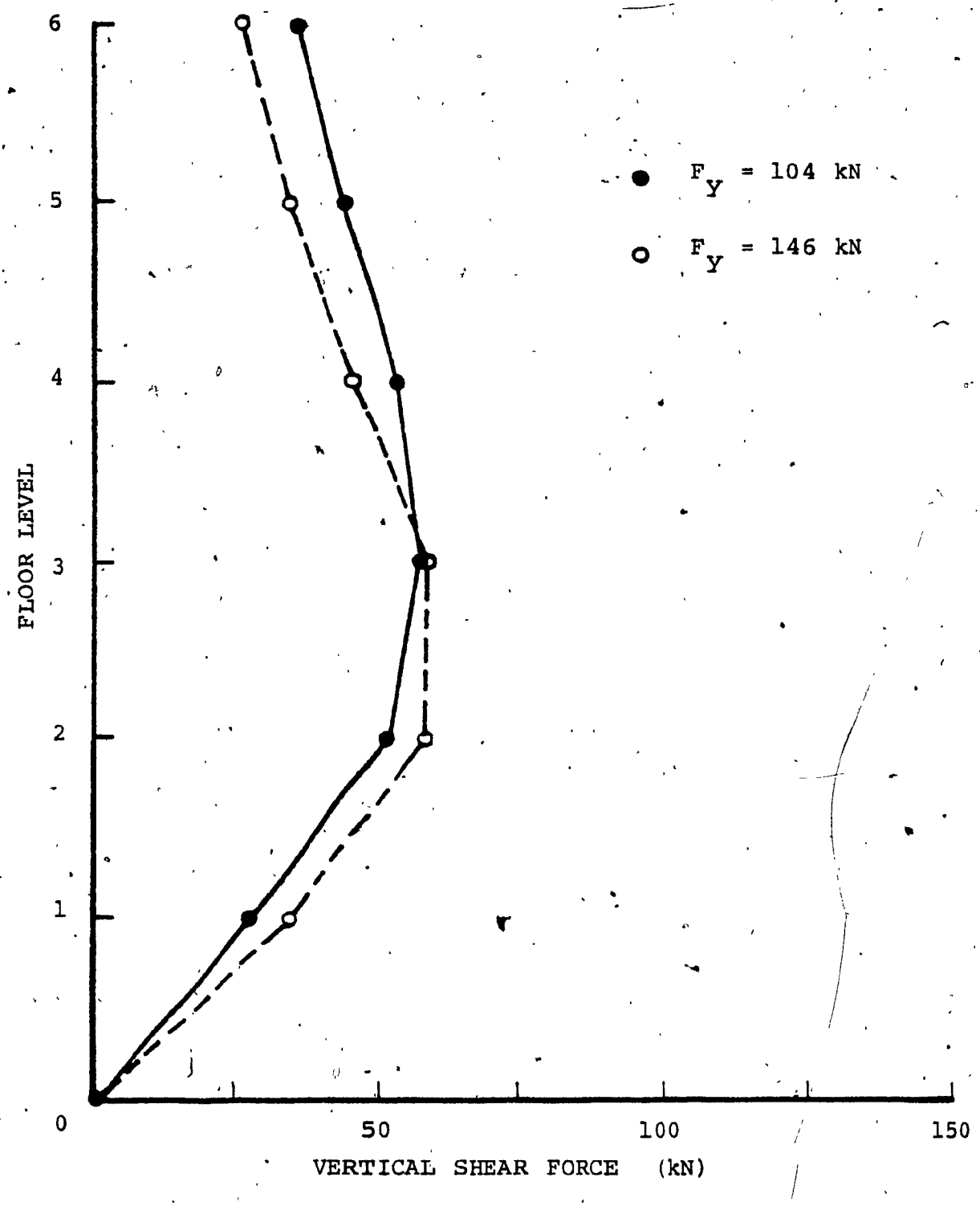

FIG. 3.24 EFFECT OF MECHANICAL CONNECTOR SHEAR STRENGTH ON DISTRIBUTION OF SHEAR FORCE IN JOINT 1 FOR 5 STOREY CANTILEVER

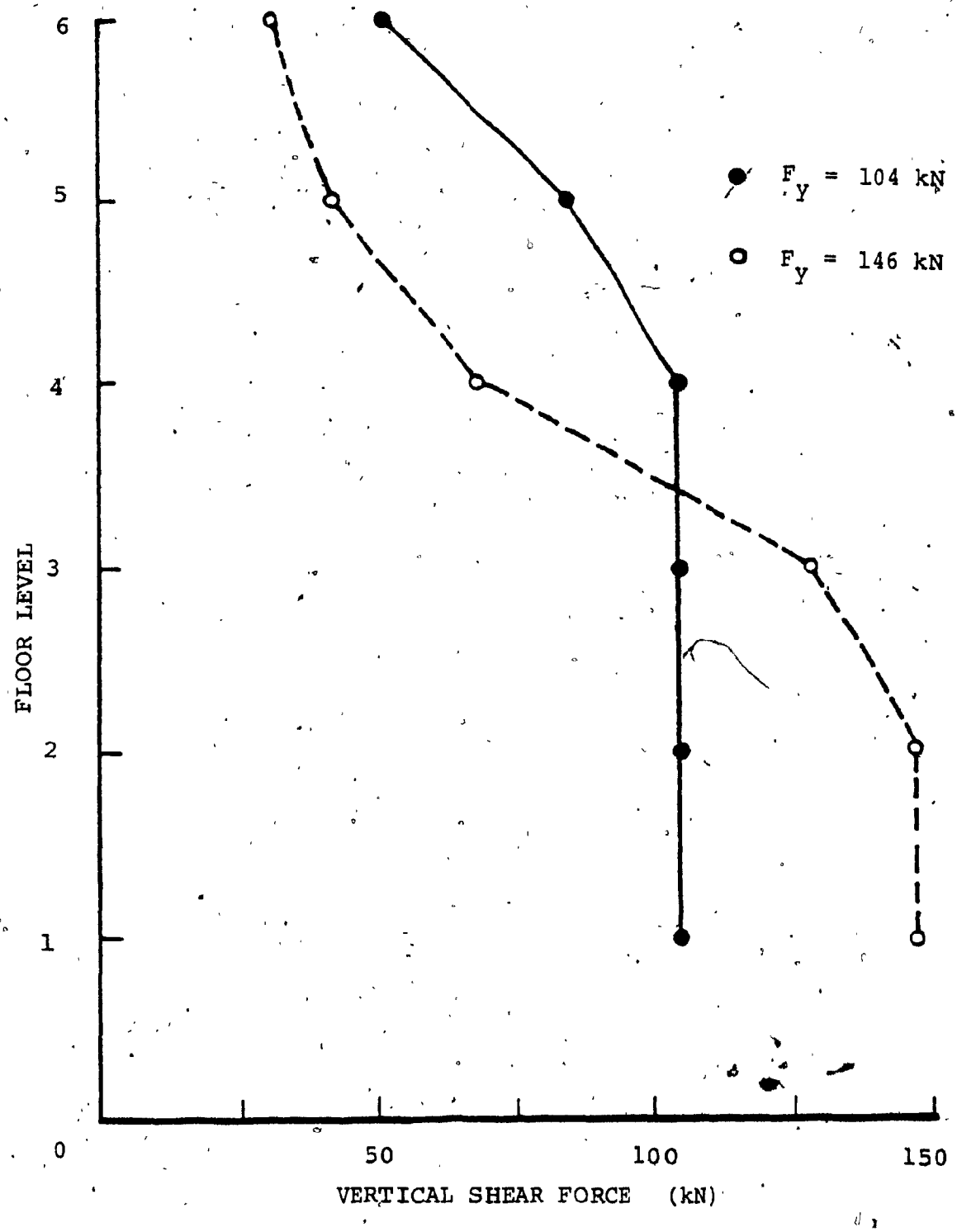

FIG. 3.25 EFFECT OF MECHANICAL CONNECTOR SHEAR STRENGTH ON DISTRIBUTION OF SHEAR FORCE IN JOINT 2 FOR 5 STOREY CANTILEVER

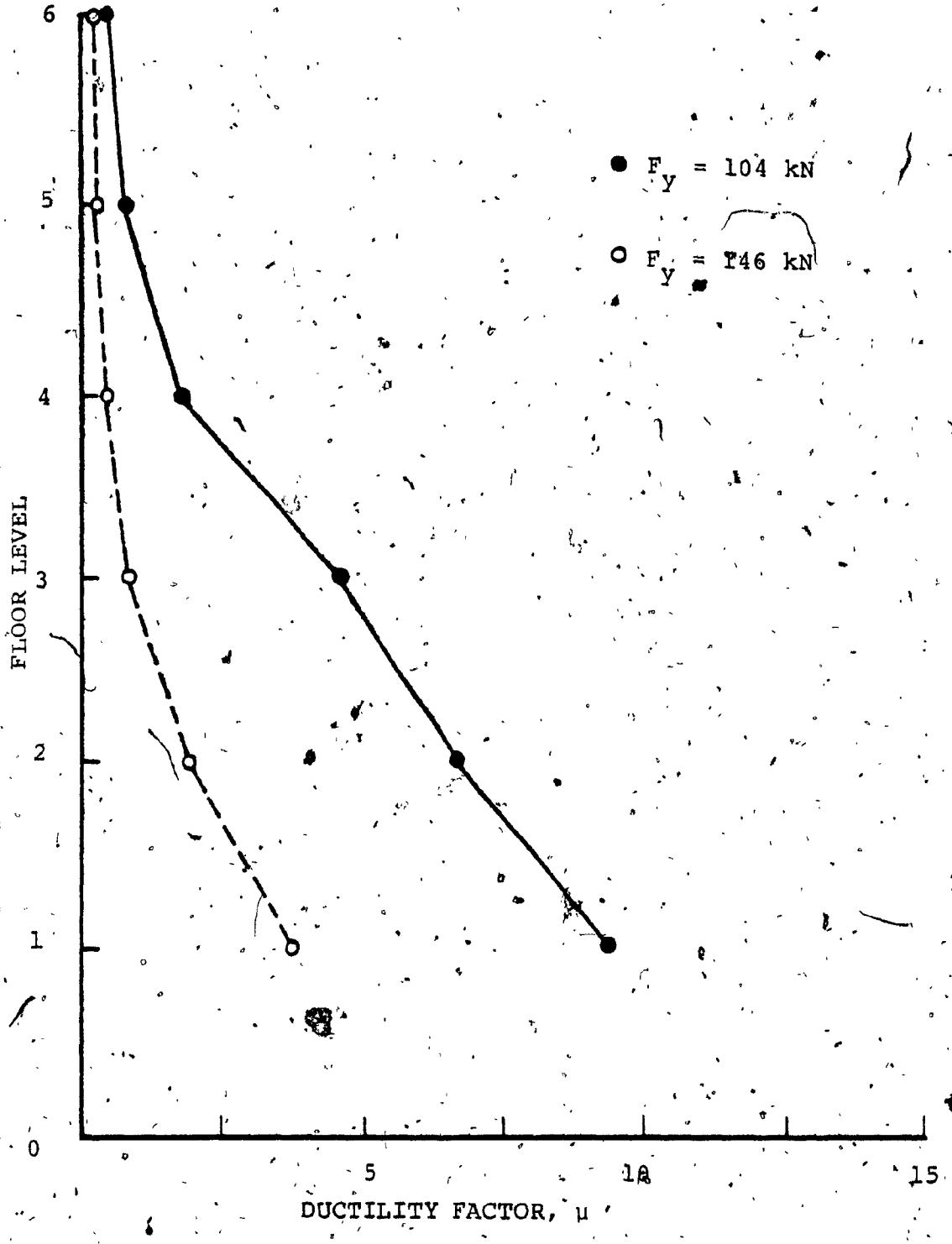

FIG. 3.26 EFFECT OF MECHANICAL CONNECTOR SHEAR STRENGTH ON DISTRIBUTION OF DUCTILITY DEMAND IN JOINT 2 FOR 5 STOREY CANTILEVER

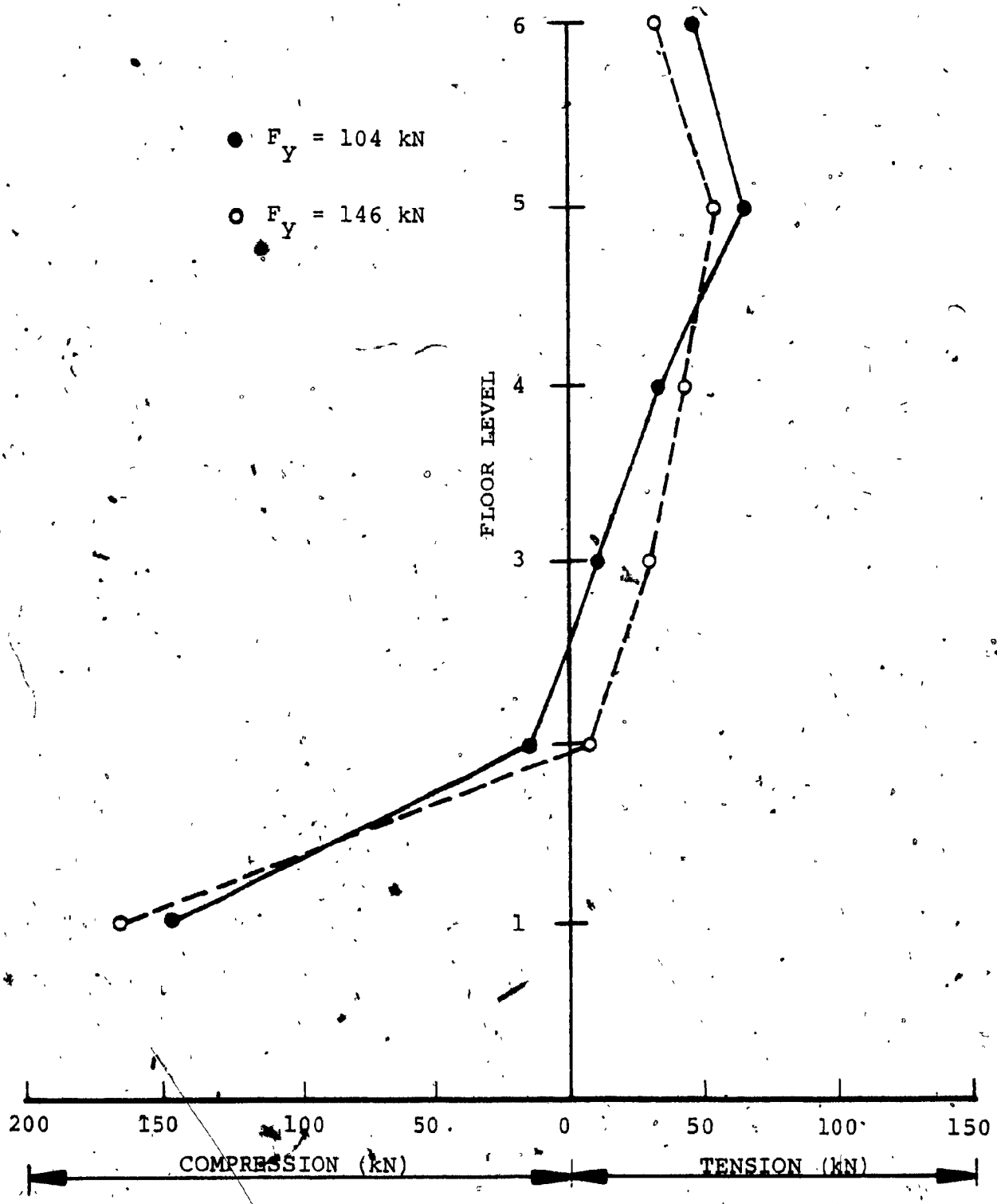

FIG. 3.27 EFFECT OF MECHANICAL CONNECTOR SHEAR STRENGTH ON DISTRIBUTION OF AXIAL FORCE IN VERTICAL JOINT FOR 5 STOREY CANTILEVER

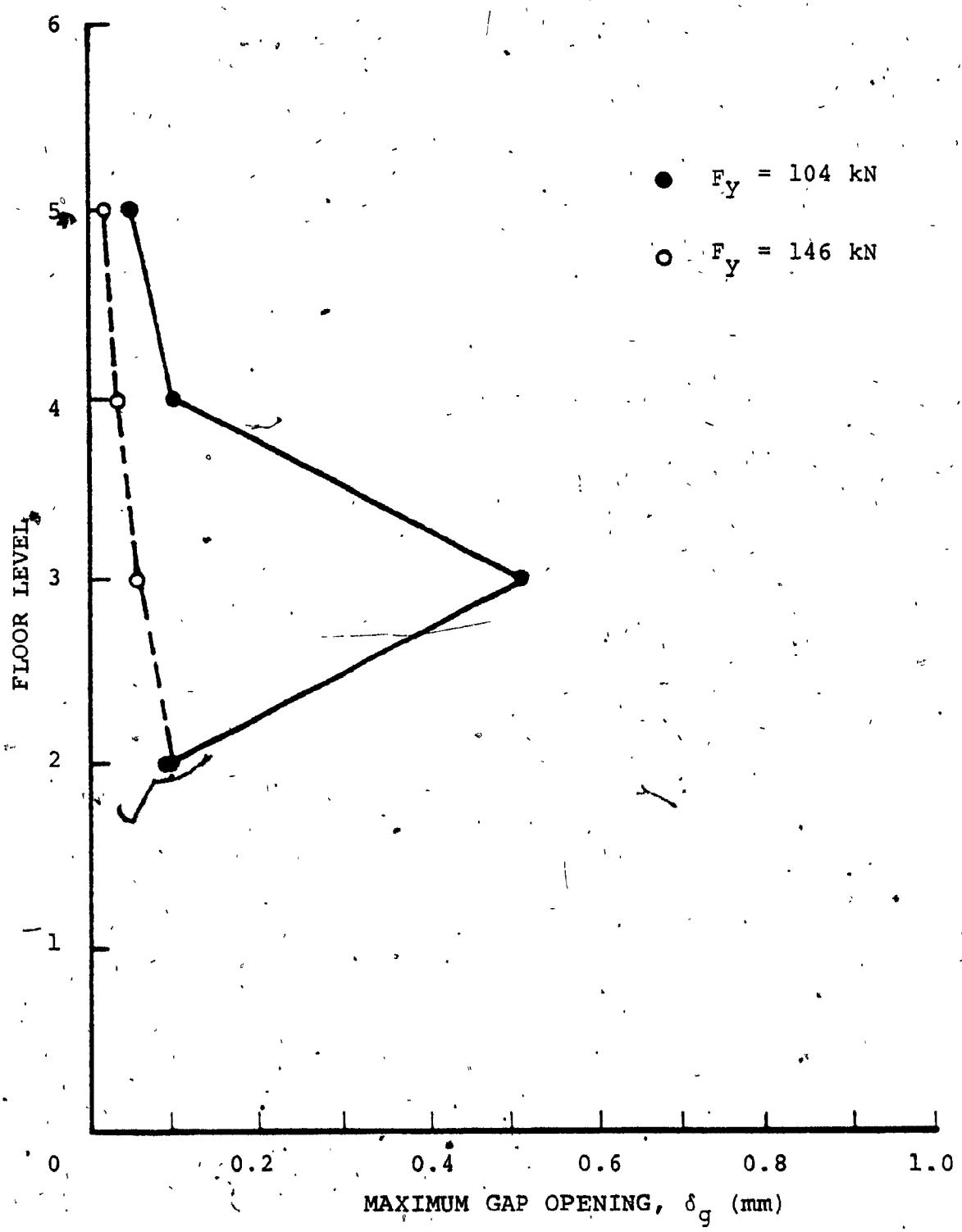

FIG. 3.28 EFFECT OF MECHANICAL CONNECTOR SHEAR STRENGTH ON DISTRIBUTION OF MAXIMUM GAP OPENING IN HORIZONTAL JOINTS OF CANTILEVER - 5 STOREY CANTILEVER

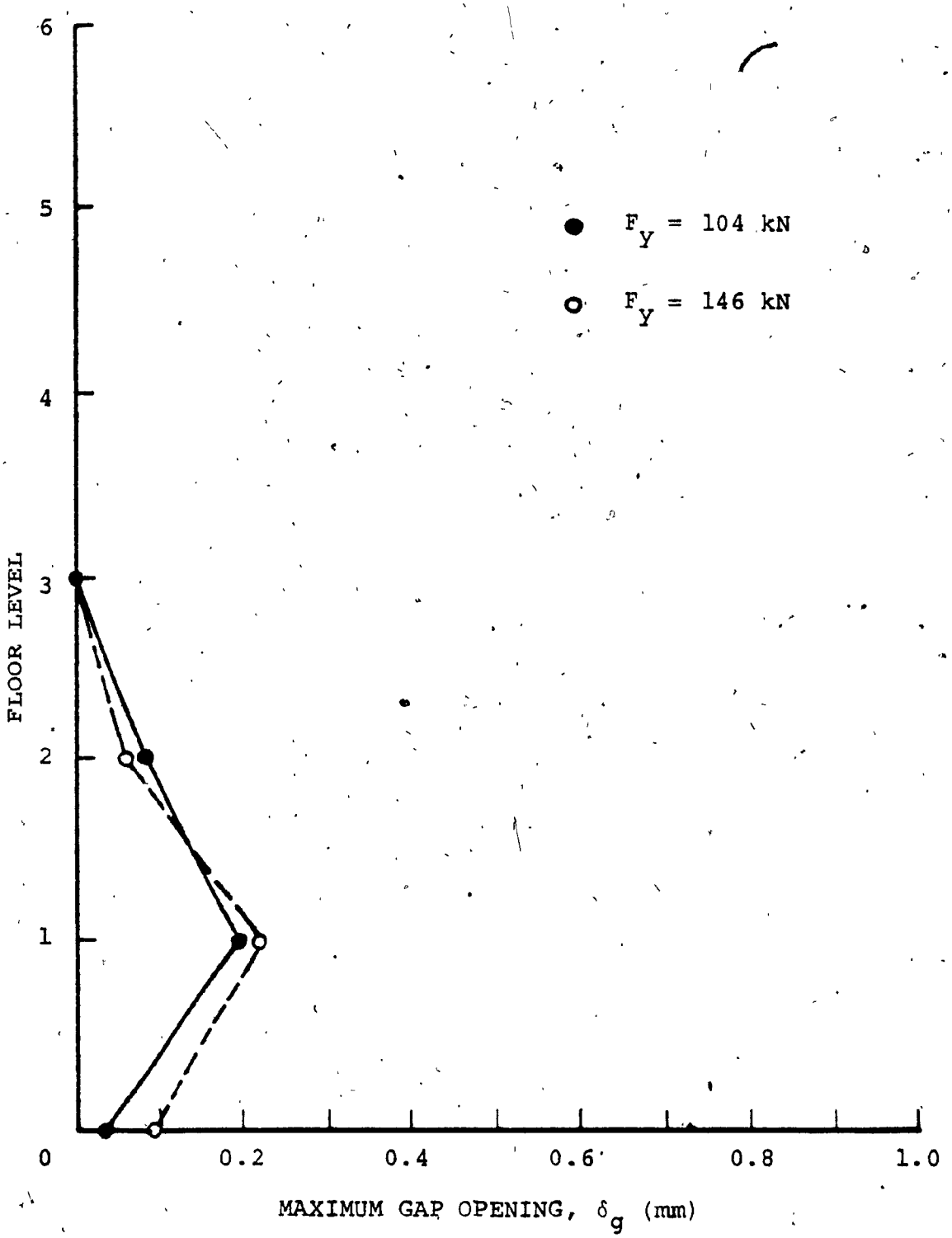

FIG. 3.29 EFFECT OF MECHANICAL CONNECTOR SHEAR STRENGTH ON DISTRIBUTION OF MAXIMUM GAP OPENING IN HORIZONTAL JOINTS OF WALL 1 - 5 STOREY CANTILEVER

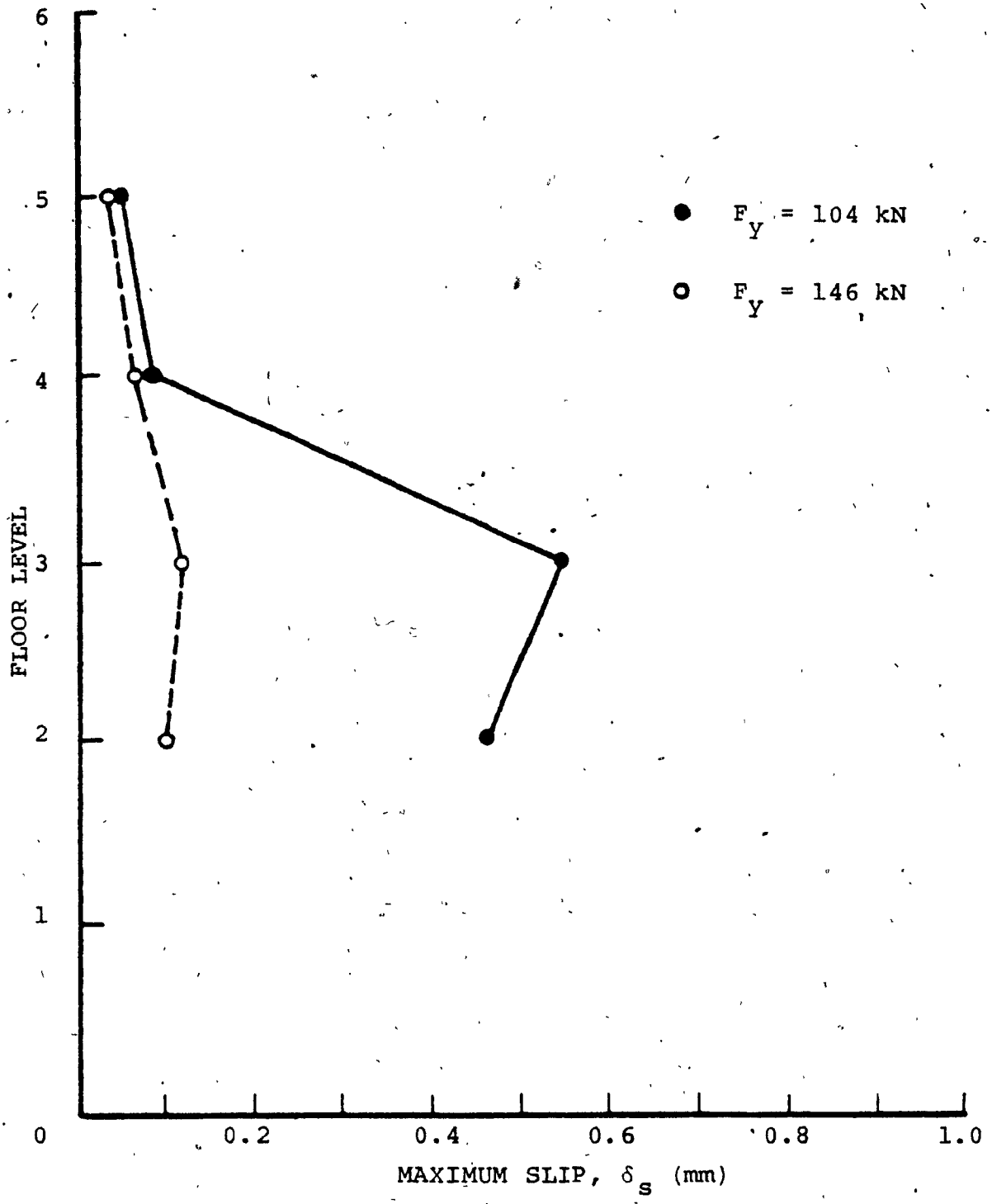

FIG. 3.30 EFFECT OF MECHANICAL CONNECTOR SHEAR STRENGTH ON DISTRIBUTION OF MAXIMUM SLIP IN HORIZONTAL JOINTS OF CANTILEVER - 5 STOREY CANTILEVER

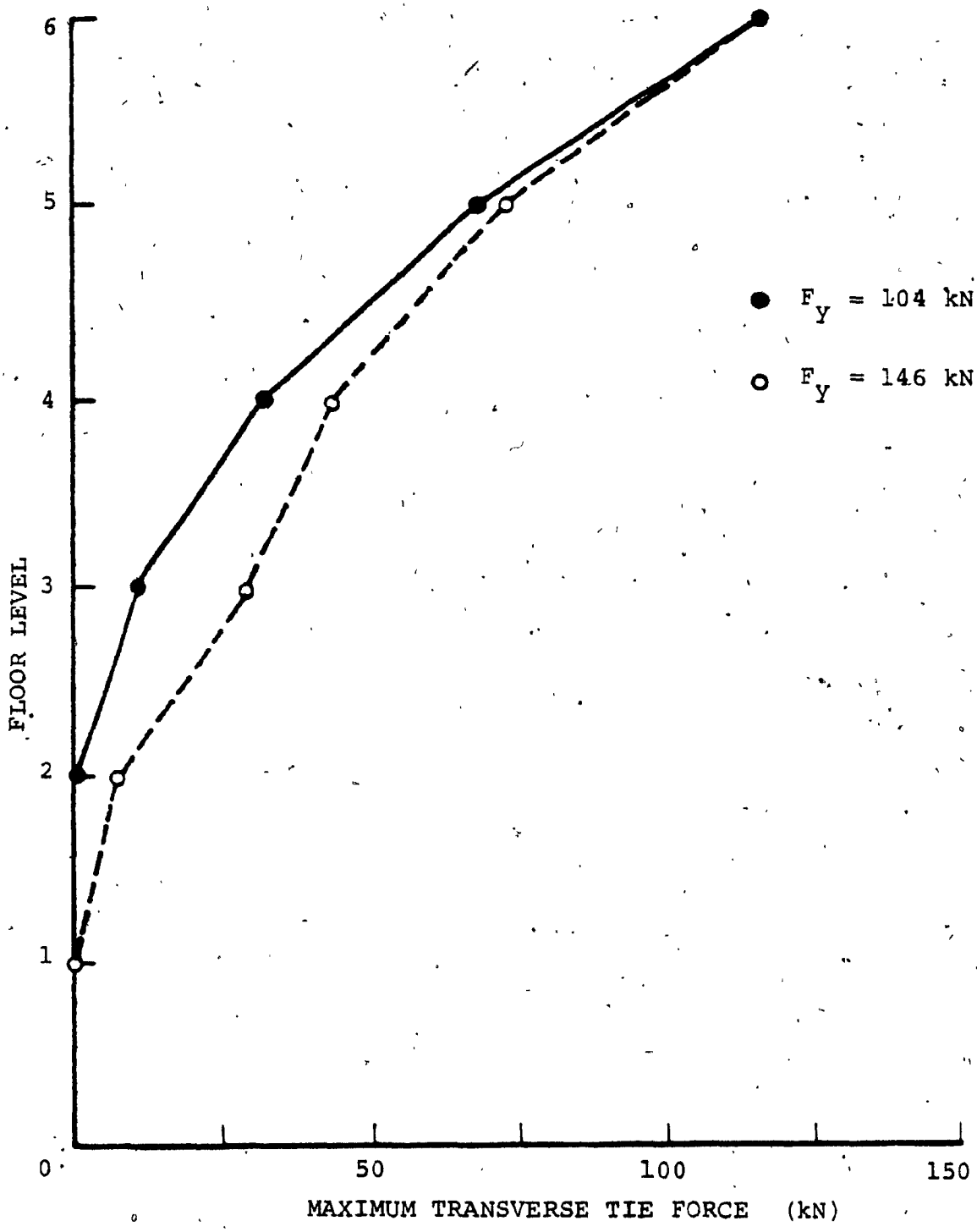

FIG. 3.31 ENVELOPES OF MAXIMUM FORCE IN TRANSVERSE TIES OF 6 STOREY PRECAST PANEL WALL FOR TWO DIFFERENT VALUES OF MECHANICAL CONNECTOR SHEAR STRENGTH

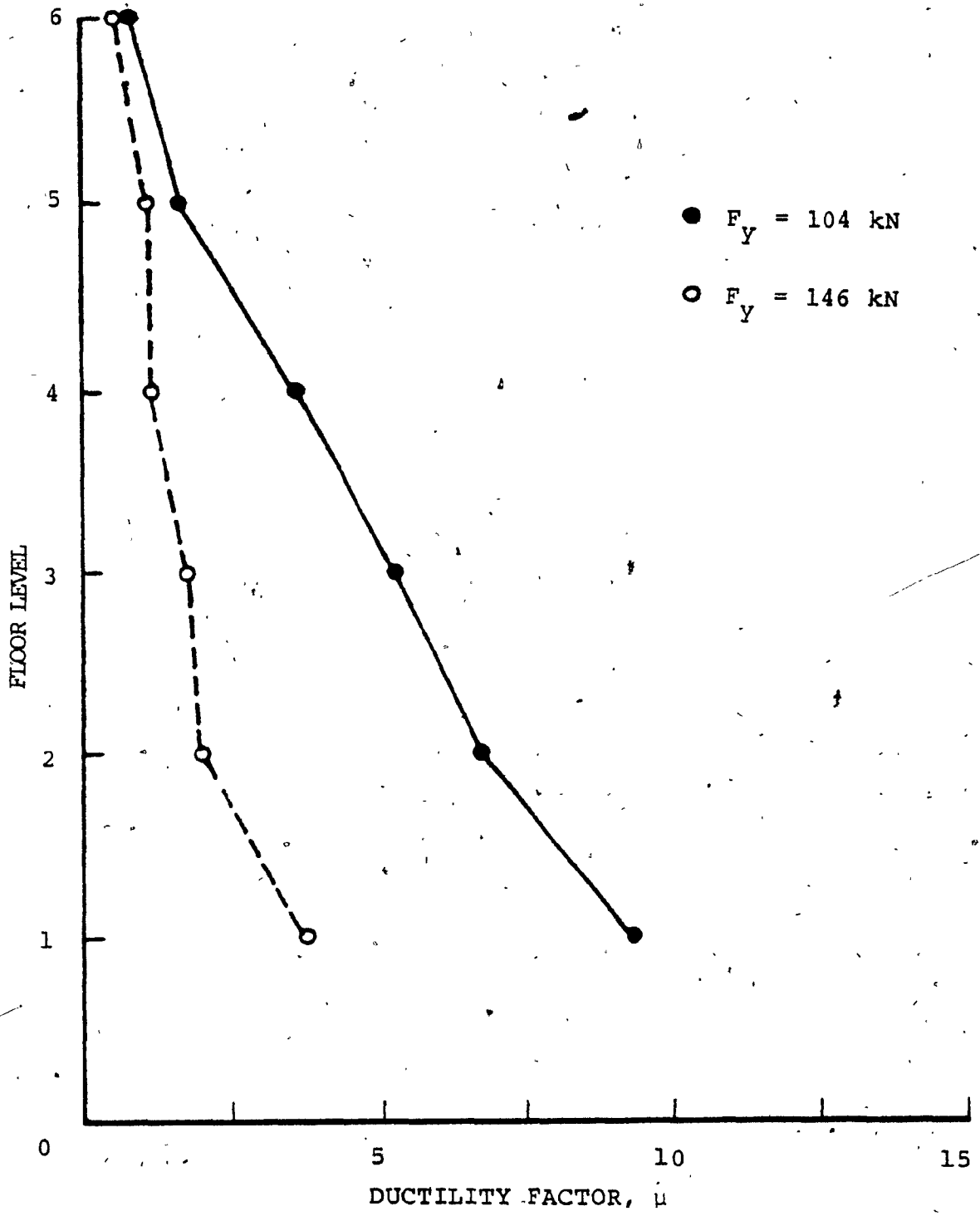

FIG. 3.32 ENVELOPES OF MAXIMUM DUCTILITY DEMAND IN VERTICAL MECHANICAL CONNECTORS OF 6 STOREY PRECAST PANEL WALL FOR TWO DIFFERENT VALUES OF CONNECTOR SHEAR STRENGTH

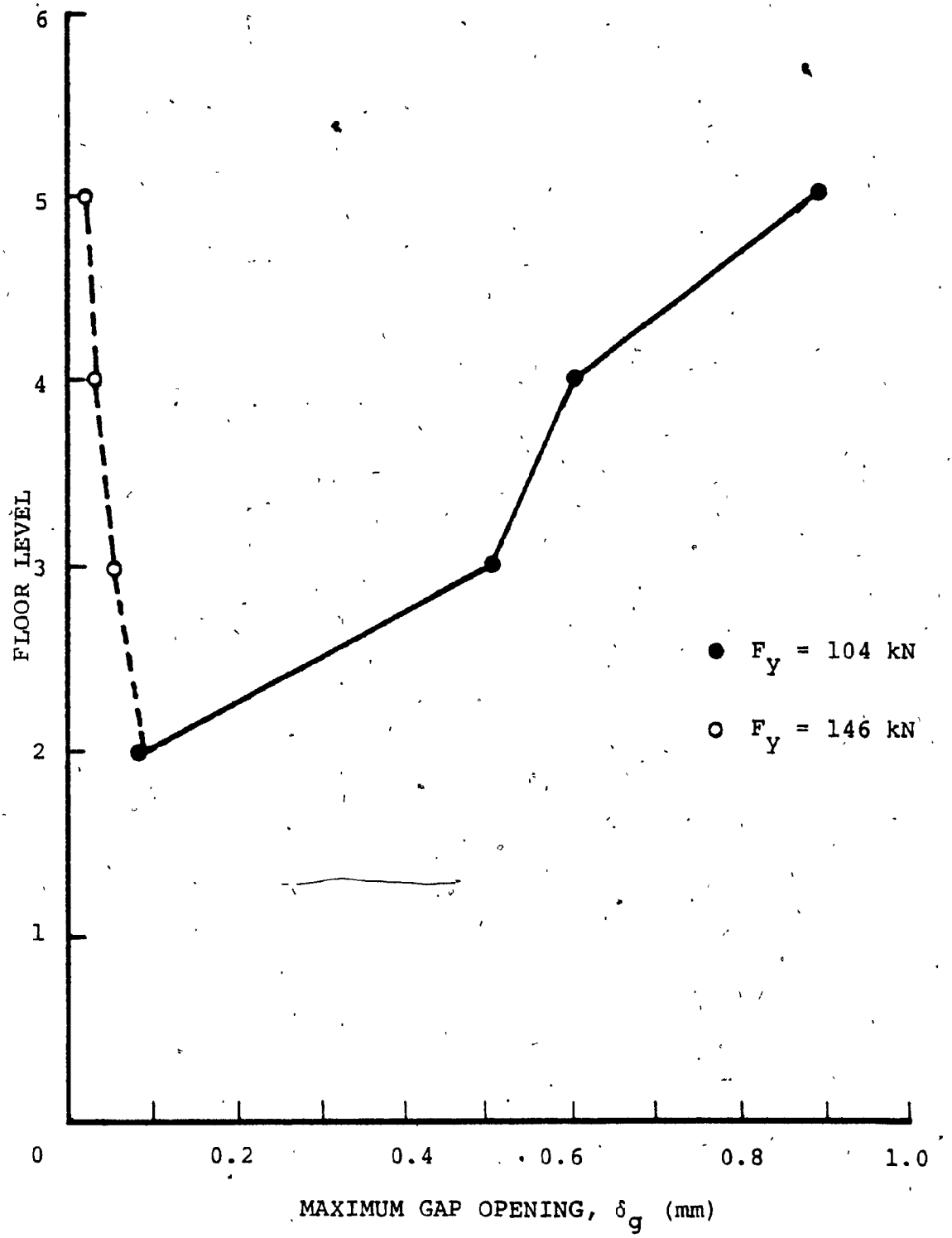

FIG. 3.33 ENVELOPES OF MAXIMUM GAP OPENING IN HORIZONTAL JOINTS OF CANTILEVER FOR TWO DIFFERENT VALUES OF MECHANICAL CONNECTOR SHEAR STRENGTH - 6 STOREY PRECAST PANEL WALL

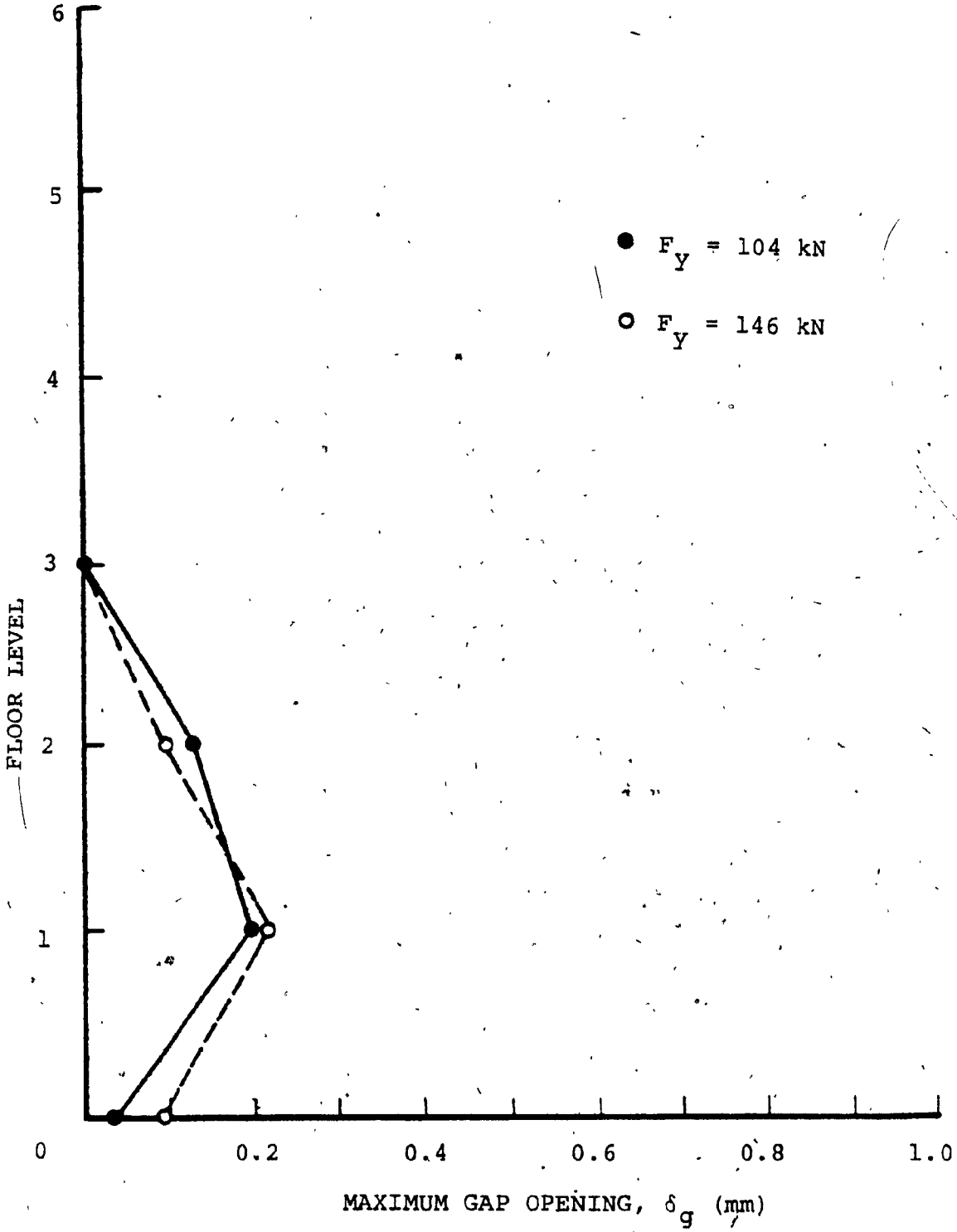

FIG. 3.34 ENVELOPES OF MAXIMUM GAP OPENING IN HORIZONTAL JOINTS OF WALL 1 FOR TWO DIFFERENT VALUES OF MECHANICAL CONNECTOR SHEAR STRENGTH - 6 STOREY PRECAST PANEL WALL

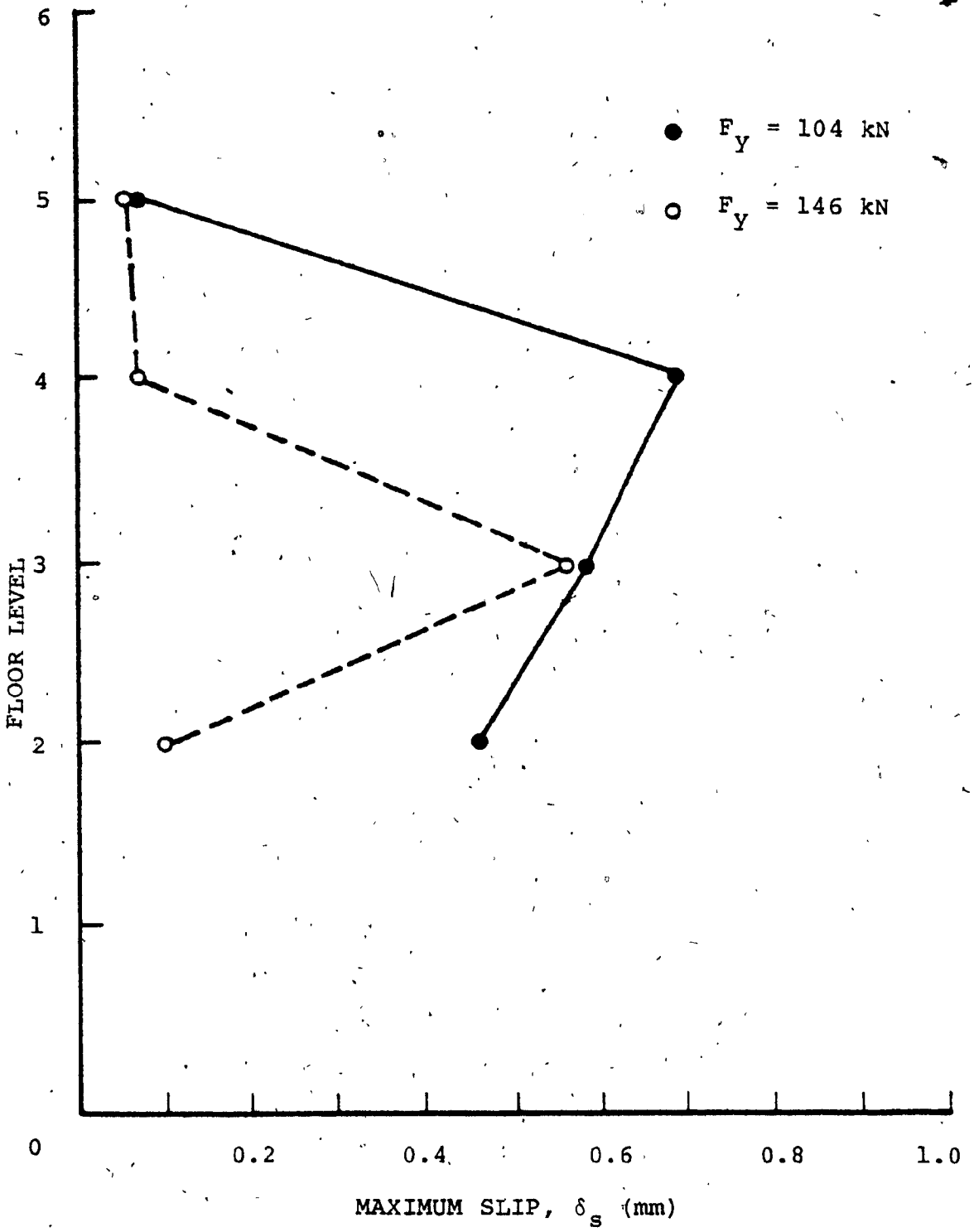

FIG. 3.35 ENVELOPES OF MAXIMUM SLIP IN HORIZONTAL JOINTS OF CANTILEVER FOR TWO DIFFERENT VALUES OF MECHANICAL CONNECTOR SHEAR STRENGTH - 6 STOREY PRECAST PANEL WALL

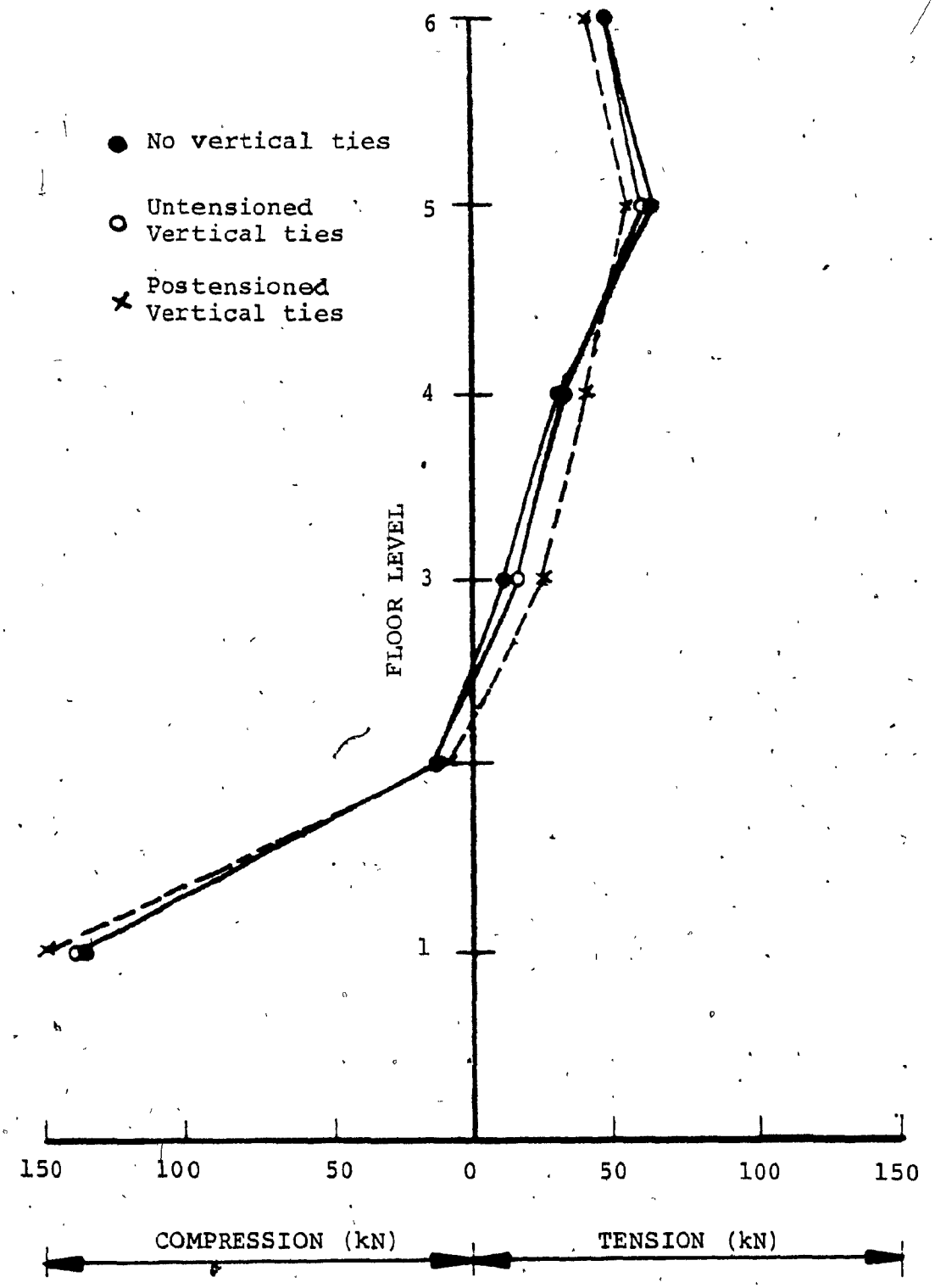

FIG. 3.36 AXIAL FORCE DISTRIBUTION IN VERTICAL JOINT OF 6 STOREY PRECAST PANEL WALL WITH AND WITHOUT VERTICAL TIES - 5 STOREY CANTILEVER

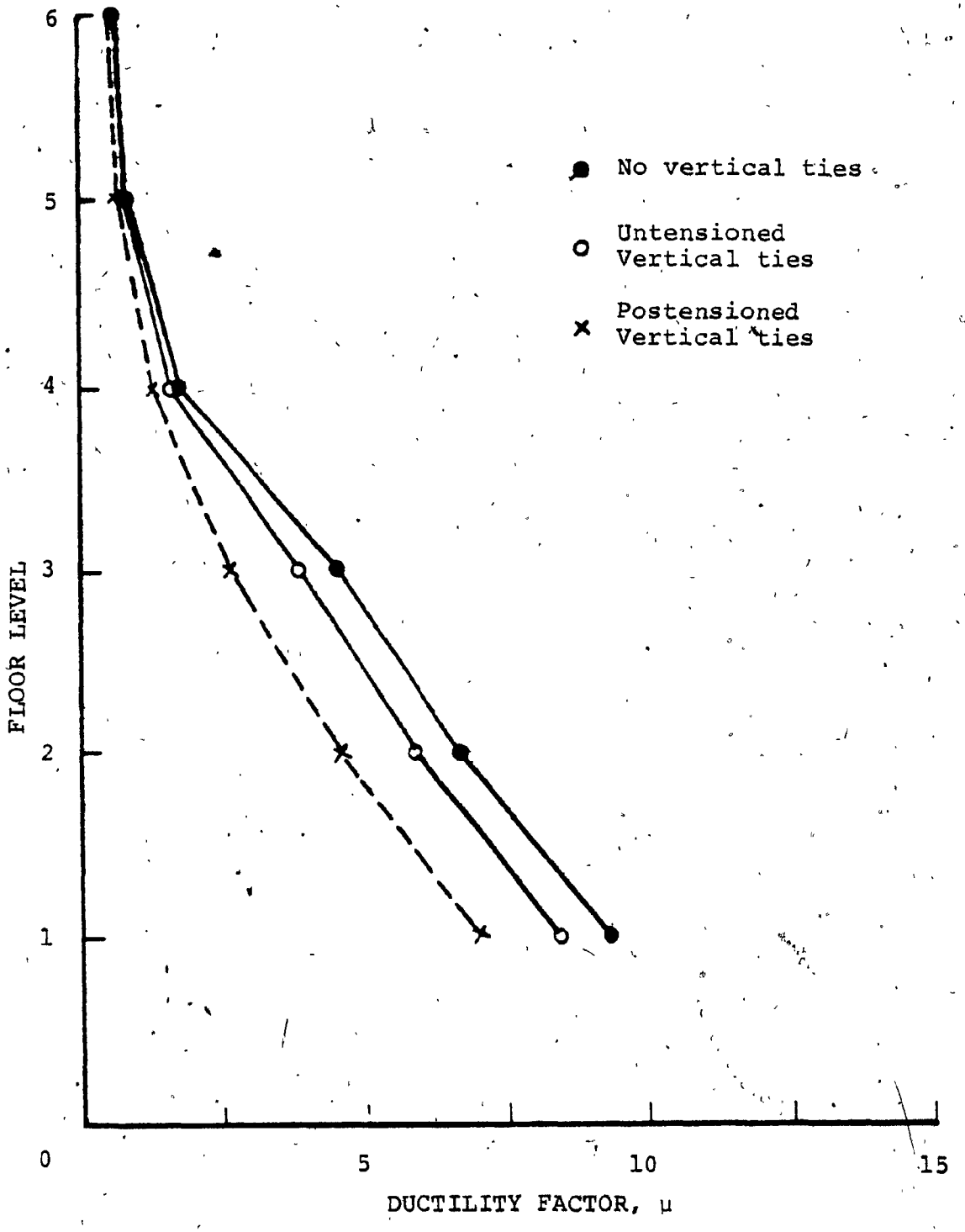

FIG. 3.37 DISTRIBUTION OF DUCTILITY DEMAND IN VERTICAL MECHANICAL CONNECTORS OF 6 STOREY PRECAST PANEL WALL WITH AND WITHOUT VERTICAL TIES - 5 STOREY CANTILEVER

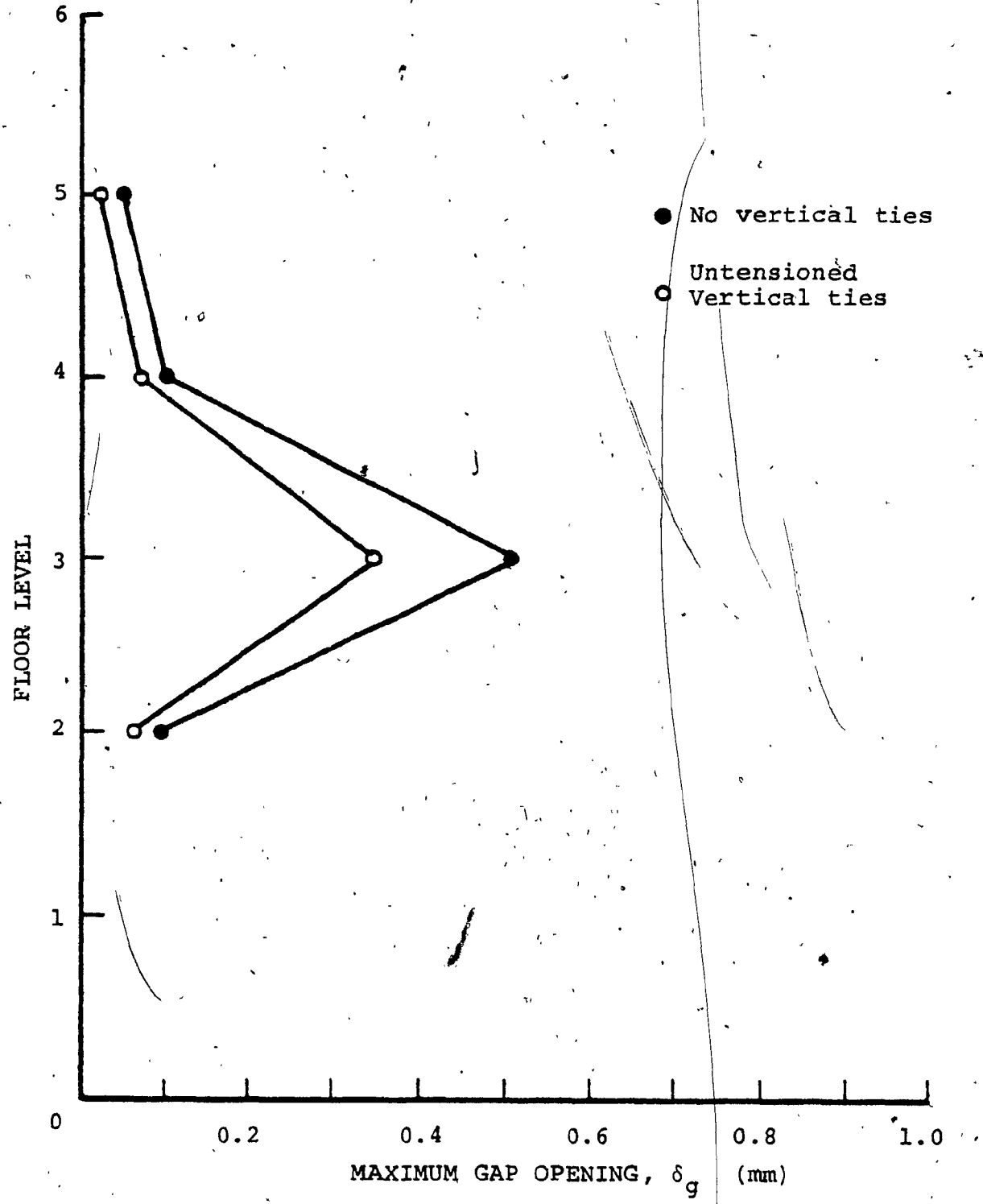

FIG. 3.38 DISTRIBUTION OF MAXIMUM GAP OPENING IN HORIZONTAL JOINTS WITH CANTILEVER OF 6 STOREY PRECAST PANEL WALL WITH AND WITHOUT VERTICAL TIES - 5-STOREY CANTILEVER

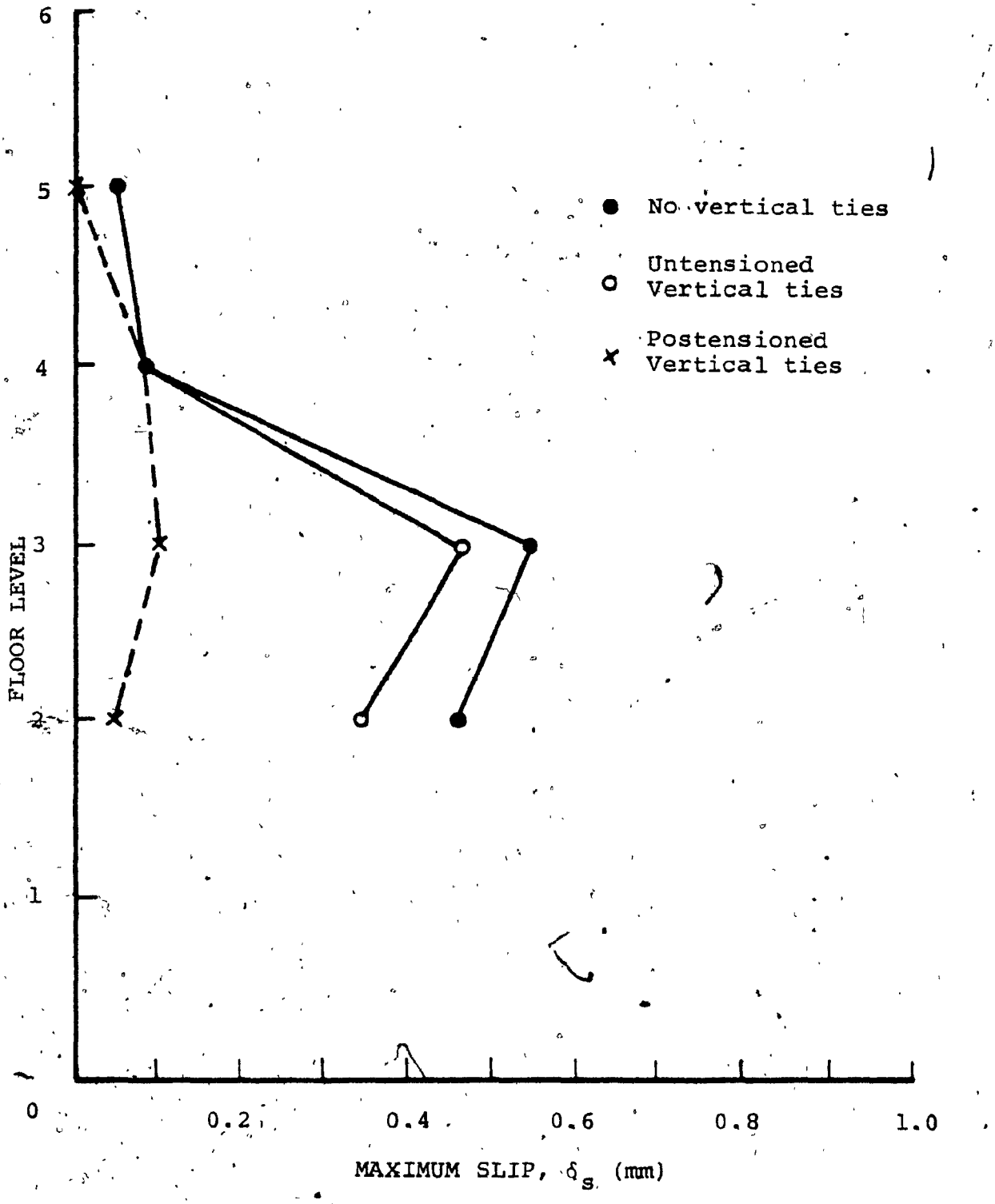

FIG. 3.39 DISTRIBUTION OF MAXIMUM HORIZONTAL SLIP IN CANTILEVER JOINTS OF 6 STOREY PRECAST PANEL WALL WITH AND WITHOUT VERTICAL TIES - 5 STOREY CANTILEVER

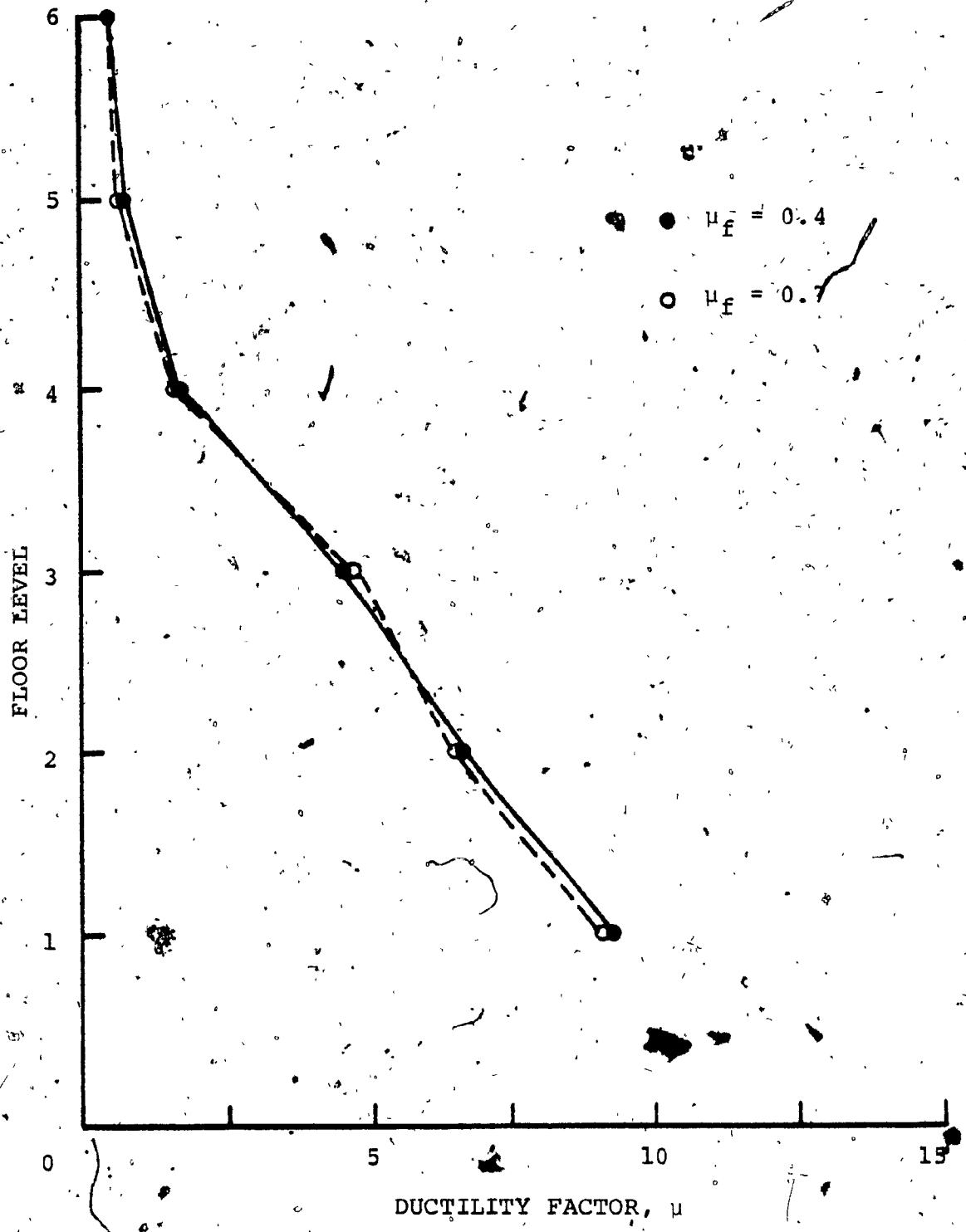

FIG. 3.40 EFFECT OF COEFFICIENT OF FRICTION ON DISTRIBUTION OF DUCTILITY DEMAND IN VERTICAL MECHANICAL CONNECTORS OF JOINT 2 - 5 STOREY CANTILEVER

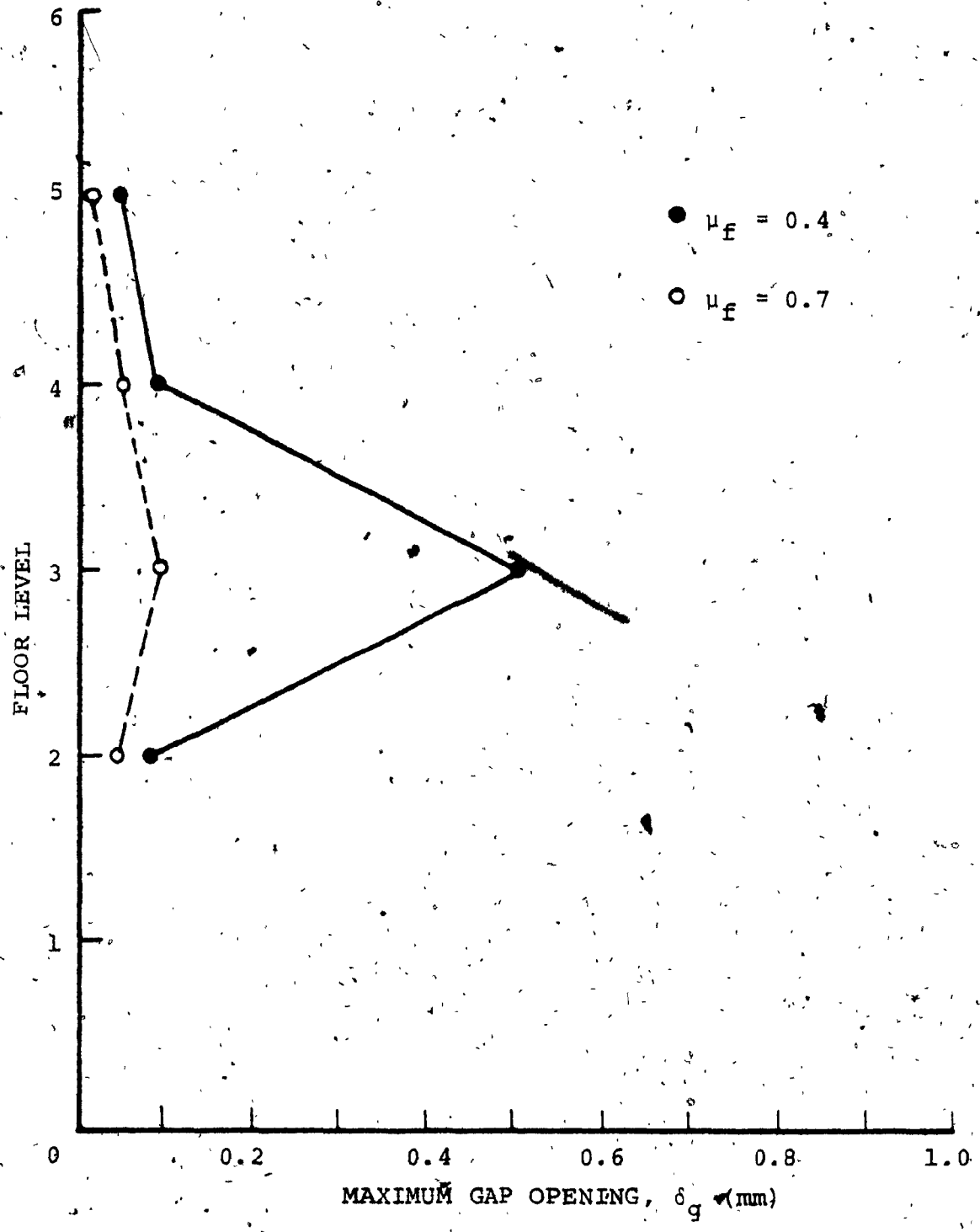

FIG. 3.41 EFFECT OF COEFFICIENT OF FRICTION ON DISTRIBUTION OF MAXIMUM GAP OPENING IN HORIZONTAL JOINTS OF CANTILEVER - 5 STOREY CANTILEVER

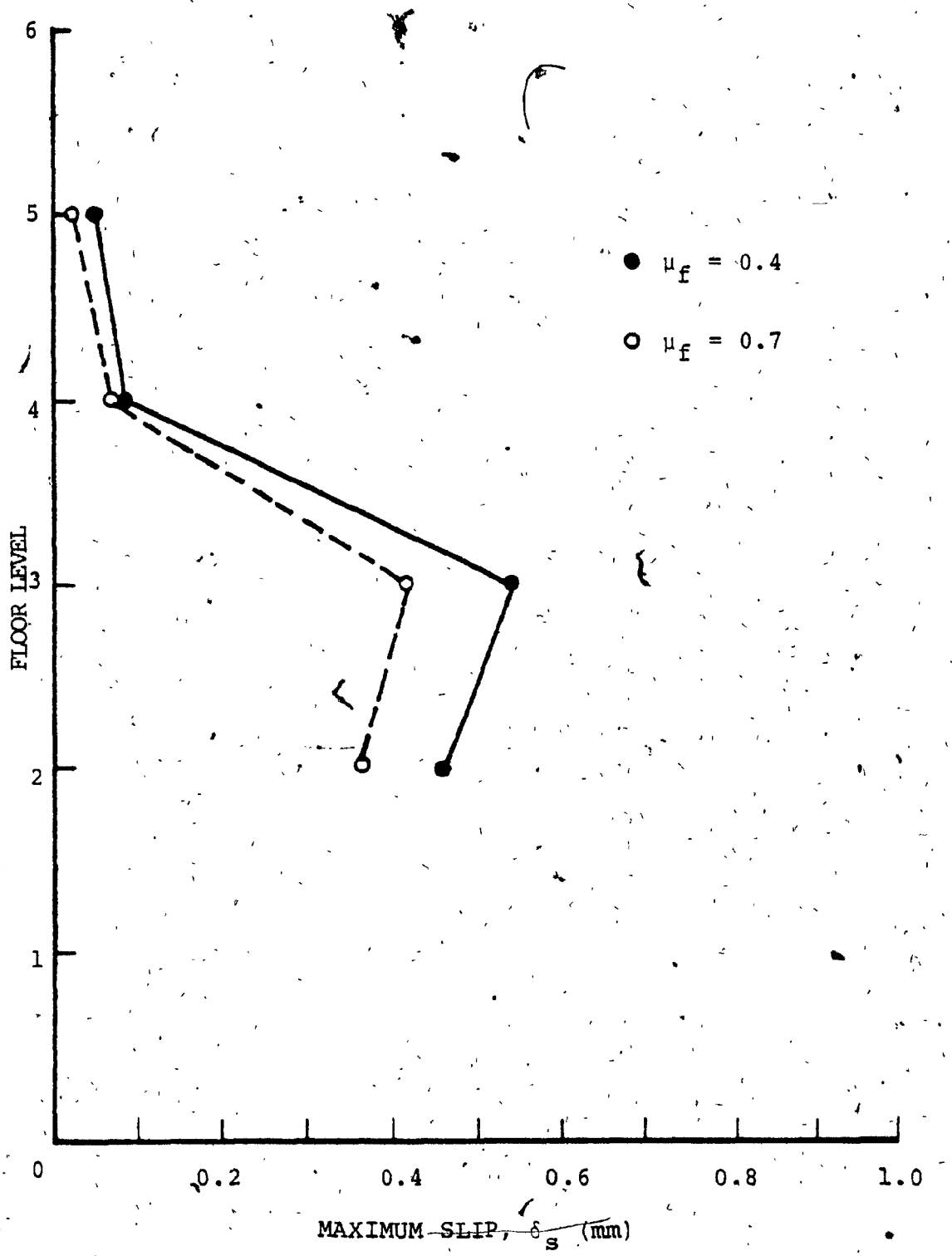

FIG. 3.42 EFFECT OF COEFFICIENT OF FRICTION ON DISTRIBUTION OF MAXIMUM SLIP IN HORIZONTAL JOINTS OF CANTILEVER - 5 STOREY CANTILEVER

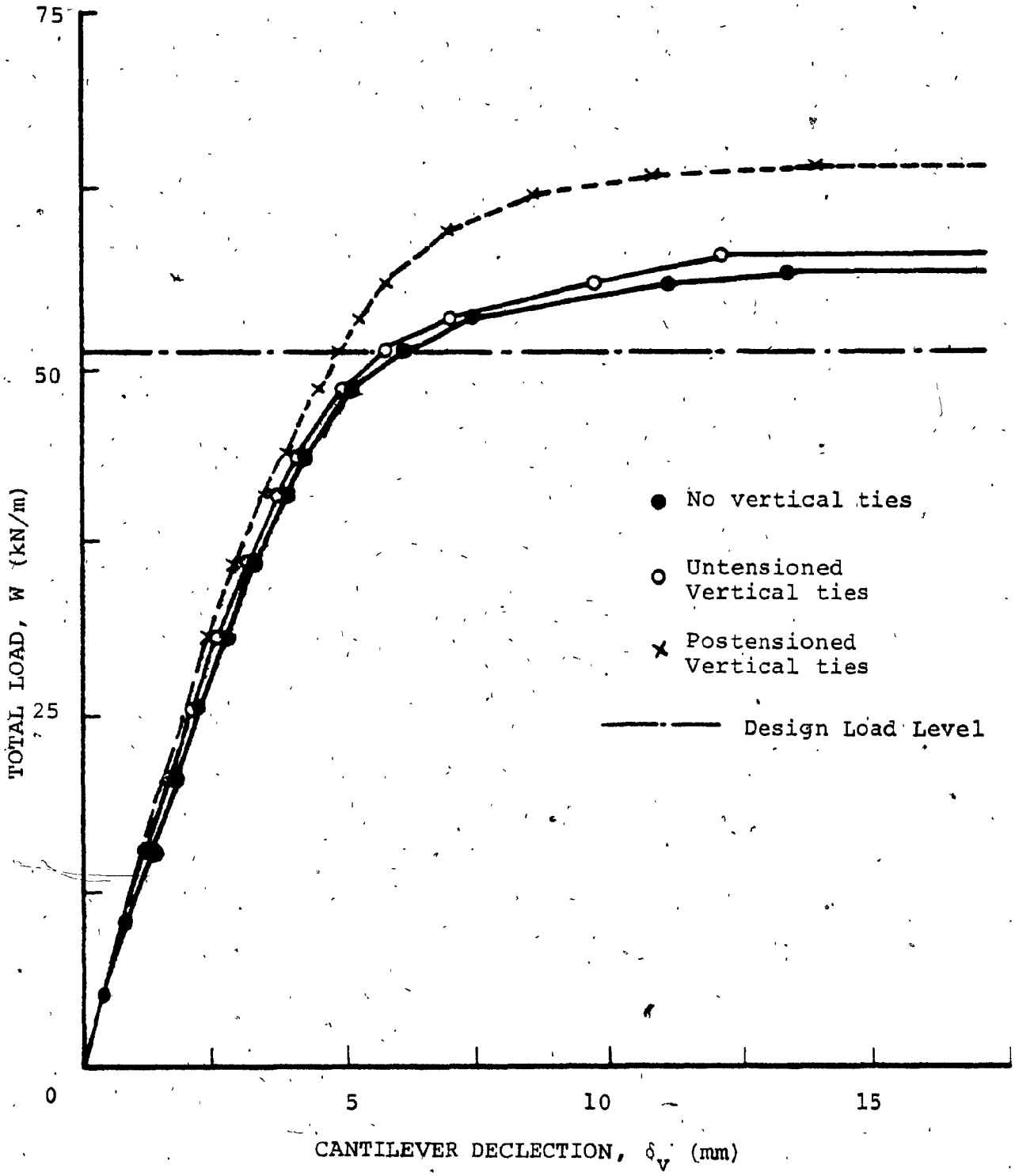

FIG. 3.43 LOAD-DISPLACEMENT BEHAVIOUR OF CANTILEVER OF 6 STOREY PRECAST PANEL WALL WITH AND WITHOUT VERTICAL TIES - 5 STOREY CANTILEVER

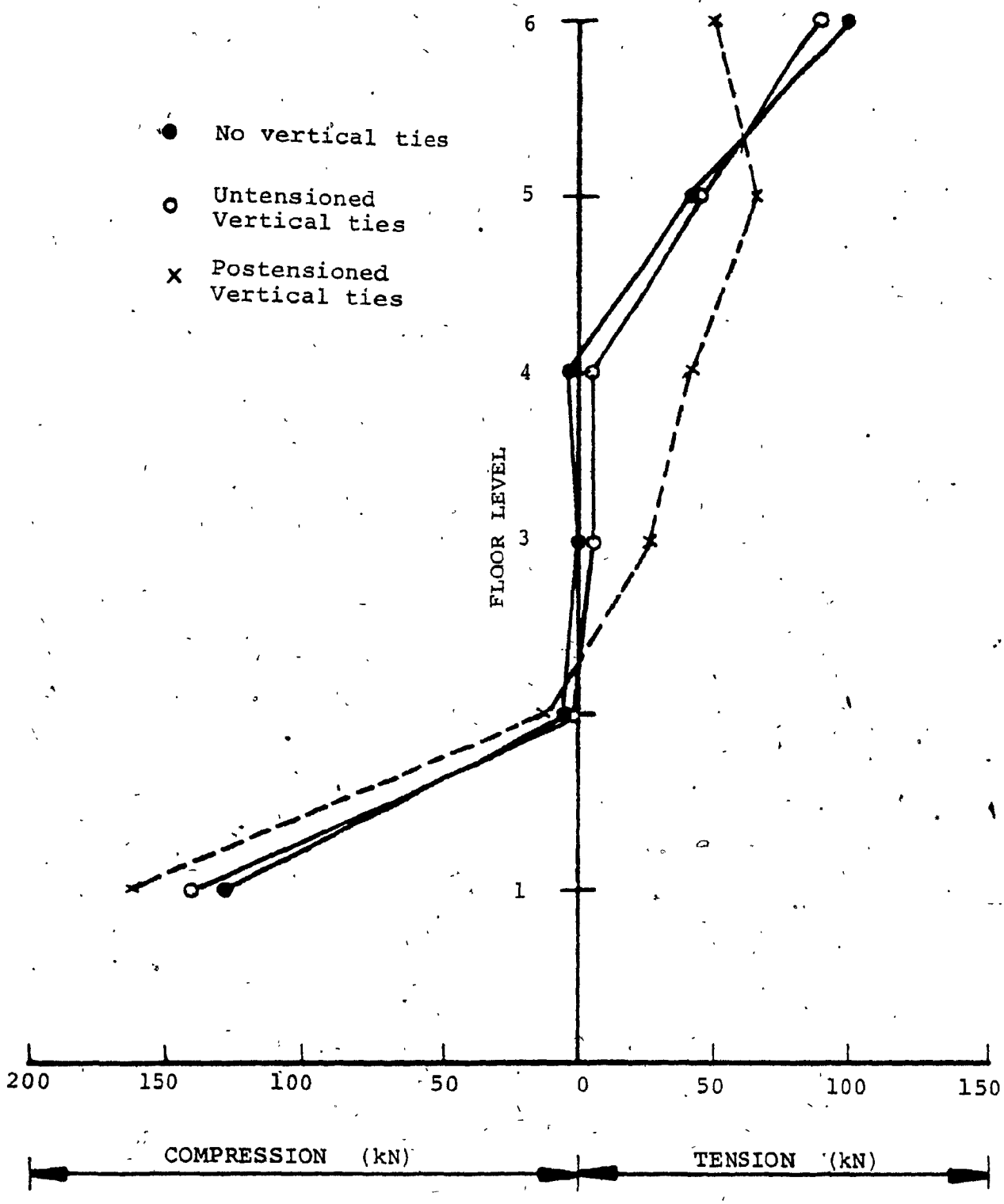

FIG. 3.44 AXIAL FORCE DISTRIBUTION IN VERTICAL JOINT OF 6 STOREY PRECAST PANEL WALL WITH AND WITHOUT VERTICAL TIES AT FAILURE - 5 STOREY CANTILEVER

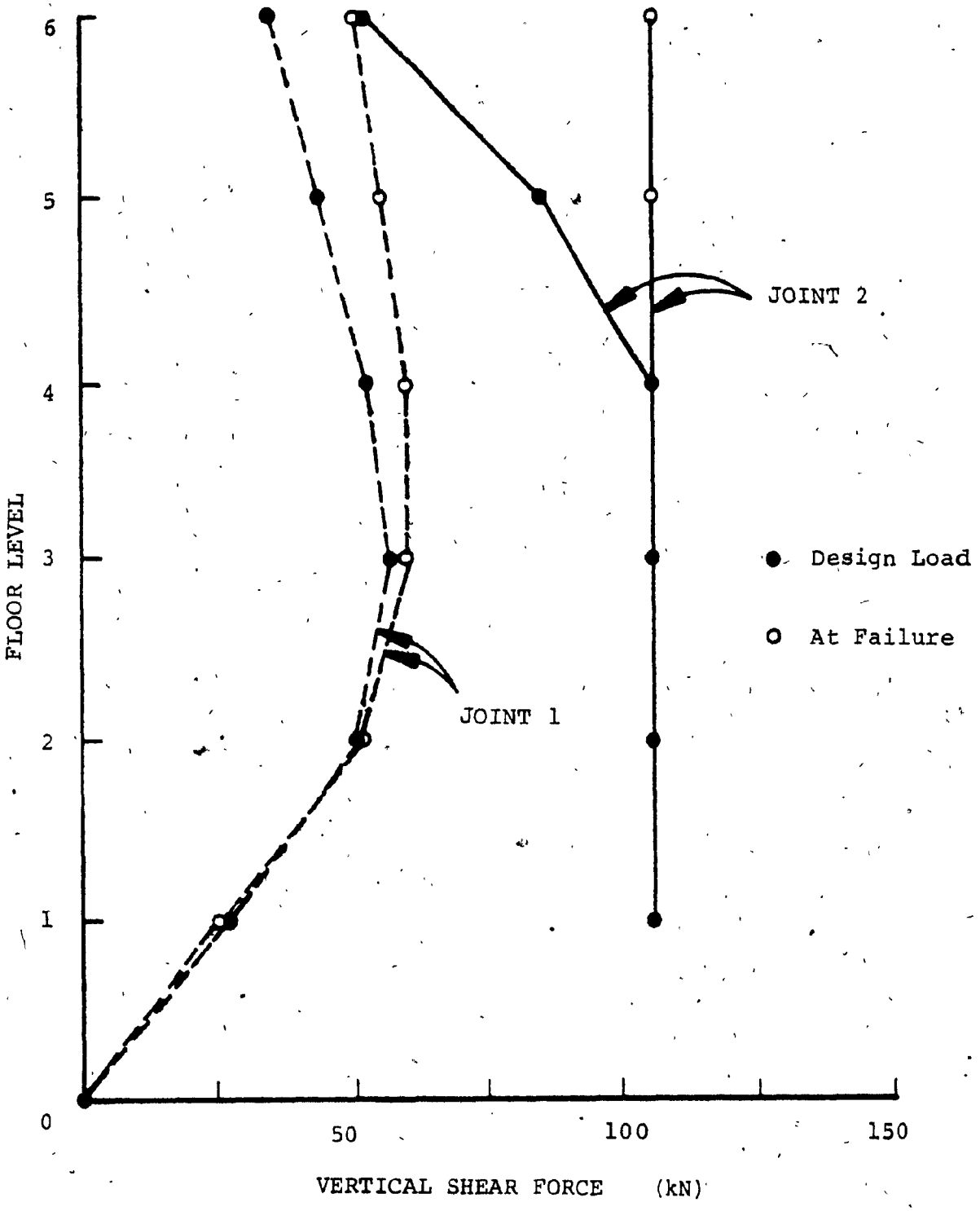

FIG. 3.45 SHEAR FORCE DISTRIBUTION IN VERTICAL JOINTS 1 AND 2 OF 6 STOREY PRECAST PANEL WALL (NO VERTICAL TIES) AT DESIGN LOAD LEVEL AND AT FAILURE - 5 STOREY CANTILEVER

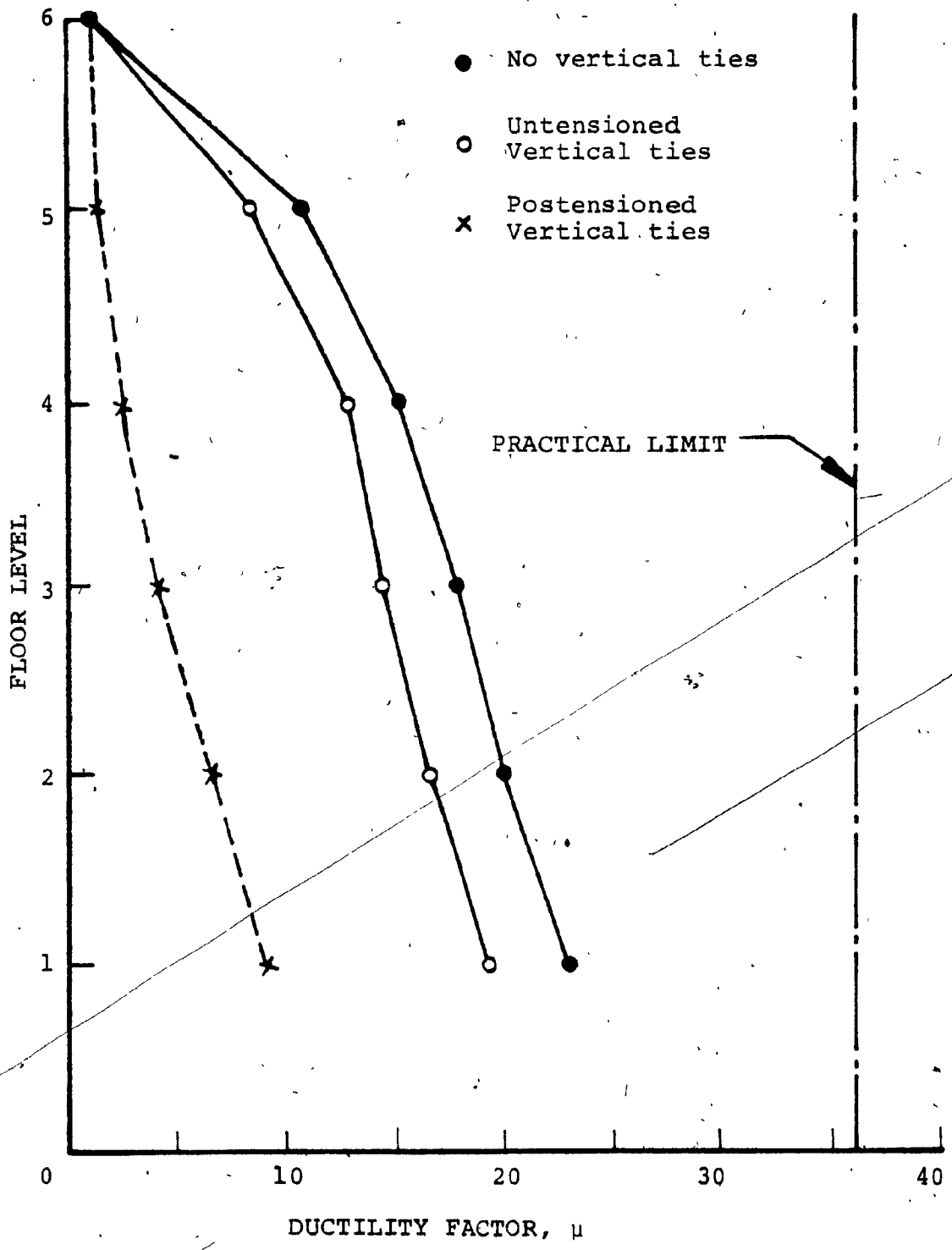

FIG. 3.46 DISTRIBUTION OF DUCTILITY DEMAND IN VERTICAL MECHANICAL CONNECTORS OF 6 STOREY PRECAST PANEL WALL WITH AND WITHOUT VERTICAL TIES AT FAILURE - 5 STOREY CANTILEVER

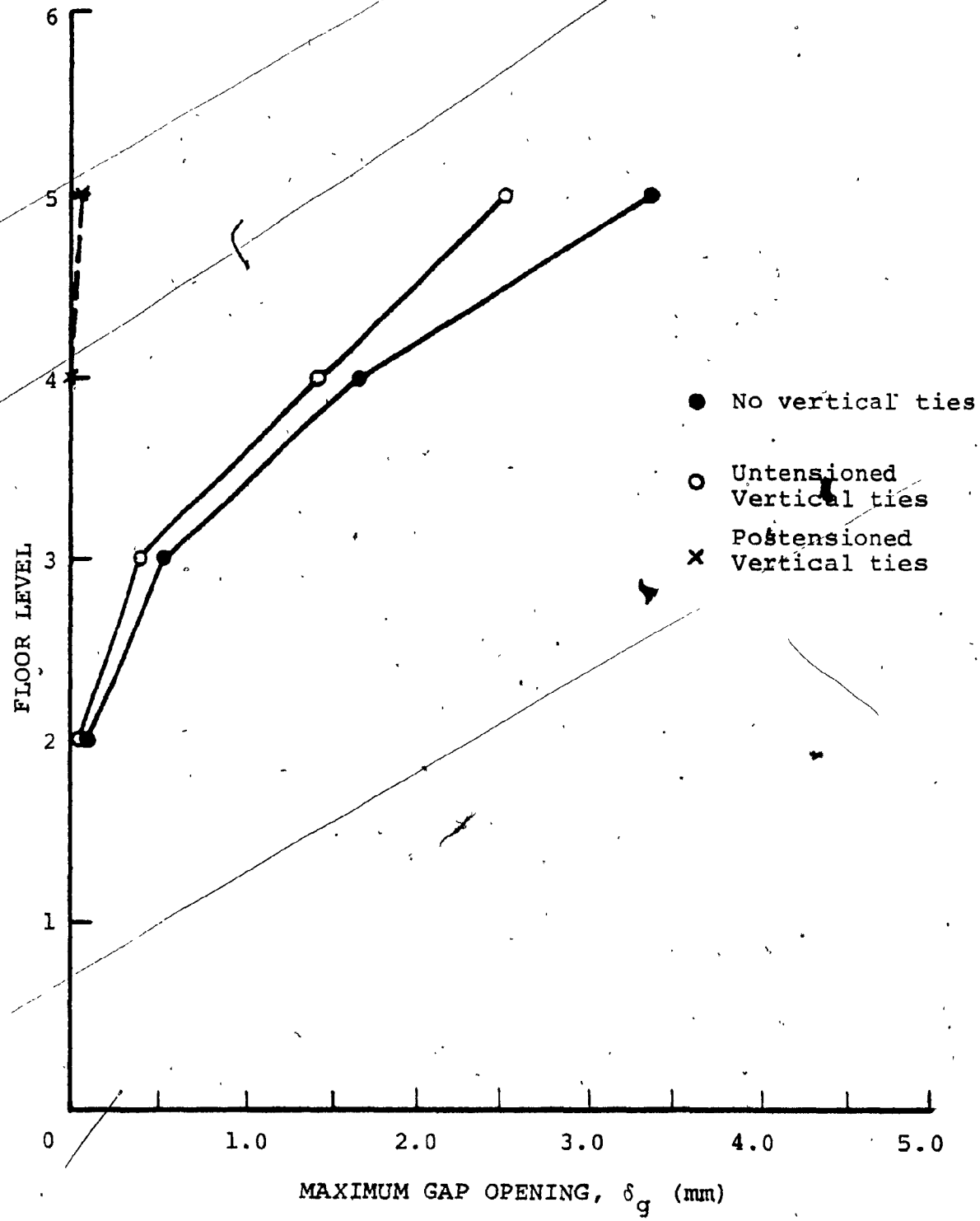

FIG. 3.47 DISTRIBUTION OF MAXIMUM GAP OPENING IN HORIZONTAL JOINTS OF CANTILEVER OF 6 STOREY PRECAST PANEL WALL WITH AND WITHOUT VERTICAL TIES AT FAILURE - 5 STOREY CANTILEVER

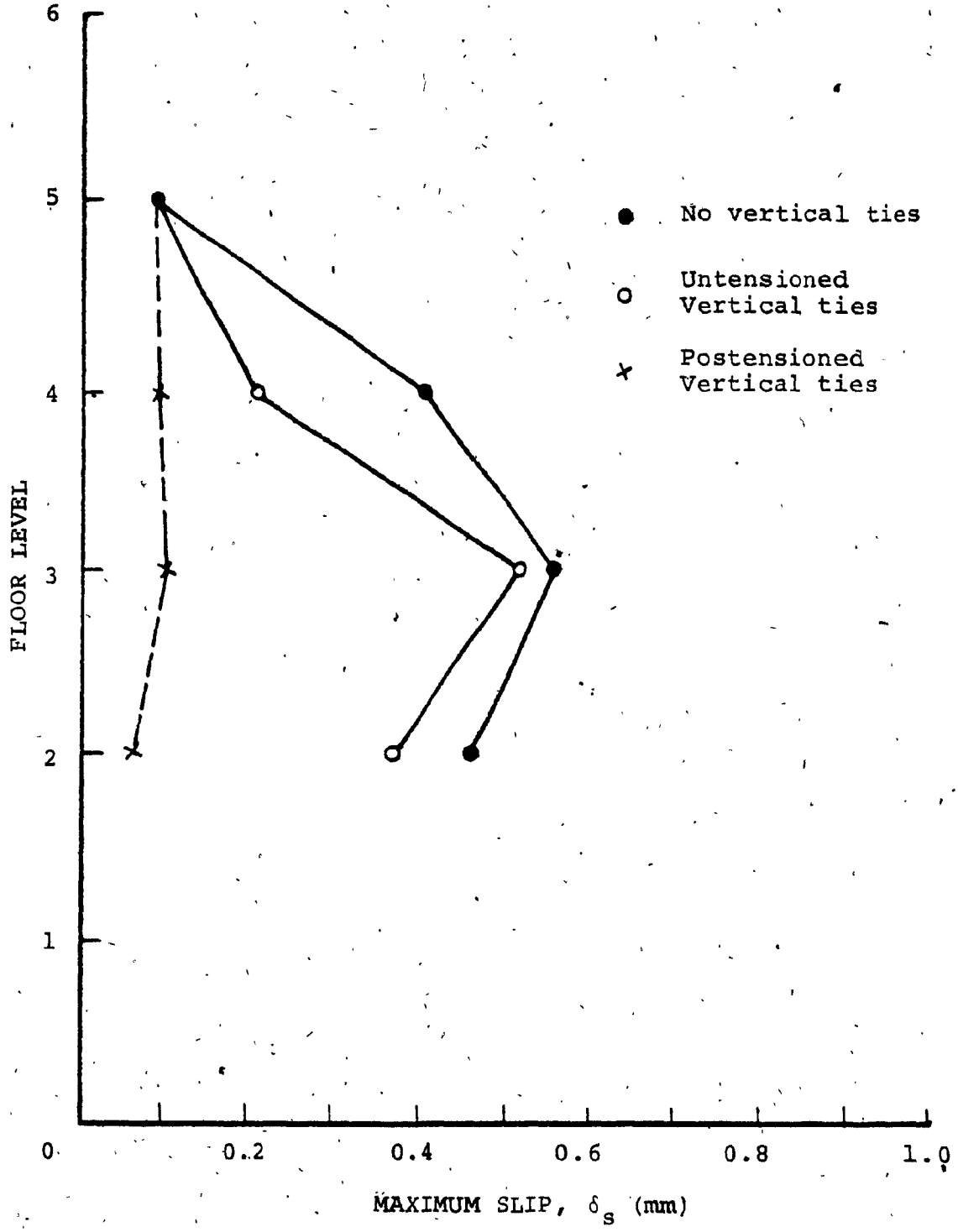

FIG. 3.48 DISTRIBUTION OF MAXIMUM HORIZONTAL SLIP IN CANTILEVER JOINTS OF 6 STOREY PRECAST PANEL WALL WITH AND WITHOUT VERTICAL TIES AT FAILURE - 5 STOREY CANTILEVER

CHAPTER IV

DYNAMIC BEHAVIOUR OF A 6-STOREY PRECAST PANEL WALL

CHAPTER IV

DYNAMIC BEHAVIOUR OF A 6-STOREY PRECAST PANEL WALL

4.1 INTRODUCTION

In recent years, the liability of large precast panel buildings to progressive collapse has been a major concern. It is recognized that structural integrity is not inherent in panelized building systems due to lack of continuity and ductility introduced by joint regions. As a result, panelized buildings are more susceptible to progressive collapse. In general, a progressive collapse condition may arise from any form of abnormal load, such as gas explosions, impact or shock loadings, earthquake excitation, etc. To preclude potential catastrophic failure under such conditions, it is generally recognized that some local damage should be permitted within the structure. However, the structure must be designed such that it has the ability to redistribute the stresses away from the point of local failure, and most importantly, to maintain the overall stability of the partially damaged structure.

The Portland Cement Association (PCA) [4],[5] has carried out comprehensive studies on the behaviour of large panel structures subjected to abnormal loads. Structural integrity is examined for panelized systems with various

panels removed to model conditions of progressive collapse. Analyses were made based on a rigid-cantilever approach for the critical condition where an exterior panel in a precast wall becomes ineffective. In related studies, Muskitvitch and Harris [6],[7] examined the experimental behaviour of a 3/32-scale large panel building under simulated progressive collapse conditions. The effects of non-linear characteristics of joints and panels on the behaviour of partially damaged precast walls were also studied using the finite element method [8]. The most critical aspects of cantilever behaviour were found to be the local bond stress transfer mechanism of the transverse ties, the shear slip behaviour of the horizontal joints, as well as the adequacy of the vertical support provided for the cantilever walls.

The recent work by Pekau [14] investigated the structural integrity of precast panel walls for elastic behaviour. The finite element method was employed for the analysis with panels modelled as multi-level substructures, whereas joints were modelled as orthogonal spring elements.

Alexander and Hambly [2] developed a method for the design of load-bearing walls and floor slabs to withstand gas explosions. It was assumed that reinforced concrete behaves rigid-plastically and hinge mechanisms form at yield conditions under the effects of dynamic loading. Equations

of motions were derived for the individual walls and slabs based on the assumed plastic hinge mechanisms. It was suggested that these elements can be designed to withstand gas explosions by providing sufficient reinforcement.

The foregoing experimental and analytical investigations, with the exception of Reference [2], have been limited to evaluations of the static stability of the damaged structure, i.e., the local failure was assumed to take place in a quasi-static manner. Corresponding studies for dynamic stability have not been reported to-date. In response to the dynamic effects of abnormal loads, local failure will typically take place in a short duration of time instead of in a quasi-static manner. As a result, it is reasonable to expect that the stability of the panelized system is more uncertain under the dynamic effects of local failure.

The purpose of this Chapter is to establish a modelling procedure which attempts to examine the dynamic stability of precast panel shear walls, when a panel becomes ineffective after failure due to transient dynamic loadings. To evaluate the response of the structure under such conditions, the complete time-history of the transient loading must be known. However, owing to the fact that the transient loading may occur due to a wide variety of causes, the essential characteristics of the loading may not be

confidently predicted. The present investigation considers the effects of domestic gas explosions, since the pressure pulses associated with this type of loading have been reported in the literature [29],[30].

The finite element procedure is employed for the nonlinear dynamic analysis of a 6-storey precast shear wall structure (Figure 4.2). The analytical model employed for this investigation is described in Section 2.5, whereas the dimensions and properties of the prototype wall are summarized in Tables 2.1 and 2.2. The conditions for local failure are simulated by assuming that a panel collapses in a short duration of time in response to a domestic gas explosion. The investigation was performed using the general purpose finite element program ANSR-I [27] modified as described in an earlier study by Pekau and Wulf [22].

4.2 DOMESTIC GAS EXPLOSIONS IN LARGE PANEL STRUCTURES

Following the inquiry of the Ronan Point incident [1], comprehensive studies have been reported in the literature[29], [30] regarding evaluations of pressure pulses associated with domestic gas explosions. The British Building Regulations [31] adopted the requirement that structural elements must be designed to resist a pressure of 34 kN/m^2 from any direction, for buildings over four storeys in height.

Figure 4.1(a) shows typical pressure-time curves for gaseous reactions associated with large and small venting areas. The dashed line indicated in Figure 4.1(a) represents pressure that would build up if no relief occurred. The maximum pressure that might be reached in a domestic explosion is affected by a large number of variables [29], which includes the characteristics of the gas mixture and the enclosure, the internal layout, the vent release pressure, and the venting area. A theoretical maximum pressure of up to 700 kN/m^2 may be reached if the gaseous reaction takes place in a closed compartment under adiabetic conditions† [30]. This considerably exceeds the pressure to which domestic structures can be designed. On the basis of tests, Rashbash [29] and others [30] suggested empirical formulae for determining the maximum pressure developed in a vented domestic gas explosion. For design purposes, Mainstone [30] recommended that the probable maximum pressure lies within the range 25-50 kN/m^2. The time taken for the maximum pressure to build up is in the order of 0.1 to 1.0 seconds, depending on the apartment size, as well as the gas composition and

---

†The system, in which the reaction takes place, is isolated from its surroundings as regards heat transfer.

available venting, which results in essentially uniform pressure over the entire surface subjected to the explosion at any instant of time [30].

As discussed earlier, it is reasonable to allow local failure to occur within the structure under gas explosions, but ensuring that overall structural stability is maintained. It is evident that this local failure will typically occur in a finite time, owing to the fact that the resistance of the structural element must be overcome by the pressure pulse to bring it to collapse.

For the purpose of this investigation, the pressure-time curve associated with an internal gas explosion is idealized as an equilateral triangle, assuming the explosion takes place in a typical domestic room where sufficient explosion relief (venting) such as windows and doors are provided. The corresponding duration of the idealized pressure-time curve t_d is taken as 0.60 seconds, with time of maximum pressure t_m of 0.30 sec., as illustrated in Figure 4.1(b).

Consider now the prototype structure (Figure 4.3) subjected to the above-mentioned gas explosion, causing the design strength of the exterior panel to be exceeded and resulting in a local collapse. The time at which the panel collapses due to the explosion is dependent primarily upon the ratio of the duration of the pressure pulse, t_d, to

the fundamental period of the panel, T_1, in the lateral direction in which the pressure acts. Assuming that the pressure due to the explosion at any instant is uniformly distributed over the panel surface, the fundamental frequency, ω_1, of a panel with simply supported edges can be expressed as [32]:

$$\omega_1 = \pi^2 \left[\frac{Et^3}{12(1-\nu^2)m}\right]^{1/2} \left(\frac{1}{h^2} + \frac{1}{b^2}\right)$$

where

E = Young's modulus

ν = Poisson's ratio, and

m = mass density

and

h,b,t are respectively, the height, the width, and the thickness of the panel.

For the values of the material properties and dimensions summarized in Table 2.1, ω_1 is calculated as 368 radians per sec. The corresponding fundamental period, T_1, is given as $2\pi/\omega_1 = 0.017$ sec., which results in $t_d/T_1 = 35.0$. For such a large ratio of t_d to T_1, the time of maximum response of the panel coincides with the time of maximum applied pressure t_m [32], considering the response is similar to that of one degree elastic undamped system (initially at rest).

As a result, the time at which the panel collapses, t_c, will be taken to correspond to the time of maximum response, i.e., $t_c = t_m$.

Under normal conditions, the horizontal joints are subjected to compressive and shear forces due to gravity loading. These joint forces are represented by the axial force, F_a, and shear force, F_s, in the discrete orthogonal spring elements modelling the horizontal joints as shown in Figure 4.3(b). However, only insignificant forces occur in the vertical mechanical connectors under such conditions. Subsequent to the gas explosion the exterior panel fails and becomes ineffective, which is accompanied simultaneously by a reduction of the forces exerted on the surrounding panels by the joints. The time at which the joint forces reduce to zero must therefore coincide with the time of collapse, t_c, of the panel which in turn equals the time of maximum pressure, t_m, as discussed earlier. In order to simulate the effect of the duration of local failure due to the explosion, the analysis of the response of the structure involves the dynamic consideration of the time dependent joint forces, $F_a(t)$ and $F_s(t)$, surrounding the ineffective panel. These joint forces are represented by a triangular dynamic load function with duration equal to t_c, shown in Figure 4.3(c).

4.3 DYNAMIC BEHAVIOUR OF PROTOTYPE WALL WITH VARIABLE CANTILEVER

Since a panel may become ineffective at any level, the study was carried out on the 6-storey prototype structure with cantilever height varying from one to five storeys in depth (see Figure 4.3). In each case, the dynamic analysis was typically preceded by a static analysis of the intact structure under gravity loading, for which the state of stress as well as the displacement configuration of the complete structure are obtained. These stresses and displacements are then used as prescribed initial conditions for the nonlinear dynamic analysis immediately to follow.

To model the force conditions of local failure due to the gas explosion with pressure-time curve shown in Figure 4.1(b), the forces exerted on the damaged structure by the collapsing panel (Figure 4.3) are assumed to decrease linearly from the start of the explosion to zero at $t_c = 0.3$ sec. (see Figure 4.3(c)). Under the influence of the sudden collapse of a panel, the maximum response of the structure is expected to be reached in a short time also; therefore, only the undamped response is considered.

The nonlinear dynamic behaviour of the prototype structure is evaluated in terms of overall structural response, the magnitude and distribution of forces and deformations in the joints, as well as forces in the ties. In particular, the

following are studied in detail:

1) Time history response of cantilever deflection;
2) Distribution of maximum force in transverse ties;
3) Ductility demand in vertical mechanical connectors;
4) Distribution of maximum gap opening in horizontal joints; and
5) Distribution of maximum shear slip in horizontal joints.

The results are compared with the nonlinear static response obtained in Section 3.2. In addition, the magnitude and distribution of design tie force are compared with those obtained using the rigid-cantilever approach proposed by the PCA [5].

Figure 4.4 shows the time history response of cantilever tip deflection, δ_v, for cantilevers of 1, 3, and 5 storeys. It can be observed that in all cases, the maximum cantilever deflection is reached shortly after the panel collapse time, t_c = 0.3 sec.

A comparison of maximum deflections between the nonlinear static and dynamic response for the damaged structure with varying cantilever depths is presented in Table 4.1. The data show that the influence of dynamic effects on the

maximum deflection increases with increasing cantilever height. For example, the dynamic response for the 5-storey cantilever is 49% larger than that for static response, whereas the corresponding increase for the 2-storey cantilever is only 16%. For design of higher structures against progressive collapse, these results suggest that it becomes increasingly more important to consider the dynamic effects of abnormal loads. The complex time history response of typical vertical and horizontal joint forces are shown in Figures 4.5 and 4.6.

Comparisons of the static and dynamic response parameters are summarized in Table 4.2. For design purposes, the dynamic effects in the response of the structure are best evaluated based on the envelopes of maximum response with cantilever height varying from one to five storeys, as presented in Figures 4.7 through 4.13, and Table 4.3. In particular, the following observations are noted:

(i) The envelope for maximum transverse tie force (Figure 4.7) obtained from the dynamic analysis shows larger tie force requirement at most levels, compared to static and rigid cantilever analysis, with values greater than the 80 kN minimum tie design force [5] for only the upper two floor levels. In particular, there is an increase of force level of 13% for the uppermost tie where the force requirement is at its

maximum. At level 5, the force obtained from the dynamic analysis shows an increase of 24% and 62%, respectively, over static and rigid-cantilever analyses.

The design strength envelope is also shown in Figure 4.7. The diagram shows that the force requirement in transverse ties is satisfied at all floor levels for nonlinear dynamic behaviour, with the exception at the fifth level, where the force (84.7 kN) exceeds the design strength of 80 kN (minimum tie force).

(ii) The pseudo-static resultant from maximum force envelopes for transverse ties with varying cantilever height is shown in Figure 4.8. The diagram shows that the resultant force increases with the height of the cantilever, in contrast with static and rigid-cantilever analysis where forces are seen to be approximately constant for cantilevers deeper than one storey. Table 4.3 summarizes the equivalent lever arm for varying cantilever depths. It can be seen that with the exception of the 1-storey cantilever, the ratio between the equivalent lever arm and the cantilever height ranges from 0.76 to 0.79 for various cantilever depths, which compares well with the corresponding ratio obtained from the static analysis (0.77 to 0.79).

In Figure 4.9 the lever arm is plotted as a function of cantilever height for the three different analyses considered. The diagram shows that the lever arms computed from the various analyses are in good agreement for cantilevers up to five storeys in height. These results demonstrate that, since the lever arm for any cantilever height is nearly the same for dynamic and static response, the dynamic increase in overturning moment is resisted by larger resultant force in the transverse ties.

(iii) Envelopes of ductility demand in the vertical mechanical connectors are shown in Figure 4.10. As indicated in the diagram, the ductility requirement increases approximately by an average of 50% at all floor levels due to dynamic effects.

(iv) The envelopes of maximum gap openings in horizontal joints show much larger values at all floor levels indicating a higher requirement for vertical continuity when loading is dynamic (Figures 4.11 and 4.12). In Figure 4.11 the maximum gap opening in cantilever joints which occurs at the uppermost horizontal joint shows an increase of 152.4% over the static response. In Wall 1, the dynamic effects lead to an increase in maximum gap opening of 336.4% at level 1 (Figure 4.12).

(v) As is expected, the envelope values of maximum slip in horizontal joints of the cantilever are substantially larger than static values at all floor levels, with a maximum increase of 89.6% at the fourth level (Figure 4.13).

Based on the above observations, it is noted that the dynamic response in terms of cantilever deflection and resultant force in transverse ties increases with the height of the cantilever. Also, the lever arm is constant at approximately 80% of the overall cantilever height for cantilevers deeper than one storey, which is the same as that obtained from static analysis. However, the corresponding resultant of maximum forces in transverse ties is generally higher with an increase of 64% for the 5 storey cantilever (see Table 4.2). These results indicate that for the design of transverse ties in higher structures, it is essential to include the dynamic effects of abnormal loads. Furthermore, it was shown that the forces in transverse ties obtained from the rigid-cantilever analysis are considerably lower at the upper floor levels. In particular, the tie forces in only the uppermost two floor levels exceeded the PCA [5] recommended minimum of 80 kN.

An important observation is that the maximum tie force was found to be 129.9 kN at the uppermost level (for a 1-storey cantilever), while the design strength is 142 kN.

However, it was shown that at the fifth floor level the tie force (84.7 kN) exceeds the design strength of 80 kN (minimum tie force). Hence, it may be concluded that at the design load level[†] the recommended minimum tie force of 80 kN by the PCA [5] is not sufficient when the dynamic collapse of a panel is considered.

Finally, it was noted in Section 4.2.4, that the ductility demand in mechanical connections may exceed the practical ductility limit for structures higher than 12 storeys under the static response. The present results suggest that the practical ductility limit will be reached in shorter structures when the dynamic collapse of a panel is considered.

4.4 PARAMETRIC INVESTIGATION OF THE DYNAMIC BEHAVIOUR FOR A 5-STOREY CANTILEVER

A parametric investigation is carried out to examine the influence of joint parameters and dynamic parameters on the response characteristics of precast panel walls to local failure initiated by abnormal loading.

[†]Design load level, $W = W_d + 0.5\, W_\ell$, where W_d and W_ℓ are the dead load and live load, respectively.

The investigation was conducted on the 6-storey precast panel wall for a maximum height cantilever, i.e., the lowest exterior panel was assumed to be affected by the gas explosion as described in Section 4.2. The dimensions and properties of panels and joints for the 6-storey precast wall are the same as those summarized in Tables 2.1 and 2.2.

Response characteristics are evaluated in terms of structural displacement, as well as the magnitude and distribution of joint forces and deformations. The investigation follows a parametric scheme where the principal parameters are:

1) Vertical tie reinforcement and postensioning;

2) Coefficient of friction μ_f;

3) Mechanical connector shear strength F_y; and

4) Dynamic response parameters R/W and t_c.

4.4.1 Effect of Vertical Tie Reinforcement and Postensioning

To provide vertical continuity, vertical ties of high strength steel bars are installed through lifts of wall panels (Figure 4.2). Additional vertical continuity

was provided in one case by postensioning each bar to a stress level equal to 60% of its ultimate capacity. Material properties and modelling of the vertical ties are described in Section 3.5.2, whereas the stiffness properties are given in Table 2.2.

Figure 4.14 shows the effect of vertical ties on the time history response of cantilever tip deflection δ_v for t_c = 0.3 sec. It can be observed that the provision of postensioned vertical ties significantly reduces the maximum deflection to a level comparable to that of nonlinear static deflection, whereas in the case of untensioned ties the maximum deflection is only reduced by 10.6%.

The effect of vertical ties on the magnitude and distribution of maximum joint forces and deformations are shown in Figures 4.15 through 4.19. The following observations are noted:

(i) The distribution of maximum axial force in the vertical joint is little affected by the presence of either untensioned or postensioned ties. In the case of postensioned ties the force at the uppermost level is reduced by 28.4%; however, this is compensated by larger tie forces at intermediate levels (Figure 4.15).

(ii) The maximum ductility requirement (at the lowest level in a cantilever) in mechanical connectors is reduced by 17.9% and 40.7%, respectively, for untensioned and postensioned ties (Figure 4.16).

(iii) The effectiveness of postensioned ties in reducing joint openings in horizontal joints within the cantilever is shown in Figure 4.17. However, in Wall 1 comparable magnitudes of joint openings in horizontal joints are observed with and without ties (Figure 4.18). In particular, the magnitudes of joint openings were found to be the largest for the upper horizontal joints in the case of untensioned ties.

(iv) Maximum slip in horizontal joints within a cantilever is considerably decreased when postensioned ties are used, as shown in Figure 4.19. The computed maximum slip in the case of untensioned ties is also reduced at all floor levels but only by an average of 15%.

It can be concluded that the addition of untensioned vertical ties has only a minor effect on computed response. However, the results show that the ductility demand and joint deformations are much reduced by postensioning.

4.4.2 Effect of Coefficient of Friction μ_f

It has been reported [4] that the coefficient of friction, μ_f, between precast concrete panels and the grout in horizontal joints ranges from 0.2 to 0.8 in various specifications. The analyses reported in Section 4.3 assumed $\mu_f = 0.4$.

In this section, the response characteristics of the precast system for two values of the coefficient of friction are examined, namely $\mu_f = 0.4$ and $\mu_f = 0.7$. Figure 4.20 shows the comparison of time history response of cantilever tip deflection, δ_v, for $\mu_f = 0.4$ and $\mu_f = 0.7$. It can be noted that the deflection is identical up to a duration of about 0.35 seconds, after which the deflection becomes slightly larger for $\mu_f = 0.7$. It can therefore be expected that for $\mu_f = 0.7$, which provides higher shear resistance in the horizontal joints, the structure will vibrate with a period slightly shorter than for $\mu_f = 0.4$. If the response of the cantilever deflection is taken to be similar to that of one-degree elasto-plastic undamped system (initially at rest) subjected to impulsive loadings of duration t_c, then maximum response must increase due to the increase of the ratio of t_c to the period of vibration [32]. The maximum axial forces at floor levels along the vertical joints were

essentially the same for $\mu_f = 0.4$ and $\mu_f = 0.7$. This indicates that the force requirement in transverse ties is not sensitive to μ_f under the dynamic effect of local failure. However, differences in joint deformations were observed as presented in Figures 4.21 through 4.24. The following are noted:

(i) For $\mu_f = 0.7$, the ductility demand in vertical mechanical connectors is increased (by approximately 10%) at all levels along the height of the cantilever, (Figure 4.21). This increase is attributable to the higher cantilever deflection shown in Figure 4.20.

(ii) The computed maximum opening in horizontal joints within the cantilever is also increased by an average of 38% for $\mu_f = 0.7$, with exception at the lowest joint where the value of joint opening is seen to be lowered by about 33% (Figure 4.22). However, the magnitude of joint opening in Wall 1 is found to be generally lower than that for $\mu_f = 0.4$ (Figure 4.23).

(iii) As indicated in Figure 4.24, the magnitude of maximum slip in horizontal joints of the cantilever were reduced at most levels, for $\mu_f = 0.7$, owing to the fact that shear resistance in the horizontal

joints is comparatively higher than that for $\mu_f = 0.4$.

The results presented show that use of a coefficient of friction higher than $\mu_f = 0.4$ in horizontal joints can result in slightly higher ductility demand in mechanical connectors, and also larger gap openings in horizontal joints within the cantilever. The magnitude of joint openings in Wall 1 and shear slip in horizontal joints within the cantilever were found to be somewhat lower for $\mu_f = 0.70$. However, it appears that the value of μ_f, if chosen within the practical range 0.2 to 0.8 will not significantly affect most of the computed response parameters.

4.4.3 Effect of Vertical Mechanical Connector Shear Strength F_y

The shear strength F_y of the welded headed stud mechanical connectors used in vertical joints (Figure 2.11(d)) is governed predominantly by several factors, which include the characteristics of the studs, the connector angles and plates, the weld quality, the embedment properties, the concrete strength and the loading history, as well as the behaviour in combined shear-tension loading. Practical design data [28] and test results [33] indicate that the shear capacity of connectors can range from 24 to 289 kN, depending on the size and number of stud anchors employed.

The analyses reported earlier employed a shear strength F_y = 104 kN, corresponding to the strength of 2 - 12.7 × 155.6 mm headed stud anchors per connector.

To evaluate the influence of the shear strength F_y on response characteristics of the damaged structure, the value of F_y has been increased to 146 kN(for 2 - 15.9 × 166.7 mm headed anchors). For comparison, analysis was also carried out using $F_y = 10^5$ kN, which represents elastic behaviour of the connectors.

Figure 4.25 shows the time history response of cantilever tip deflection, δ_v, using various shear strengths; namely, F_y = 104 kN, F_y = 146 kN, and $F_y = 10^5$ kN (elastic behaviour). It can be seen that for F_y = 104 kN, the maximum deflection is considerably larger for F_y = 146 kN and $F_y = 10^5$ kN. Therefore, it can be expected that F_y will significantly affect the nonlinear dynamic response of the structure in the damaged state.

The distribution of maximum shear force in vertical joints 1 and 2 are shown in Figures 4.26 and 4.27. In vertical joint 1, the distribution is similar to that obtained in static analysis (Section 3.2.3) for all three cases, with no yielding occurring throughout the joint. However, in vertical joint 2 the shear strength is reached at most connectors for F_y = 104 kN, except at the uppermost connector. For the case of F_y = 146 kN, yielding occurs in the

connectors at the lower three floor levels, with the forces in the upper connectors remaining elastic. The force distribution for $F_y = 10^5$ kN deviates considerably from the above two cases, with significantly larger shear force concentrated at the lowest connector in the cantilever. The corresponding ductility factors of the mechanical connectors for two values of F_y are shown in Figure 4.28. It can be noted that ductility demand is substantially larger for $F_y = 104$ kN.

The distributions of maximum axial force in the vertical joint, as well as the deformations in horizontal joints for various cases are shown in Figures 4.29 through 4.31. The following are to be noted:

(i) The force requirement in the uppermost transverse tie is substantially higher (about 50%) for $F_y = 104$ kN, as compared to the other two cases. The latter, however, produce relatively higher tie forces for the intermediate floor levels as illustrated in Figure 4.29.

(ii) For $F_y = 104$ kN, significantly larger joint openings are observed in the horizontal joints within the cantilever, as can be seen in Figure 4.30. In Wall 1, more comparable magnitudes of joint openings were obtained for all three cases (Figure 4.31).

(iii) In Figure 4.32, it can be noted that there is a considerable difference in the distribution of maximum slip in the horizontal joints within the cantilever for various values of F_y. In general, the value of maximum slip obtained is much higher at all floor levels for F_y = 104 kN.

Based on the above observations, the nonlinear dynamic response of the system appears to be greatly influenced by the shear strength parameter under the effects of abnormal loads. For large values for F_y, it may be expected that the distributions of maximum axial and shear force in the vertical joints follow those for elastic behaviour in shear accompanied by reduced deformations in the joints. In particular, the ductility demand in the mechanical connectors can be effectively reduced by providing relatively higher shear strength.

4.4.4 Effect of Dynamic Response Parameters R/W and t_c

In the previous analyses, the collapse time t_c of the exterior panel associated with a typical domestic gas explosion was established as 0.3 sec. For dynamic analysis the value of t_c also represents the rate of decrease of forces in the joints connecting the affected panel, modelled by the triangular load-time function shown in Figure 4.3(c).

Therefore, for design purposes the collapse time t_c is an important parameter which requires careful consideration. Furthermore, the essential response characteristics of the cantilever are dependent primarily upon the relationship between the ratio of the maximum resistance to the applied load, and the ratio of the collapse time to the effective period of the structure.

For the following discussions, it is convenient to define the parameter R as the maximum resistance of the cantilever, which is numerically equal to the total shear strength of mechanical connectors in the vertical joint adjacent to the cantilever (Section 3.3.4). Also, the parameter W will refer to the load on the cantilever. The investigation presented in this section involves the variation of the ratio R/W and the panel collapse time t_c. In particular, the following cases are considered:

1) R/W = 1.02 (R = 1464 kN; W = 1431 kN)
2) R/W = 1.12 (R = 1044 kN; W = 936 kN)
3) R/W = 1.56 (R = 1464 kN; W = 936 kN)

It should be noted that the ratio R/W = 1.12 represents the prototype structure, where R = 1044 kN corresponds to the shear strength of 2 - 12.7 × 155.6 mm headed stud anchors per mechanical connector (F_y = 104 kN); and

W = 936 kN is the specified design load level,† recommended by the PCA [5]. On the other hand, the ratio R/W = 1.02 corresponds to the strength of 2 - 15.9 × 166.7 mm headed stud anchors per connector (F_y = 146 kN) and the factored load level.†† Furthermore, the ratio R/W = 1.56 represents the strength of 2 - 15.9 × 166.7 mm head stud anchors per connector and the design load level.

For each of the above cases, the collapse time is varied from 0.1 to 1.0 sec. The range of collapse time considered here corresponds to the time taken for the maximum pressure to build up during a typical domestic gas explosion (Section 4.2). It can be expected that, for large ratios of R/W, the dynamic response of the cantilever will be essentially elastic.

Table 4.4 contains a summary of the values of maximum nonlinear static response for each of the ratios of R/W considered, which are used as normalizing factors in the data reported herein.

---

†Design load level, $W = W_d + 0.5\ W_\ell$.

††Factored load level, $W = 1.4\ W_d + 1.7\ W_\ell$.

Figures 4.33 through 4.35 show the time history response of cantilever deflection, δ_v, for varying collapse time and three different ratios of R/W. It can be observed that the parameter t_c has a significant effect on the response characteristics of the cantilever deflection. In general, the maximum deflection increases with decreasing collapse time. This is particularly evident for R/W = 1.02, where it can be seen that the displacement response increases abruptly for relatively short t_c (Figure 4.33).

The influence of the ratio R/W on the time history response of cantilever deflection for t_c = 0.3 sec. is shown in Figure 4.36. Clearly, the diagram shows that the response of the cantilever is influenced greatly by the parameter R/W. For R/W = 1.02, the maximum deflection is seen to be several times larger than those of R/W = 1.12 and R/W = 1.56.

The values of maximum response, normalized with respect to the corresponding static response from Table 4.4, are plotted for three different values of R/W as functions of collapse time t_c in Figures 4.37 through 4.42. The following observations are noted:

(i) In Figure 4.37, for all three ratios of R/W, the normalized maximum cantilever tip deflection, δ_v, is seen to be significantly affected by a variation in the collapse time t_c, particularly for $t_c < 0.4$ sec.

For t_c = 0.1 sec., the maximum dynamic response of cantilever deflection is 3.42, 2.15 and 1.82 times the corresponding static deflection, for R/W = 1.02, R/W = 1.12 and R/W = 1.56, respectively. However, for $t_c \geq 0.4$ sec., the dynamic effects lead to increases in cantilever deflection of 52 - 70%, 20 - 30% and 8 - 18%, respectively, for R/W = 1.02, R/W = 1.12 and R/W = 1.56.

(ii) The influence of the collapse time t_c on the normalized maximum force in transverse ties, T_{max}, is presented in Figure 4.38. For R/W = 1.02, the increase in maximum tie force due to the dynamic effects ranges from 64% to 42% for increasing values of t_c, with an increase of 49% at t_c = 0.3 sec. The variation in maximum tie force with the panel collapse time is similar for R/W = 1.12 and R/W = 1.56 with increases of 20 - 74% (R/W = 1.12) and 11 - 69% (R/W = 1.56) for decreasing values of t_c, compared to the corresponding static response. At t_c = 0.3 sec., the increases in maximum tie force are 38 and 35%, respectively, for R/W = 1.12 and R/W = 1.56.

(iii) As noted previously, the maximum ductility demand in vertical mechanical connectors occurs at the lowest level of the cantilever. Figure 4.39 shows the normalized maximum ductility factor, μ, for varying

values of t_c. For R/W = 1.02, it is noted that the maximum ductility demand increases considerably with values ranging from 1.95 to 5.85 times that of the static response for decreasing values of t_c ($\mu/\bar{\mu}$ = 3.19 at t_c = 0.3 sec.). The corresponding increase in maximum ductility demand for R/W = 1.12 varies from 26 to 251%, with an increase of 67% at t_c = 0.3 sec. For R/W = 1.56, however, the increase in maximum ductility demand ranges from 19 to 61% over the static response for $t_c \leq 0.3$ sec. ($\mu/\bar{\mu}$ = 1.19 at t_c = 0.3 sec.), whereas the increase is approximately constant for $t_c \geq 0.4$ sec. (9 - 14%).

(iv) The normalized maximum gap opening, δ_g, in horizontal joints of cantilever and Wall 1 for varying values of t_c are presented in Figures 4.40 and 4.41. The diagram shows that gap openings in horizontal joints of the cantilever (Figure 4.40) is substantially higher than that of the static response for R/W = 1.12 with an increase of 2.13 to 5.66 times the static response for decreasing values of t_c ($\delta_g/\bar{\delta_g}$ = 3.13 at t_c = 0.3 sec.). For R/W = 1.56, the maximum gap opening in cantilever is seen to be unaffected by the dynamic effects for $t_c \geq 0.3$ sec. ($\delta_g/\bar{\delta_g}$ = 0.52 at t_c = 0.3 sec.). Furthermore, the

maximum gap opening in cantilever joints for R/W = 1.02 is approximately constant (54 - 70%) for the range of t_c considered ($\delta_g/\overline{\delta_g}$ = 1.55 at t_c = 0.3 sec.).

In Wall 1 (Figure 4.41) the magnitude of maximum gap opening is observed to be more comparable for all three ratios of R/W. The increases at t_c = 0.3 are 90%, 257% and 184%, respectively for R/W = 1.02, R/W = 1.12 and R/W = 1.56.

(v) For R/W = 1.56, the increase in normalized maximum slip, δ_s, in horizontal joints of the cantilever (Figure 4.42) is influenced greatly by the variation in the value of t_c with substantial increase over that of the static response ($\delta_s/\overline{\delta_s}$ = 7.65 at t_c = 0.3 sec.). However, the corresponding increase is considerably lower for R/W = 1.12 ($\delta_s/\overline{\delta_s}$ = 2.08 at t_c = 0.3 sec.). On the other hand, the maximum slip is approximately constant for R/W = 1.02 with values generally lower than that of the static response (40 to 16%).

The foregoing investigation has examined maximum response for a precast panel wall under dynamic loading associated with a domestic gas explosion. Once the maximum static response is computed, the corresponding

dynamic response can be estimated from the diagrams provided with the aid of Table 4.4.

For t_c < 0.3 sec., the results indicate that the ductility demand in vertical mechanical connectors will substantially exceed the limit to which domestic structures can be designed. For example, the ductility demand in the lowest mechanical connector in the cantilever is 101.7 for R/W = 1.02 at t_c = 0.1 sec., which represents an increase of 485% over that of the static response (μ = 17.4). This considerably exceeds the practical ductility limit of μ = 36 for welded headed stud connectors (Section 3.2.4).

For the prototype structure (R/W = 1.12) at t_c = 0.3 sec., the dynamic effects lead to increases of 74, 115 and 151%, respectively, for the maximum force in transverse ties, the cantilever deflection and the maximum ductility demand in mechanical connectors. The maximum transverse tie force which occurs at the fifth floor level is equal to 84.7 kN, still below the design strength (F_y = 142 kN). In addition, the maximum ductility demand in mechanical connectors is 15.5, compared to the practical ductility limit of 36. It can therefore be concluded that for t_c = 0.3 sec., the performance of the prototype structure will be satisfactory. Furthermore, it also appears that the design value of the panel collapse

time t_c = 0.3 sec. represents a reasonable limit for design consideration.

4.5 CONCLUSIONS

The studies reported herein have examined the response characteristics of a 6-storey precast panel shear wall structure, subjected to a domestic gas explosion. Conclusions which can be made from the studies are as follows:

1) Under the dynamic effects of local panel failure, the pseudo-static resultant from maximum force envelopes for transverse ties increases with increasing cantilever depth. The corresponding lever arm represents approximately 80% of the overall cantilever height for cantilevers deeper than one storey (i.e., d/H = 0.8). The force requirement in transverse ties is shown to be substantially higher than that of the non-linear static behaviour at all floor levels, with maximum increase of 12.4 to 177.2%. On the other hand, the forces produced from the rigid-cantilever [5] are relatively lower at the upper floor levels. In particular, it was shown that the transverse tie force exceeds the design strength (recommended minimum tie force of 80 kN from Ref. [5]) at the fifth floor level at design load.

2) The ductility demand in mechanical connectors increases with the height of the cantilever. Moreover, it was shown that the maximum ductility demand increases by an average of 50% at all floor levels due to dynamic effects.

3) Maximum gap openings in horizontal joints of the cantilever and Wall 1 are substantially larger than those of nonlinear static behaviours. The maximum gap opening in cantilever joints which occurs at the uppermost horizontal joint shows an increase of 152.4%, whereas in Wall 1 the dynamic effects lead to an increase in maximum gap opening of 336.4% at floor level 1.

4) As was expected, significantly larger horizontal shear slip was observed at all floor levels in the cantilever joints, compared with the nonlinear static behaviour. The maximum increase in horizontal shear slip was shown to be 89.6%.

The results of the parameter study allow the following conclusions:

5) The shear strength parameter has a significant effect on the nonlinear dynamic response of the system. For large values of F_y, the magnitudes of joint deformations and ductility demand are found to be much reduced.

6) The results indicate that the use of a higher coefficient of friction μ_f can result in higher ductility demand in mechanical connectors. However, it appears that the value of μ_f if chosen within the practical range 0.20 to 0.80 will not significantly affect the computed response.

7) The provision of untensioned vertical ties can have a minor effect on the computed response. It was noted that the ductility demand and joint deformations are considerably reduced when vertical ties are postensioned.

8) For $t_c < 0.3$ sec., the results indicate that the ductility demand in mechanical connectors will substantially exceed the limit to which domestic structures can be designed. It was observed that for $t_c = 0.3$ sec. the performance of the prototype wall will be satisfactory. Finally, the design value of the panel collapse time, $t_c = 0.3$ sec., was shown to be a reasonable limit for design consideration.

TABLE 4.1 COMPARISON OF MAXIMUM CANTILEVER DEFLECTION FOR NONLINEAR STATIC AND DYNAMIC RESPONSE - 6 STOREY PROTOTYPE STRUCTURE

CANTILEVER HEIGHT IN NO.OF STOREYS, H	MAXIMUM CANTILEVER DEFLECTION (mm)		$\delta_v/\bar{\delta}_v$
	STATIC RESPONSE $\bar{\delta}_v$	DYNAMIC RESPONSE δ_v	
1	9.89	10.75	1.09
2	7.10	8.27	1.16
3	6.81	8.93	1.31
4	6.90	9.65	1.40
5	6.85	10.20	1.49

TABLE 4.2 COMPARISON OF MAXIMUM NONLINEAR STATIC AND DYNAMIC RESPONSE OF 6 STOREY PROTOTYPE WALL - 5 STOREY CANTILEVER

PARAMETER	NONLINEAR RESPONSE		DYNAMIC/ STATIC
	STATIC	DYNAMIC	
Cantilever deflection, δ_v, in mm	6.85	10.20	1.49
Maximum force in transverse ties, T_{max}, in kN	61.3	84.7	1.38
Maximum ductility factor in mechanical connectors, μ	9.30	15.54	1.67
Maximum gap opening in horizontal joints, δ_g, in mm			
- in cantilever	0.507	1.586	3.13
- in Wall 1	0.192	0.684	3.56
Maximum slip in horizontal joints of cantilever, δ_s, in mm	0.539	1.121	2.08

TABLE 4.3 SUMMARY OF RESULTANT FORCE AND EFFECTIVE LEVER ARM FOR 6 STOREY PROTOTYPE WALL - NONLINEAR DYNAMIC BEHAVIOUR

CANTILEVER HEIGHT IN NO.OF STOREYS, H	RESULTANT FORCE T_R OR C_R (kN)	EFFECTIVE LEVER ARM IN NO. OF STOREYS, d	d/H
1	244.52	1.00	1.00
2	224.66	1.58	0.79
3	204.27	2.31	0.77
4	173.84	3.05	0.76
5	129.94	3.83	0.77

TABLE 4.4 VALUES OF MAXIMUM NONLINEAR STATIC RESPONSES FOR THREE DIFFERENT RATIOS OF R/W - 5 STOREY CANTILEVER

PARAMETER	R/W = 1.02*	R/W = 1.12†	R/W = 1.56††
Cantilever deflection, δ_v, in mm	20.71	6.85	5.49
Maximum force in transverse ties, T_{max}, in kN	133.40	61.30	54.62
Maximum ductility factor in mechanical connectors, μ	17.38	9.30	3.72
Maximum gap opening in horizontal joints, δ_g, in mm.			
- in cantilever	3.941	0.507	0.091
- in Wall 1	0.410	0.192	0.215
Maximum slip in horizontal joints, δ_s, in mm	6.913	0.539	0.106

* R = 1464 kN; W = 1431 kN.
† Prototype structure, R = 1044 kN; W = 936 kN.
†† R = 1464 kN; W = 936 kN.

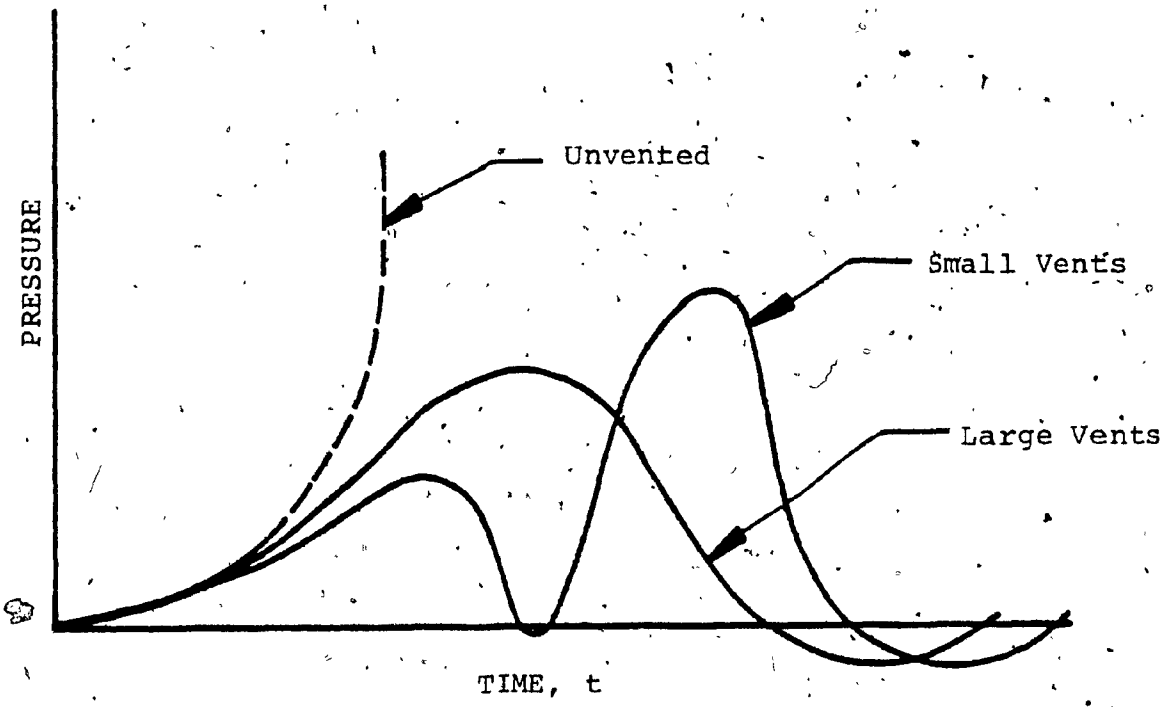

(a)

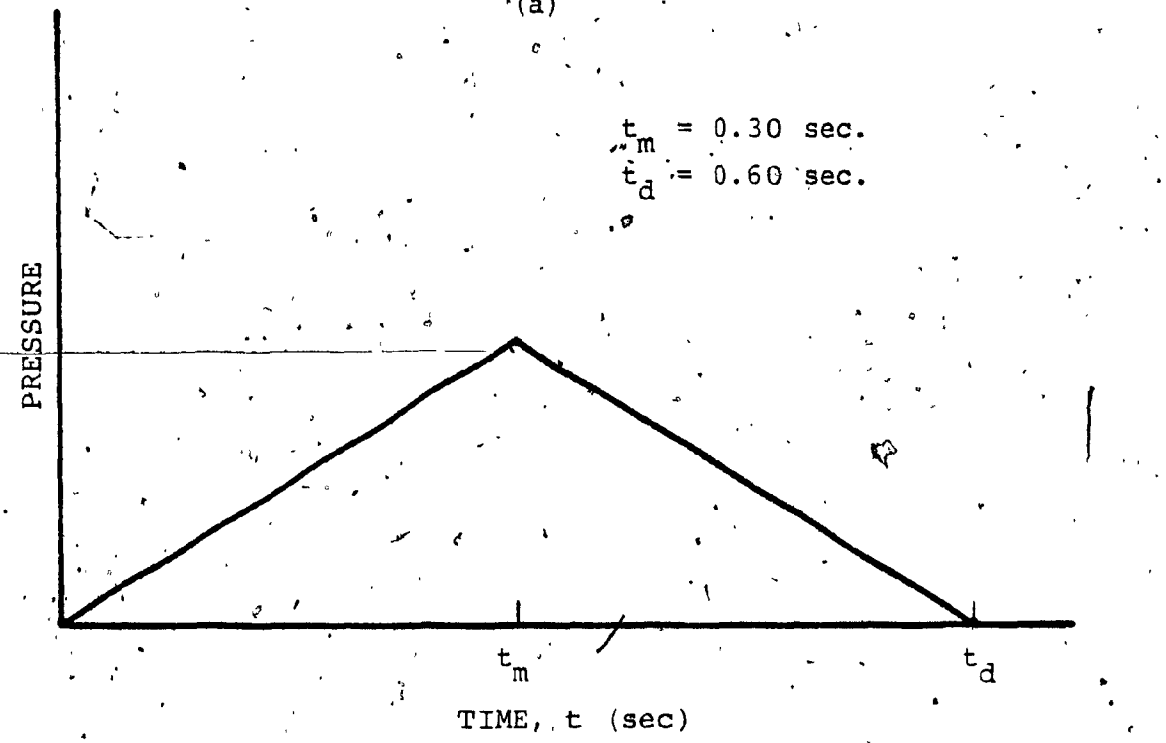

(b)

FIG. 4.1 PRESSURE-TIME CURVES FOR TYPICAL GAS EXPLOSIONS: (a) ACTUAL PRESSURE-TIME CURVE; (b) IDEALIZED PRESSURE-TIME CURVE

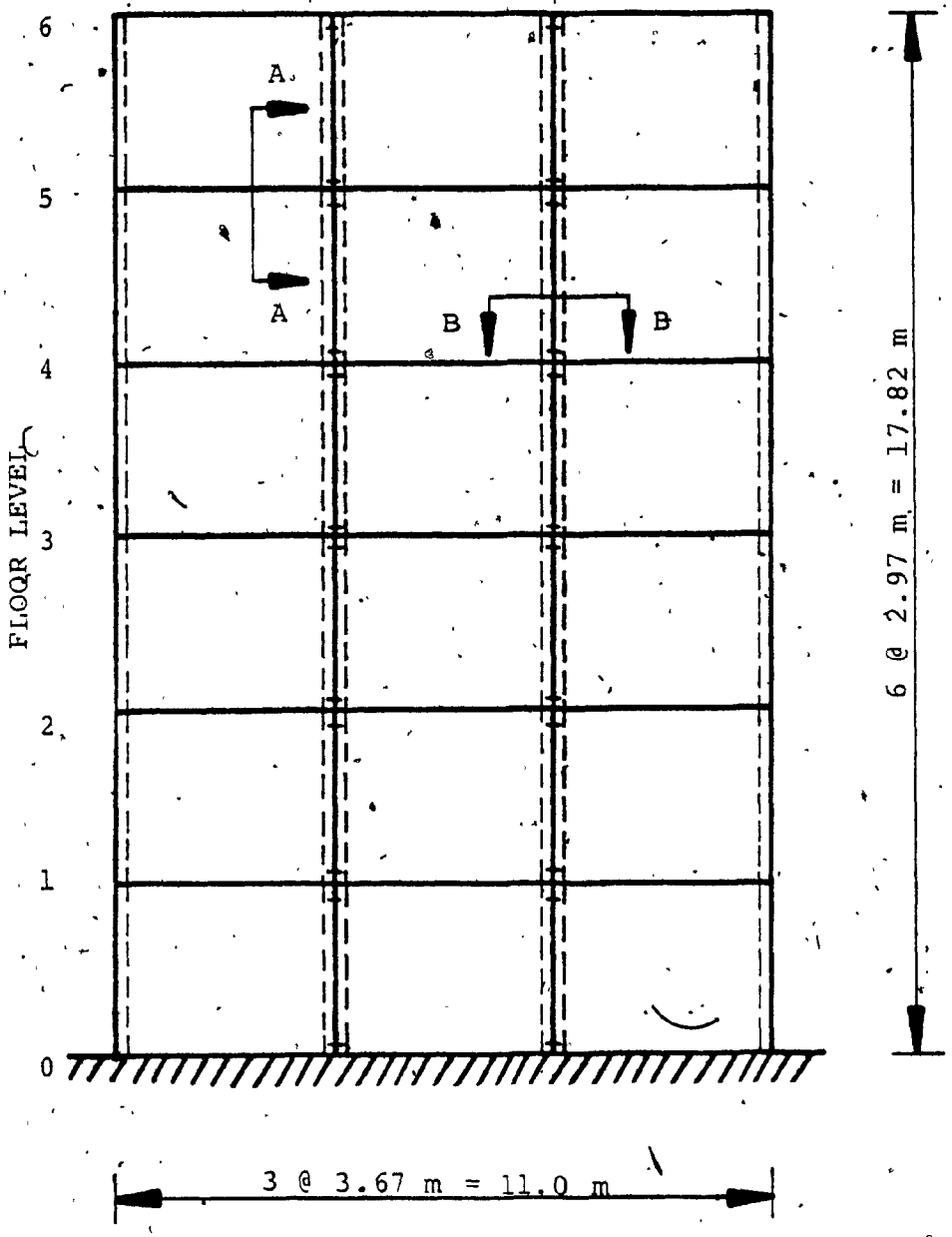

NOTE: For details A-A and B-B, see Figs. 2.11(c) and 2.11(d)

FIG. 4.2 TYPICAL PRECAST PANEL WALL

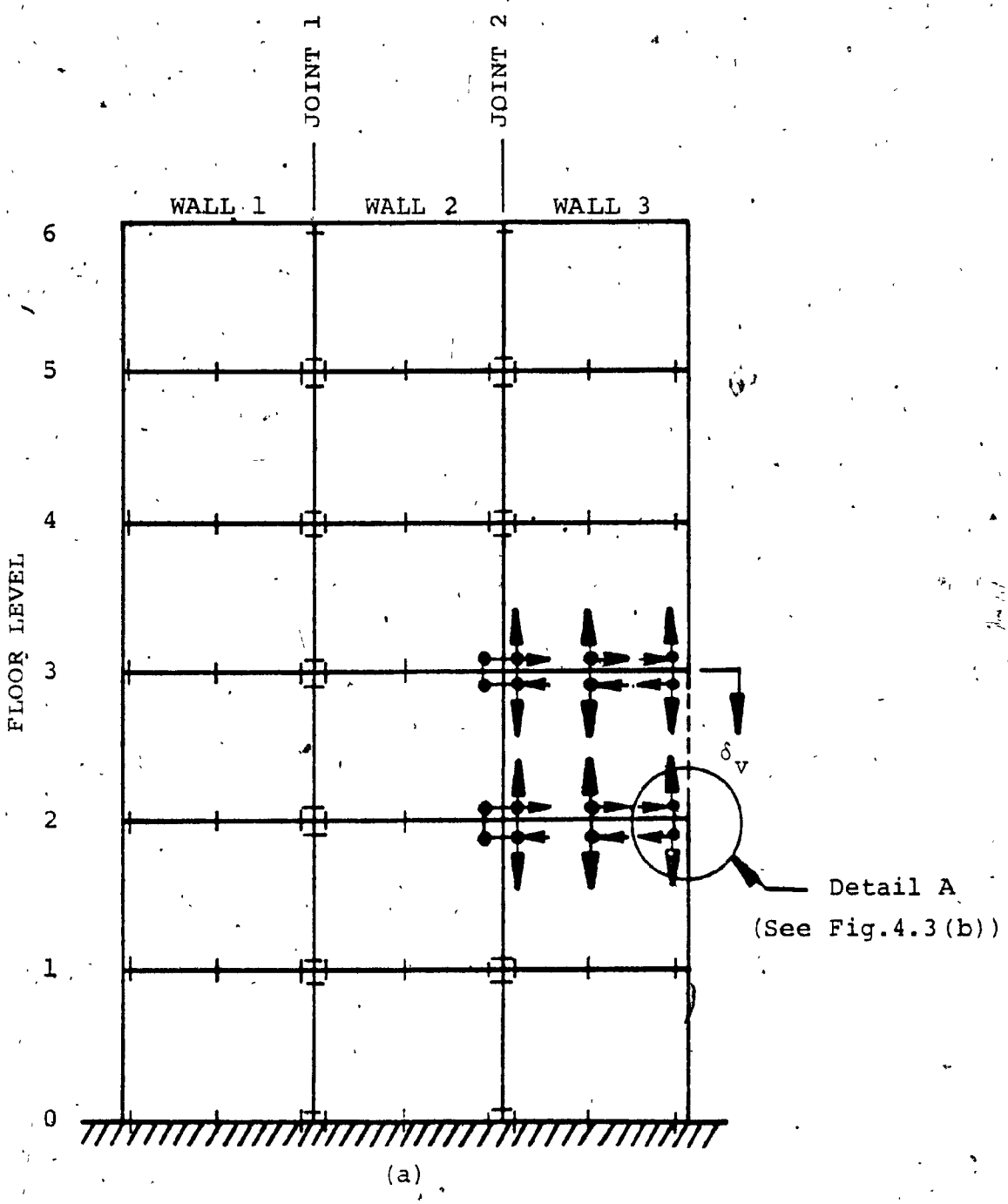

FIG. 4.3 FORCE CONDITIONS OF PANEL FAILURE IN 6 STOREY PROTOTYPE WALL SUBJECTED TO TYPICAL GAS EXPLOSION: (a) TYPICAL DAMAGED CONFIGURATION AND FINITE ELEMENT IDEALIZATION ; (b) TYPICAL JOINT FORCES EXERTED ON PANELS; (c) JOINT FORCE-TIME FUNCTION

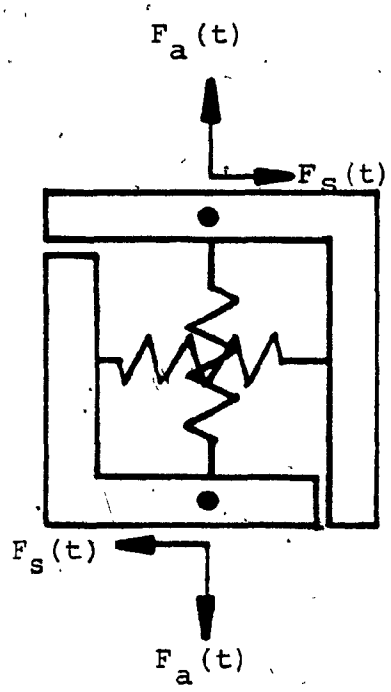

DETAIL A - TYPICAL JOINT FORCES EXERTED ON PANELS

(b)

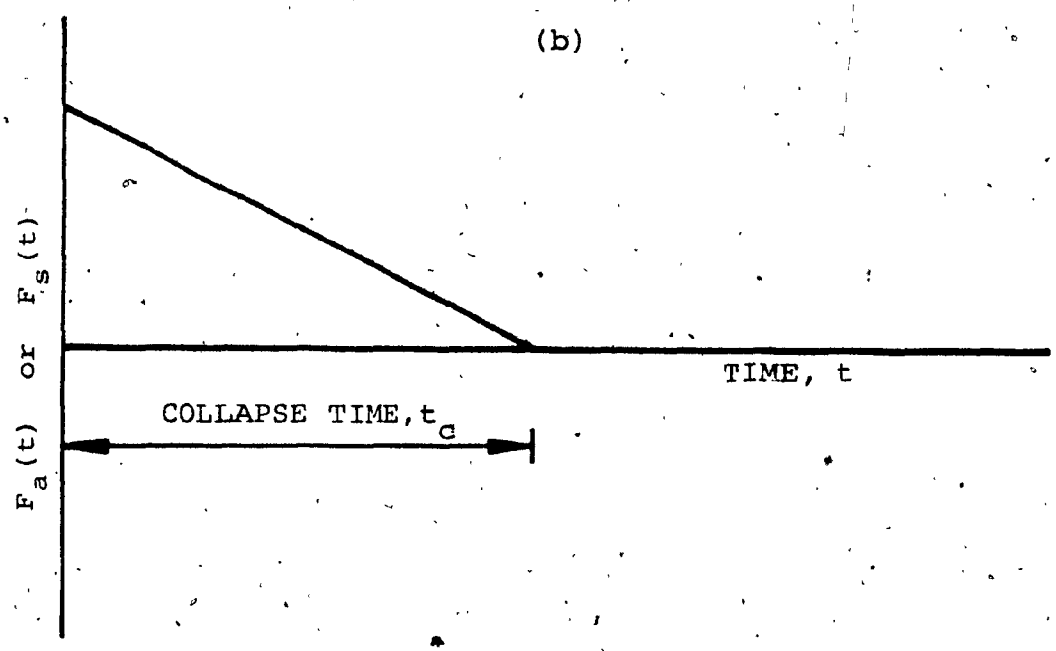

(c)

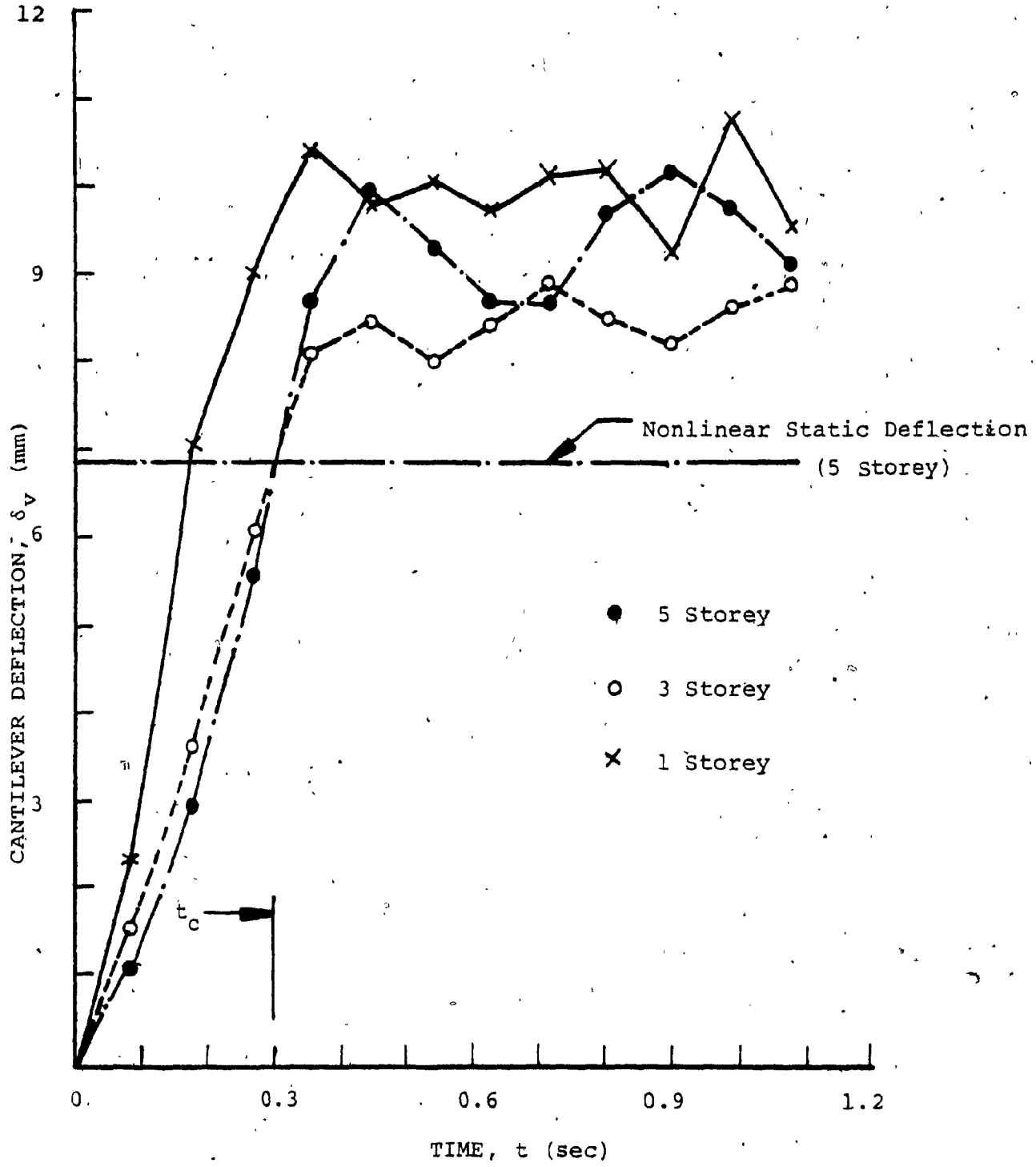

FIG. 4.4 TIME HISTORY RESPONSE OF CANTILEVER DEFLECTION FOR VARIOUS CANTILEVER DEPTHS - t_c = 0.3 SEC.

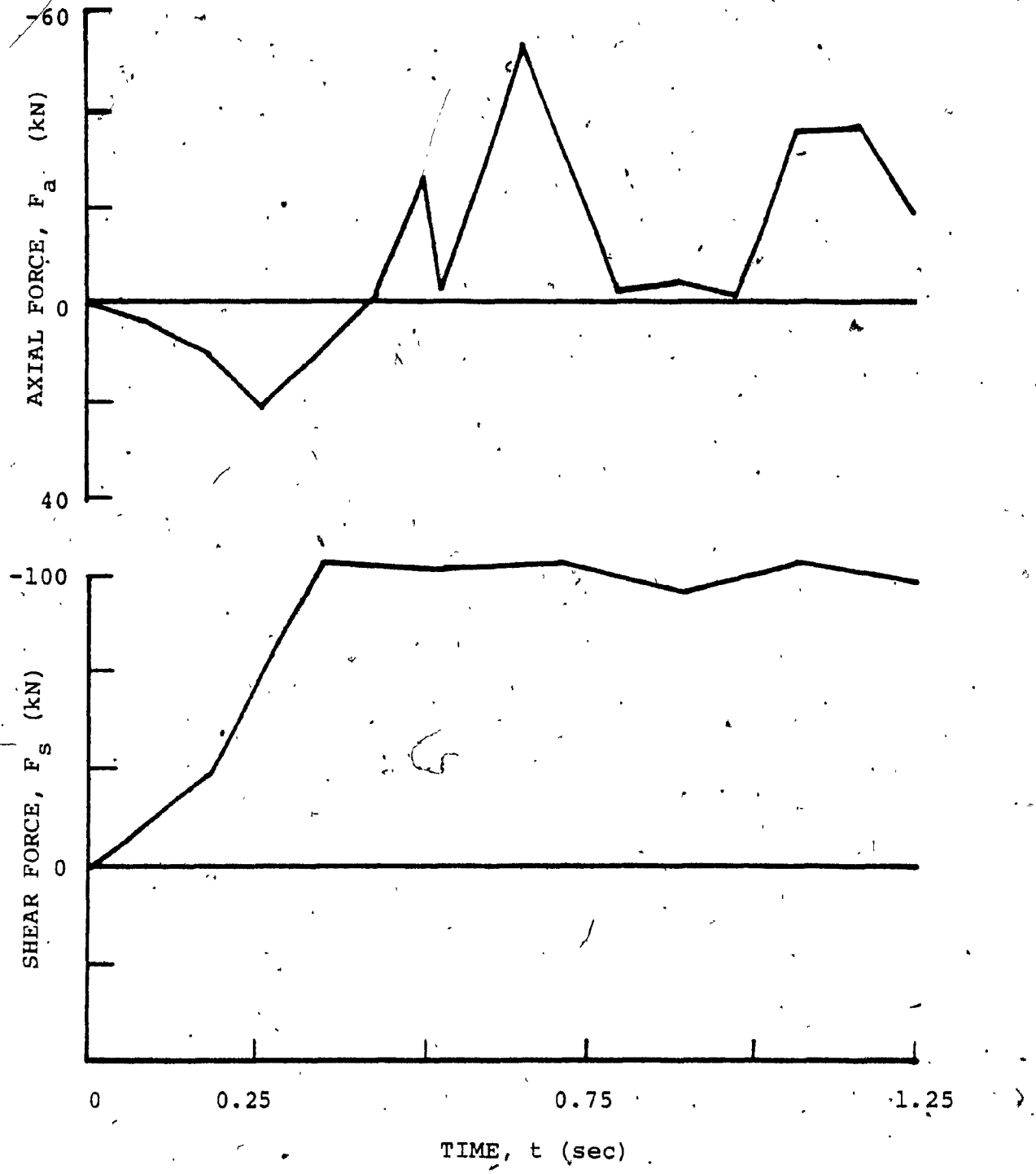

FIG. 4.5 TYPICAL TIME HISTORY RESPONSE OF FORCES IN VERTICAL JOINT 2 (FLOOR LEVEL 4) FOR t_c = 0.3 SEC. - 5 STOREY CANTILEVER

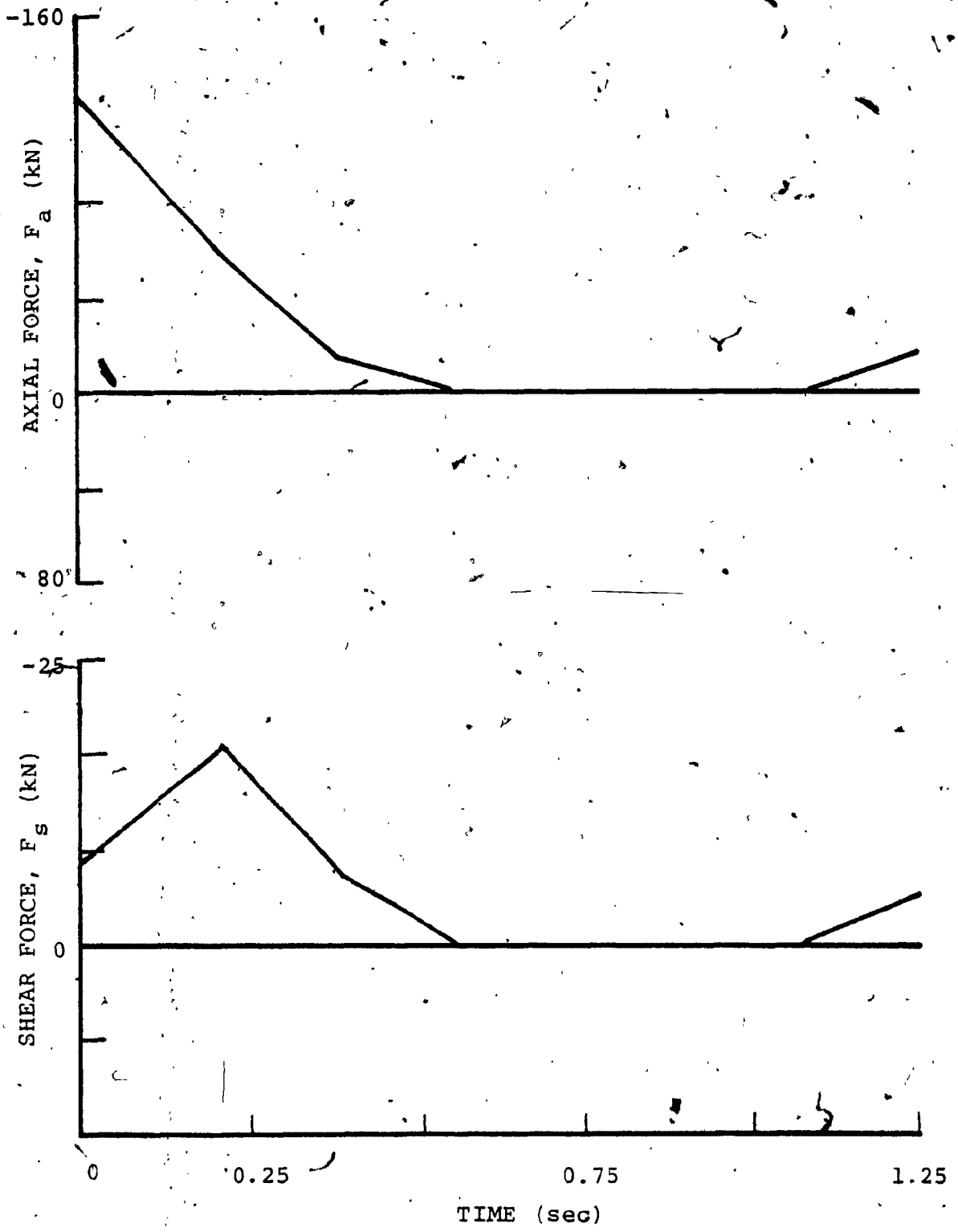

FIG. 4.6 TYPICAL TIME HISTORY RESPONSE OF COUPLED AXIAL-SHEAR FORCES IN HORIZONTAL JOINT OF CANTILEVER (FLOOR LEVEL 4) FOR t_c = 0.3 SEC. - 5 STOREY CANTILEVER

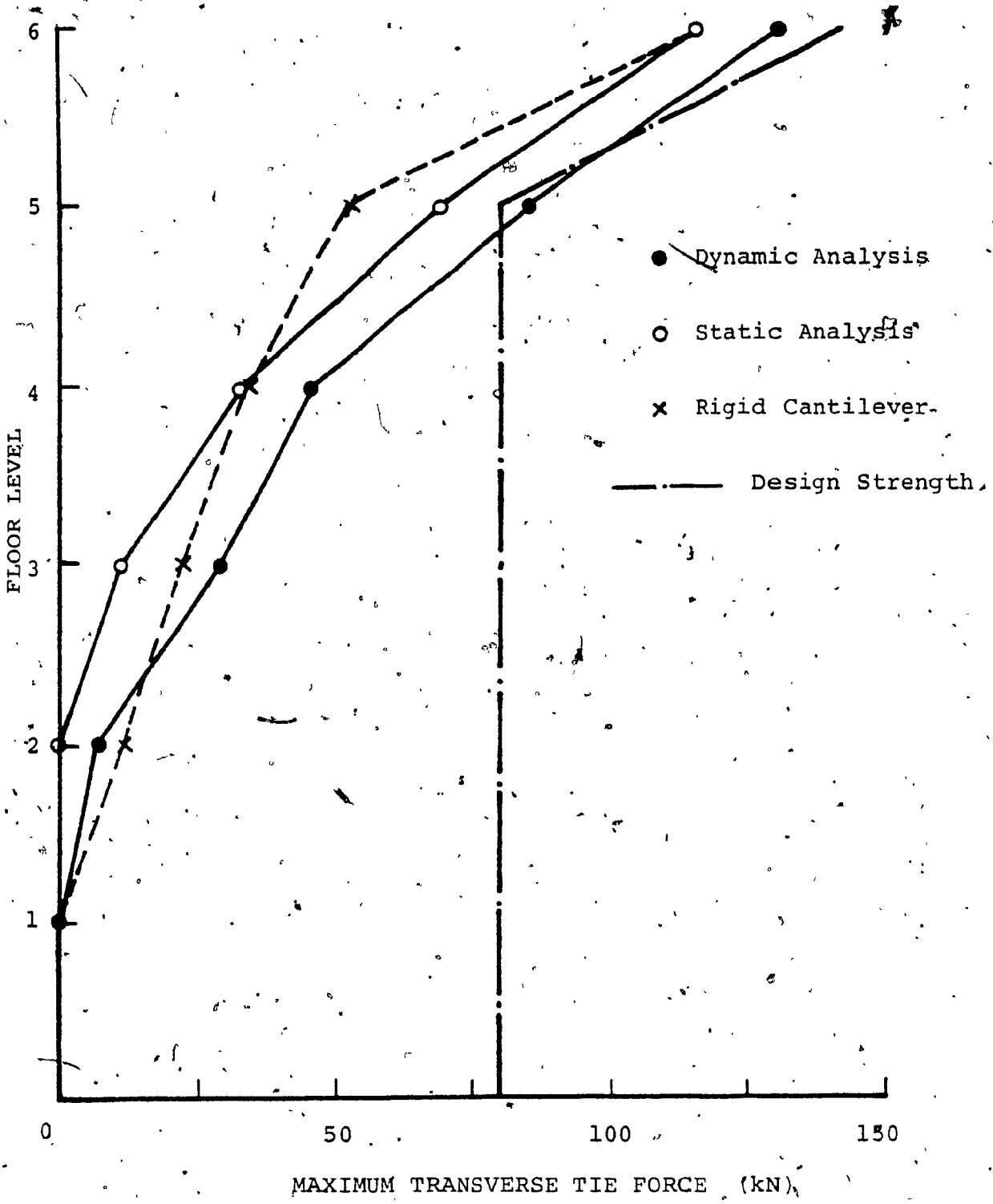

FIG. 4.7. ENVELOPES OF MAXIMUM FORCE IN TRANSVERSE TIES OF 6 STOREY PROTOTYPE WALL FOR NONLINEAR STATIC, NONLINEAR DYNAMIC (t_c = 0.3 SEC.) AND RIGID CANTILEVER BEHAVIOUR

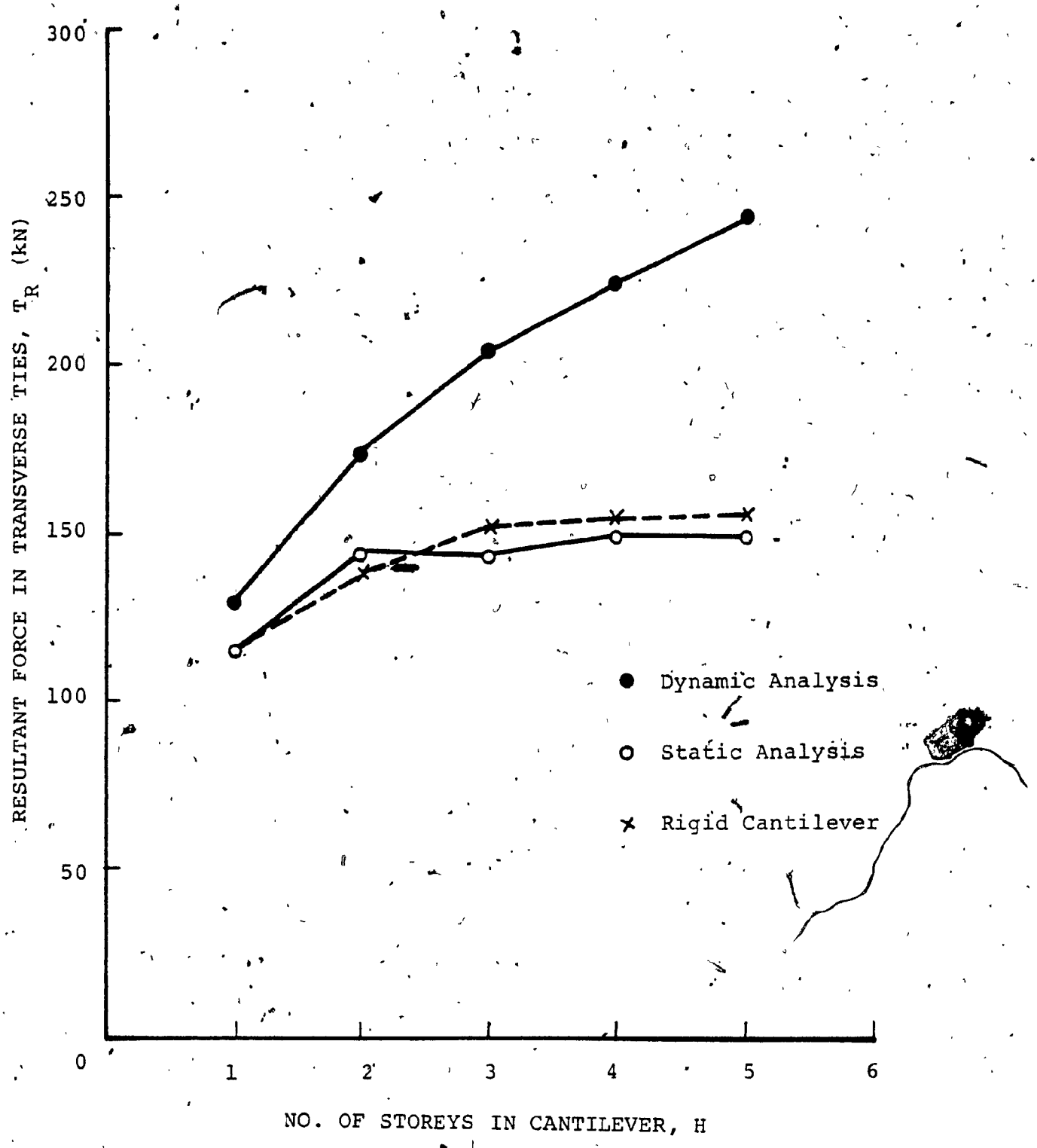

FIG. 4.8 VARIATION IN RESULTANT FORCE OF TRANSVERSE TIES WITH CANTILEVER DEPTH FOR NONLINEAR STATIC, NONLINEAR DYNAMIC (t_c = 0.3 SEC.) AND RIGID CANTILEVER BEHAVIOUR

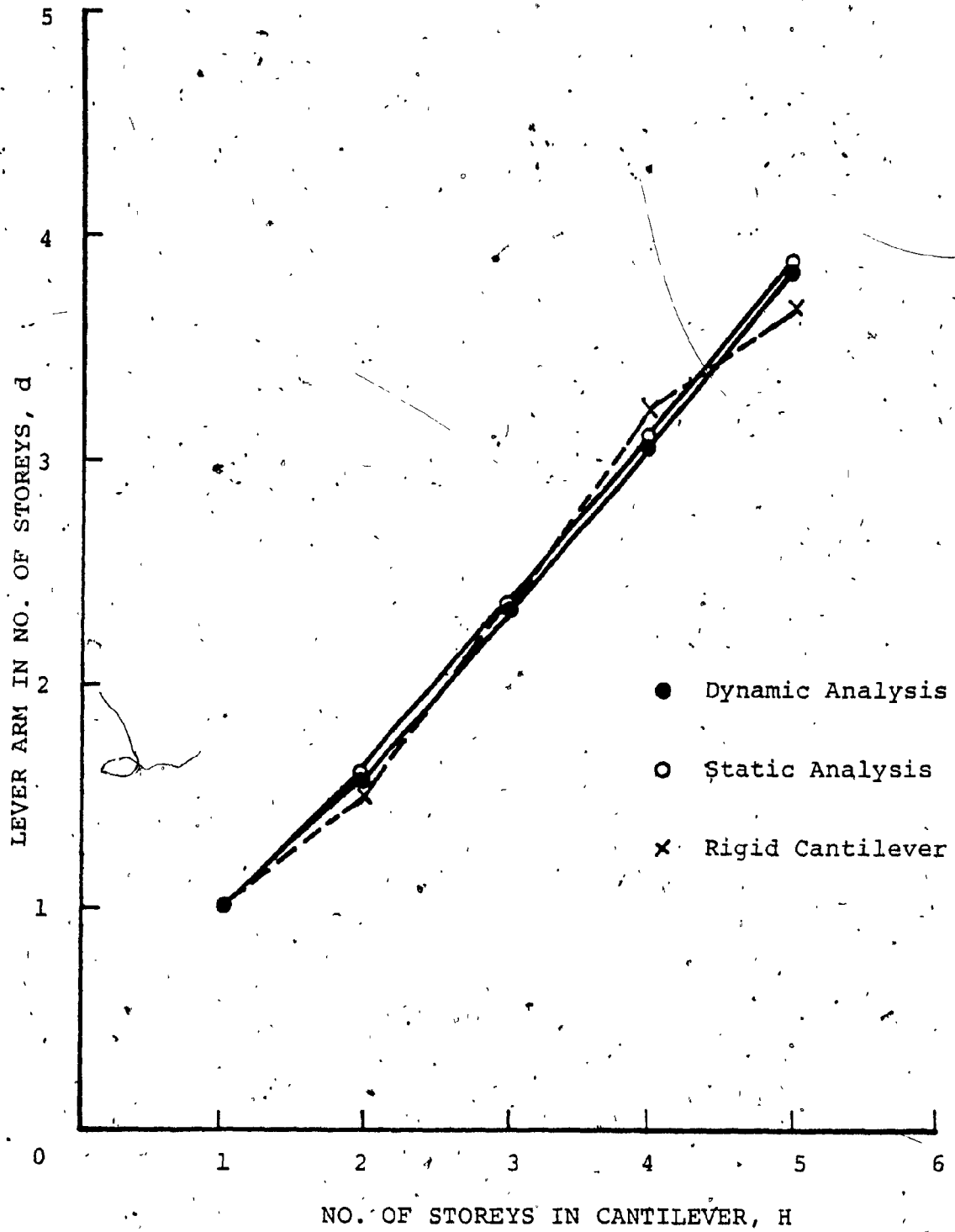

FIG. 4.9 VARIATION IN EFFECTIVE LEVER ARM WITH CANTILEVER DEPTH FOR NONLINEAR STATIC, NONLINEAR DYNAMIC AND RIGID CANTILEVER BEHAVIOUR

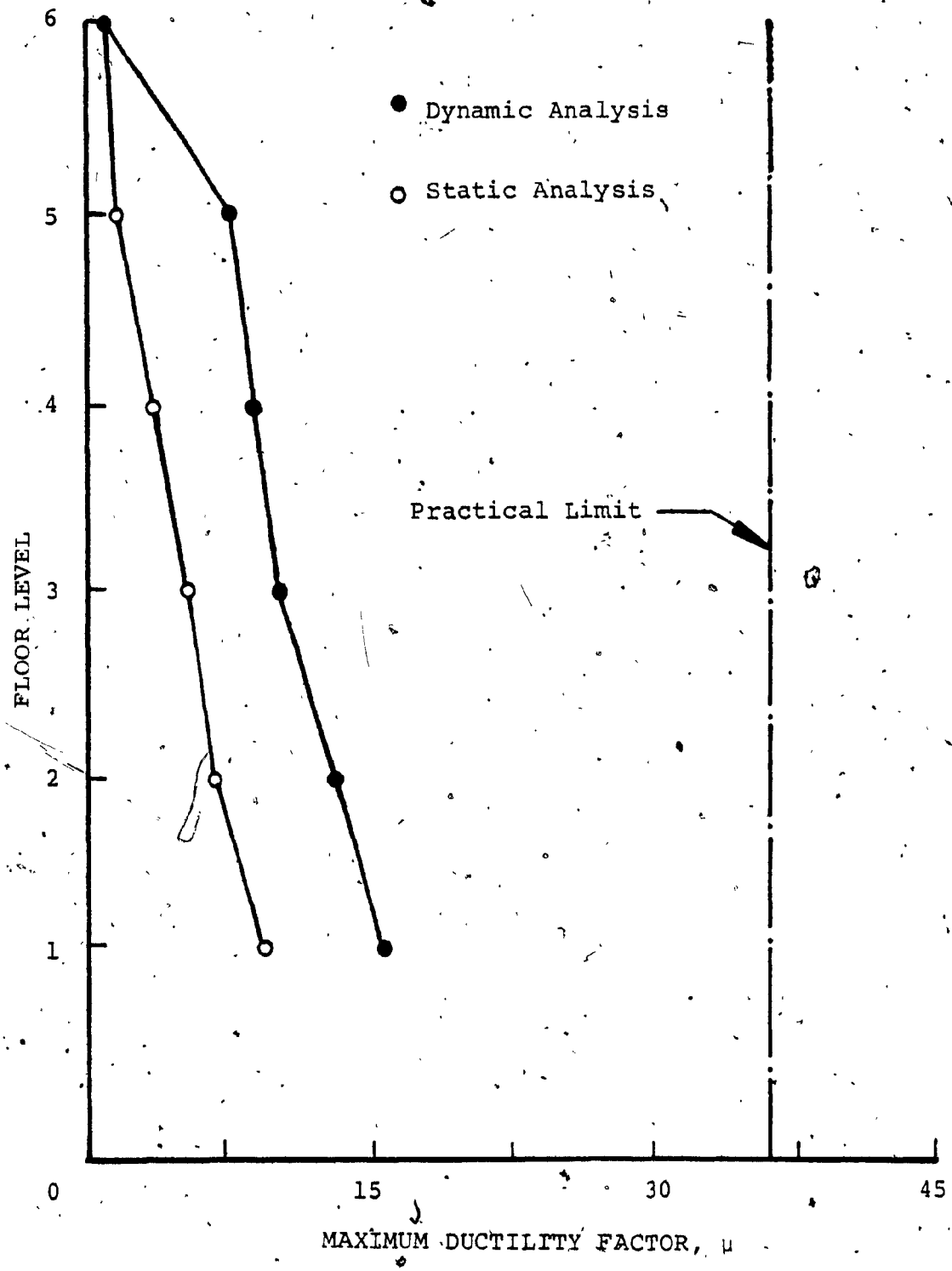

FIG. 4.10 ENVELOPES OF MAXIMUM DUCTILITY DEMAND IN VERTICAL MECHANICAL CONNECTORS OF 6 STOREY PROTOTYPE WALL (t_c = 0.3 SEC.) FOR NONLINEAR STATIC AND DYNAMIC BEHAVIOUR

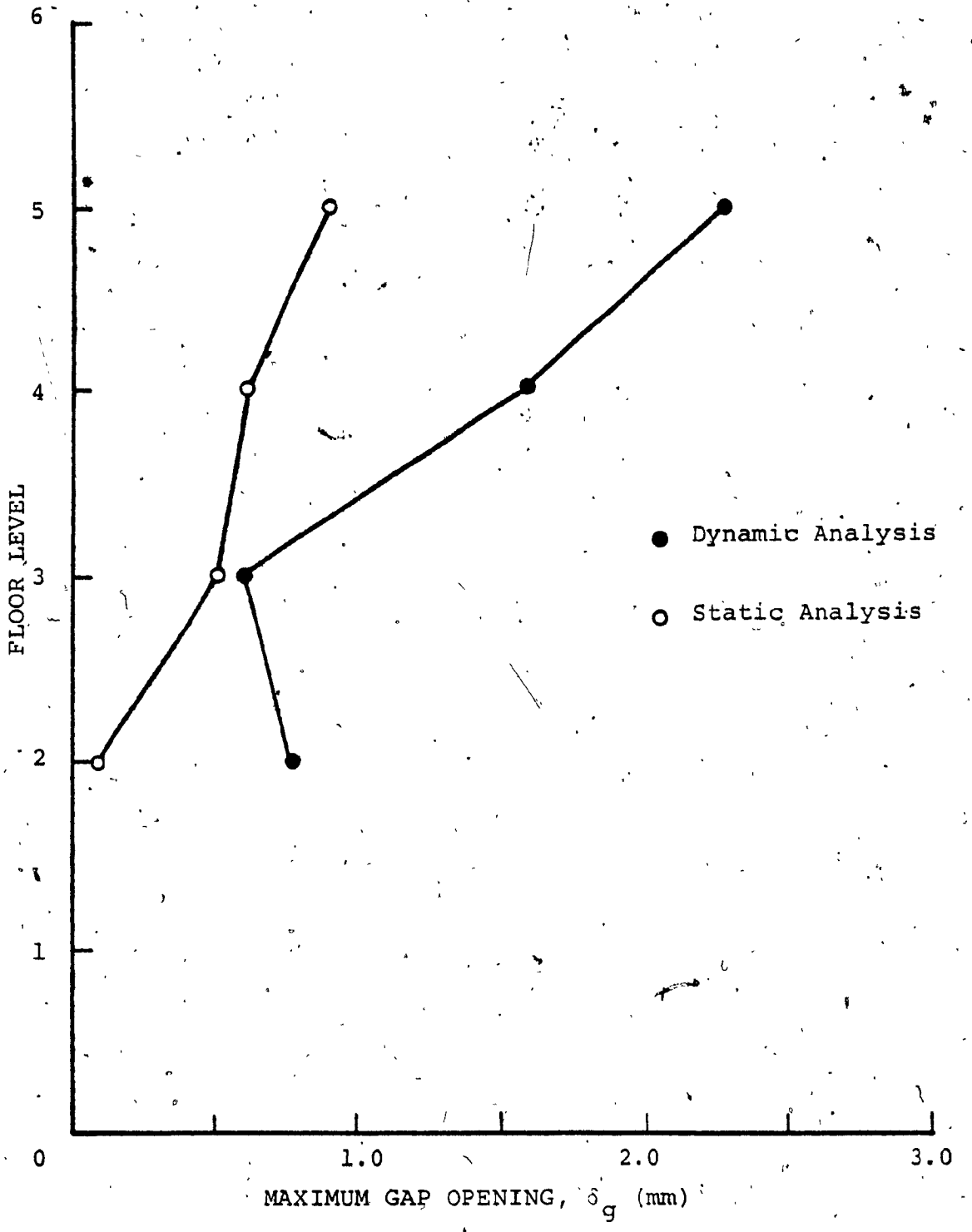

FIG. 4.11 ENVELOPES OF MAXIMUM GAP OPENING IN HORIZONTAL JOINTS OF CANTILEVER OF 6 STOREY PROTOTYPE WALL (t_c = 0.3 SEC.) FOR NONLINEAR STATIC AND DYNAMIC BEHAVIOUR

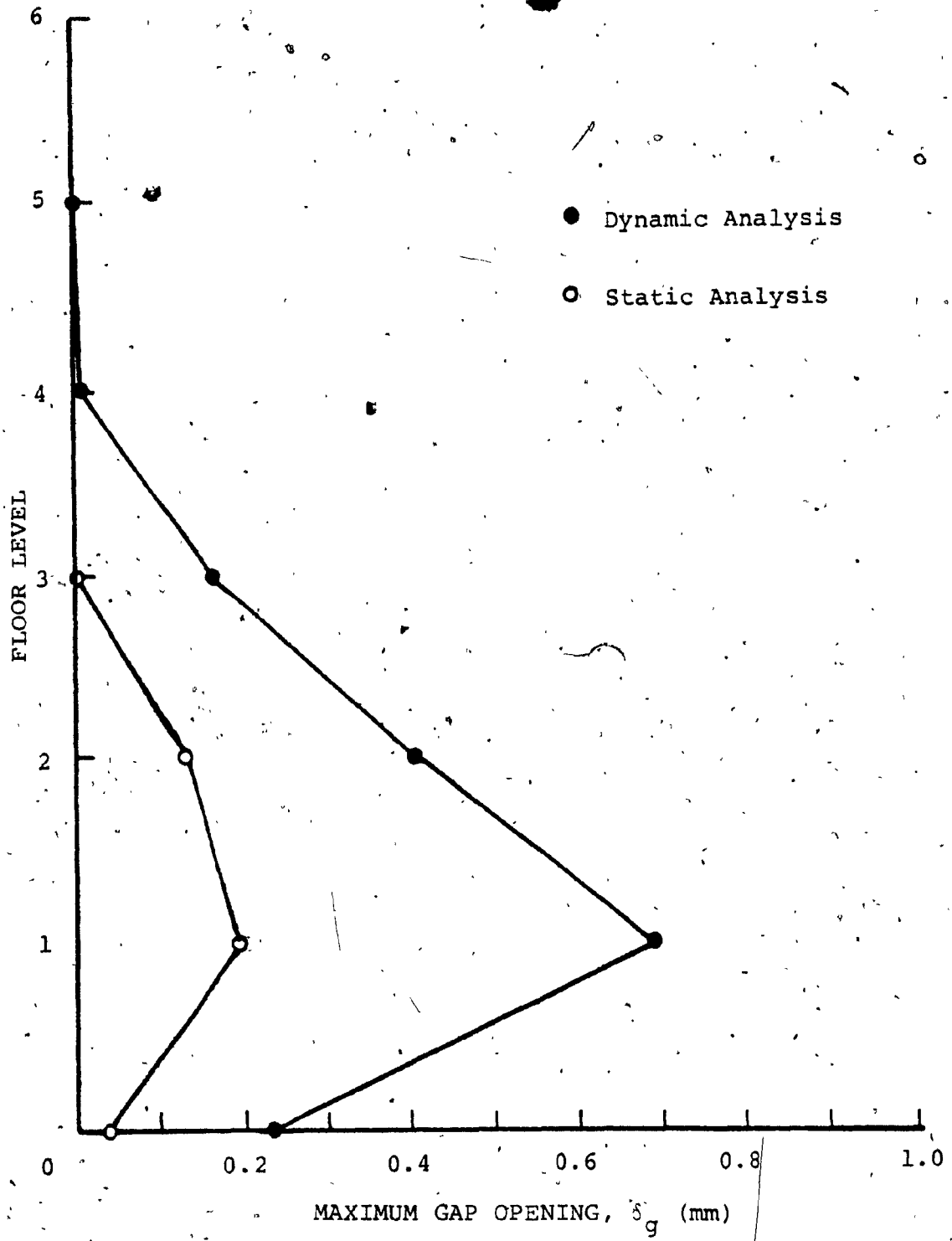

FIG. 4.12 ENVELOPES OF MAXIMUM GAP OPENING IN HORIZONTAL JOINTS OF WALL 1 OF 6 STOREY PROTOTYPE WALL (t_c = 0.3 SEC.) FOR NONLINEAR STATIC AND DYNAMIC BEHAVIOUR

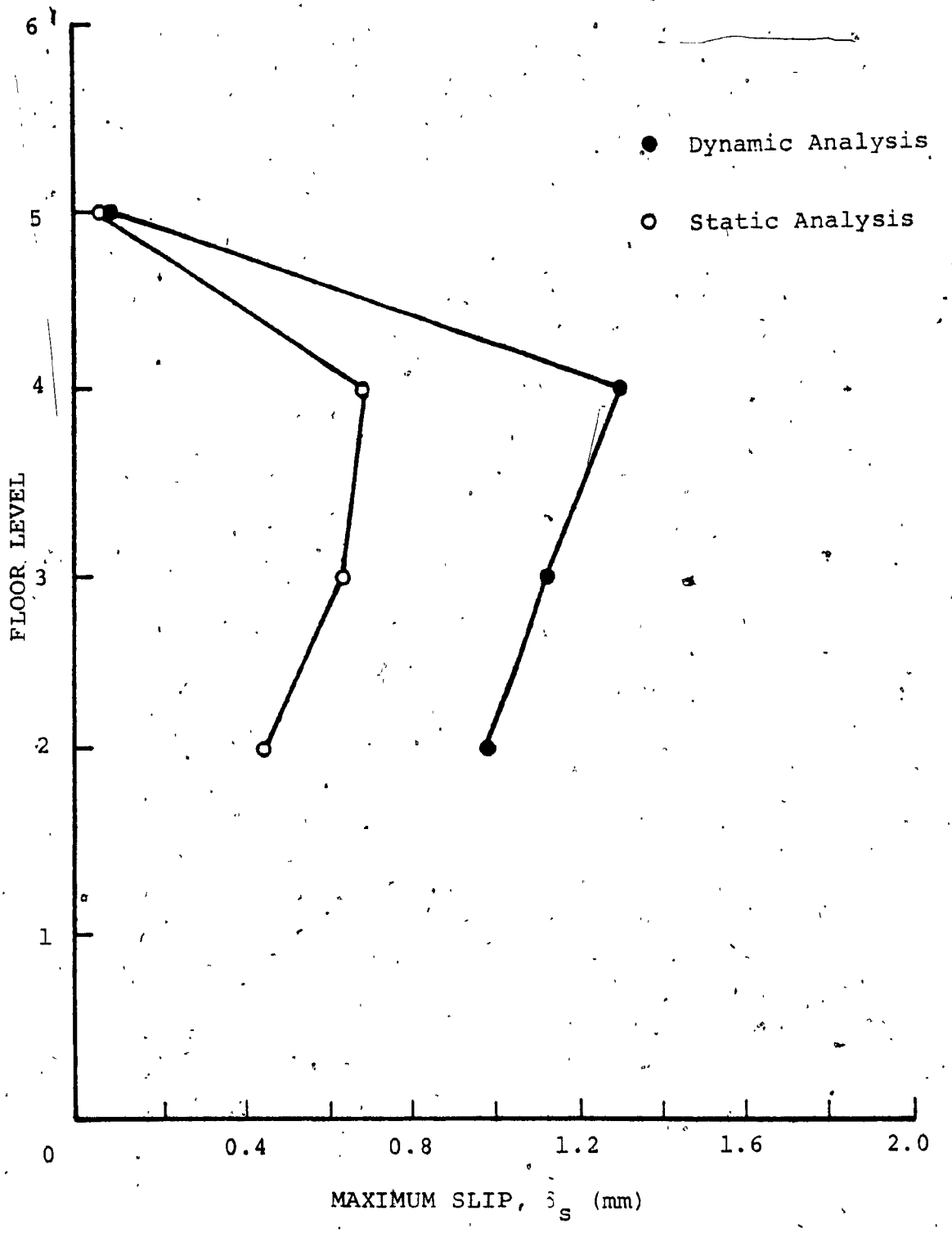

FIG. 4.13 ENVELOPES OF MAXIMUM SLIP IN HORIZONTAL JOINTS OF CANTILEVER OF 6 STOREY PROTOTYPE WALL (t_c = 0.3 SEC.) FOR NONLINEAR STATIC AND DYNAMIC BEHAVIOUR

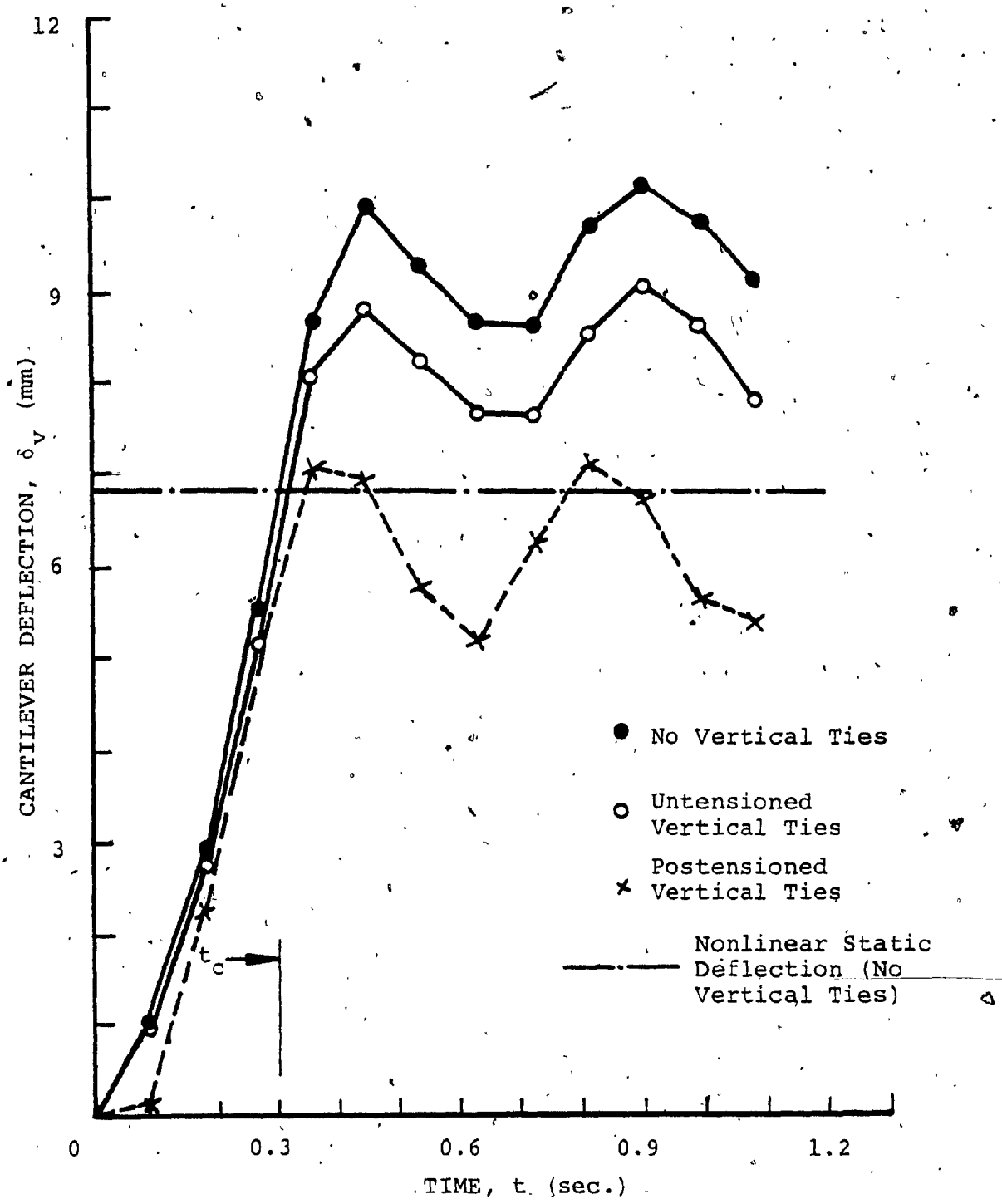

FIG. 4.14 TIME HISTORY RESPONSE OF CANTILEVER DEFLECTION OF 6 STOREY PRECAST PANEL WALL WITH AND WITHOUT VERTICAL TIES FOR t_c = 0.3 SEC. - 5 STOREY CANTILEVER

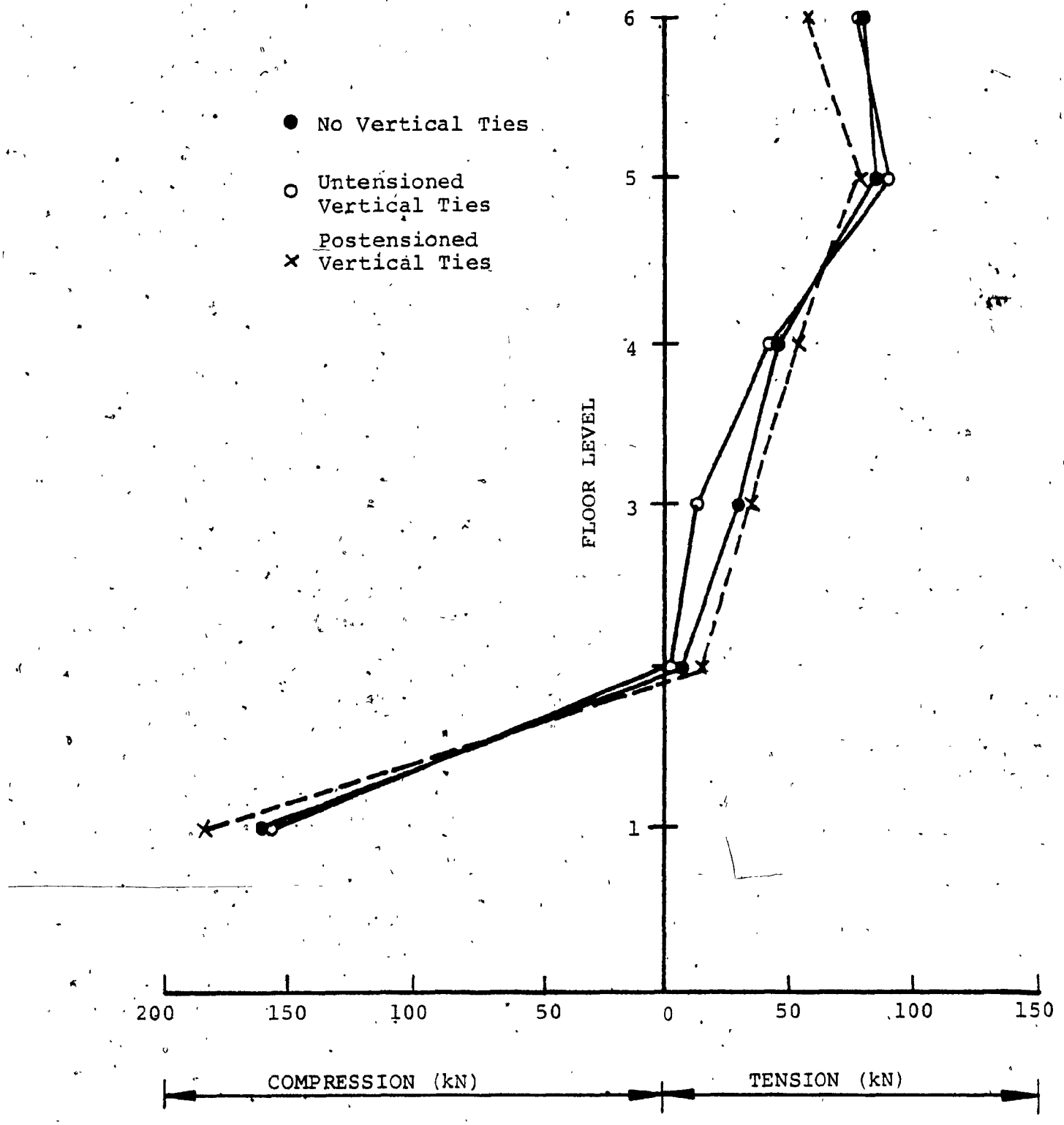

FIG. 4.15 DISTRIBUTION OF MAXIMUM AXIAL FORCE IN VERTICAL JOINT OF 6 STOREY PRECAST PANEL WALL WITH AND WITHOUT VERTICAL TIES FOR t_c = 0.3 SEC. - 5 STOREY CANTILEVER

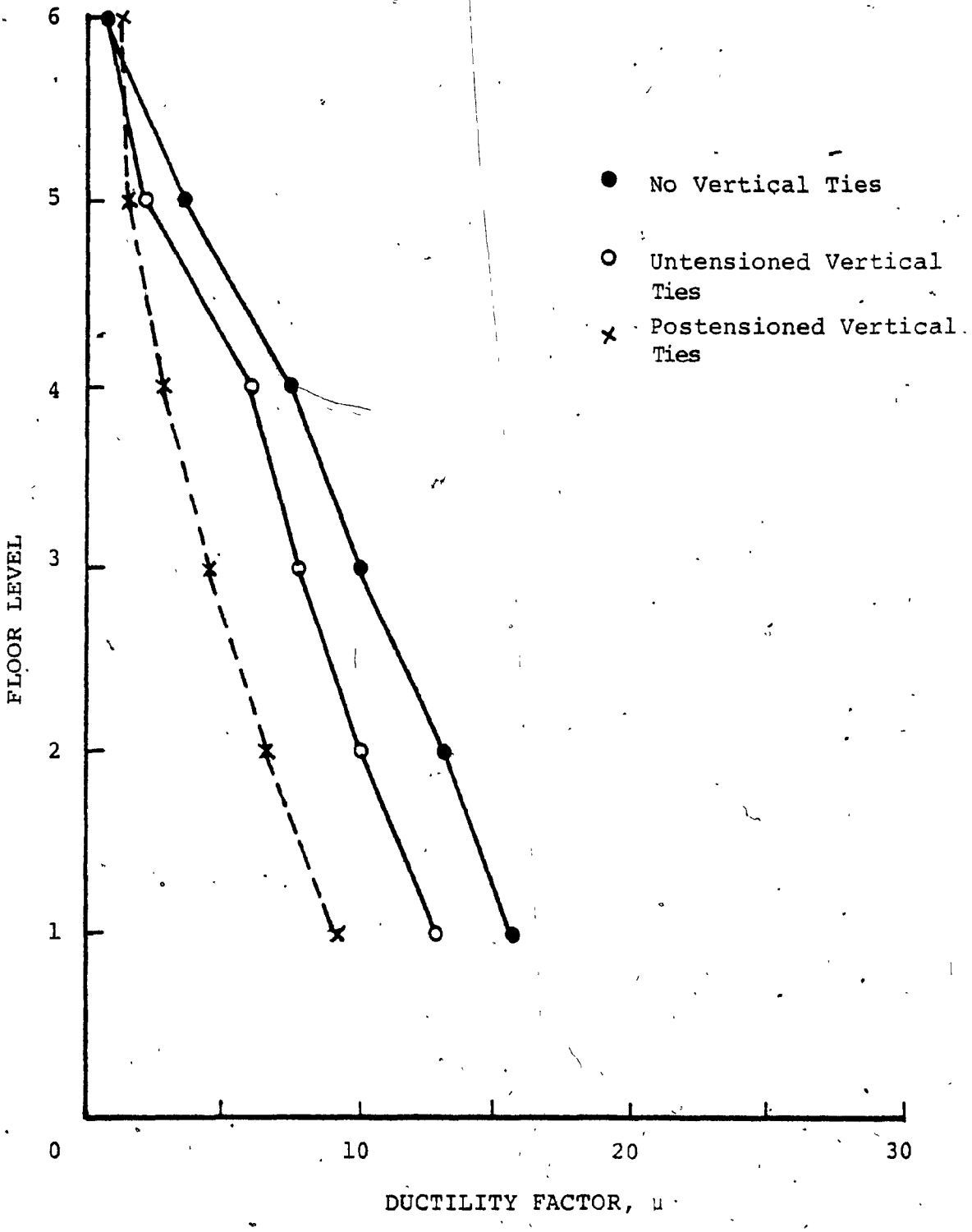

FIG. 4.16 DISTRIBUTION OF MAXIMUM DUCTILITY FACTOR IN VERTICAL MECHANICAL CONNECTORS OF JOINT 2 OF 6 STOREY PRECAST PANEL WALL WITH AND WITHOUT VERTICAL TIES FOR t_c = 0.3 SEC. - 5 STOREY CANTILEVER

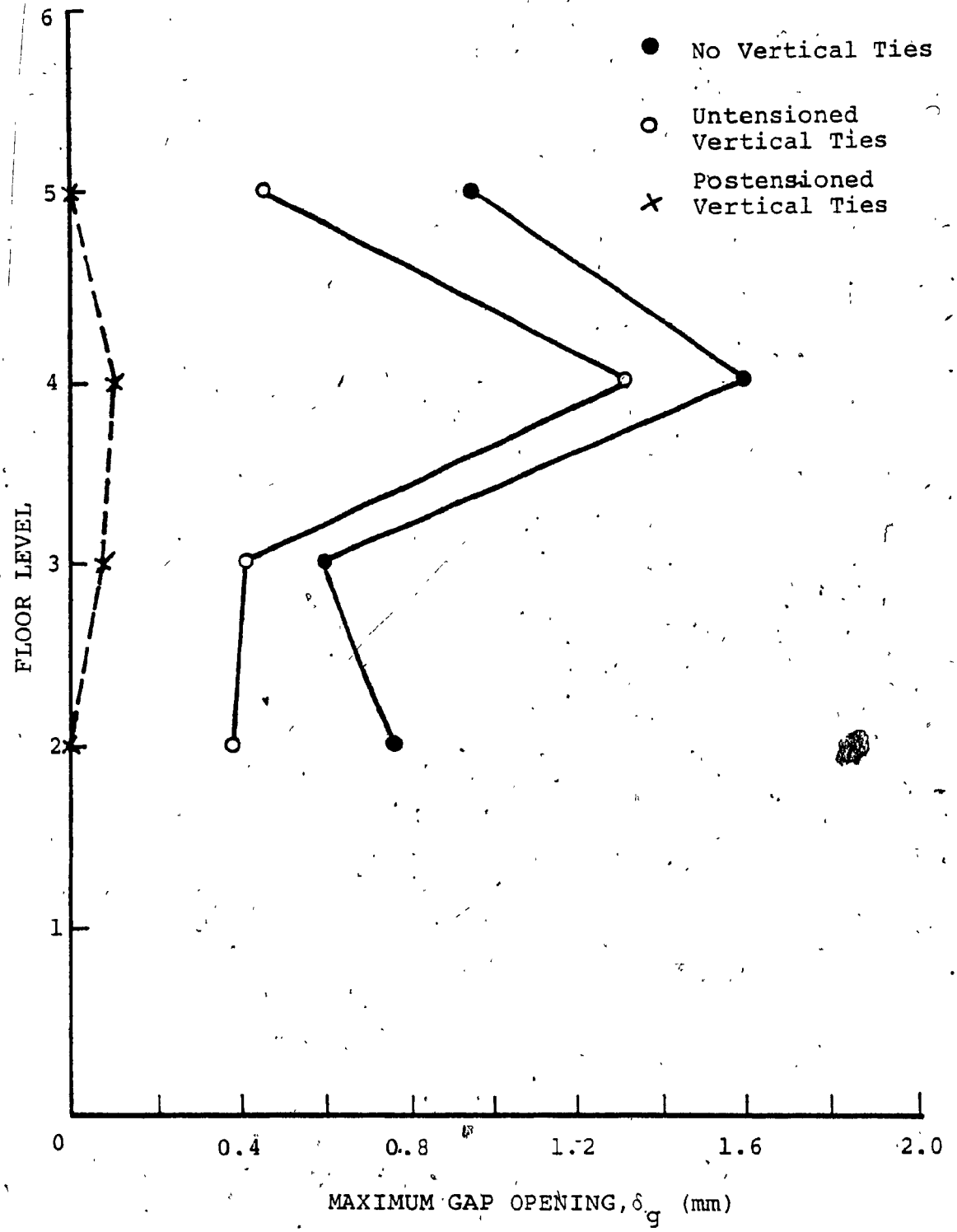

FIG. 4.17 DISTRIBUTION OF MAXIMUM GAP OPENING IN HORIZONTAL JOINTS OF CANTILEVER OF 6 STOREY PRECAST PANEL WALL WITH AND WITHOUT VERTICAL TIES FOR t_c = 0.3 SEC. - 5 STOREY CANTILEVER

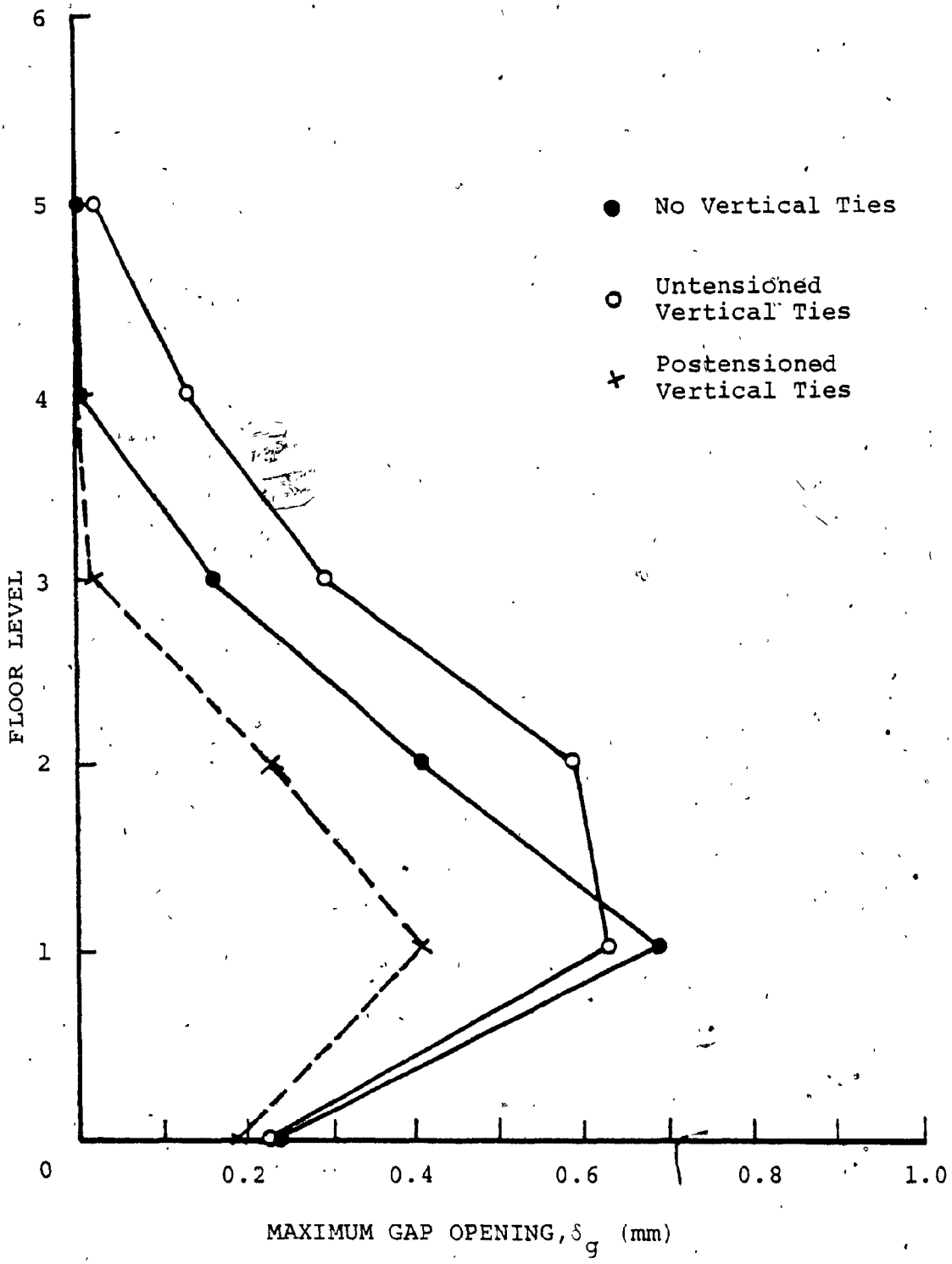

FIG. 4.18 DISTRIBUTION OF MAXIMUM GAP OPENING IN HORIZONTAL JOINTS OF WALL 1 OF 6 STOREY PRECAST PANEL WALL WITH AND WITHOUT VERTICAL TIES FOR t_c = 0.3 SEC. 5 STOREY CANTILEVER

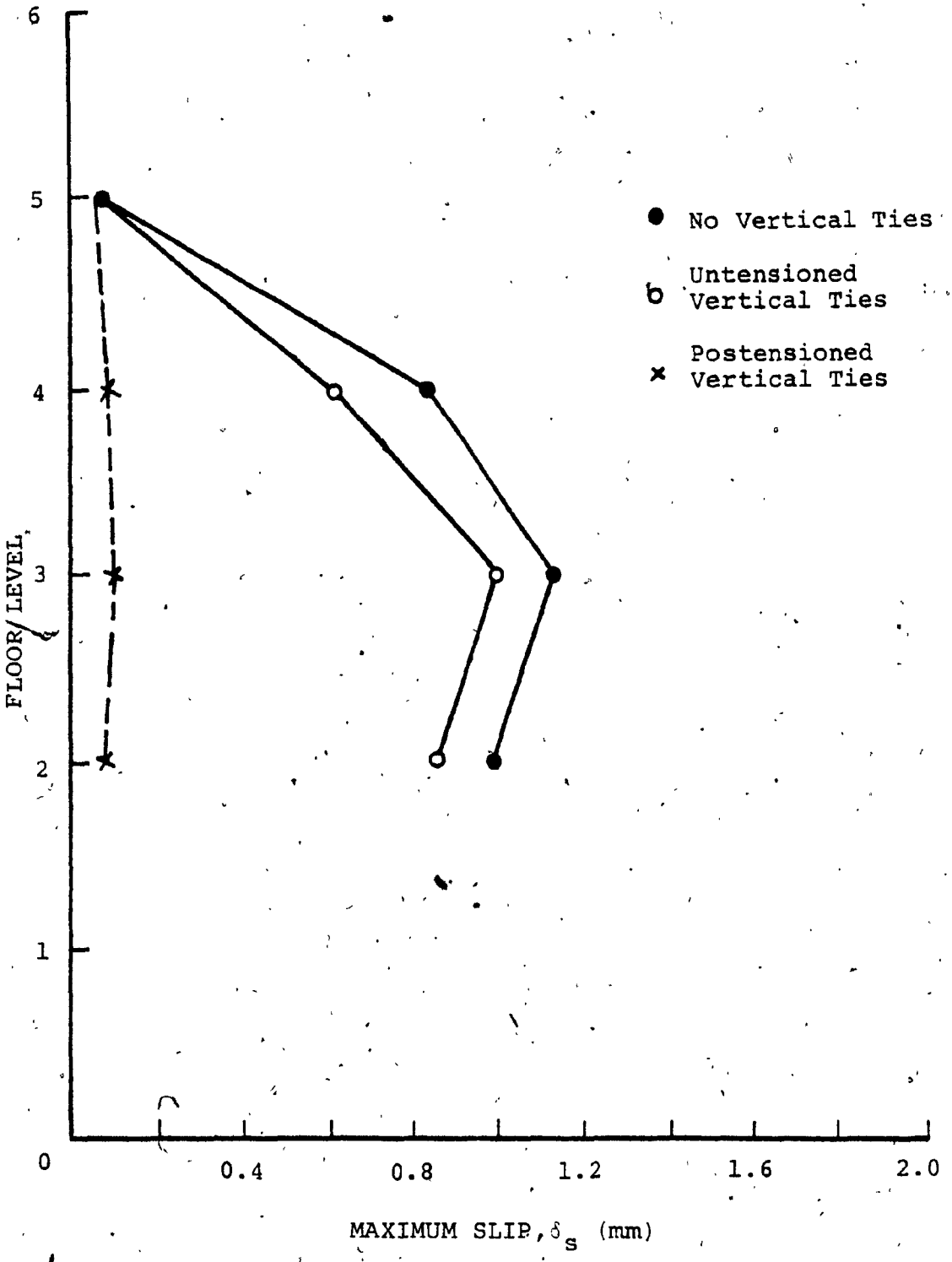

FIG. 4.19 DISTRIBUTION OF MAXIMUM SLIP IN HORIZONTAL JOINTS OF CANTILEVER OF 6 STOREY PRECAST PANEL WALL WITH AND WITHOUT VERTICAL TIES FOR t_c = 0.3 SEC. - 5 STOREY CANTILEVER

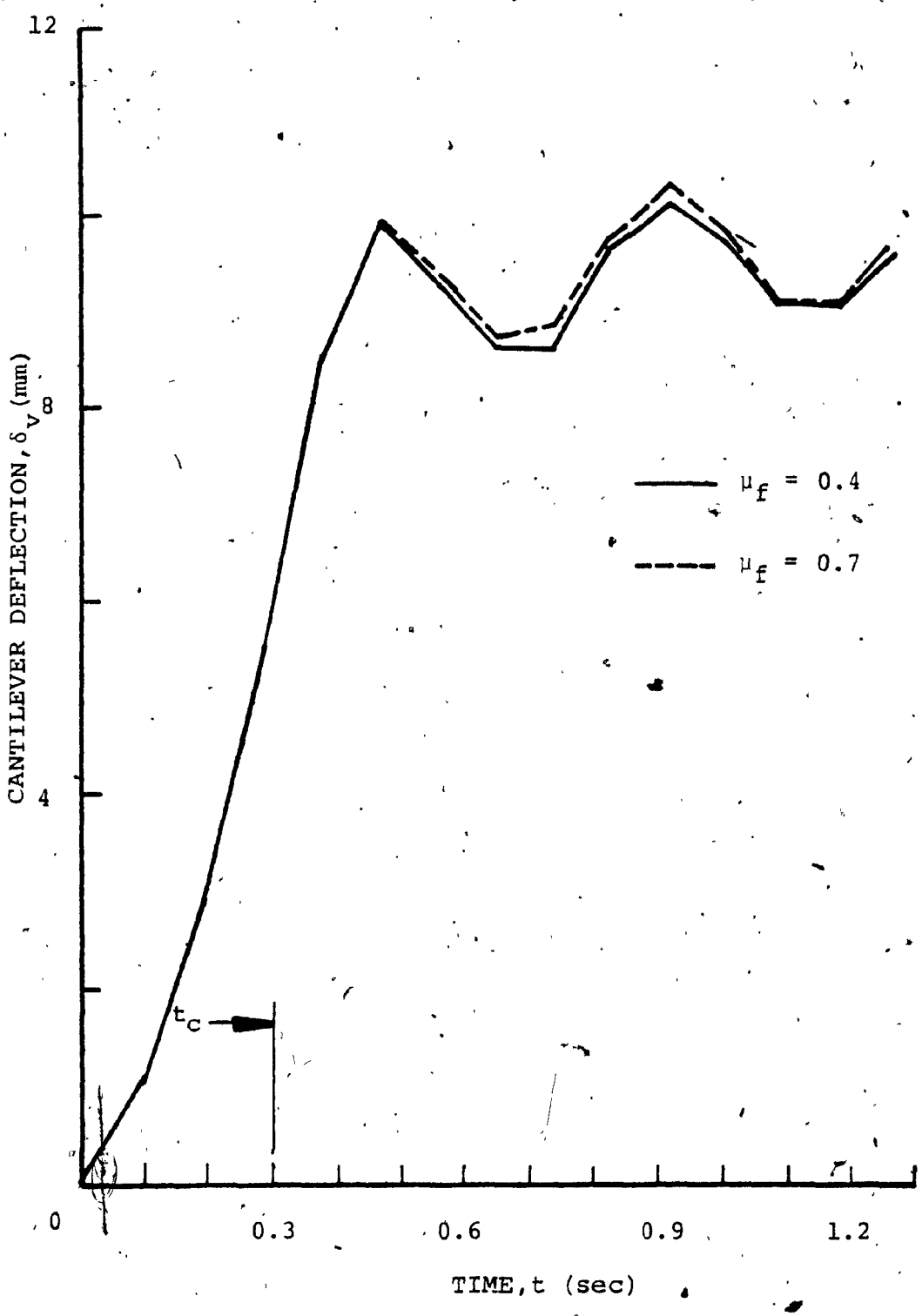

FIG. 4.20 EFFECT OF COEFFICIENT OF FRICTION ON TIME HISTORY RESPONSE OF CANTILEVER DEFLECTION FOR t_c = 0.3 SEC. - 5 STOREY CANTILEVER

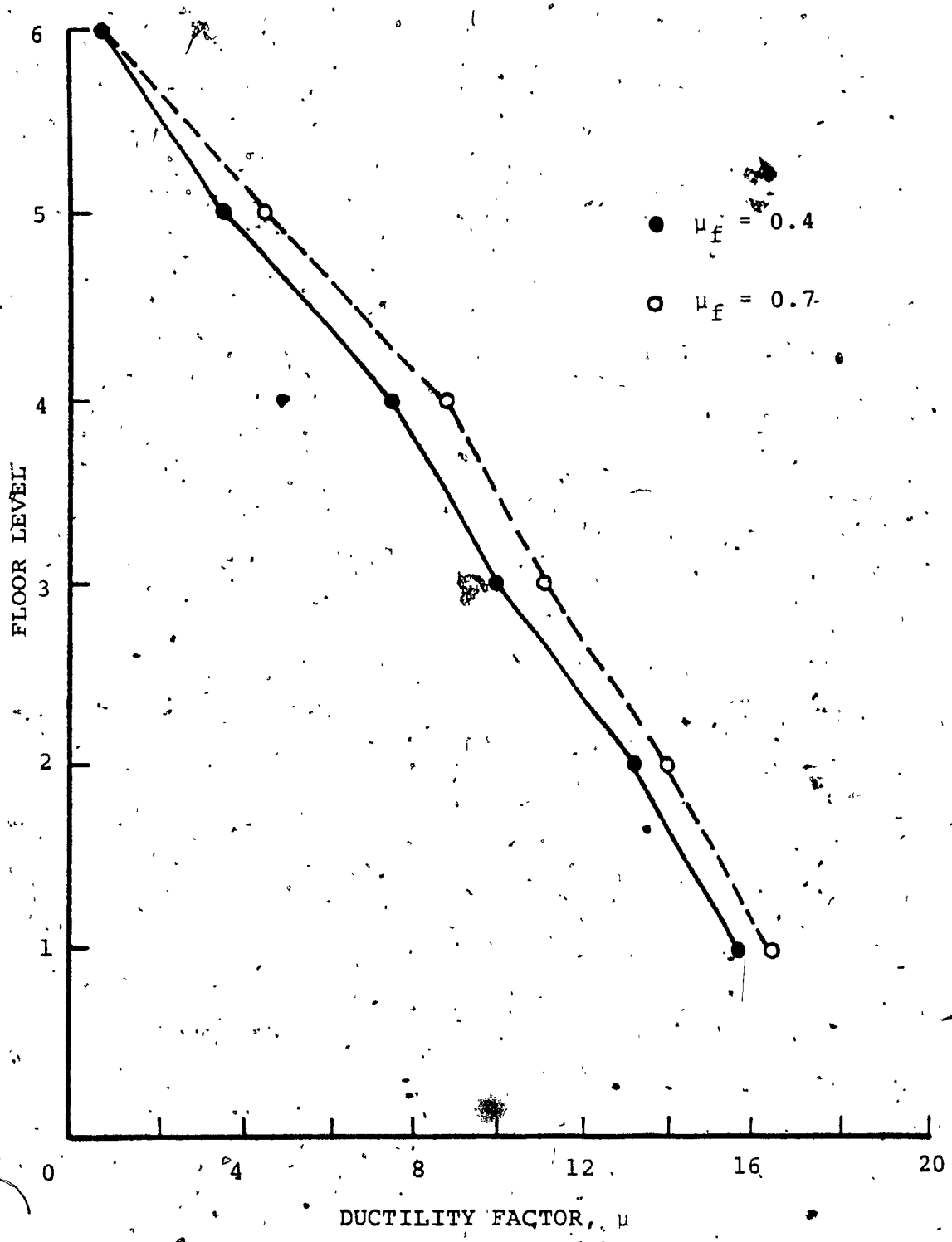

FIG. 4.21 EFFECT OF COEFFICIENT OF FRICTION ON DISTRIBUTION OF MAXIMUM DUCTILITY DEMAND IN VERTICAL MECHANICAL CONNECTORS OF JOINT 2 FOR t_c = 0.3 SEC. - 5 STOREY CANTILEVER

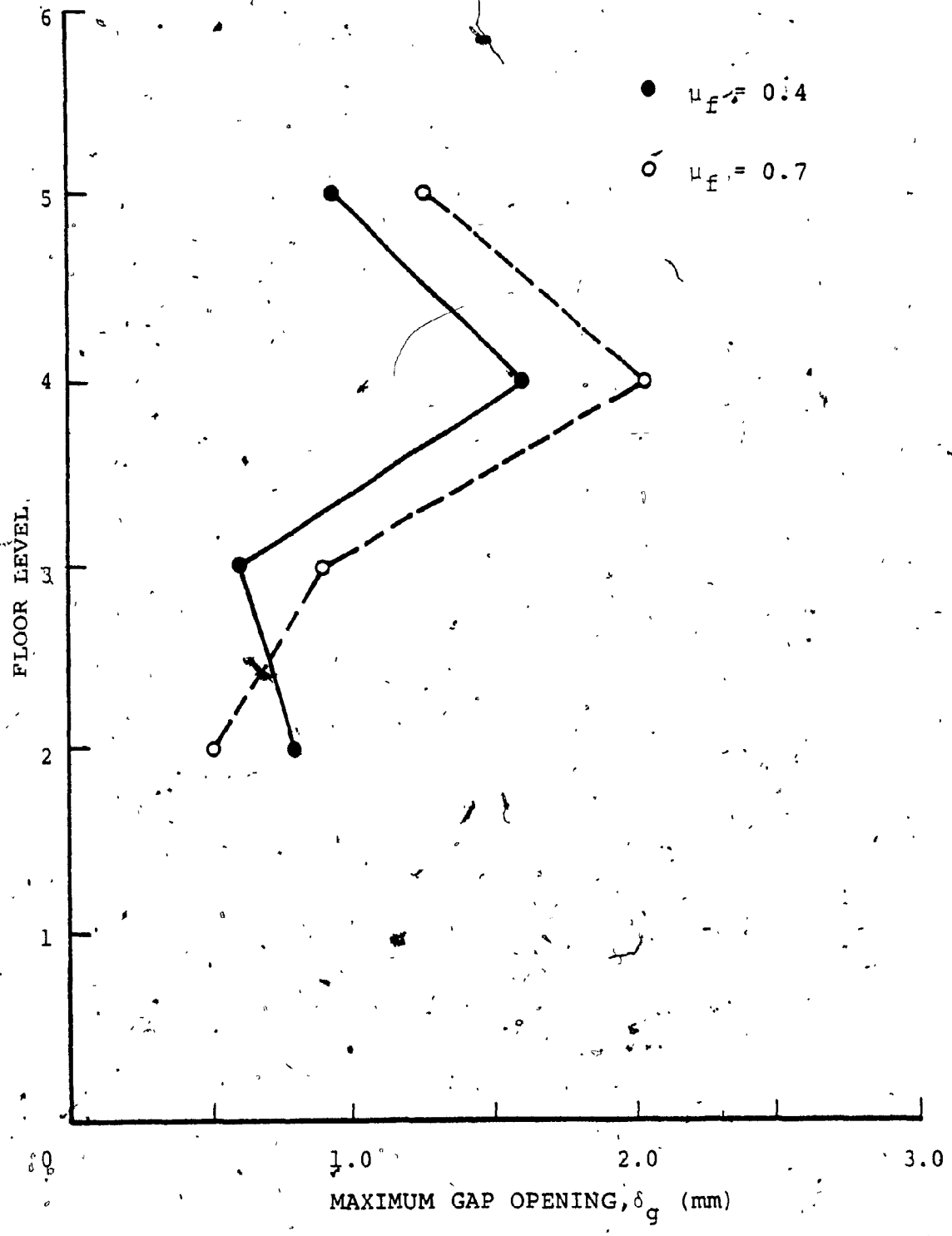

FIG. 4.22 EFFECT OF COEFFICIENT OF FRICTION ON DISTRIBUTION OF MAXIMUM GAP OPENING IN HORIZONTAL JOINTS OF CANTILEVER FOR t_c = 0.3 SEC. - 5 STOREY CANTILEVER.

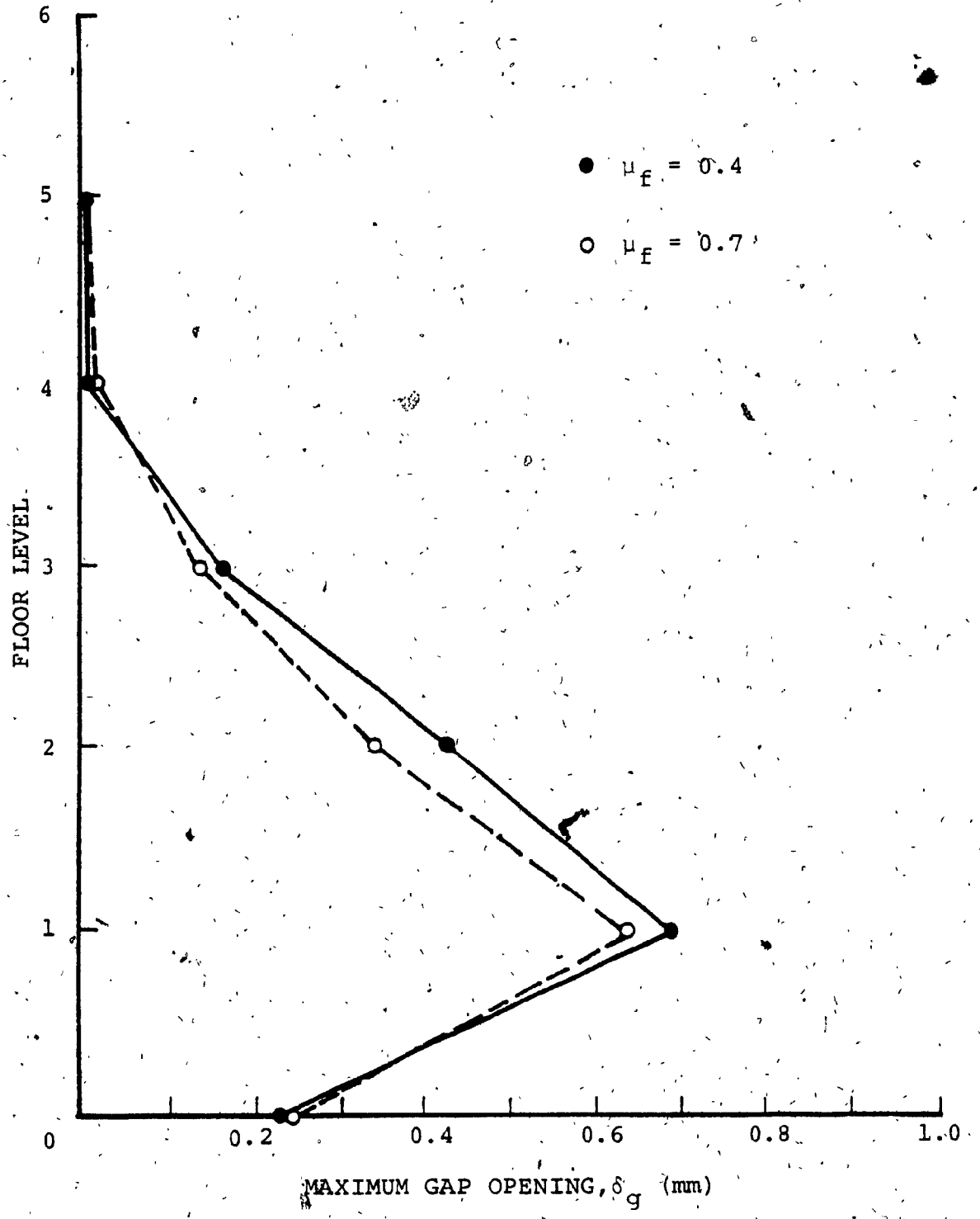

FIG. 4.23 EFFECT OF COEFFICIENT OF FRICTION ON DISTRIBUTION OF MAXIMUM GAP OPENING IN HORIZONTAL JOINTS OF WALL 1 FOR t_c = 0.3 SEC. - 5 STOREY CANTILEVER

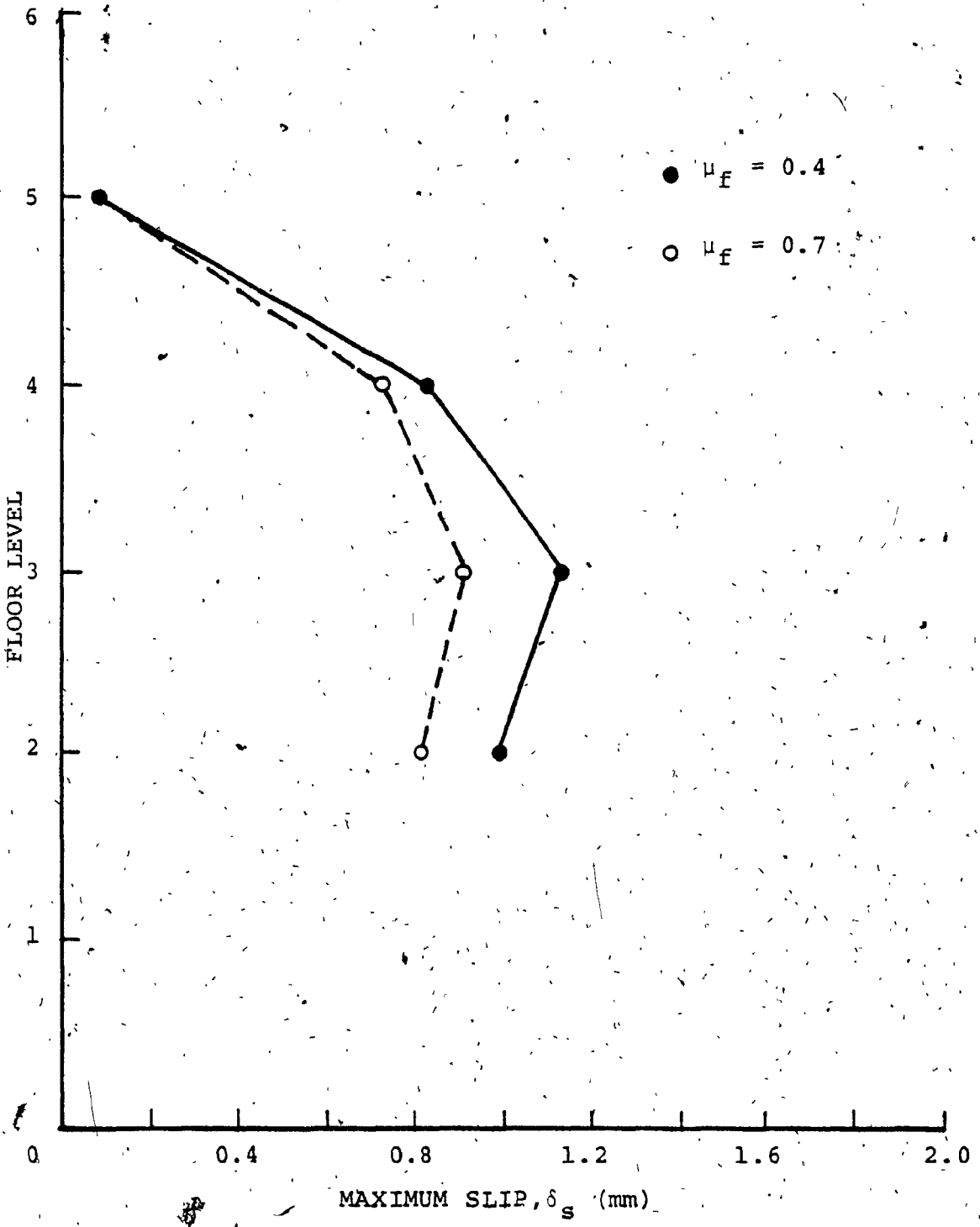

FIG. 4.24 EFFECT OF COEFFICIENT OF FRICTION ON DISTRIBUTION OF MAXIMUM SLIP IN HORIZONTAL JOINTS OF CANTILEVER FOR t_c = 0.3 SEC. - 5 STOREY CANTILEVER

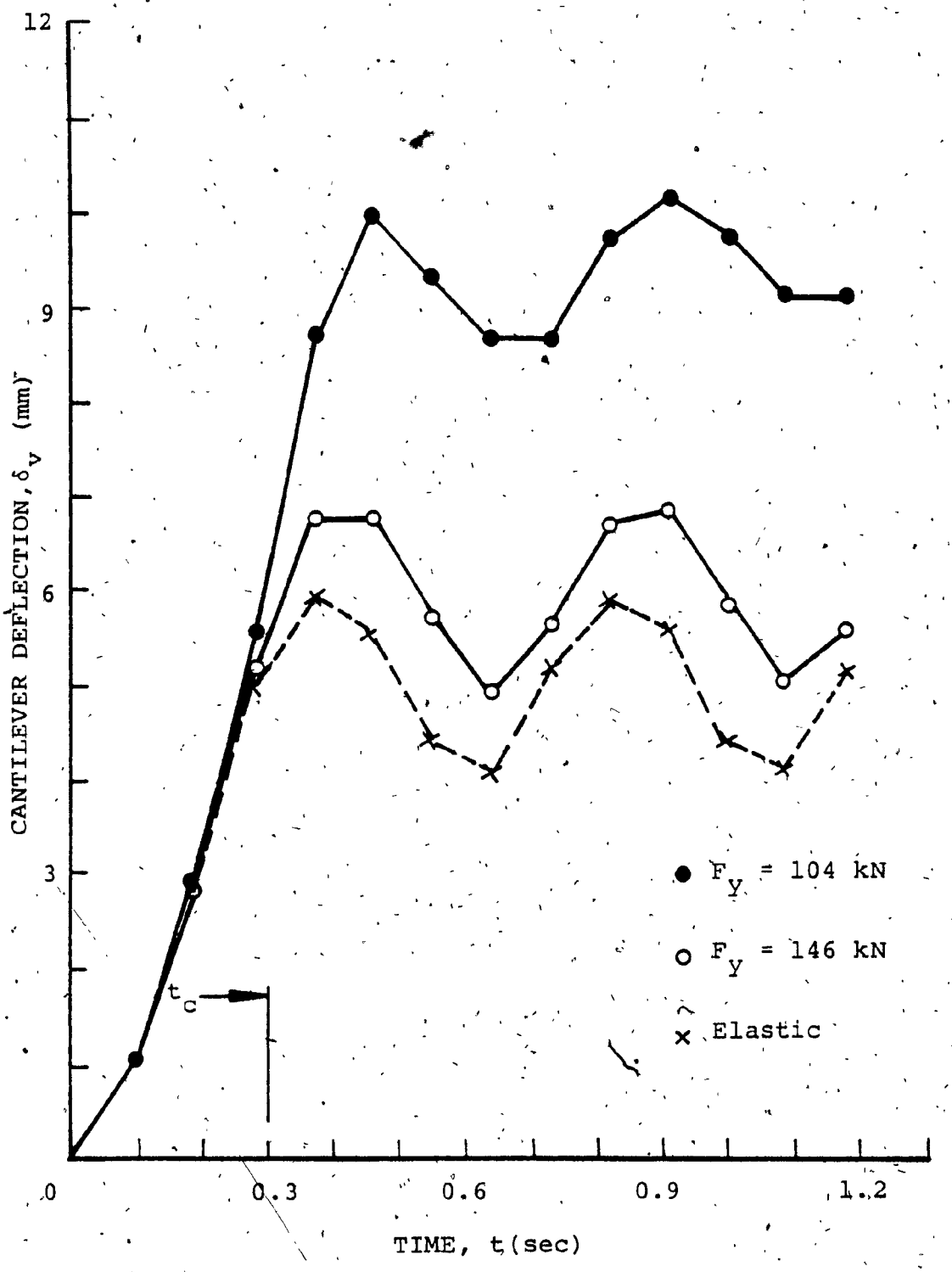

FIG. 4.25 EFFECT OF VERTICAL MECHANICAL CONNECTOR SHEAR STRENGTH ON TIME HISTORY RESPONSE OF CANTILEVER DEFLECTION FOR t_c = 0.3 SEC. - 5 STOREY CANTILEVER

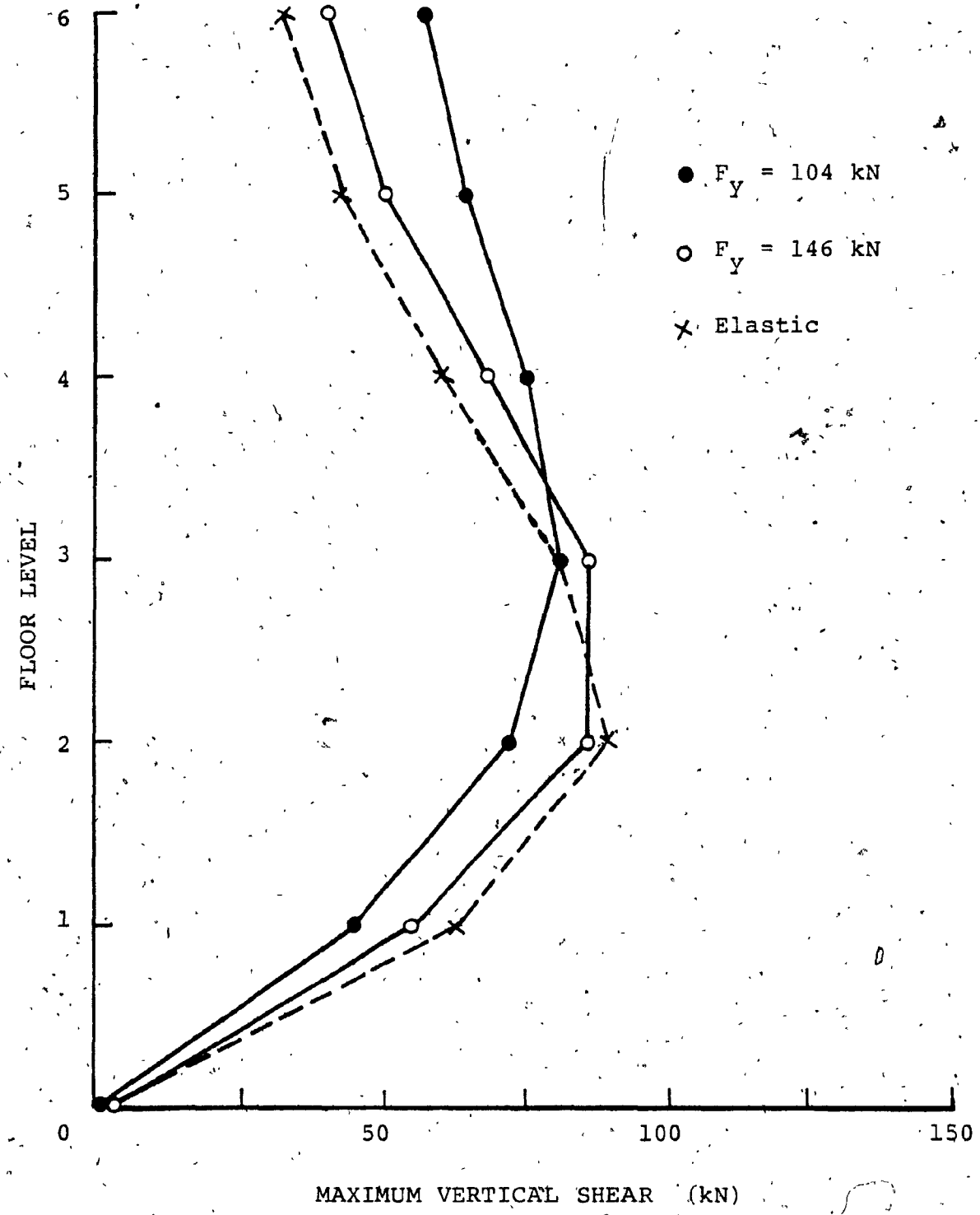

FIG. 4.26 EFFECT OF VERTICAL MECHANICAL CONNECTOR SHEAR STRENGTH ON DISTRIBUTION OF MAXIMUM SHEAR FORCE IN JOINT 1 FOR t_c = 0.3 SEC. - 5 STOREY CANTILEVER

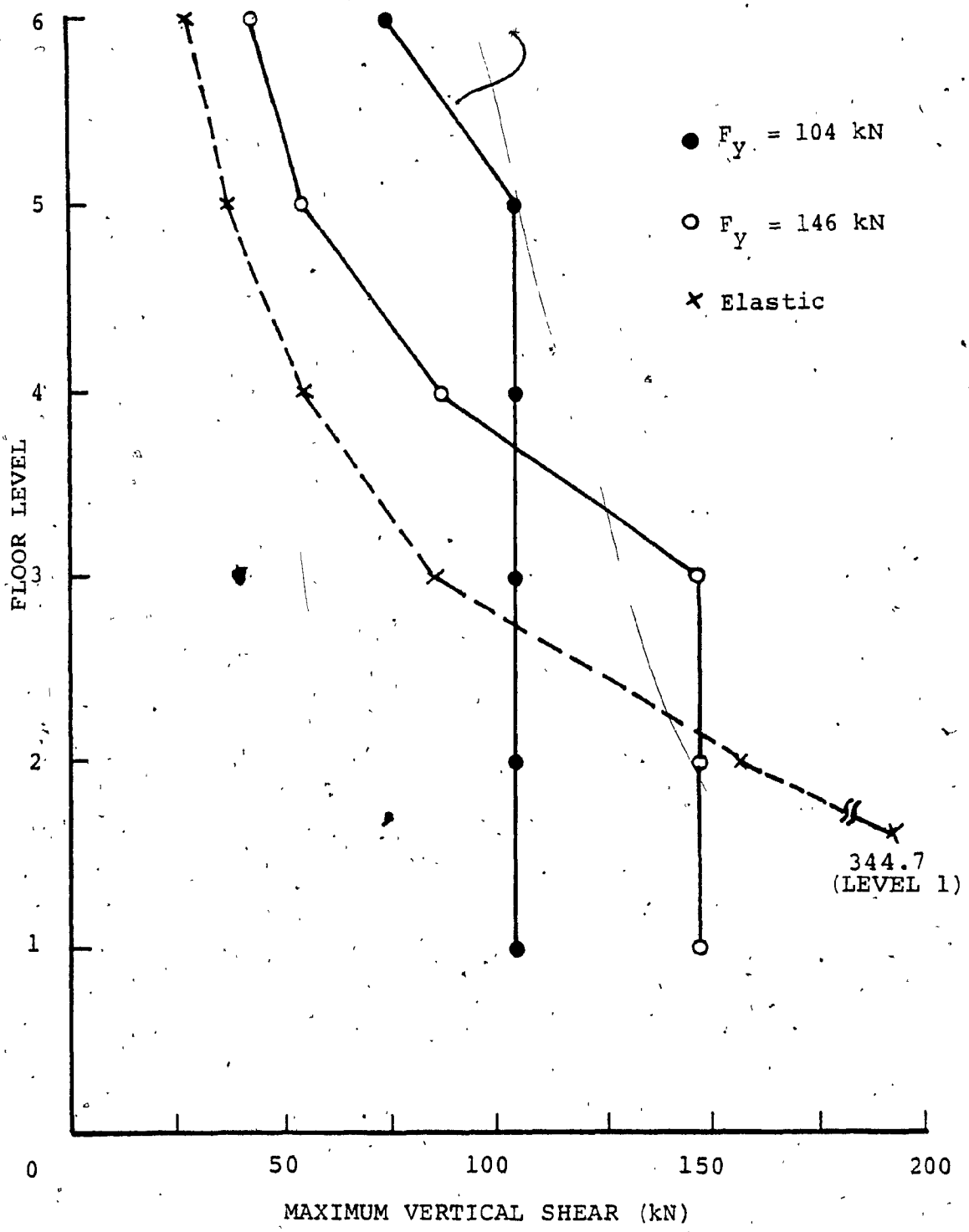

FIG. 4.27 EFFECT OF VERTICAL MECHANICAL CONNECTOR SHEAR STRENGTH ON DISTRIBUTION OF MAXIMUM SHEAR FORCE IN JOINT 2 FOR t_c = 0.3 SEC. - 5 STOREY CANTILEVER

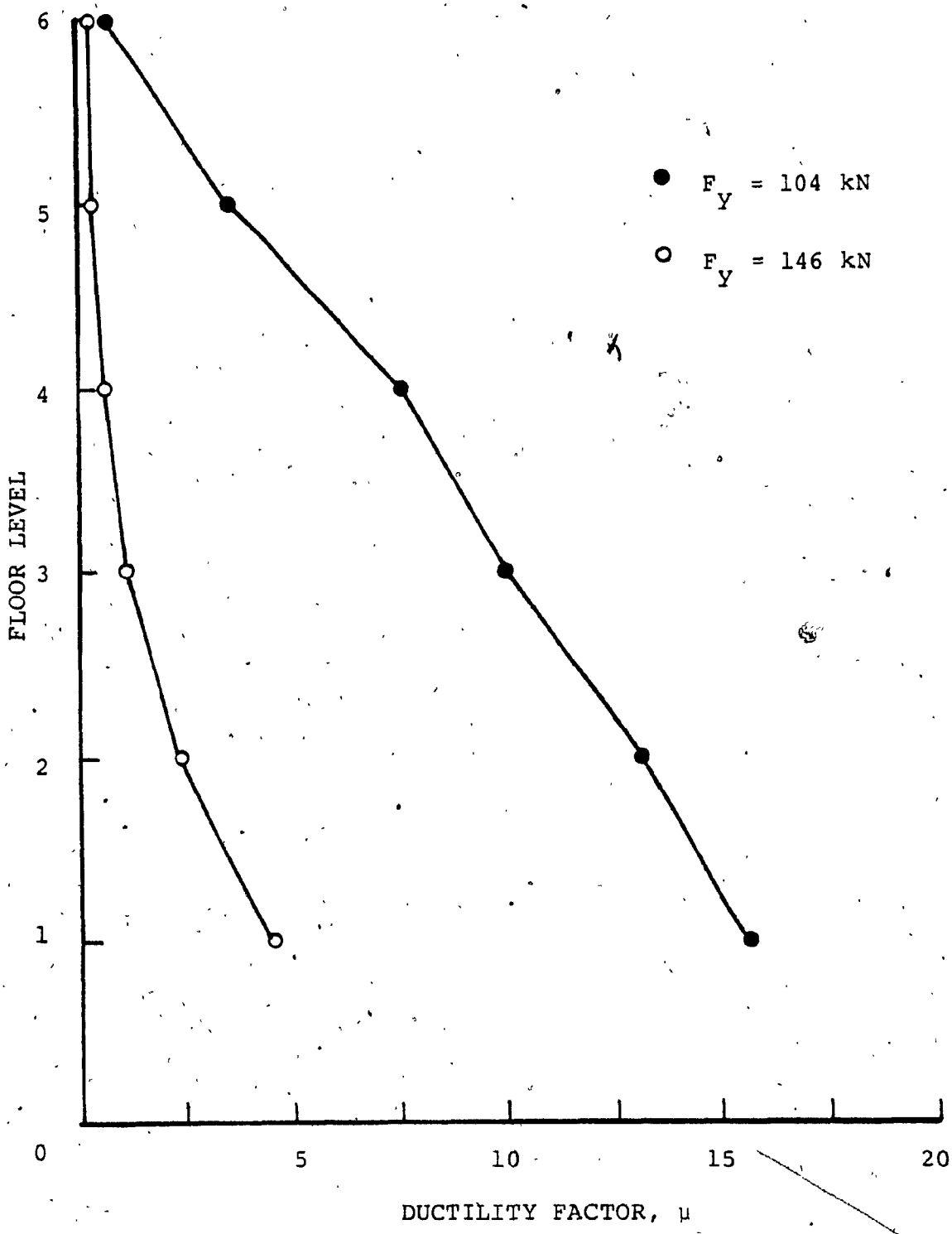

FIG. 4.28 EFFECT OF VERTICAL MECHANICAL CONNECTOR SHEAR STRENGTH ON DISTRIBUTION OF MAXIMUM DUCTILITY DEMAND IN JOINT 2 FOR t_c = 0.3 SEC. - 5 STOREY CANTILEVER

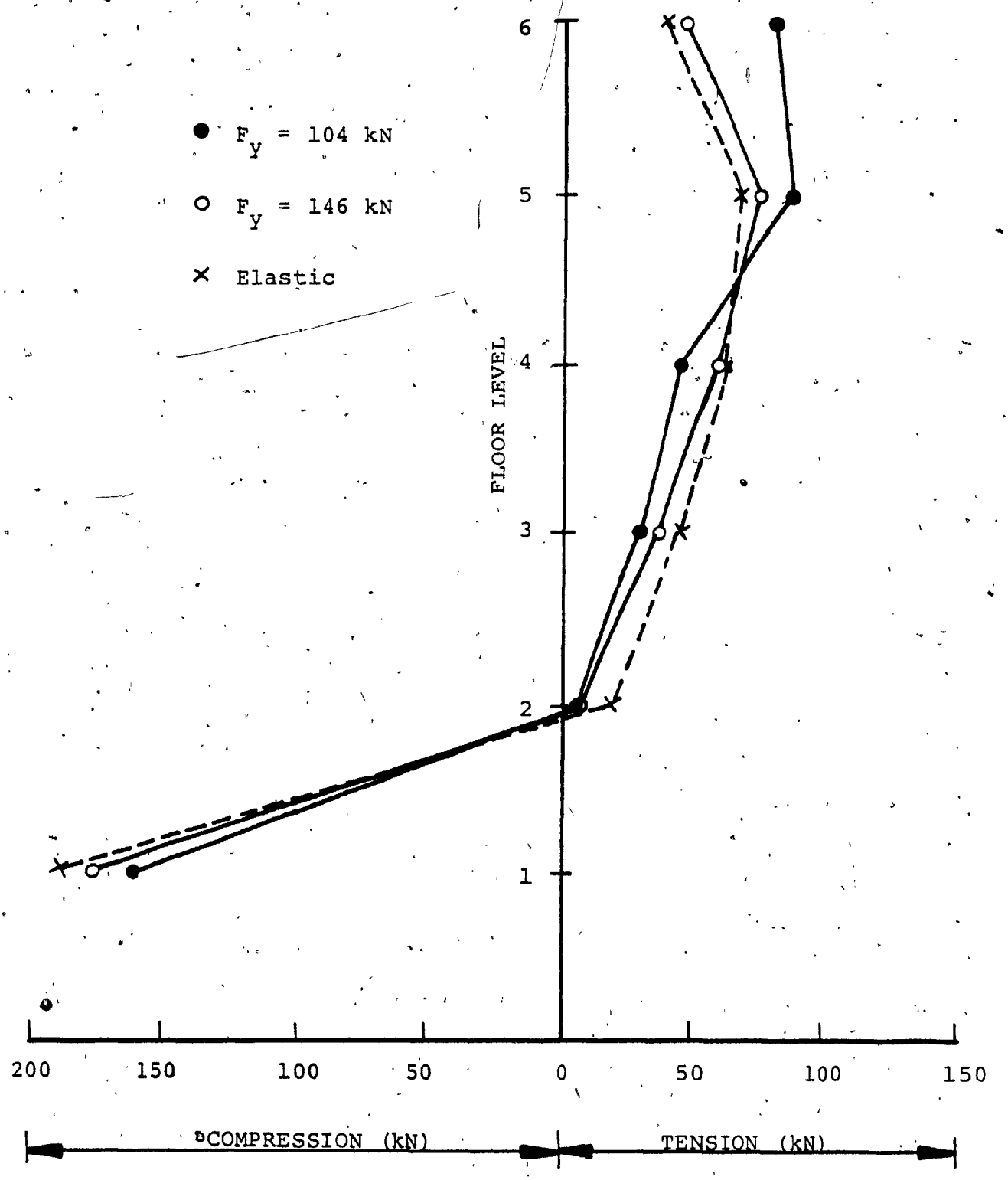

FIG. 4.29 EFFECT OF VERTICAL MECHANICAL CONNECTOR SHEAR STRENGTH ON DISTRIBUTION OF MAXIMUM AXIAL FORCE IN VERTICAL JOINT FOR t_c = 0.3 SEC. - 5 STOREY CANTILEVER

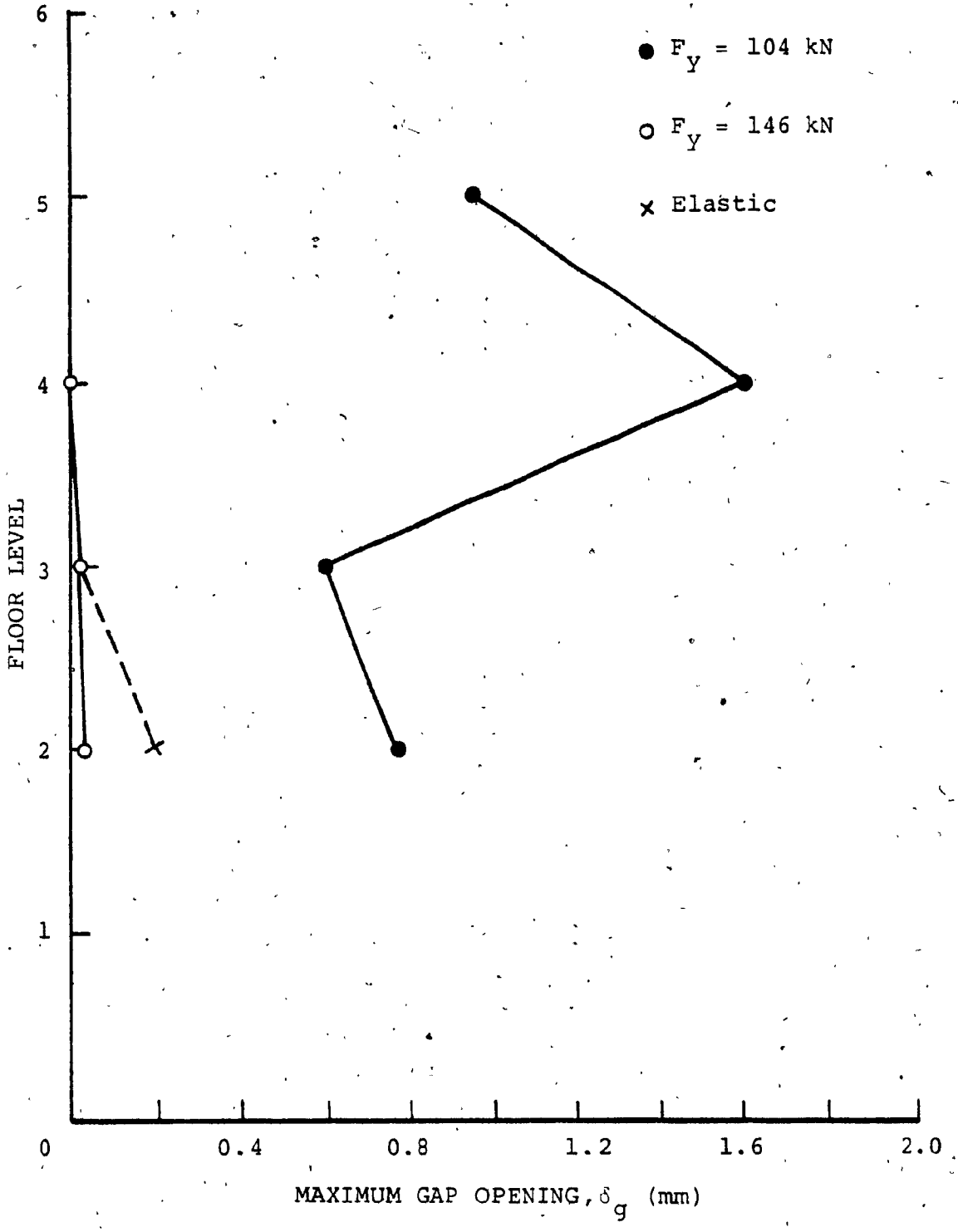

FIG. 4.30 EFFECT OF VERTICAL MECHANICAL CONNECTOR SHEAR STRENGTH ON DISTRIBUTION OF MAXIMUM GAP OPENING IN HORIZONTAL JOINTS OF CANTILEVER FOR t_c = 0.3 SEC. - 5 STOREY CANTILEVER

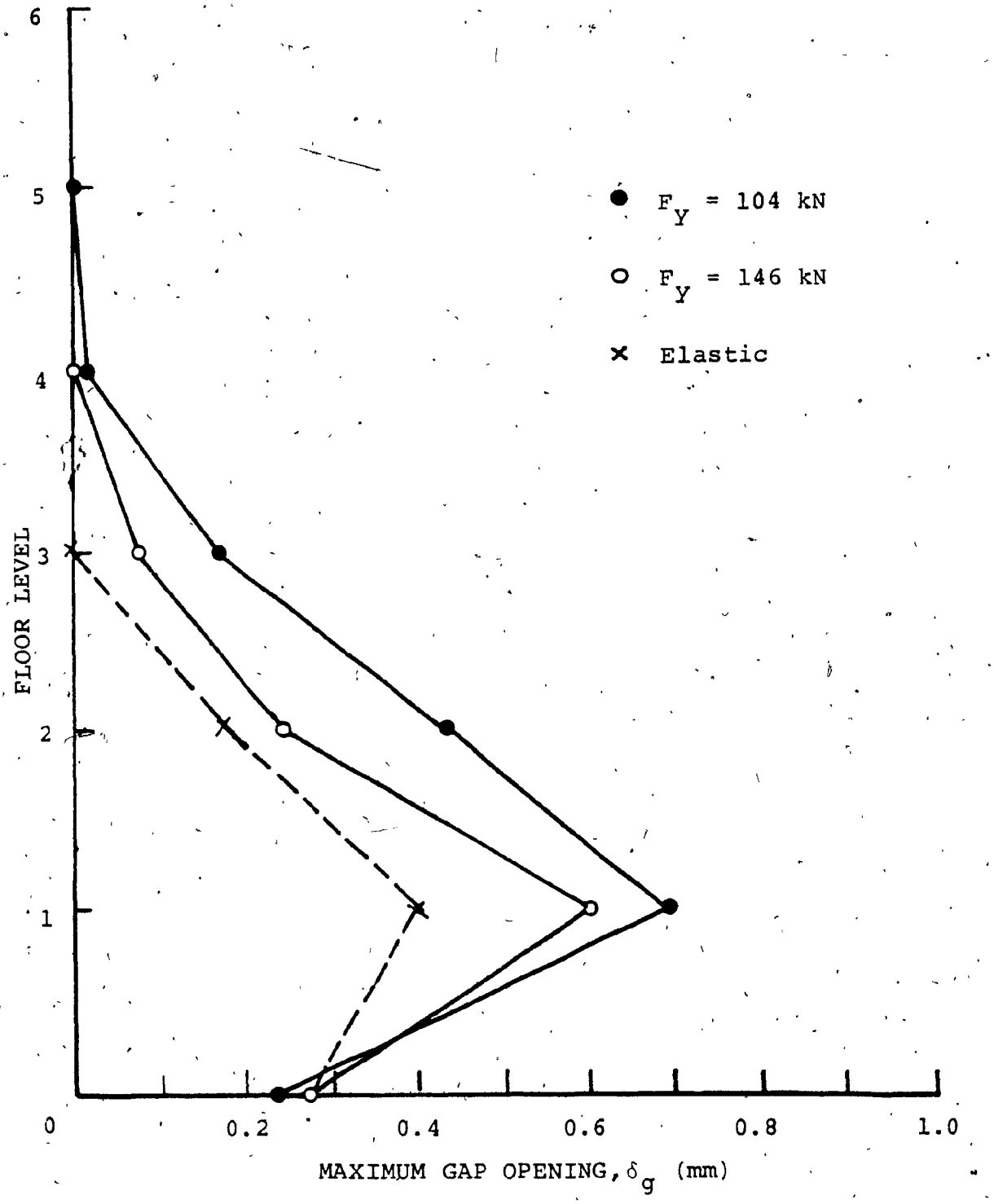

FIG. 4.31 EFFECT OF VERTICAL MECHANICAL CONNECTOR SHEAR STRENGTH ON DISTRIBUTION OF MAXIMUM GAP OPENING IN HORIZONTAL JOINTS OF WALL 1 FOR t_c = 0.3 SEC. - 5 STOREY CANTILEVER

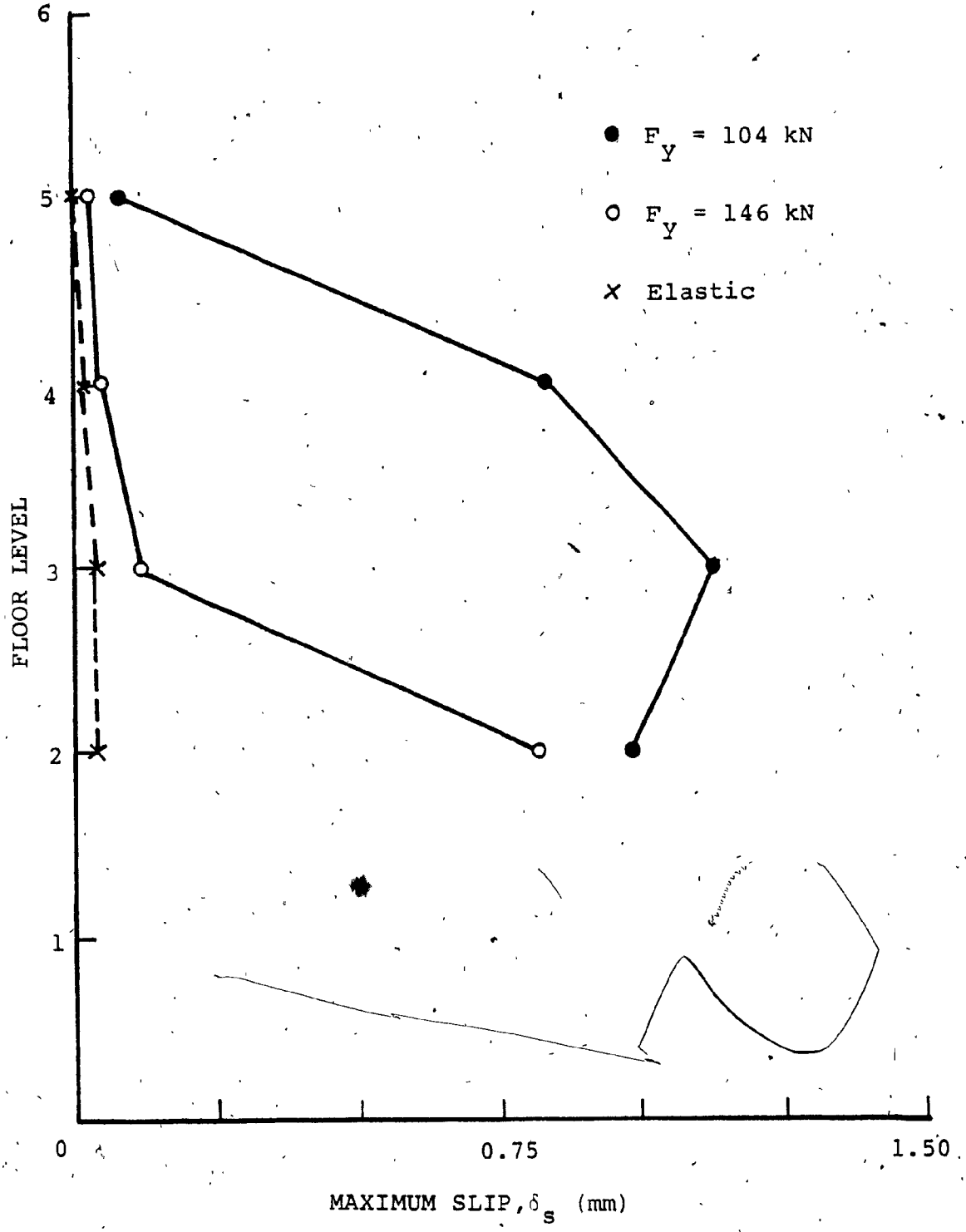

FIG. 4.32 EFFECT OF VERTICAL MECHANICAL CONNECTOR SHEAR STRENGTH ON DISTRIBUTION OF MAXIMUM SLIP IN HORIZONTAL JOINTS OF CANTILEVER FOR t_c = 0.3 SEC. - 5 STOREY CANTILEVER

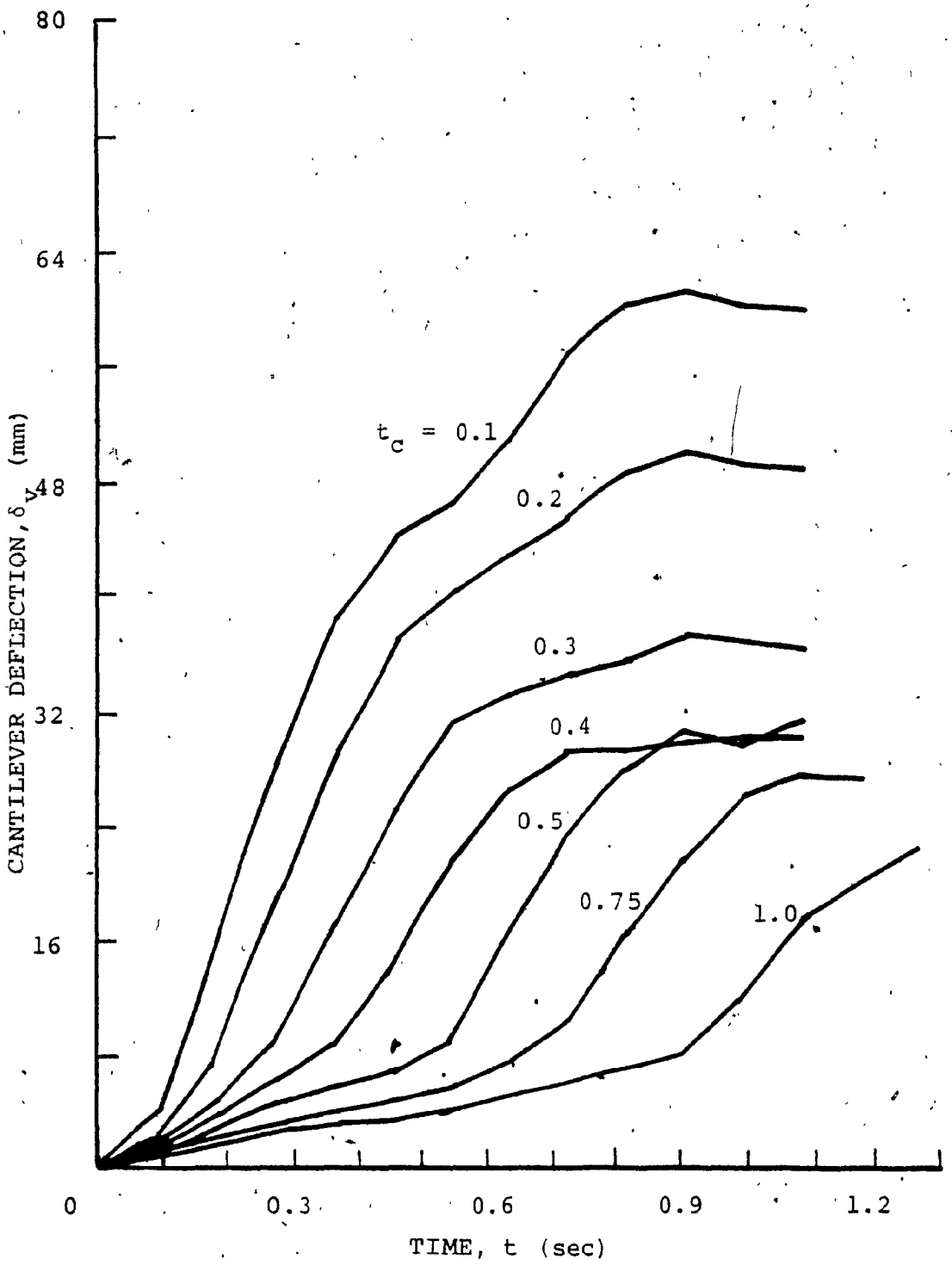

FIG. 4.33 TIME HISTORY RESPONSE OF CANTILEVER DEFLECTION FOR VARIOUS PANEL COLLAPSE TIMES WITH R/W = 1.02 (R = 1464 kN; W = 1431 kN) - 5 STOREY CANTILEVER

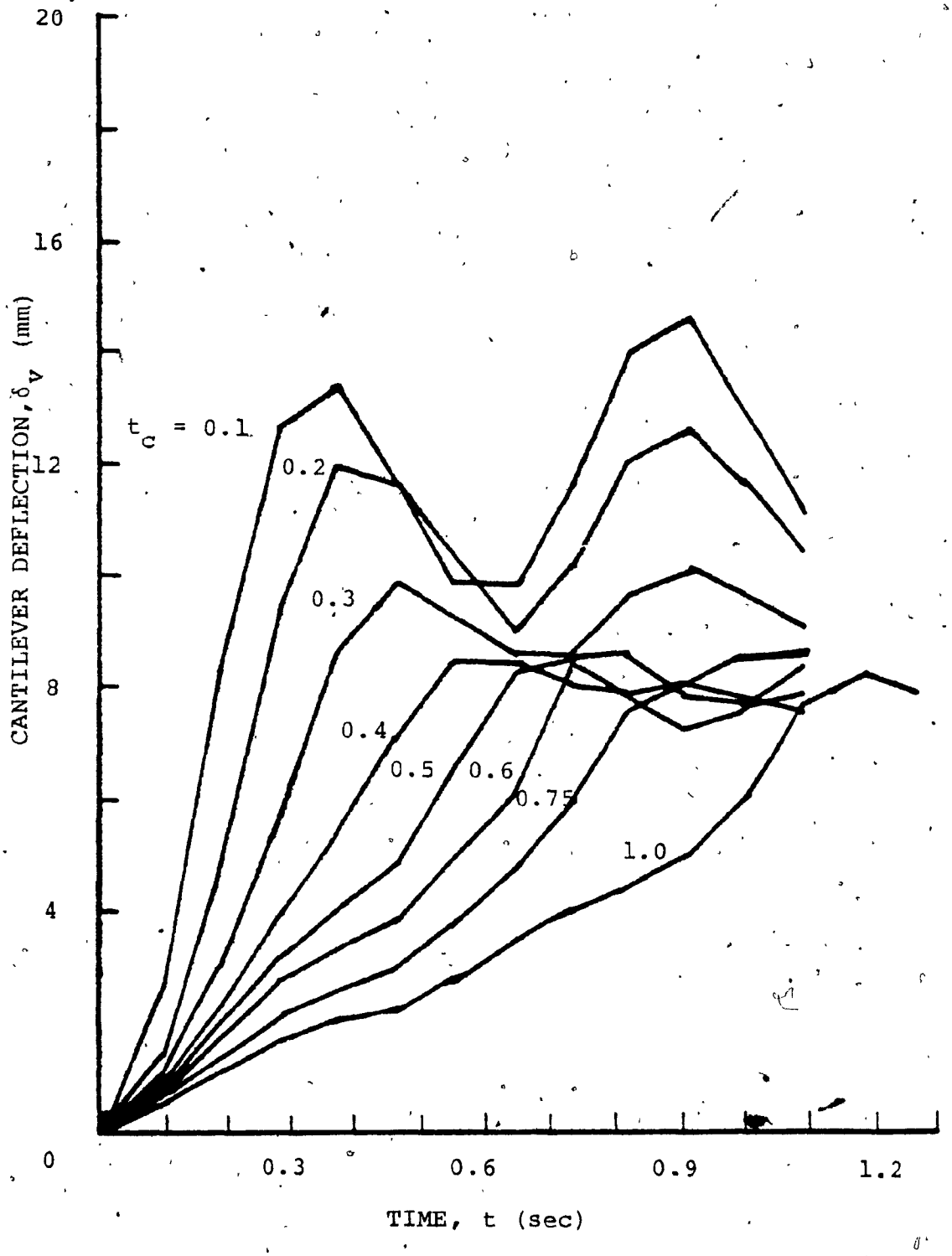

FIG. 4.34 TIME HISTORY RESPONSE OF CANTILEVER DEFLECTION FOR VARIOUS PANEL COLLAPSE TIMES WITH R/W = 1.12 (PROTOTYPE WALL: R = 1044 kN; W = 936 kN) - 5 STOREY CANTILEVER

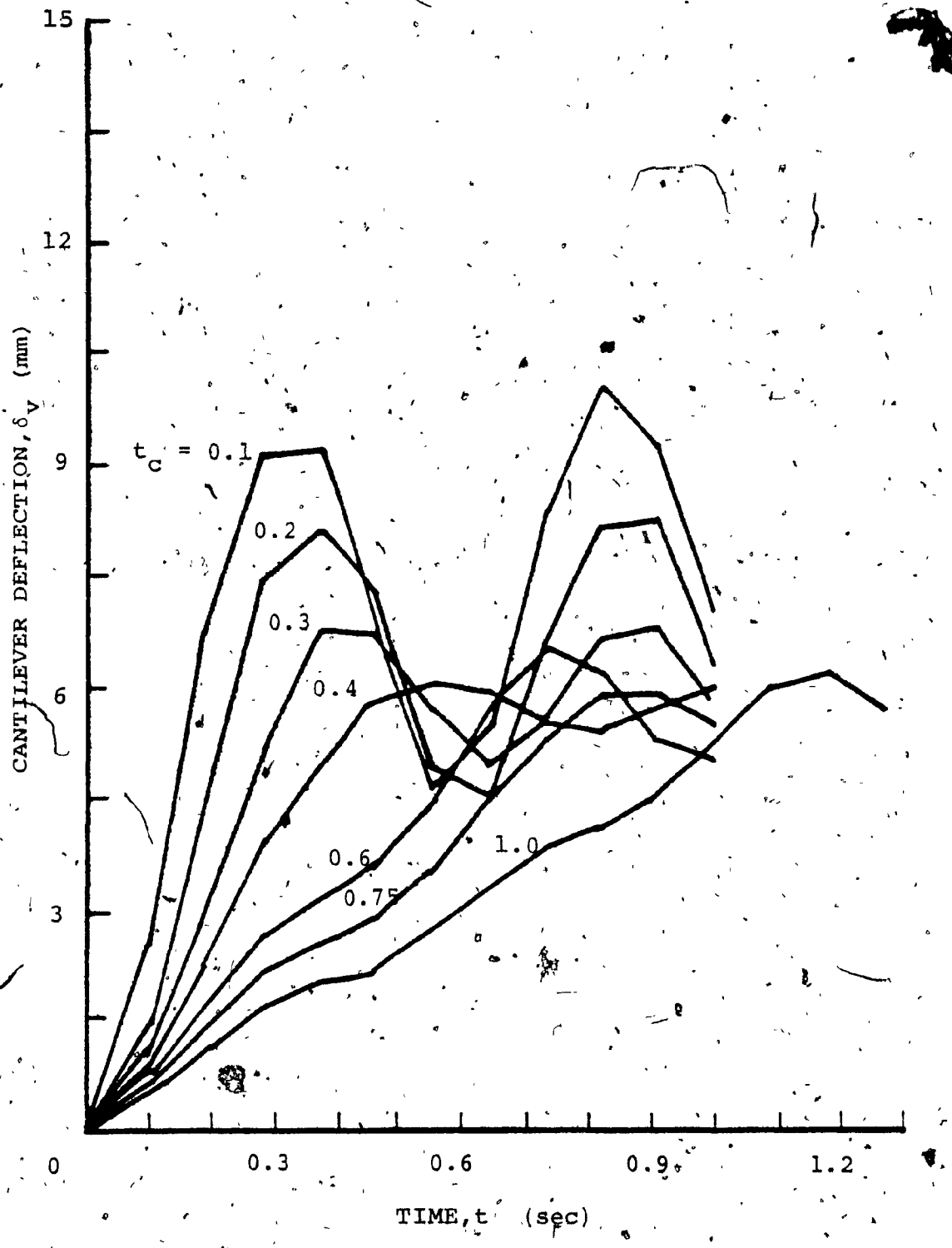

FIG. 4.35 TIME HISTORY RESPONSE OF CANTILEVER DEFLECTION FOR VARIOUS PANEL COLLAPSE TIMES WITH R/W = 1.56 (R = 1464 kN; W = 936 kN) - 5 STOREY CANTILEVER

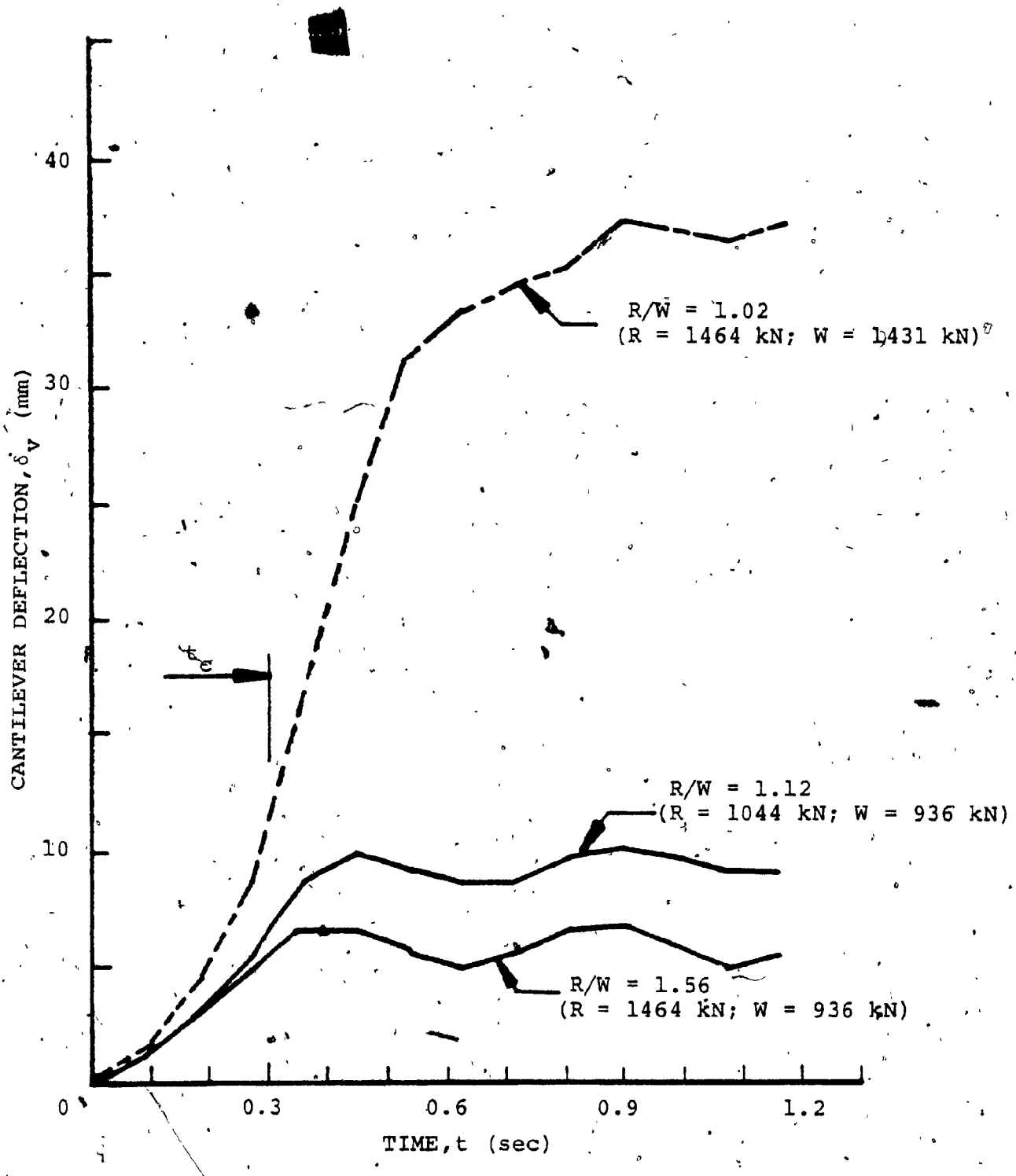

FIG. 4.36 EFFECT OF R/W ON TIME HISTORY RESPONSE OF CANTILEVER DEFLECTION FOR t_c = 0.3 SEC. - 5 STOREY CANTILEVER

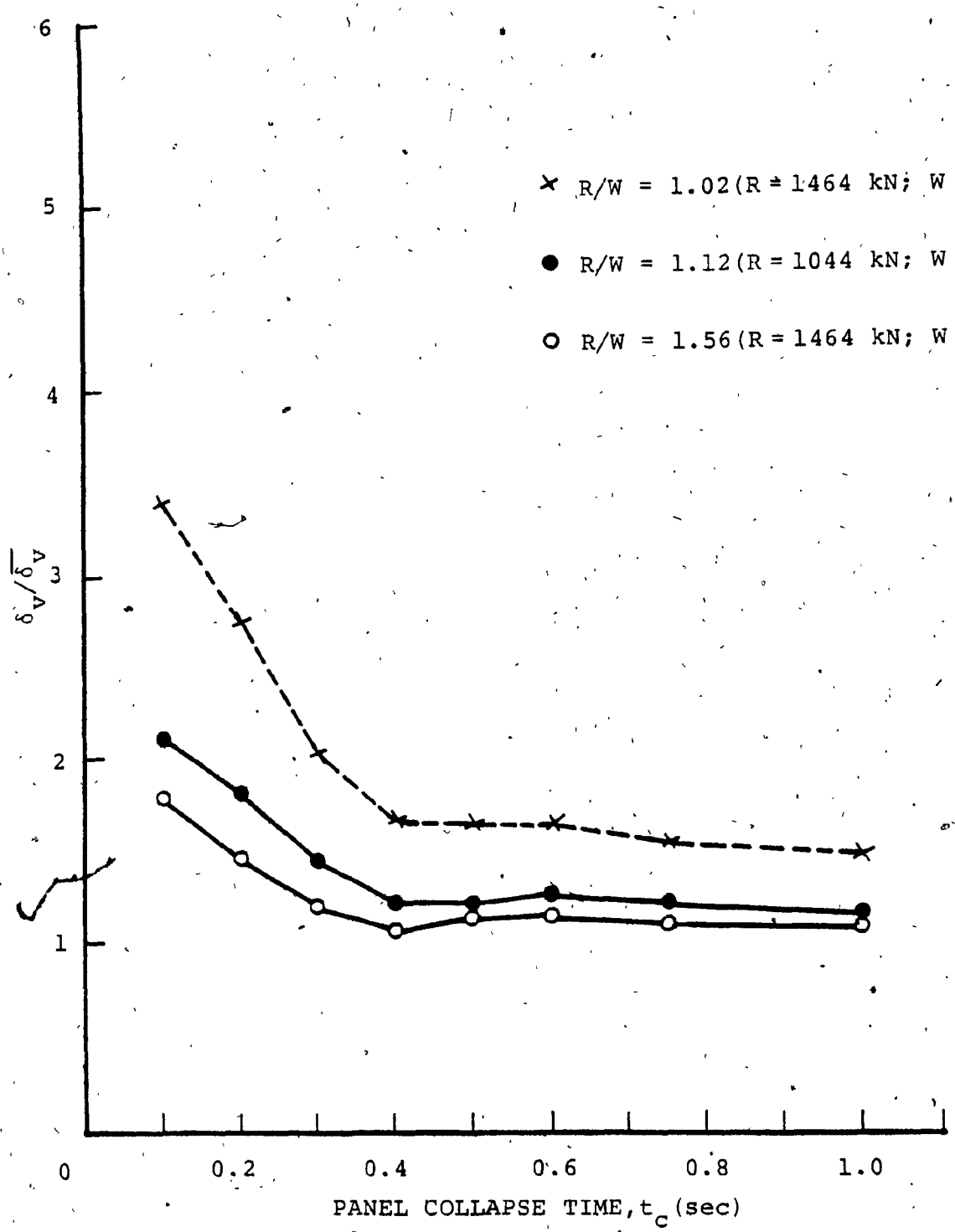

FIG. 4.37 MAXIMUM DYNAMIC RESPONSE OF CANTILEVER DEFLECTION FOR VARYING PANEL COLLAPSE TIMES AND THREE DIFFERENT RATIOS OF R/W - 5 STOREY CANTILEVER

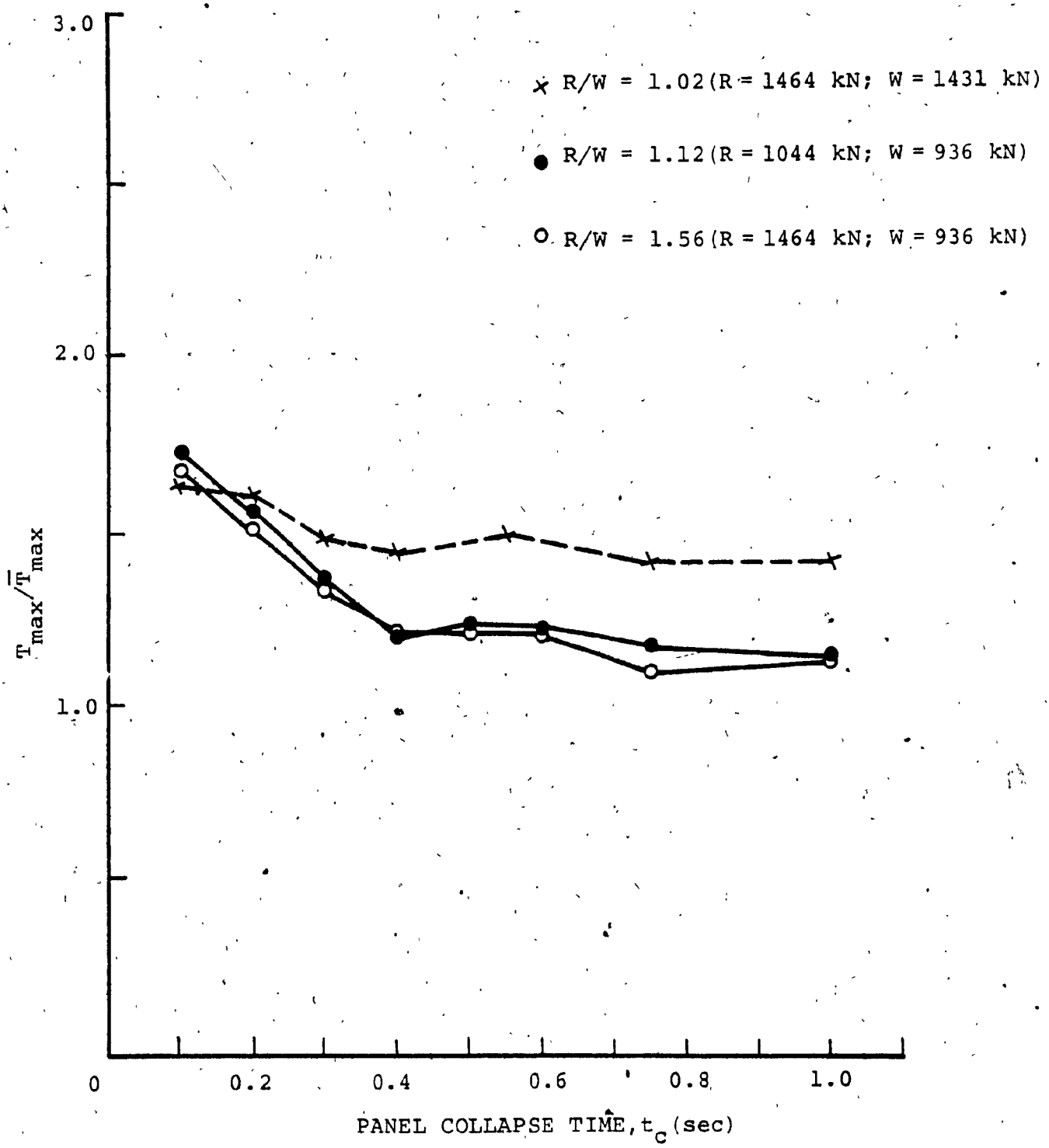

FIG. 4.38 MAXIMUM DYNAMIC RESPONSE OF TRANSVERSE TIE FORCE FOR VARYING PANEL COLLAPSE TIMES AND THREE DIFFERENT RATIOS OF R/W - 5 STOREY CANTILEVER

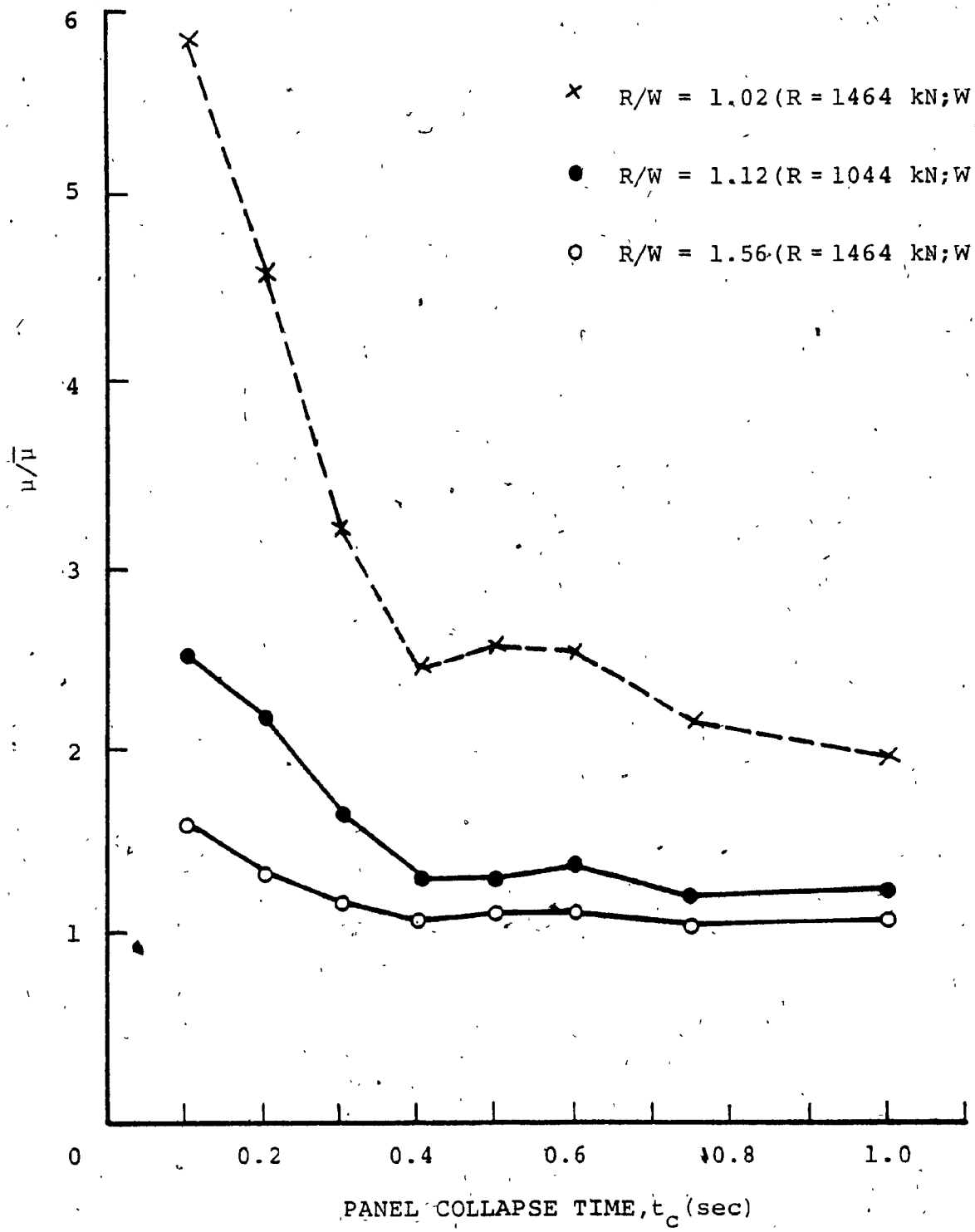

FIG. 4.39 MAXIMUM DYNAMIC RESPONSE OF DUCTILITY DEMAND IN VERTICAL MECHANICAL CONNECTORS FOR VARYING PANEL COLLAPSE TIMES AND THREE DIFFERENT RATIOS OF R/W - 5 STOREY CANTILEVER

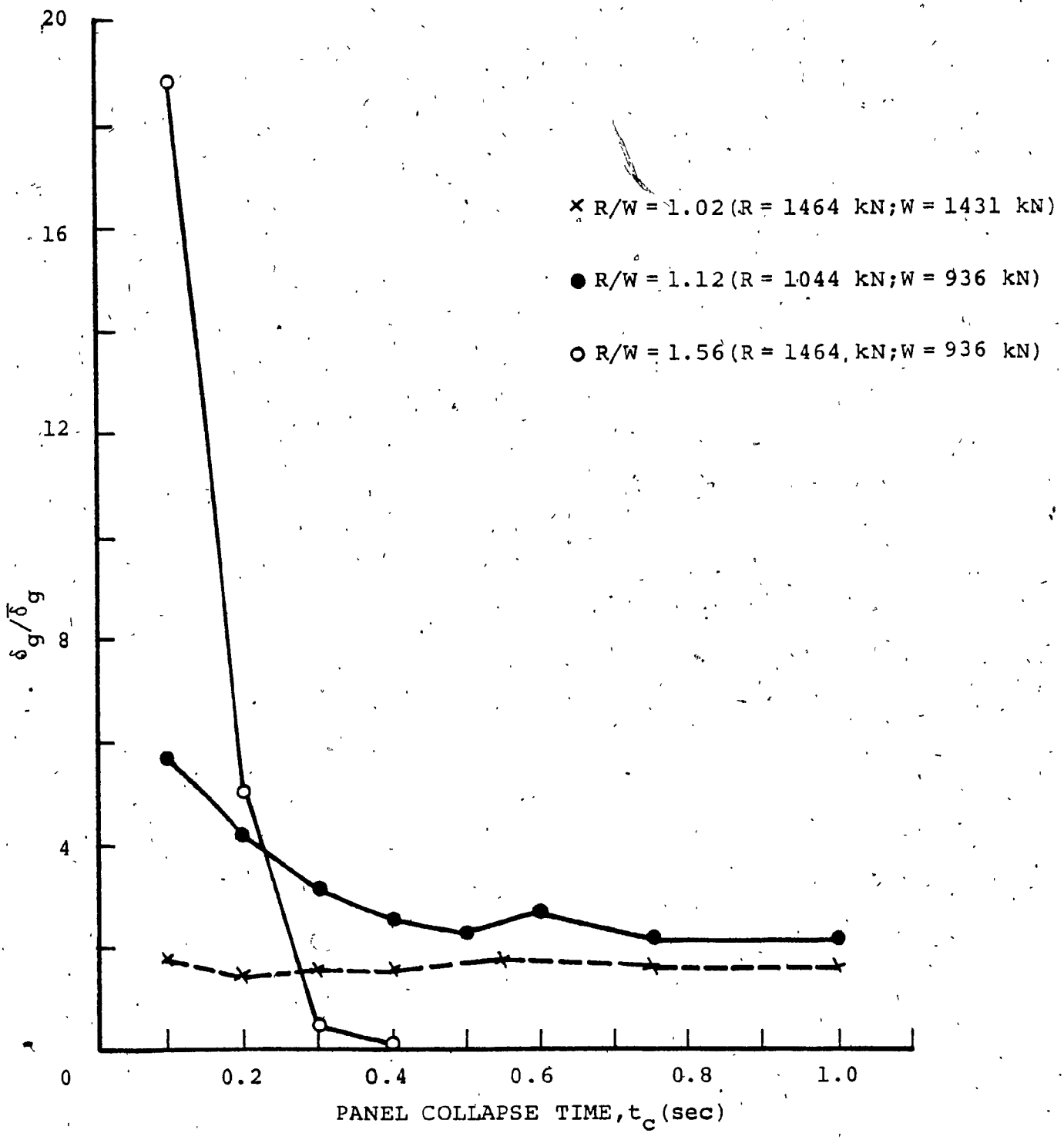

FIG. 4.40 MAXIMUM DYNAMIC RESPONSE OF GAP OPENING IN HORIZONTAL JOINTS OF CANTILEVER FOR VARYING PANEL COLLAPSE TIMES AND THREE DIFFERENT RATIOS OF R/W - 5 STOREY CANTILEVER

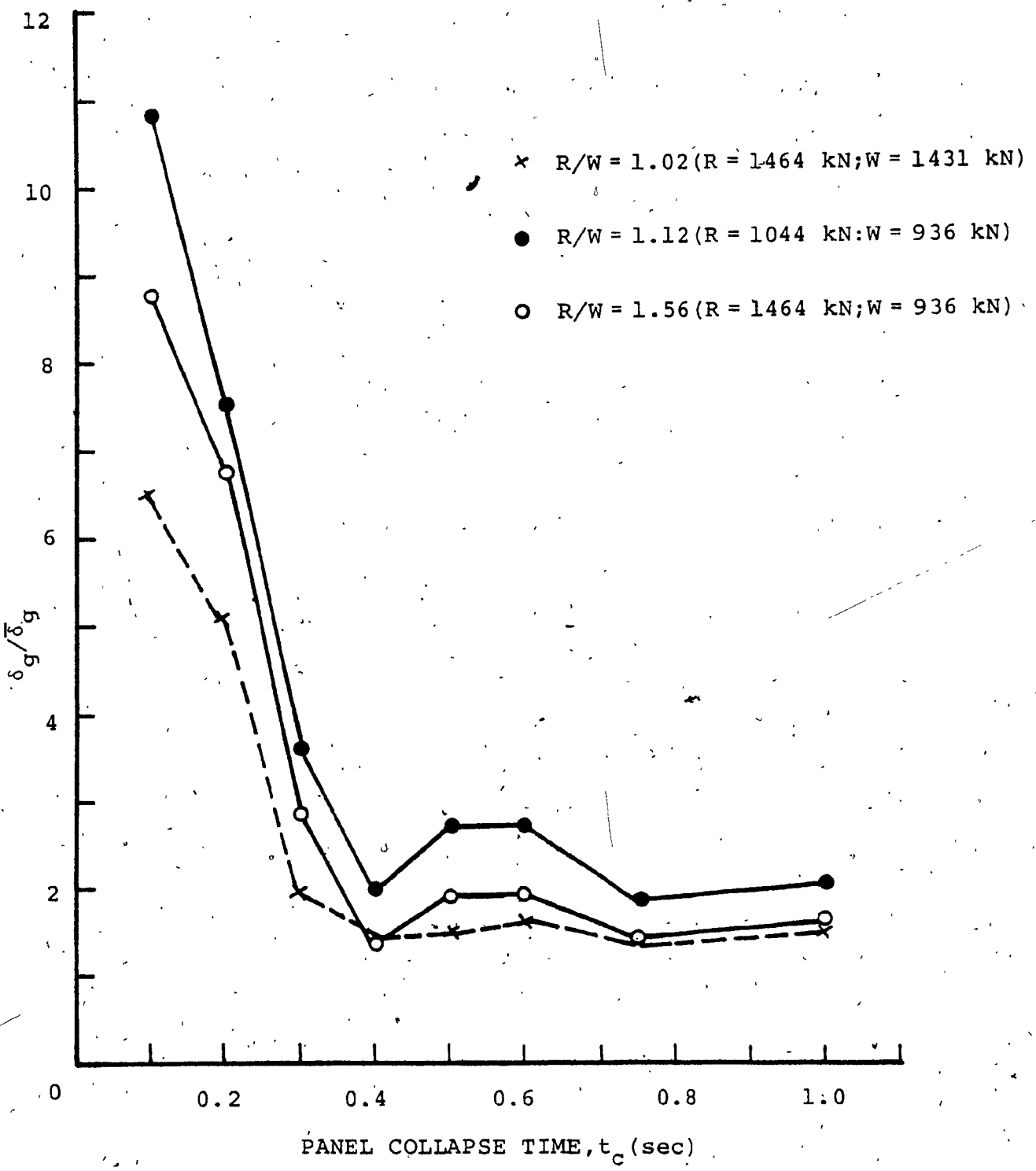

FIG. 4.41 MAXIMUM DYNAMIC RESPONSE OF GAP OPENING IN HORIZONTAL JOINTS OF WALL 1 FOR VARYING PANEL COLLAPSE TIMES AND THREE DIFFERENT RATIOS OF R/W - 5 STOREY CANTILEVER

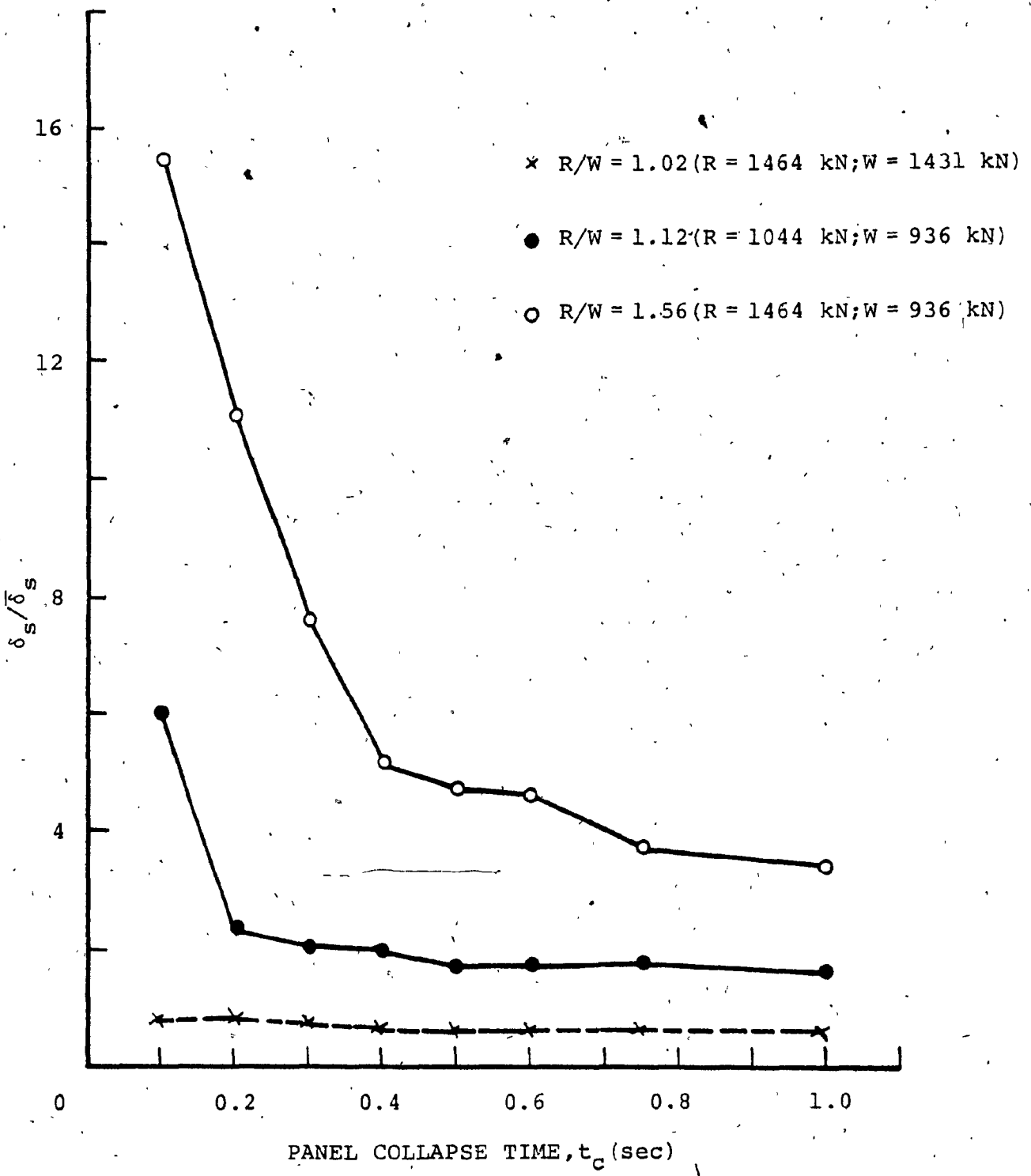

FIG. 4.42 MAXIMUM DYNAMIC RESPONSE OF SHEAR SLIP IN HORIZONTAL JOINTS OF CANTILEVER FOR VARYING PANEL COLLAPSE TIMES AND THREE DIFFERENT RATIOS OF R/W - 5 STOREY CANTILEVER

CHAPTER V

SUMMARY AND CONCLUSIONS

CHAPTER V

SUMMARY AND CONCLUSIONS

A study of precast panel walls has been performed for simulated quasi-static and dynamic conditions of local panel collapse. A finite element procedure was employed to examine the nonlinear static and dynamic behaviour of a large precast panel shear wall structure of the cross-wall type. Individual precast panels were modelled as multilevel finite element substructures comprising 4-node plane stress rectangular elements with linear elastic behaviour. Horizontal and vertical joints were represented by discrete orthogonal spring elements with nonlinear constitutive relationships, whereas uniaxial spring elements with elastic behaviour were used to model the transverse and vertical ties.

A 12-storey prototype wall with variable cantilever depths was studied for static loading. To simulate static conditions for local collapse, individual exterior panels are assumed to fail quasi-statically at various levels within the precast system. For comparison, analyses were also performed for:

(a) Elastic behaviour based on the assumption that all joints remain elastic but allowing slip and gap openings to occur in the horizontal joints; and

(b) The rigid-cantilever approach recommended for design by the PCA [5].

The following observations were noted concerning the nonlinear static behaviour of the prototype wall.

(1) Regardless of the number of storeys in the cantilever, tensile forces developed in transverse ties are confined within the upper six floor levels. For cantilevers deeper than one storey, the resultant force in transverse ties is essentially constant, whereas the effective lever arm increases with increasing cantilever depth. However, it was noted that the ratio between the effective lever arm d and the overall cantilever height H is approximately constant ($d/H = 0.80$). Furthermore, it was observed that the rigid-cantilever approach produces conservative design forces for transverse ties below the upper four floor levels, compared to those of the nonlinear behaviour. In particular, it was noted that the transverse ties which are designed according to the PCA recommendations [5] will remain elastic at design load level.

(2) The ductility demand in mechanical connectors increases with increasing cantilever height. An important observation was that the demand will exceed the practical ductility limit for structures higher than 12 storeys.

(3) Significant gap openings were observed in the horizontal joints of the cantilever and Wall 1, demonstrating the necessity for reinforcement across the horizontal joints to resist the vertical tensile stresses developed.

(4) Horizontal shear slip occurs at all floor levels of the cantilever joints. This implies that the resistance provided by friction between precast concrete panels and in-situ joint grout is not adequate to resist the induced shear force in the horizontal joints.

A parametric study was performed for a 6-storey precast panel wall for static loading. The following conclusions were noted:

(5) The nonlinear static behaviour of the precast system is significantly influenced by the design shear strength of mechanical connectors. In particular, it was shown that the ductility demand in mechanical connectors can be effectively reduced by introducing connectors with higher design shear strength.

(6) The coefficient of friction between the precast concrete and the in-situ joint grout in horizontal joints, if specified within the range 0.2 - 0.8 used in current design codes, has insignificant effect on the performance of the precast system.

(7) Vertical ties reduce the magnitude of nonlinear joint deformations and ductility demand in the structure. In particular, vertical ties with postensioning were shown to be more effective.

(8) The ultimate load capacity of the cantilever is governed by the shear capacity of the mechanical connectors in the vertical joint.

A nonlinear dynamic analysis has also been carried out for a 6-storey prototype wall with variable cantilever depths for simulated dynamic force conditions of local panel collapse. The latter was simulated by assuming that an exterior panel collapses in a short duration of time in response to a domestic gas explosion. The following observations were noted concerning the dynamic effects of local panel collapse on the prototype wall.

(9) The pseudo-static resultant from maximum force envelopes for transverse ties increases with increasing cantilever depth. However, the ratio between the effective lever arm and overall cantilever height remains constant at 0.80 for cantilever deeper than one storey. The force requirement in transverse ties was shown to be substantially higher than that of the nonlinear static behaviour at all floor levels (12.4 to 177.2%). At design load level, it was observed that the transverse tie force

at the fifth floor level surpasses the minimum design strength of 80 kN recommended by the PCA [5].

(10) The ductility demand in mechanical connectors is approximately 50% higher than that of the nonlinear static behaviour at all floor levels.

(11) Maximum gap openings and shear slip in the horizontal joints of the cantilever and Wall 1 are significantly higher than those of the nonlinear static response, with maximum increases of 89.6%, 152.4% and 336.4%, for maximum shear slip, maximum gap opening in the cantilever and Wall 1, respectively.

The results of the parameter study on the nonlinear dynamic behaviour of a 6-storey precast panel wall of 5-storey cantilever allows the following conclusions:

(12) The results indicate that the use of a coefficient higher than $\mu_f = 0.4$ in horizontal joints can result in slightly higher ductility demand in mechanical connectors.

(13) For panel collapse time $t_c < 0.3$ sec., it was shown that the ductility demand in mechanical connectors will significantly exceed the limit to which domestic structures can be designed.

(14) The design value of the panel collapse time, $t_c = 0.3$ sec., appears to be a reasonable limit for design consideration.

REFERENCES

REFERENCES

[1] Griffiths, H., Pugsley, Sir A. and Saunders, Sir O., Report of the Inquiry into the Collapse of Flats at Ronan Point, Canning Town, Ministry of Housing and Local Government, H.M.S.O., London, 1968.

[2] Alexander, S.J., and Hambly, E.C., "The Design of Structures to Withstand Gaseous Explosions," Concrete, Feb. 1970, pp. 107-114.

[3] Stafford-Smith, B., and Rahman, K.M.K., "A Theoretical Study of the Sequence of Failure in Precast Panel Shear Walls," Proceedings of the Institution of Civil Engineers, Vol. 55, Paper 7620, Sept. 1973, pp.581-592.

[4] Fintel, M., Schultz, D.M. and Iqbal, M., "Report 2: Philosophy of Structural Response to Normal and Abnormal Loads," Design and Construction of Large-Panel Concrete Structures. Office of Policy Development and Research, U.S. Department of Housing and Urban Development, Washington, D.C., 1976.

[5] Schultz, D.M., Burnett, S.F.P. and Fintel M., "Report 4: A Design Approach to General Structural Integrity," Design and Construction of Large-Panel Concrete Structures. Office of Policy Development and Research, U.S. Department of Housing and Urban Development, Washington, D.C., 1977.

[6] Harris, H.B. and Muskivitch, J.C., "Report 1: Study of Joints and Sub-Assemblies - Validation of the Small Scale Direct Modeling Techniques," Nature and Mechanism of Progressive Collapse in Industrialized Buildings. Office of Policy Development and Research, U.S. Department of Housing and Urban Development, Washington, D.C., 1977.

[7] Muskivitch, J.C. and Harris, H.G., "Report 2: Behaviour of Precast Large Panel Buildings Under Simulated Progressive Collapse Conditions," Nature and Mechanism of Progressive Collapse in Industrialized Buildings. Office of Policy Development and Research, U.S. Department of Housing and Urban Development, Washington, D.C., 1979.

[8] Muskivitch, J.C. and Harris, H.G., "Report 3: Analytical Investigation of the Internal Load Distribution and the Mechanism of Progressive Collapse in Precast Concrete Large Panel Buildings," Nature and Mechanism of Progressive Collapse in Industrialized Buildings. Office of Policy Development and Research, U.S. Department of Housing and Urban Development, Washington, D.C., 1981.

[9] Llorente, C., "The Effect of Opening of Horizontal Connections on the Dynamic Response of Precast Panel Buildings," M.Sc. Thesis, Department of Civil Engineering, Massachusetts Institute of Technology, June 1977.

[10] Llorente, C., Becker, J.M. and Roesset, J.M., "The Effect of Nonlinear-Inelastic Connection Behaviour on Precast Panelized Shear Walls," Symposium on Mathematical Modelling of Reinforced Concrete Structures, American Concrete Institute National Convention, Toronto, Canada, April 1978.

[11] Mueller, P. and Becker, J.M., "Seismic Behavior of Precast Walls Coupled Through Vertical Connections," Proceedings of Seventh World Conference on Earthquake Engineering, Istanbul, Turkey, Sept. 1980.

[12] Mueller, P. and Becker, J.M., "Seismic Characteristics of Composite Precast Walls," Proceedings Third Canadian Conference on Earthquake Engineering, Montreal, Canada, June 1979.

[13] Schricker, V. and Powell, G.H., "Inelastic Seismic Analysis of Large Panel Buildings," Report No. UCB/EERC - 80/38, EERC, College of Engineering, University of California, Berkeley, California, Sept. 1980.

[14] Pekau, O.A., "Structural Integrity of Precast Panel Shear Walls," Canadian Journal of Civil Engineering, Vol. 9, No. 1, 1982, pp. 13-24.

[15] Burnett, E.F.P. and Howson, C., "Cantilever Wall Action in Concrete Panelized Buildings - Design Procedures for the Avoidance of Progressive Collapse," Building Engineering Group, Civil Engineering Department, University of Waterloo, March 1978.

[16] Verbic, B. and Terzic, N., "Test of Panel Connections in "Vranica" Type Large Panel Buildings," Institute za Materijale: Konstruckcije, Sarajevo, Yugoslavia, April 1977.

[17] Mattock, A.H., "Effect of Reinforcing Bar Size on Shear Transfer Across a Crack in Concrete," Report SM77-2, Department of Civil Engineering, University of Washington, Sept. 1977.

[18] Mattock, A.H., "Shear Transfer Under Cyclically Reversing Loading, Across an Interface Between Concretes Cast at Different Times," Report SM77-1, Department of Civil Engineering, University of Washington, June 1977.

[19] Spencer, R.A. and Neille, D.S., "Cyclic Tests of Welded Headed Stud Connections," Journal of the Prestressed Concrete Institute, Vol. 21, No. 3, May/June, 1976. pp.71-114.

[20] Pekau, O.A., and Huttelmaier, H.P., "A Versatile Panel Element for the Analysis of Shear Wall Structures," Computers and Structures, Vol. 12, No. 3, Pergamon Press, New York, 1980, pp. 349-359.

[21] Huttelmaier, H.P., "Dynamic Analysis of Shear Walls and Discretely Connected Panel Structures Using a Super Finite Element Technique," Ph.D. Thesis, Department of Civil Engineering, Concordia University, Montreal, 1979.

[22] Pekau, O.A., and Wulf, A., "A Computer Program for the Nonlinear Analysis of Precast Panel Structures," Research Report, Department of Civil Engineering, Concordia University and the Technical University of Berlin, August 1979 (47 pages).

[23] Karsan, I.D. and Jirsa, J.O., "Behaviour of Concrete Under Compressive Loadings," Journal of Structural Division, ASCE, Vol. 95, No. ST12, December 1969, pp. 2543-2563.

[24] Pekau, O.A., "Influence of Vertical Joints on the Earthquake Response of Precast Panel Walls," Building and Environment, Vol. 16, No. 2, Pergamon Press, New York, 1981, pp. 153-162.

[25] Takeda, T., Sozen, M.A., and Neilson, N.N., "Reinforced Concrete Response to Simulated Earthquakes," Journal of the Structural Division, ASCE, Vol. 96, No. ST12, Dec. 1970, pp. 2557-2573.

[26] Desayi, P. and Krishnan, S., "Equation for Stress-Strain Curve of Concrete," Journal of the American Concrete Institute, Vol. 61, No. 3, Detroit, Michigan, 1964, pp. 345-350.

[27] Mondkar, D. and Powell, G., "ANSR-I General Purpose Computer Program for Analysis of Non-Linear Structure Response," Report No. 75-37, Earthquake Engineering Research Center, University of California Berkeley, California, 1975.

[28] Embedment Properties of Headed Studs, Design Data 10, Nelson Division, Ohio, 1970.

[29] Rashbash, D.J. and Stretch, K.L., "Explosions in Domestic Structures," The Structural Engineer, Vol. 47, No. 10, October 1969, pp. 403-411.

[30] Mainstone, R.J., "Internal Blast," Proceedings of the International Conference on Planning and Design of Tall Buildings, Vol. 1b, Lehigh University, Pennsylvania, August 21-26, 1972, pp. 643-660.

[31] Statutory Instruments 1970, No.109, Building and Buildings, The Building Regulations 1970, HMSO, London, England, 1970.

[32] Biggs, J.M., Introduction to Structural Dynamics, McGraw-Hill Book Company, New York, 1964.

[33] Ollgaard, J.G., Slutter, R.G., and Fisher, J.W., "Shear Strength of Stud Connectors in Lightweight and Normal-Weight Concrete," American Institute of Steel Construction Engineering Journal, Vol.8, No.2, April 1971, pp.55-64.

APPENDIX A

LOADING CONDITIONS AND TIE DESIGN DETAILS

APPENDIX A

LOADING CONDITIONS AND TIE DESIGN DETAILS

A.1 LOADING CONDITIONS

The loading conditions for the structure shown in Figure 3.13 are given below:

LOADINGS

Floor:	Live load	=	1915.2	N/m^2
	Partition load	=	478.8	N/m^2
	Mechamical load	=	239.4	N/m^2
	Slab dead load	=	2633.4	N/m^2
Roof:	Live load	=	1915.2	N/m^2
	Built-up roof	=	287.3	N/m^2
	Slab dead load	=	2633.4	N/m^2

EQUIVALENT DISTRIBUTED LOAD ON PANEL - FLOOR LEVEL

Dead load: = (478.8 + 239.4 + 2633.4) × 8.46/1000 = 29 kN/m

Panel self-weight : = 23.562 × 2.97 × 0.2 = 14 kN/m

Total dead load: W_d = 29 + 14 = 43 kN/m

Total live load: W_ℓ = 1915.2 × 8.46/1000 = 16 kN/m

EQUIVALENT DISTRIBUTED LOAD ON PANEL - ROOF LEVEL

Dead load: = (287.3 + 2633.4) × 8.46/1000 = 25 kN/m

Panel self-weight : = 14 kN/m

Total dead load: W_d = 25 + 14 = 39 kN/m

Total live load: W_ℓ = 16 kN/m

A.2 LOAD COMBINATION

When wind load is not included in the design, the required strength, U, provided to resist dead load, D, and live load, L, should be at least equal to the following [5]:

$$U = D + 0.5\ L$$

Accordingly, the roof and floor loads to be used in the analysis are determined as follows:

Roof load: $W_r = 39.0 + 0.5 \times 16.0 = 47.0$ kN/m

Floor load: $W_f = 43.0 + 0.5 \times 16.0 = 51.0$ kN/m

Since the value of W_r is nearly the same as W_f, the value of W_f will also be used at the roof level, i.e., the design load, $W = W_f$.

A.3 LUMPED MASS AT FLOOR LEVELS

Based on the design load distributed at floor levels, the resulting lumped masses assigned to the individual walls at each floor level are as follows:

Lumped mass at floor levels: $= 51{,}000.0 \times 11.0/9.81$

$= 57.24 \times 10^3$ N.s^2/m

$= 57.24 \times 10^3$ kg

A.4 DESIGN OF TRANSVERSE TIES

It is given that the tensile force, F_x, in the transverse tie at a particular storey is expressed as [5]:

$$F_x = \frac{\alpha_x W \ell_d^2}{2h_s}$$

where

α_x is a coefficient depending on the particular building height and cantilever depth.

The constant height of each storey, h_s, the design floor load, W, and the unsupported length of the cantilever, ℓ_d, are, respectively,

$$h_s = 2.97 \text{ m}; W = 51.0 \text{ kN/m}; \text{and } \ell_d = 3.67 \text{ m}.$$

To determine the transverse tie requirements, the α_x-value for each storey is chosen from the design chart [5].

The required transverse tie forces are as follows:

Floor Level	α	F_x (kN)
12	1.00	115.6
11	0.45	52.0
10	0.29	33.5
9	0.21	24.3
8	0.17	19.7
7	0.14	16.2
6	0.12	13.9
Below 5	0.10	11.6

It can be noted that with the exception at the uppermost level, the required tie force is below the recommended minimum tie force of 80 kN [5] at all floor levels. Accordingly, the unstressed prestressing strands selected for use as transverse ties are given below:

Floor Level	Transverse Tie Details
Roof	1-12.7 mm diameter strand; $A_s = 92$ mm^2; $f'_{pu} = 1{,}720 \times 10^3$ kN/m^2
11-1	1-9.5 mm diameter strand; $A_s = 51.6$ mm^2; $f'_{pu} = 1{,}720 \times 10^3$ kN/m^2

The design strength of a strand employed as a transverse tie is calculated as [5],

$$F_y = 0.9\ f_{pu}\ A_s$$

For 12.7 mm diameter strands,

$$F_y = 0.9 \times 1,720 \times 10^3 \times 92 \times 10^{-6} = 142\ kN$$

For 9.5 mm diameter strands,

$$F_y = 0.9 \times 1,720 \times 10^3 \times 51.6 \times 10^{-6} = 80\ kN$$

The tensile stiffness per strand, k_t, to be used in the analysis is calculated based on the debonding length, expressed as,

$$k_t = \frac{A_s\ E_s}{60d}$$

For d = 12.7 mm,

$$k_t = \frac{92 \times 200}{60 \times 12.7} = 24.0\ \ kN/mm$$

For d = 9.5 mm,

$$k_t = \frac{51.6 \times 200}{60 \times 9.5} = 18.1\ \ kN/mm$$

A.5 DESIGN OF VERTICAL TIES

The horizontal shear force at each floor level is given as [5],

$$V_x = \frac{\beta_x W \ell_d^2}{2h_s}$$

where

β_x is a coefficient depending on the particular building height and cantilever depth.

The other variables in the above equation are the same as those described in Section A.4. Hence, the horizontal shear force at each floor level is calculated as follows,

Floor Level	β_x	V_x (kN)
12	1.00	115.6
11	1.20	138.8
10	1.29	149.2
9	1.33	153.8
8	1.37	158.4
7	1.39	160.7
6	1.40	161.9
5	1.41	163.1
4	1.42	164.2
3	1.43	165.4
2	1.44	166.5
1	1.45	167.7

In addition to the above horizontal shear forces, the vertical ties must also act as tensile ties to resist any tensile forces induced by the suspension mechanism. Thus, by using two ties per panel, the required tensile force per tie is calculated as follows,

$$\text{Tensile force per tie} = V_x/2 + W\,\ell_d/2$$

It is clear that the highest tensile force requirement occurs at the first floor level, hence, the required force per tie is,

$$\text{Tensile force per tie} = \frac{167.7}{2} + \frac{51 \times 3.67}{2}$$

$$= 177.5 \text{ kN}$$

High strength steel bars ($d = 17.5$ mm, $A_s = 240$ mm^2) are employed as vertical ties with an ultimate tensile strength, $f_{pu} = 1{,}035 \times 10^3$ kN/m^2, with two per panel. The design strength of the bars is computed as [5],

$$F_y = \phi f_{pu} A_s = 0.9 \times 1{,}035 \times 10^3 \times 240 \times 10^{-6}$$

$$= 224.0 \text{ kN}$$

Hence, the tensile stiffness per tie, is expressed as

$$k_t = \frac{A_s E_s}{h} = \frac{240 \times 200}{h}$$

where

h is the height of the building to be inserted in the analysis for the particular building under consideration.